Microbial electrolysis cells with both anode and cathode catalysed by microorganisms

Swee Su Lim

A thesis presented for the degree of

Doctor of Philosophy

School of Engineering

Newcastle University

May 2019

Abstract

Microbial electrolysis cells (MECs), which simultaneously produce hydrogen and treat wastewater, is an innovative technology. This study not only focused on the acquirement of self-sustained biocatalysts but also meant to understand bioelectrodes' interaction in a single MEC which are crucial to improve the technology and make it economically feasible. For such MECs, further increases in overall performance were successfully done with the information from the studies. Those improvement methods included controlling bioelectrode reactions and cell configuration modification.

The bioanodes and biocathodes were enriched separately in half-cell condition at +0.2 and -0.9 V vs. standard hydrogen electrode (SHE) and tested with chronoamperometry to check the best operating potentials. The bioanode achieved a maximum current density of 0.30 ± 0.05 A/m^2 between -0.2 and +1.0 V while the biocathode only started to produce hydrogen below -0.8 V vs. SHE. It is preferable to maintain those potentials when both bioelectrodes are utilised in a MEC.

The interactions between the bioanode and biocathode were studied in a two-chamber MEC (2cMEC). Both bioelectrodes were enriched simultaneously at a 0.3 V applied voltage. The bioanode grew faster and produced less current than the biocathode required, due to different redox reactions (acetate oxidation vs. proton reduction). Therefore, a fed-batch feeding mode was deployed in order to keep the bioanode active and produce sufficient current output. Three main regions of behaviour were identified under a range of applied voltages: cathode activation (< 0.7 V), maximum production (0.7–1.2 V) and anode limitation (> 1.2 V). The potentials of the biocathode fell from -0.6 to -1.0 V while the bioanode maintained a value of ~ -0.3 V, when the voltage was increased from 0.3 to 0.7 V. Between 0.7 and 1.2 V, the bioanode potential started to increase from -0.3 V to -0.1 V when biocathode potential reached its minimum at -1.1 V. Applied voltages higher than 1.2 V, further increased the current density up to 2.5 ± 0.5 A/m^2 and the bioanode potential to +0.5 V. The greatest hydrogen production rate (20.0 ± 5.0 $dm^3\ H_2/m^2/day$) occurred after 0.9 V when an external power supply (increased from 0 to 75 %) took over the bioanode (decreased from 100 to 25 %) energy contribution. Cyclic voltammetry revealed a lower catalytic activity in the bioanode at 2.0 V compared to 0.3 V and the result was opposite for biocathode.

Further study involved a three-chamber MEC (3cMEC) where a gas chamber was attached next to the cathodic chamber for the accumulation of CO_2 from a gas phase into catholyte. This proof-of-concept MEC showed CO_2 can be separated in a single step under specific solubility conditions. The 3cMEC performed almost the same as 2cMEC except it could accumulate a higher concentration of carbonates (550 ± 200 mg/L accumulated vs. 150 ± 50 mg/L pre-added) and alleviate pH increase (10.0 ± 0.5 vs. 11.0 ± 0.5) in the cathode as a result of the CO_2 dissolution.

Acknowledgements

I would like to acknowledge my indebtedness and render my warmest thanks to my supervisor, Prof. Keith Scott, who made this work possible. His friendly guidance and expert advice have been invaluable throughout all stages of the work. I would also wish to express my gratitude to Dr. Eileen Yu for extended discussions and valuable suggestions which have contributed greatly to the improvement of the thesis.

My thanks are given to the technical workshop team of the Chemical Engineering department. Ian Strong and Ian Ditchburn assisted me kindly with the reactor designs and constructions. Paul Sterling who constantly support me in the operation of CEAM autoclave service. I must also thank Rob Dixon for his reliability and advice on chemical supplies and other technical related help. In the Civil Engineering department, I received a thorough understanding of the various analytical techniques I employed from David Race and I also thank Henriette Christensen for assistance with the running of the Total Organic Carbon and Ion Chromatography analysis.

Completing this work would have been all the more difficult were it not for the support and friendship provided by the colleagues and friends of the School of Engineering. I am indebted to them for their help, especially Martin Spurr for giving advice and assistances, and Jean-Marie for countless lunchtime discussions. Those people, such as the postdocs and postgraduate students at Newcastle, who provided a much-needed form of escape from my studies, also deserve thanks for helping me keep things in perspective: Tobechi Okoroafor, Paniz Izadi, Valentina Gogulancea, Victor Hugo Grisales Diaz and Orlando Do Nascimento.

I dedicate this work to my parents and family. Thank you for giving me the supports and encouragements during my study.

Table of contents

List of Figures

List of Tables

List of Abbreviations

Abb.	Definition
2c-	Two-chamber
3c-	Three-chamber
ATP	Adenosine triphosphate
BES	Bioelectrochemical system
BID	Barrier Ionization Discharge
CA	Chronoamperometry
CV	Cyclic voltammetry
D	Diffusion properties
DET	Direct electron transfer
EAB	Electrochemically-active biofilm
EAM	Electrochemically-active microorganisms
EGB	Electricity-generating bioanode
EIS	Electrochemical impedance spectroscopy
ES	Electrochemical system
ET	Electron transfer
FAD	Flavin adenine dinucleotide
FBEB	Flavin-based electron bifurcation
Fd	Ferredoxin
FlxABCD	Flavin oxidoreductase
HdrABC	Heterodisulfide reductase
HPB	Hydrogen-producing biocathode
MDC	Microbial desalination cell
MEC	Microbial electrolysis cell
MECC	Microbial electrochemical carbon capture
MET	Meditated electron transfer
MFC	Microbial fuel cell
MIC	Microbial influenced corrosion
MSC	Microbial electrosynthesis cell
NaAc	Sodium acetate
NAD	Nicotinamide adenine dinucleotide
ORR	Oxygen reduction reaction
PEMFC	Proton-exchange membrane fuel cell
PBS	Phosphate buffer solution
CPE	Constant phase element
SCFA	Short-chain fatty acid
SHE	Standard hydrogen electrode
SMFC	Sediment microbial fuel cell
SRB	Sulphate-reducing bacteria

List of Nomenclature

Symbol	Description	Units
A	Cross-sectional area	cm^2
A_{cat}	Cathode surface area	m^2
b	Activation coefficient	V
υ	Stoichiometric number	-
c	Concentration at specific time	mol
c_o	Initial concentration	mol
COD	Chemical oxygen demand	mg/L
DO	Dissolved oxygen	mg/L
D_o	Diffusion coefficient	cm^2/s
e^-	Electron charge	C
E_{cell}'	Open circuit cell voltage	V
e_e	Energy contribution by external power input	%
E_o	Open circuit potential	V
E_o'	Standard reduction potential	V
e_s	Energy contribution by substrate oxidation	%
F	Faraday constant (96485)	C/mol
HRT	Hydraulic retention time	hr
I_D	Current density	A/m^2
k_o	Mass transfer coefficient	cm/s
K_s	Half-saturated substrate concentration	mM
L	Membrane thickness	cm
OCP	Open circuit potential	V
Q_{H2}	Hydrogen production rate	$L/m^2/day$
$Q_{oxidise}$	Electrical charge produced from substrate oxidation	C
$Q_{produce}$	Electrical charge measured from electrical current	C
$Q_{recovery}$	Electrical charge recovered from a reducing product	C
Q_{supply}	Electrical charge supplied from the power supply	C

R	Ohmic coefficient	Ω
r_{cat}	Cathodic recovery	%
r_{CE}	Columbic efficiency	%
R_s	Electrolyte resistance	Ω
R_t	Charge transfer resistance	Ω
S	Substrate concentration	mg/L or mM
t_p	Production time	day
t_d	diffusion time	s
TC	Total carbon	mg/L
TDS	Total dissolved inorganic salt	%
V	Reactor volume	L
V_{gas}	Gas chamber volume	cm^3
V_{ap}	Applied voltage	V
V_{cell}	Cell voltage	V
V_h	Headspace volume	m^2
V_{H2}	Hydrogen volume	m^2
V_r	Anodic reactor volume	L
W_e	Supplied electrical energy	J
W_h	Energy content of hydrogen	J
W_s	Energy released from substrate oxidation	J
X	Fraction	-
z	Valency number of product formation	-
γ	Diffusion coefficients	V
n	Product recovery	mol
η_e	Energy yield relative to electrical input	%
η_{e+s}	Overall energy yield	%
η_s	Energy yield relative to substrate oxidation	%
ω	Diffusion coefficients	m^2/A

List of articles as part of this thesis

1. Kim, B.H., Lim, S.S., Daud, W.R.W., Gadd, G.M. and Chang, I.S. (2015) 'The biocathode of microbial electrochemical systems and microbially-influenced corrosion', *Bioresource Technology*, 190, pp. 395-401.
2. Lim, S.S., Yu, E.H., Daud, W.R.W., Kim, B.H. and Scott, K. (2017) 'Bioanode as a limiting factor to biocathode performance in microbial electrolysis cells', *Bioresource Technology*, 238, pp. 313-324.
3. Lim, S.S., Kim, B.H., Li, D., Feng, Y., Daud, W.R.W., Scott, K. and Yu, E.H. (2018) 'Effects of applied potential and reactants to hydrogen-producing biocathode in a microbial electrolysis cell', *Frontiers in Chemistry*, 6, p. 318.
4. Lim, S.S., Fontmorin, J., Izadi, P., Daud, W.R.W., Scott, K. and Yu, E.H. (-) 'Impact of applied cell voltage on the performance of a microbial electrolysis cell fully catalysed by microorganisms for the production of hydrogen', *Applied Energy*, Submitted.
5. Lim, S.S., Daud, W.R.W., Scott, K. and Yu, E.H. (-) 'Improvement of hydrogen production in two-chambered microbial electrolysis cell fully catalysed by microorganisms', *under preparation*.
6. Lim, S.S., Daud, W.R.W., Scott, K. and Yu, E.H. (-) 'The potential usage of three-chamber microbial electrolysis cell fully catalysed by microorganisms for direct CO_2 separation', *under preparation*.

Chapter 1. Introduction

1.0. Chapter summary

Microbial electrolysis cell (MEC) was introduced in this chapter by pointing out the importance of assisting sustainable energy generation in conjunction with wastewater treatment. Few research problems have been pointed out due to the insufficiency or shortage of this technology at the current stage. Following the drawbacks, a theory of improving the technology towards practical application has been suggested. It is aimed to increase MEC performance while decreasing overall operating cost by systematic control and studies. Several critical objectives were laid out in subsequent order to thoroughly study the theory and achieve the final aim.

1.1. Renewable energy, wastewater treatment and microbial electrolysis cell

Electrochemical system (ES) refers to a device that can perform oxidation-reduction process involve electron transfer to or from a molecular or ion by then changing its oxidation state (Hoogers, 2002). A most common example is the proton-exchange membrane fuel cells (PEMFCs) where oxidation of hydrogen (to proton) and reduction of oxygen (to water) occurred simultaneously in the system (consisted anode and cathode) separated by a proton exchange membrane. Different from the ES, the terminology of (bio)electrochemical system (BES) is mainly focused on the usage of biocatalysts to promote oxidation and/or reduction reaction(s) rather than abiotic catalysis as in the ES (Bajracharya *et al.*, 2016b). The BES is a wide research subject included several important research fields in microbial fuel cell (MFC), microbial electrolysis cell (MEC), microbial desalination cell (MDC), microbial electrosynthesis cell (MSC). Either these cells are power-generating or power-consuming system depending on their final aim to produce specific products (Harnisch and Schroder, 2010; Bajracharya *et al.*, 2016b; Choi and Sang, 2016; Zhen *et al.*, 2017). For instance, MFC is a method to reduce energy requirement for energy-intensive wastewater treatment, and also harness energy in wastewater while MEC is targeted to produce low-cost hydrogen and other chemicals under the assistance of less electrical input than conventional electrolysis process.

Whatever the aim of the systems, they must consist of at least a bioelectrode to enable them to be grouped in the BES category. Otherwise, the BES is not a BES but only an ES like PEMFC, which involved only in chemical reactions under abiotic catalysis. For the reason, most of BES consists of at least a biotic electrode in the system. Figure 1.1 shows the principle of operation of a BES based on microbial fuel cell system. Notes that a layer of biofilm is growth on the anode surface called bioanode catalysing substrate oxidation reaction. Electrons collected from the reaction are sent to cathode as driven by electromotive force between anode and cathode through an external circuit.

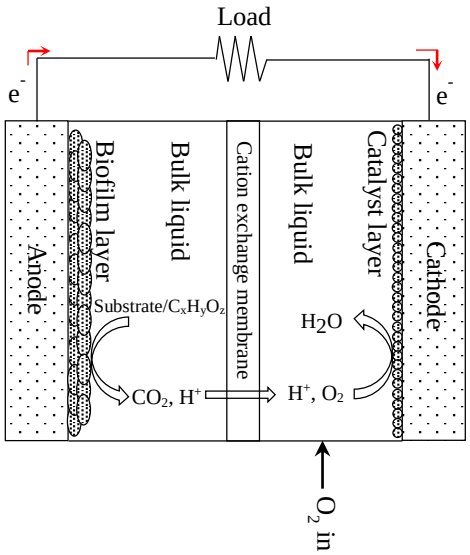

Figure 1.1 Principle of microbial fuel cell based on proton transfer and oxygen reduction.

Up to these days, fossil fuels still contribute a large portion of our energy sources and usages. In order to respond to the increasing energy demand and maintain the growth of human society, alternative and environmental-friendly energy sources such as hydrogen should be considered. Various approaches have been proposed to produce hydrogen and microbial electrolysis cell (MEC) is one of the alternatives. The innovative technologies have attracted the attention of researchers around the world because it not only can produce clean and safe energy but at the same time can be used to treat wastewaters and reduce CO_2 emissions.

Typical MECs deploy electricity-generating bioanode as part of energy source to support hydrogen generation in cathode. The bioanode serves as an important part in most of the bioelectrochemical system (BES) including MEC due to its ability to produce electrical current by oxidising organic matters in wastewaters (Santoro *et al.*, 2017). In MEC, the main

product, hydrogen, is generated in the cathode with the assistance of bioanode and external power supply. Either abiotic cathode or biocathode can be used in the MEC to generate hydrogen and other value-added chemicals. In the case of MEC fully catalysed by microorganisms, the research involved multidisciplinary fields like bioelectrochemistry, microbiology, chemical and environmental engineering (Kadier *et al.*, 2016). Therefore, the study of bioanode and biocathode in one system aimed for hydrogen production is an attractive and interesting subject. Deploying both bioanode and biocathode in a single BES required in-depth study. Information on the requirements of each bioelectrode are the main keys to control oxidation and reduction reactions in a MEC system while optimising the processes of wastewater treatment and hydrogen production. As living microorganisms are used as biocatalysts in both bioelectrodes, a clear understanding of the operating conditions and limitations when they are utilised in the system is essential. Up to the date, most of MEC study are half-cell experiments only focused on biocathode and there is still a lack of information on a MEC system utilised both bioelectrodes (Lim *et al.*, 2017).

Wastewater treatment industry is the fourth most energy-intensive sector in the United Kingdom. In England and Wales, almost 1% of the average daily electricity consumption is used to treat over 10 billion litres of sewage every day (Anonymous, 2007). This is the result of conventional treatment methods use pumps and energy-intensive aerated system during the treatments. Further tightening of water quality standards suggests energy cost will increase in the next coming year. In a recent study, researchers found that wastewaters actually hold more internal energy than was previously thought which can be used to offset operating cost. As reported by (Heidrich *et al.*, 2011), two wastewaters originated from North East of England but different treatment plant were collected and analysed. The analysis results show that mixed and domestic wastewaters content usable energy up to 16.8 kJ/L and 7.6 kJ/L, respectively. Therefore, more effective and energy-harvesting technology such as MEC should be utilised to conserve energy usage and improve treatment quality. However, the MEC technology is still premature at the current stage and requires further study to improve the treatment performance and recovery efficiency before can be applied in a large scale application.

1.2. Research problem and hypothesis

There are an anode and a cathode in a MEC responsible in oxidation and reduction reactions as shown in Figure 1.2. In the anode, electrochemically-active microorganisms are usually grown and used as a biocatalyst to oxidise organic matters in wastewaters. Meanwhile, the cathode

either containing abiotic or biotic catalysts is meant to perform proton reduction reaction to produce hydrogen. Both electrodes are divided by a separator to avoid reactant and product crossovers that can affect the redox reactions and poisoning the catalysts. In most MEC, the abiotic cathode is coupled with bioanode because the combination provides better control to the production of hydrogen in the cathode as long as the bioanode is maintained at optimal condition (Liu *et al.*, 2005; Rozendal *et al.*, 2006). In order to use biocatalysts in both anode and cathode of MEC, one has to consider the limitation of both biocatalysts in the MEC system in term of standard reduction potential and current supply. Firstly, the standard reduction potential is important for prediction of minimum potential in order to initiate redox reactions between the electrodes in MEC (Harnisch and Schroder, 2010; Rosenbaum *et al.*, 2011; Kumar *et al.*, 2017). Theoretically, a bioanode which uses acetate as its main carbon source could oxidise electron donors to form proton and electron as described in (Reaction 1.1). The electrons contribute electrical energy to power the system or to lower the total energy need into the MEC system. At the cathode, protons react with the electrons to form hydrogen (Reaction 1.2). The standard reduction potentials, E_o' of acetate and proton at standard condition (pH 7, 25°C and 1atm) are described as

$CH_3COO^- + 2H_2O \rightarrow 2CO_2 + 7H^+ + 8e^-$ E_o' = -0.28V vs. SHE, pH 7.0 (Reaction 1.1)

$2H^+ + 2e^- \rightarrow H_2$ E_o' = -0.41V vs. SHE, pH 7.0 (Reaction 1.2)

The minimal electrical potential that is required to drive the reaction is 0.13 V. However, more energy is required (>0.13 V) due to overpotentials to overcome energy barriers in the system (Rozendal *et al.*, 2006; Geelhoed *et al.*, 2010). Thermodynamically, this voltage is relatively smaller required to derive hydrogen from water electrolysis compared to 1.21 V at neutral pH. Meanwhile, it could go up to 1.80 - 2.00 V for water electrolysis under alkaline condition due to overpotential at the electrodes (Liu *et al.*, 2005). Secondly, the robustness of anode should be considered for better MEC performance as it could limit the current supply to cathode (Wang *et al.*, 2010; Rago *et al.*, 2016; Kumar *et al.*, 2017). Weak anode with more positive open-circuit potential tends to perform poorly in supporting cathode reduction reaction when a fixed voltage was applied between the electrodes (Wang *et al.*, 2010). As a result of the weak anode, more electrical energy was required from external power to drive the reduction reaction in cathode resulting in higher energy consumption. These phenomena were mainly found in conventional MECs using bioanode coupled with the abiotic cathode. It is hypothesised that by replacing the cathode with biocathode could reduce overall overpotentials of the MEC and increase hydrogen production. A similar study has been conducted by using both bioanode and biocathode

(Jeremiasse *et al.*, 2010). However, the system was suffered from overpotential and lower hydrogen yield compared to their previous study when only biocathode (half-cell setup) was operated (Rozendal *et al.*, 2008). Therefore, a detailed study on using both bioanode and biocathode is required.

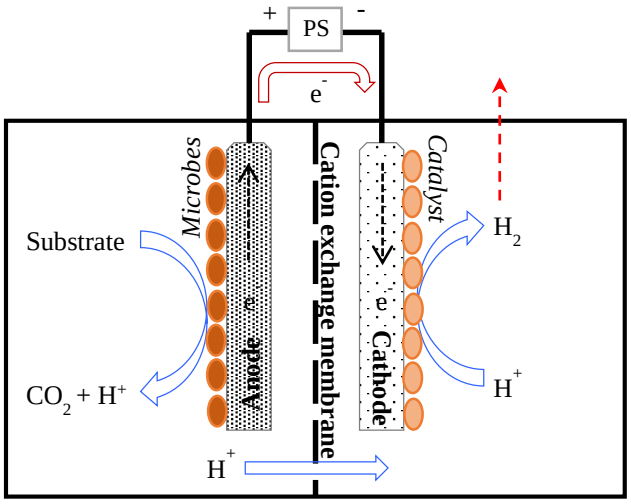

Figure 1.2 Typical microbial electrolysis cell (MEC). Bioanode is coupled with cathode either abiotic or biotic for hydrogen generation.

Hydrogen-producing biocathode is getting attention in recent years due to their ability to grow and sustain in the cathode without necessary to be replaced after a long term operation (Rozendal *et al.*, 2006; Aulenta *et al.*, 2012; Jeremiasse *et al.*, 2012; Liang *et al.*, 2014; Jourdin *et al.*, 2015). Additionally, the biocathode can be obtained freely from natural environments and resisted to organic toxicity such as sulphate and ammonium compounds (Coma *et al.*, 2013; Luo *et al.*, 2014; Zheng *et al.*, 2014). However, there is still little information about bioanode and biocathode coupling MEC in current research. As both bioelectrode perform different reactions, it is hypothesised that the reaction rates are also varied among bioanode and biocathode. Therefore, understanding their limitations and behaviours in one system are important to improve MEC performance. Once their interactions are elucidated, proper strategies can be planned to further improve and scale up the system. It is believed that sufficient electron supply from substrate oxidation by bioanode activity is vital to support the hydrogen evolution in a biocathode and therefore maintaining the external energy demand from a power supply as low as possible. In order to have an optimum hydrogen production rate from the biocathode, the anode plays an important role as a support to the biological MEC system. It may lower external energy supply to the system and increase energy recovery in term of

hydrogen evolution on the one hand and it could be a limiting factor to the whole system together with other problems like substrate crossover and precipitation of mineral on the electrodes on the other (Jeremiasse *et al.*, 2010).

Two hypotheses are proposed as mentioned above: 1. overall overpotential could be reduced by using bioanode and biocathode in one MEC system, and 2. hydrogen production in the MEC system could be increased by controlling and balancing the bioelectrodes' reactions and growth rates. To fully understand the operational conditions of hydrogen-producing biocathode in a MEC, the study of operating parameters and community interaction is essential. It was also suggested that studying the correct growth conditions with a carbon source and applied voltage, longevity of the biocathode could be the key issues for further understanding the electron transport mechanism. Various cell configurations have been tested and used in laboratory for biocathode-driven processes, especially hydrogen production. The technology has advanced from half-cell to full cell configuration, two chambers to single chamber, batch to continuous tubular mode, and laboratory to large scale aimed in reducing overpotentials and cutting down operation cost and development time (Escapa *et al.*, 2016; Kadier *et al.*, 2016; Zhen *et al.*, 2017). Nonetheless some questions still remain unanswered in these systems including the optimum operational environments for bioelectrodes (e.g. pH, conductivity, cell voltage), time of growth for both bioanode and biocathode (e.g. 1 vs. 4 weeks), optimum reducing power or potential required by biocathodes to produce certain products (e.g, HCO_3^- /CH_3COO^- E_o'=-0.28 V vs. H^+/H^2 E_o'=-0.41 V) when coupled with bioanode for wastewater treatment and the most important how the bioanode and biocathode interact in a single cell system (e.g. current response and how biofilms evolve) even during the beginning of the enrichment?

1.3. Aim and objectives

This study is aimed to develop self-sustained biocatalysts for a MEC fully catalysed by microorganisms. To carry out the study, four main objectives are set:

1. To understand operating and optimum conditions of electricity-generating bioanode and hydrogen-producing biocathode.
2. To study the interaction between bioanode and biocathode, and how bioanode affects hydrogen production and the stability of the whole system.

3. To improve MEC overall performance by controlling and balancing bioanode and biocathode reactions and growth rates.
4. To develop a three-chamber MEC with an extra gas chamber next to the cathode for direct dissolution of CO_2 into catholyte.

1.4. Thesis summary

This thesis contents 8 chapters included 4 experimental chapters as described below:

1. Introduction
2. Literature review
3. Materials and methods
4. Bioanode as a limiting factor to microbial electrolysis cell (MEC)
    - The study was started with the investigations of bioanode in a two-chamber microbial fuel cell and parameter that might affect the performance.
5. Effects of energy input and reactants to hydrogen-producing biocathode (HPB)
    - The second study was focused on biocathode and its basic requirements to produce hydrogen aimed for hydrogen production.
6. Operational applied voltage of two-chamber microbial electrolysis cell (2cMEC) and the potential usage of three-chamber microbial electrolysis cell (3cMEC)
    - Microbial electrolysis cells fully catalysed by microorganisms were used in this study to check the interactions between bioanode and biocathode especially under a range of applied potentials.
7. Improvement of hydrogen production in 2c- and 3cMEC by feed controlling in bioanode
    - As both bioanode and biocathode posted different reaction rates and underwent different reactions, microbial fuel electrolysis cell performance can be increased by a simply bioanode control mode
8. Conclusions and recommendation for future work

Chapter 2. Literature review

2.0 Chapter summary

A microbial electrolysis cell (MEC) fully catalysed by microorganism was intended to use in this study. The importance of bioanode in bioelectrochemical system (BES) was revised followed by biocathode and its abiotic counterparts. The properties and how the characteristic of the bioanode affected by its microbial community was discussed in depth. In addition, current developments and future applications of the bioanode were discussed to give readers a general overview. Meanwhile, the biocathodes involved in hydrogen generation were revised included typical hydrogen formation mechanisms in MECs. Electron transfer and energy conservations in biocathodes were also examined. As bioelectrochemical CO_2 reduction is quite similar and highly related to the hydrogen formation in biocathode, current developments of the CO_2 reduction activity were also revised in this chapter. Production of valuable or longer chain organic carbons was the main focus in the revision. At the end of the topic, utilisation of bioanode and biocathode in single BES was revised including the advantages, bottlenecks and potential of using them in MEC or microbial synthesis cell (MSC) applications.

*Part of this chapter has been published in *Bioresource Technology*, 190, pp. 395-401 in 2015 with the title 'The biocathode of microbial electrochemical systems and microbially-influenced corrosion'. All author (Byung Hong Kim, Swee Su Lim, Wan Ramli Wan Daud, Geoffrey Michael Gadd and In Seop Chang) were equally contributed to the paper.

2.1 Electricity-generating bioanode in bioelectrochemical system (BES)

2.1.1. Bioanode as a vital part in bioelectrochemical system (BES)

Electricity-generating bioanode (EGB) produced from the growth of electrochemically-active-biofilm (EAB) or microorganisms (EAM) on the electrode surface have received attentions for their potential applications in the field of bio-green energy. The bioanode studies were attracted attention based on the knowledge on iron-reducing bacteria of their ability to utilise ferric ion

as their electron acceptors (Lovley, 1991; Caccavo *et al.,* 1994). Since then the studies of bioanode in MFC was flourished especially under the Fe(III)-reducing bacteria such as *Geobacter sp.* and *Shewanella sp.* (Kim *et al.,* 2002; Bond and Lovley, 2003). On top of these bacteria, the studies of the mechanisms that articulated the electron transfer from the bacteria to the anode were also been carefully studied in order to understand the principle of EGB (LaBelle, 2009; Harnisch and Schroder, 2010; Kracke *et al.,* 2015). Based on the explanation, electrons were transferred according to the electrode's potential and reactant's standard reduction potential. A common example of the reactant is acetate. The standard reduction potential is -0.28 V (E_o' for reaction CH_3COO^-/CO_2) in ideal conditions (e.g. neutral pH and room temperature) (Bajracharya *et al.,* 2016a). If electrochemically-active microorganisms conserve energy from the acetate, they are going to use the anode as an electron sink. The difference potential of the anode and reactant can be used to estimate the energy that possibly conserved by the microorganisms (Fricke *et al.,* 2008; Lim *et al.,* 2017). Therefore, the anode potential should higher than -0.28 V in order to transfer the electrons (Aelterman *et al.,* 2008; Cheng *et al.,* 2008; Ketep *et al.,* 2013). In a BES system, a reduction reaction is always coupled with an oxidation reaction. When a substrate is oxidised, high energy electron was released from breaking the molecular bond and in the same time anode acted as an electron sink for bacteria to dispose of the electron after the energy (in term of ATP (Adenosine triphosphate)) is harvested through electron transport chain. Under normal MFC operational condition, the anode potential is always higher than the potential of disposed electrons to facilitate the collection of those electrons. A higher potential cathode is then used by connecting to the anode through an external wire in order to bring the anode potential up. In this way, iron-reducing bacteria such as *Geobacter sp.* and *Shewanella sp.* are enriched under such conditions by oxidising available substrate in bulk solution while thrive on the anode surface forming a layer of electrochemical active biofilm. Oxygen is abundance in the atmosphere and has higher reduction potential which is suitable for cathodic reduction process. Normally platinum is applied to the cathode surface to lower activation energy and facilitate the reaction (Kim *et al.,* 2002; Burkitt *et al.,* 2016; Kodali *et al.,* 2017). Technically the functionality and performance of the bioanode are actually depended on the cathode. Therefore some researchers suggested that the size of cathode should be bigger than the size of anode to overcome cathode limitation (Oh *et al.,* 2004; Cheng and Logan, 2011; Li *et al.,* 2011). In addition, higher potential the cathode must post higher potential than anode in order to serve as the driving force to transfer electrons from anode to cathode. Therefore, MFCs consist of both bioanode and biocathode did not work well in many cases and experienced low performance after a long term operation. In

addition, the functionality of the aerobic biocathode was depended on the level of dissolved oxygen which consumed large amount of electrical energy to dissolute the oxygen into catholyte (Gil *et al.*, 2003; Milner *et al.*, 2016; Milner and Yu, 2018).

Apart from MFC, other systems have been benefited from the usage of EGB. In the case of microbial electrolysis cell (MEC), the bioanode not only served as part of electrical energy provider to hydrogen-producing cathode but also treat wastewater at the same time. The whole system required less energy (0.7 V) than conventional water electrolysis process (2.0 V) (Liu *et al.*, 2005). The same principles laid in other type of BES such as microbial desalination cell (MDC) and microbial electrosynthesis cell (MSC), the bioanode still remained as an inevitable part of the systems. Figure 2.1 shows the different type of BES consists of bioanode as a natural power source. The utilisation of the bioanode in those systems is due to its natural metabolism activity and electrogenic character to treat wastewaters by reducing organic contaminants and able to grow and regenerate by itself. As long as the given environmental conditions are favourable to the bioanode, which for electrogenic microorganisms, it will stay active even under long term operational conditions (Santoro *et al.*, 2017).

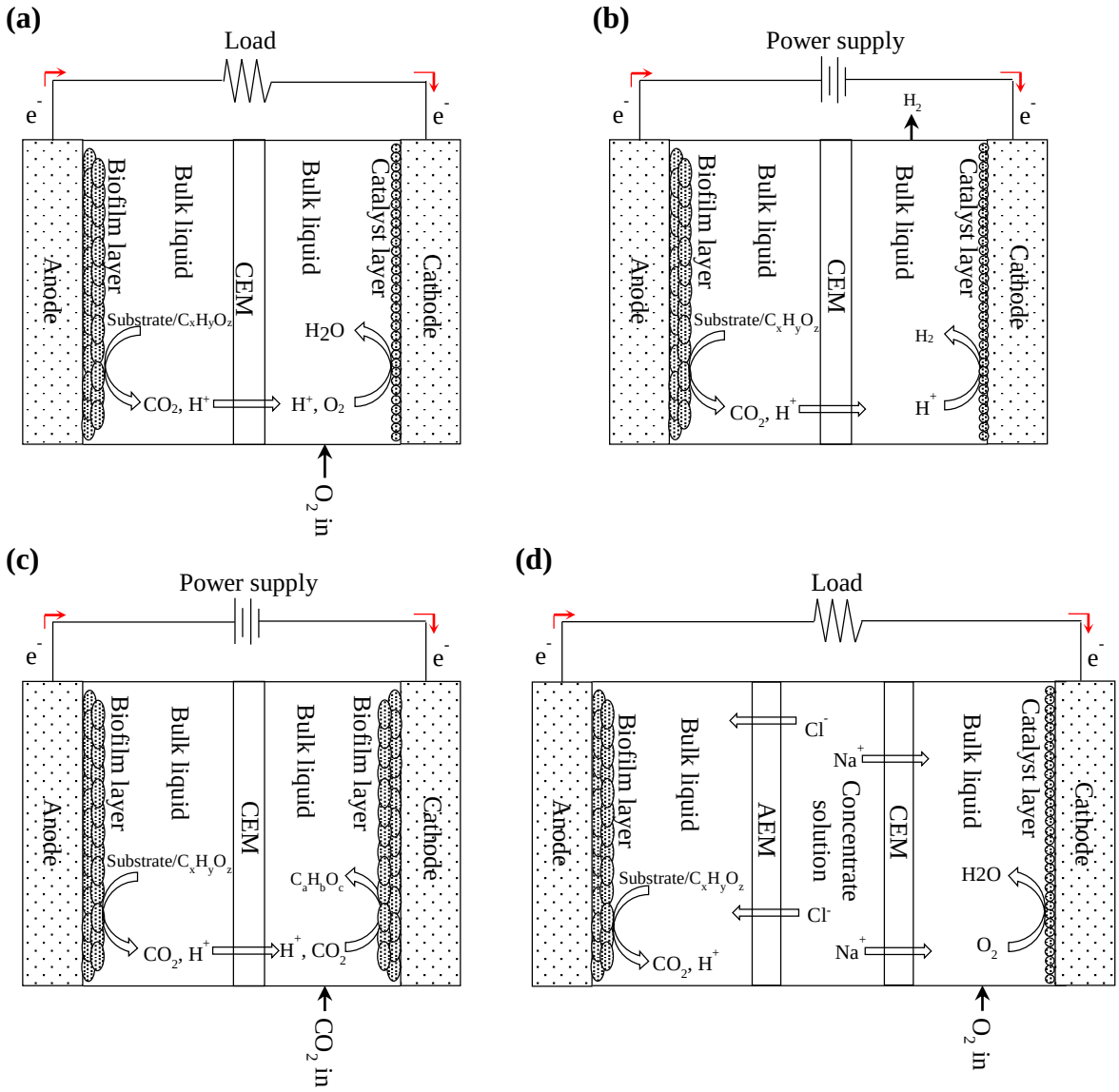

Figure 2.1 Schematic of BES: (a) microbial fuel cell, (b) microbial electrolysis cell, (c) microbial electrosynthesis cell, and (d) microbial desalination cell

2.1.2. Microbial community of bioanode

Electrochemically-active microbes are important in electricity-generating bioanode. They worked as biocatalysts to oxidise and release potential energy by breaking down organic compounds in wastewaters (Kim *et al.*, 2011; Kadier *et al.*, 2016). It makes the interaction of these microbes with their environments crucial in order to maintain their number and dominance in entire population (Kim *et al.*, 2004; Kim *et al.*, 2005; Liu *et al.*, 2008; Torres *et al.*, 2009). The well-known electrochemically-active microbes are iron-reducing bacteria

especially *Shewanella sp.* and *Geobacter sp.* as the primary examples. The bacteria are able to transfer electrons to an electrode which they obtained from oxidising substrates such as acetate and propionate. The electrons transfer beyond cell membrane required specific transport agents either through direct and/or indirect contacts with the electrode. *Geobacter sp.* is the example which use outer membrane cytochromes for direct transfer of the electron to an electrode while *Shewanella sp.* use self-secreted mediators such as flavin molecules shuttled between outer membrane proteins and the electrode (Bond and Lovley, 2003; Fricke *et al.*, 2008; LaBelle, 2009; Wei *et al.*, 2010; Jain *et al.*, 2012; Carmona-Martínez *et al.*, 2013). In order to facilitate the electron transfer, anode as electron acceptor should possess higher potential than the cytochromes and/or electron shuttles. These cytochromes and electron shuttles can show a wide range of redox potentials depended on physiological and environmental conditions (Kracke *et al.*, 2015). In a BES, practical bioanode redox potential tends to occur in between -0.15 - -0.20 V vs. SHE which is related to cytochrome or electron shuttle redox potentials. As a result, the anode potential should be higher than -0.20 V vs. SHE to smooth the electron transfer mechanism between the microbes and anode (Cheng *et al.*, 2008; Wang *et al.*, 2009; Wei *et al.*, 2010). Meanwhile, cathode plays an important role to raise and maintain the anode potential which is connected to the anode through an external circuit where electrical power is harvested (Oh *et al.*, 2004; Rismani-Yazdi *et al.*, 2008; Ketep *et al.*, 2013; Bajracharya *et al.*, 2016a). Different range of microbial community could possible grow depending on the anode potential, available organic matters and environmental conditions such as electrolyte pH and conductivity (Fan *et al.*, 2007; Torres *et al.*, 2009; Logan, 2010; Yates *et al.*, 2012). However, benign interactions between electrochemical- and non-electrochemical-active microbes are essential within the community to some extent. A mixed community is always preferable and enriched as bioanode to treat various type of wastewaters such as landfill leachate, and anaerobic digestion effluents (Freguia *et al.*, 2010; Kim *et al.*, 2011; Puig *et al.*, 2011a; Cerrillo *et al.*, 2017). This is to ensure the ability of the biofilm to produce electricity especially when treating complex organic matters in wastewaters. For example, in glucose-fed bioanode, non-electrochemically-active fermentative bacteria utilise glucose and produce short-chain fatty acids like acetate and butyrate which in turn consumed by electrochemically-active microbes and release the electron to anode (Xing *et al.*, 2009; Zhang *et al.*, 2011). However, those non-electrochemical-active microbes are mostly found dominated in solution than on anode surfaces.

2.1.3. Practical applications and future perspectives

2.1.3.1. Scaling up of bioanode for wastewater treatment and power generation

The scaling up of bioanode is mainly related to microbial fuel cell (MFC) applications in which aim to generate electricity from treating domestic or industrial wastewaters. However, the technology still infeasible in large scale applications due to its low performance but rather than using it as a scientific tools for understanding microbial, bioelectrochemical, material surface properties, substrate toxicity and chemical compounds (Aelterman *et al.*, 2008; LaBelle, 2009; Carmona-Martínez *et al.*, 2013; Spurr, 2016). Despite the fact that the technology has never been considered as a serious contender in the sectors of wastewater treatment or renewable energy, several studies have shown the implementations of MFC and the practical value of the technology in various applications. This included the first pilot-scale MFC (up to 1000 L) treating brewery wastewater in Yatala, Queensland, Australia (Logan, 2010), and MFC reactor (100 L) used for charging and discharging external ultra-capacitors (Ge *et al.*, 2015). Various approaches have been studied based on system geometry to increase bioanode outputs and performance in large scale applications. These include cell staking, bigger electrode size per operating volume, anode to cathode size ratio, and etc. (Cheng and Logan, 2011; Logan and Rabaey, 2012; Rahimnejad *et al.*, 2012). However, the successfulness of scaling up the process seems impractical by only considering the geometry aspects. The main constraints of low current output bioanode are also caused by low rates of microbial metabolic activities and electron transfer mechanisms (Logan and Rabaey, 2012; Kracke *et al.*, 2015). Those limitations in bioanode have restricted engineers to design a larger and viable scale-up system to be deployed in real environments. For instance, voltage reversal is a common issue in staked MFC as a result of anode overpotential with sluggish kinetic reaction (An and Lee, 2014). Low conductivity of influents could cause slow ion transport between electrode while requiring more activation energy to move the ions (Ahn and Logan, 2013). Other factors such as pH, temperature, internal resistance and substrate availability could also cause adverse effects on the bioanode performances (Abbas *et al.*, 2017). Inconsistent organic matters and heavy metal content in wastewaters can cause starvation and toxicity in the bioanode. As a result, the bioanode required more time to recover and respond when the conditions are reverted back to norm (Spurr, 2016). Another example of microbial metabolism working in real practical environment included Gastrobot, EcoBot-I, -II, and – III (Santoro *et al.*, 2017). The applications demonstrated the used of microbes metabolising sugars and organic matters to power self-sustained robots after a few generations of improved models.

2.1.3.2. Development of bioanode-based biosensor

Besides wastewater treatment, electricity-generating bioanode has also been developed as biosensors e.g. to detect biochemical oxygen demand (BOD) and toxicity in wastewaters (Schneider *et al.*, 2016; Spurr, 2016). The bioanode has been used in remote sensor applications such as benthic MFCs, for example, had been reported for powering a meteorological buoy and wireless temperature sensors and other environmental sensors (Tender *et al.*, 2008). The bioanode electrical output is directly related to microbial redox metabolite activities which could serve as a monitoring system in wastewaters. Bioanode microbes offer promising platforms for biosensing development since they are resistance toward different toxic compounds and sensitive to local environment changes. In addition, they are able to metabolise a wide range of chemical or organic compounds in wastewaters. Once a balance microbial community has been cultivated, it would thrive even under unfavourable adverse conditions. The concept of the sensor is based on microbial fuel cell (MFC)-based technology in which the bioanode is coupled with a cathode. The purpose of the cathode is to drive the redox reaction and complete the circuit with the bioanode. Due to the emerging interest in the microbial fuel cell-based sensors, more research has been focused on reducing the size of the sensors and enhancing the sensitivity of the bioanode. The key parameter is the internal resistance of the system included ohmic and non-ohmic losses. The ohmic losses are due to electrical resistance in the structure and electrode surface quality. While the non-ohmic losses are associated with electron transfer resistances between biotic and abiotic counterparts of the MFC system. The flow of electron from bacteria to the electrode is hindered by the non-ohmic loses, also known as activation potential or overpotential, where certain amount of energy is conquered to assure change transfer between two surfaces.

2.1.3.3. Hypersaline wastewater treatment using bioanode technique

Another practical application of the bioanodes is based on their abilities to survive under extreme conditions such as saline and hypersaline environments. Saline wastewaters normally produced and discharged by different industrial sectors including the fish industry, food processing, textile and leather and petroleum industries. The wastewaters are distinguished in saline, highly saline and hypersaline according to the total dissolved inorganic salt content (TDS), is between 0 and 1%, 1 to 3.5% and over 3.5% w/v, respectively (Pernetti and Di Palma, 2005). The bioanodes in MFC system treating saline wastewaters have been reported. For

instance, the usage of seawater for toilet flushing. Additional treatment is required before disposal of the seawater-based domestic wastewater sewage sludge back into natural environments. In this case, Karthikeyan *et al.* (2016) used the sludge as feedstock and source of inoculum for their MFCs and successfully generated a maximum power density of 35 w/m^3 with 72% chemical oxygen demand (COD) removal and 20% Coulombic efficiency. The sludge was pre-analysed and reported contains 13.3 g/L of TDS. The sludge was further studied by mixing it with freshwater-based wastewater sludge for investigating the effect of ionic conductivity to the bioanode and MFC performances. The TDS value of the mixture was decreased to about 8 g/L while the initial COD was similar. The mixed sludge MFCs showed higher power density (41 w/m^3) and Coulombic efficiency (28%) but with lower COD removal (59%). The authors deducted that strong buffering capacity of the freshwater-based wastewater sewage sludge could mitigate the effect of excessive ionic conductivity and pH drop in the sea-based wastewater sewage sludge. Another example of the bioanode applications is the treatment of oilfield wastewaters under hypersaline conditions. The wastewater is the largest waste stream generated in oil and gas industries and usually rich in dissolved and dispersed oil while the content of salt can reach up to 300g TDS/L. In recent developments, Ghasemi Naraghi *et al.* (2015) obtained inoculum from the last sedimentation unit tank of treating oilfield wastewater for their bioanode. The inoculum was pre-enriched with grow medium containing 250 g/L of NaCl before it was used in spiral-type MFC for oilfield wastewater treatment. Halophile and halotolerant microbes were found dominated in the pre-enriched inoculum. The MFC was then used to treat oilfield wastewater contained 200 g/L TDS and 3000 mg/L COD. A maximum power density of 0.65 mW/m^3 with 90% of COD removal was observed from the MFC operations. The final TDS was also decreased to 40 g/L, however, low CE (0.2%) suggested that the bioelectrochemical activities were limited and further study is required for optimising the process. These examples showed the possibility of saline wastewater treatment using MFC technology. Nevertheless, exposure of the extreme and unstable conditions in MFC devices could cause a breakdown of the whole treatment system. Robust anode materials and specific cell setup which could withstand the conditions should be carefully sorted and tested for long term effects.

2.1.3.4. Bioremediation of heavy metal using sediment bioanode

Recently, sediment microbial fuel cell (SMFC) have been attracted the attention of the research community due to its ability to remediate heavy metal or hydrocarbon polluted soils while

producing sustainable energy source. The SMFC are distinguished from normal MFC due to their completely anoxic operating condition and lack of a separator between anode and cathode (Wang *et al.*, 2018). The anodes are normally buried underneath sediments to provide a growing surface for electroactive microbes (Ewing *et al.*, 2014). The electroactive microbes utilise any available organic contaminants in the sediments to power the cathode, located on the sediment surfaces, to reduce heavy metals and absorb them onto the surface that can be easily removed. Besides simultaneously produce electricity by oxidising the available organic matters, they can also bioremediate any organic contaminants such as hydrocarbon or petroleum pollutants in the vicinity of the sediment where they are installed. Inocula are normally obtained and originated from areas which required the bioremediations. These areas included river sediment, marine sediment, paddy field, or wastewater sludge (Chen *et al.*, 2012; Liu *et al.*, 2016; Liu *et al.*, 2018). In the case of heavy metals, the function of the SMFC is to reduce the metal ions from soluble to insoluble redox state thus reduce their toxicity under low potential conditions. The heavy metals such as Cr(VI), Cd(II), Cu(II) and Zn(II) are toxic to ecosystem especially aquatic organisms. Regardless not all heavy metals can be removed by reduction process, for instances, arsenic and mercury required to be oxidised at the anode with easy removal precipitation forms. The combination of electrochemically induced precipitation and bioremediation has provided novel insights to remove multiple heavy metals from sediments (Chen *et al.*, 2015). Moreover, the energy generated by the SMFC can be used to power conventional environmental sensors such as temperature sensor, humidity sensor and BOD monitoring sensor in a remote area (Ewing *et al.*, 2014).

2.2 Hydrogen-producing biocathode in microbial electrolysis cell (MEC)

2.2.1. Importance of biocathode in BES

Bioelectrochemical system (BES) have been studied extensively since the first discovery of electrochemically active bacterium in an anode microbial fuel cell (MFC) (Kim *et al.*, 1999). Electrochemically active bacteria are also found in cathode where it can consume available electrons instead of transferring electrons to electrode as in anode (Bergel *et al.*, 2005). Since then, researchers start to use the term “biocathode” to describe the electrochemically active microbes as a catalyst in cathode either in MFCs that reduce oxygen or in MECs that reduce proton to hydrogen. In MFC application, aerobic biocathodes have a higher affinity for oxygen than abiotic catalysts that included precious metals such as platinum (Milner *et al.*, 2016). In

addition, these biocathodes are cost-effective, self-generated and resistant to sulphide poisoning. Pham (2004) reported that minimum dissolved oxygen concentration (DO) required to produce maximum current from plain and platinum-catalysed graphite felts was 6.6 mg/L and 2.0 mg/L. However, aerobic bacteria can respire oxygen at maximum capacity with DO as low as 0.12 mg/L (Chen *et al.*, 1985). It would be a great advantage for a biocathode enriched with microorganisms that can use alternative electron acceptors. Nitrate (Jia *et al.*, 2008; Desloover *et al.*, 2011; Puig *et al.*, 2011b; Lee *et al.*, 2012; Cai *et al.*, 2014), chlorinated hydrocarbons (Aulenta *et al.*, 2010; Huang *et al.*, 2012), perchlorate (Shea *et al.*, 2008; Butler *et al.*, 2010; Xie *et al.*, 2014), chromate (Li *et al.*, 2009; Tandukar *et al.*, 2009; Huang *et al.*, 2011; Zhang *et al.*, 2012a) and nitro-compounds (Mu *et al.*, 2009; Wang *et al.*, 2011b) are among the alternative electron acceptors other than oxygen which have been studied in BES biocathode to treat wastewaters containing these substances. It was reported that a biofilm that formed on a stainless steel coupon electrochemically polarized in the range of -0.14 - +0.16 V vs. SHE in seawater for several days was able to catalyse the oxygen reduction reaction (ORR) efficiently, but this activity was reduced after the biofilm was removed (Bergel *et al.*, 2005). The electrochemically-active biocathode could be enriched in a two-chamber MFC using graphite felt (Rabaey *et al.*, 2008), granular graphite (Chen *et al.*, 2008), or a carbon fibre brush with graphite granules (Zhang *et al.*, 2012b) as the cathode. Alternatively, a cathode was polarized at a potential lower than +0.24 V vs. SHE to enrich a cathode biofilm in a two-chamber MFC (Liang *et al.*, 2009). It was expected that the cathode redox potential of a two-chamber MFC becomes low enough for electrochemically-active microbes to grow when the cathode was connected to an actively metabolising bioanode through a suitable external resistance. It is assumed that the increase in electrochemical activities during the enrichment process is the result of the growth of electrochemically-active microorganisms on the electrode. It has been reported that the anode biofilm could be used as an aerobic (Cheng *et al.*, 2012a) or denitrifying biocathode (Cheng *et al.*, 2012a). It is not known if the same organisms catalyse anode reactions, oxidizing electron donors to transfer electrons to the electrode with the cathode reaction consuming electrons available from the electrode to reduce oxygen or nitrate.

In addition to the biocathode in a MFC catalysing ORR, H^+-reducing biocathodes have been studied in microbial electrolysis cells (MECs). A MEC is a microbial electrochemical system where electrons available from the anode reaction are used to reduce H^+ producing H_2. Since the redox potential of the anode reaction is higher than that of the H^+/H_2 half reaction, energy is supplied to the cathode in the form of electricity (Liu *et al.*, 2005; Rozendal *et al.*, 2008). The first MEC biocathode was developed through a three-phase start-up procedure that

effectively turned an acetate- and hydrogen-oxidizing bioanode into a hydrogen-producing biocathode by reversing the polarity of the electrode (Rozendal *et al.*, 2008). Microbial population analysis of a biocathode developed in a similar way showed predominant strains of *Eubacterium limosum* and *Desulfovibrio* sp. A2, that were not found in the enriched anode (Pisciotta *et al.*, 2012). These results show that during the start-up procedure, the microbial population changes from electrode-reducing to electrode-oxidizing strains. The MEC setup was also used to enrich the H_2-producing biocathode at various cathode potentials either under closed (Jeremiasse *et al.*, 2012; Marshall *et al.*, 2012) or open circuit conditions (Batlle-Vilanova *et al.*, 2014). CO_2 was the sole carbon source added to the cathode compartment (Marshall *et al.*, 2012; Batlle-Vilanova *et al.*, 2014) while acetate enhanced the development of a H_2-producing microbial biocathode (Jeremiasse *et al.*, 2012). Community analysis showed that *Hoeflea* sp. and *Aquiflexum* sp. were present in the H_2-producing biocathode (Batlle-Vilanova *et al.*, 2014) while a MEC biocathode producing acetate was dominated by *Acetobacterium* sp., which are homoacetogens (Marshall *et al.*, 2012). In another report (Croese *et al.*, 2011), *Desulfovibrio* sp. was dominant, and a strain of *Desulfovibrio* from a culture collection was capable of catalysing H_2 production in a MEC (Aulenta *et al.*, 2012). *Eubacterium limosum* and *Desulfovibrio* sp. were dominant in a H_2-producing biocathode (Pisciotta *et al.*, 2012). As in the MEC biocathode, carbon metabolism has not been extensively studied. CO_2 was used as the sole carbon source in most cases, and acetate enhanced the enrichment process as stated above (Jeremiasse *et al.*, 2012). These results suggest that those microorganisms enriched in MEC biocathodes are chemolithotrophs that can grow mixotrophically with acetate.

2.2.2. Hydrogen production in MEC

Global energy consumption is increasing significantly for the last 50 years due to the fast industrial developments and human demands. Conventional fossil fuels are provided to support a major portion of those demands which releasing mass CO_2 to the atmosphere and creating global warming. Inevitably, huge pollutions and environment destructions caused by excessive usage of the fuels endangering and irreversibly damage the balance of the natural ecosystem. Therefore, current research that focuses on the finding of clean and renewable energy is highly motivated and encouraged by the incentive from local authorities. One of these major researches is the production of H_2 as a sustainable clean energy source to replace fossil fuels and alleviate the pollutions. The potential of H_2 has attracted the attention of researchers is due to its

characteristic of high-energy bond that can produce higher power during chemical reaction meanwhile generating water as the only by-product. Serious attention has been paid by researchers over the years on the recovery of the H_2 effectively through various process technology such as fermentation, anaerobic digestion, bio-electrochemistry process, chemical gasification, etc. (Hay *et al.*, 2013; Zhu *et al.*, 2013). However, to recover the energy in the form of H_2 while treating the wastewater simultaneously is a great challenge due to the organic and inorganic matters in the wastewater. In addition to the wastewater complexities, the uncertainty of microbial community and metabolism behaviour also affect the catalysed reaction to form H_2 and treat wastewater (Krieg *et al.*, 2014).

Microbial electrolysis cells (MECs) which had evolved from microbial fuel cells (MFCs) basic reactor was first studied and published by few researchers about 10 years ago (Liu *et al.*, 2005; Rozendal *et al.*, 2006). Since then, many studies have been focused on MEC to seek insight knowledge with the purpose of increasing the efficiency of H_2 evolution and reducing the cost of construction and operation (Rozendal *et al.*, 2008; Villano *et al.*, 2011; Jeremiasse *et al.*, 2012; Fu *et al.*, 2013; Zaybak *et al.*, 2013; Batlle-Vilanova *et al.*, 2014). The researchers believed that MECs are environmental friendly and economically to produce valuable products such as notably H_2 compared to MFCs with present achievement on power output. The production of desired products that can be stored and transported from the site is more attractive than electricity output.

Microbial electrolysis cells are devices capable of producing hydrogen using electrical energy generated by microbial oxidations. The reactions happened when electricity-generating bacteria or electrogens in anode oxidising organic-rich matters in wastewater and transferring utilised electrons to anode. The anode functioned as electron sink to collect the electrons and further transfer them to cathode through an external circuit. Hydrogen is produced in cathode when protons are reduced by the electrons. Hydrogen is produced in cathode when protons are reduced. At standard condition, the potential that generated based on biodegradation of substrate (e.g. acetate to CO_2) in an electrochemically active bioanode (Chapter 1: Reaction 1.1). At the cathode, H^+ ions may be reduced by the external electron from bioanode oxidation and an extra power supply to produce H_2 (Chapter 1: Reaction 1.2). Based on the redox reactions, a minimum applied voltage of 0.13 V is needed to drive the redox reaction in MECs. However, more than 0.5 V is practically applied to the MECs to overcome the overpotentials in activation and mass transport losses. Despite the overpotentials in MECs, the applied voltage is still relatively lower compared to conventional electrolysis (1.2 V) to make the H_2 reductive reaction possible and spontaneous (Rozendal *et al.*, 2006).

Platinum was the first catalyst applied in the cathode with the purpose of catalysing the reductive reaction and decreasing the activation overpotential (Liu *et al.*, 2005; Cheng *et al.*, 2006; Jeremiasse *et al.*, 2010). This expensive precise catalyst had displayed promising results in producing a significant amount of H_2 yet inevitably increased the capital cost of scaling up and operational in wastewater industry. Then, other metal-based catalysts such as stainless steels, nickel and cobalt were employed in the cathode to replace the scarce catalyst. Even though the cost of catalyst reduces significantly, the similar problem still occurred because of the non-sustainable catalysts that easily deactivated by CO and cations such as sulphate and nitrate which are normally found wastewater (Selembo *et al.*, 2009). An alternative approach is the use of microorganisms as a catalyst in the cathode. Rozendal *et al.* (2008) showed that a biocathode functions better than platinum catalyst in hydrogen production in MEC for the first time, and this has been verified by various research groups around the world (Aulenta *et al.*, 2012; Jeremiasse *et al.*, 2012; Pisciotta *et al.*, 2012; Fu *et al.*, 2013; Zaybak *et al.*, 2013; Batlle-Vilanova *et al.*, 2014). Since the anaerobic bacteria have a much higher affinity for electron than any known abiotic cathode catalysts, the performance of a MEC can be improved using the bacteria acting as the cathode catalyst. These electrochemically-active anaerobic bacteria are able to accept electron directly or indirectly from the cathode and use them to reduce protons to hydrogen.

2.2.3. Mechanisms of H_2 production on MEC biocathodes

Anaerobic bacteria can employ various mechanisms to conserve biological energy for growth and produce hydrogen as a by-product. Strictly and facultative anaerobes are known for their ability to use proton as an electron acceptor to produce hydrogen or carbon-based compounds such as methane and acetate (Croese *et al.*, 2011; Lu *et al.*, 2011; Mohanakrishna *et al.*, 2015; van Eerten-Jansen *et al.*, 2015). The reduction of the proton to hydrogen is catalysed by hydrogenase. They can divided in different classes, [*FeFe*], [*FeNi*] and [*FeNiSe*] hydrogenase depend on the anaerobes species (Nonaka *et al.*, 2013; Bagyinka, 2014; Peters *et al.*, 2015). Typically, [*FeFe*] hydrogenase is hydrogen-producing hydrogenase while [*FeNi*] and [*FeNiSe*] hydrogenases can catalyse the reversible reaction between proton and hydrogen. From a chemical point of view, hydrogen production from protons is a simpler reaction. However, microbial conversion of proton to hydrogen is rather a complex reaction and limited by thermodynamic constraints. To promote H_2 formation in cathode, at least -0.41 V of reduction potential is needed to couple the H^+/H_2 reaction at pH 7.0. In the microbial cell, electron transfer

mediators are involved with the following standard potential, E_o' of the couple ferredoxin Fd_{ox}/Fd_{red} is -0.44 V, nicotinamide adenine dinucleotide NAD/NADH -0.32 V and Flavin adenine dinucleotide FAD/$FADH_2$ -0.22 V. As the lower the potential, the higher the energy level of the electron that takes part in the couple reaction of hydrogen formation. Therefore, only the reduced ferredoxin, Fd_{red} is the most suitable candidate to generate higher hydrogen partial pressures when coupling with hydrogen formation. NADH oxidation coupled with hydrogen formation only happen at the lower hydrogen partial pressures than the Fd_{red}. Meanwhile, $FADH_2$ oxidation coupled with hydrogen formation is impossible without extra energy input. The limitation of the energy level is the reason why anaerobic bacteria cannot oxidise organic substrate such as glucose and acetate to CO_2 coupled with hydrogen formation. One of the solutions is to invest additional energy into the reaction to make the coupled reaction feasible and promote hydrogen formation (Rozendal *et al.*, 2007; Zaybak *et al.*, 2013; Batlle-Vilanova *et al.*, 2014).

2.2.4. Electron transfer and energy conservation in MEC biocathodes

There are a few energy conservation mechanisms proposed to explain the electron transfer and the activity of hydrogenase in biocathode MEC. The first mechanism was discussed in a review paper by Geelhoed *et al.* (2010). According to the hypothesis, a proton gradient is developed through the action of membrane-bound energy-converting hydrogenase that translocates proton out of the cytoplasm and consumes proton with the cytoplasm. The hydrogen formed from the reduction of proton and diffused out through the cytoplasm membrane (Figure 2.2 (a)). The second hypothesis was made by Rosenbaum *et al.* (2011). The authors proposed that the cathodic reaction of hydrogen formation is occurred within the periplasm of electrochemically active microbes and not necessarily an energy conservation mechanism (Figure 2.2 (b)). For the sustainable growth of the MEC biocathode, microbes involved in proton reduction should grow under the given conditions. Finally, Keller and Wall (2011) suggested that the energy mechanism in biocathode was similar to hydrogen cycling mechanism in a species of *Desulfovibrio*. The authors used the well-studied mechanism to explain the energy conservation and electron transfer. According to the original hypothesis, electrons from oxidation of lactate as well as pyruvate are used to reduce protons in cytoplasm by the action of a hydrogenase and the hydrogen is diffused to periplasm where another hydrogenase oxidizes it reducing membrane-bound cytochrome c_3. Electrons from this electron carrier are transferred into the cytoplasm to reduce sulphate consuming protons. Because of the redox potential of

pyruvate/lactate ($E^{o'}$ = -0.19 V) too high to be coupled with proton reduction, a modified hydrogen cycling mechanism has been proposed (Keller and Wall, 2011) (Figure 2.2 (c)). According to the modified hypothesis lactate oxidation is coupled to the sulphate reduction while pyruvate reduction is coupled to proton reduction.

Attempts were made to analyse the microbial population employing 16S rDNA analysis method (Croese *et al.*, 2011). They reported that the bacterial population consisted of 46% *Proteobacteria*, 25% *Firmicutes*, 17% *Bacteroidetes*, and 12% related to other phyla. The dominant ribotype belonged to the species *Desulfovibrio vulgaris*. The second major ribotype cluster constituted a novel taxonomic group at the genus level, clustering within uncultured *Firmicutes*. The third cluster belonged to uncultured *Bacteroidetes* and grouped in a taxonomic group from which only clones were described before; most of these clones originated from soil samples. In the paper, the authors showed a type of culture of *Desulfovibrio sp.* can catalyse hydrogen production as the cathode catalyst in MEC. The authors discussed the possible function of the bacterium with high hydrogenase activity. A type culture of *Desulfovibrio paquesii* was also reported can catalyse hydrogen production in a MEC (Aulenta *et al.*, 2012). It is believed that *Desulfovibrio sp.* may conserve energy through the reduction of proton using available and high-energy electron (< -0.41V) from cathode in similar way to the hydrogen cycling mechanism in Figure 2.3. Protons are reduced by hydrogenase that located in both periplasm and cytoplasm. Hydrogen produced from the reduction of protons is then diffused out across cytoplasmic membrane resulting in a proton gradient and proton motive force across the cytoplasmic membrane. The proton motive force is used to create ATP to support the bacteria growth from the translocation of the proton through ATPase.

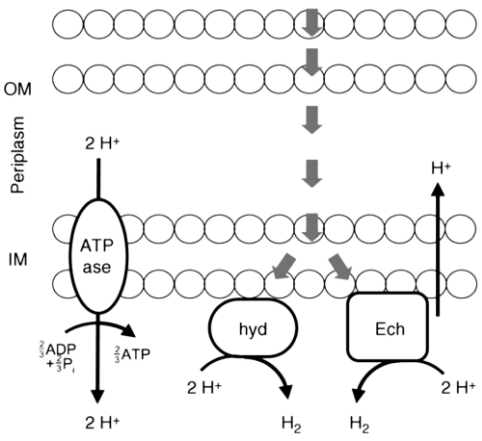

(a)

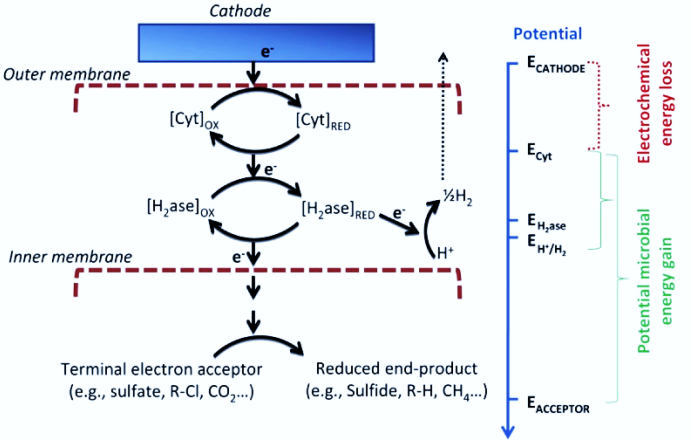

(b)

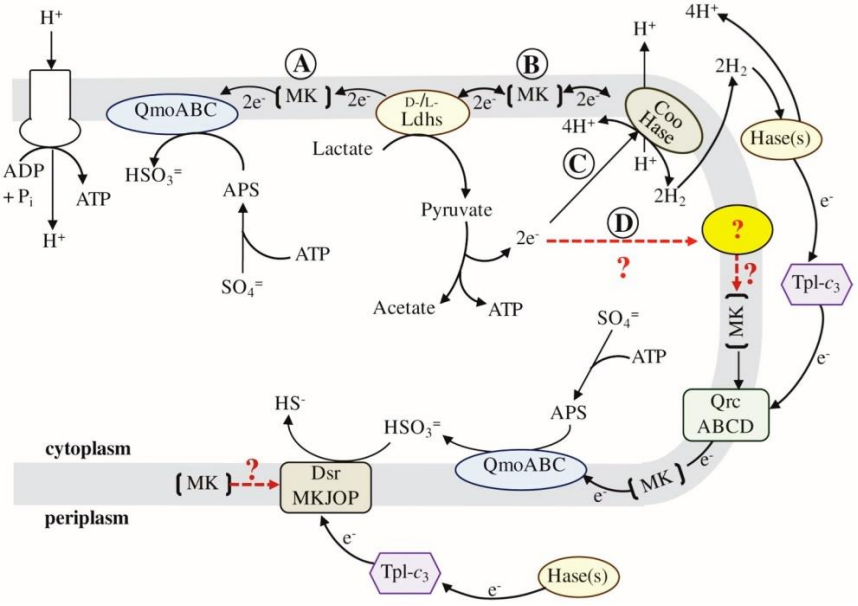

(c)

Figure 2.2 Geelhoed *et al.* (2010) suggested that the couple of hydrogen production and energy conservation mechanism are coupled to proton translocation in a microbial cell of the biocathode. (b) Electron transfer mechanism in a MEC biocathode proposed by Rosenbaum *et al.* (2011). (c) Hypothesised energy conservation used by Keller and Wall (2011) based on the hydrogen cycling mechanism in *Desulfovibrio* sp.

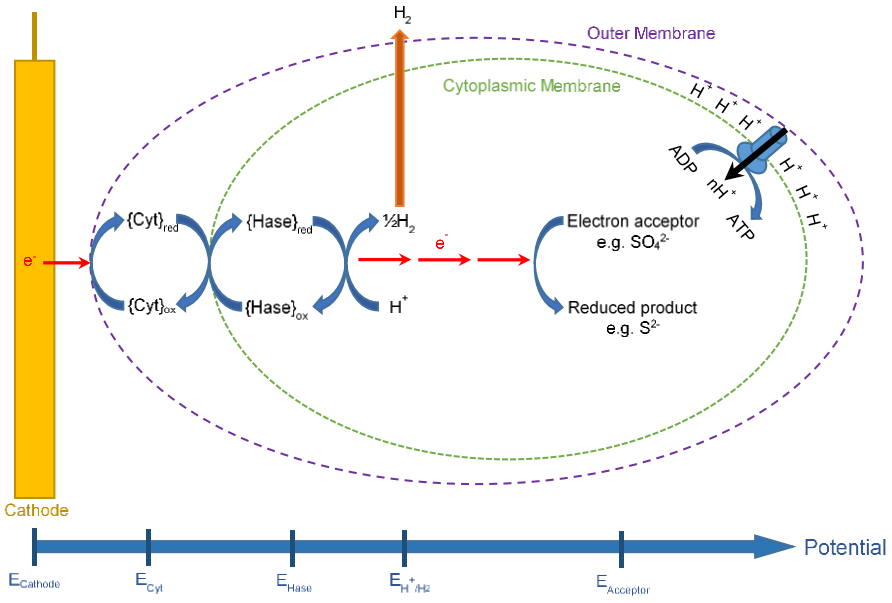

Figure 2.3 Proposed energy conservation mechanism used by *Desulfovibrio* sp. during H^+ reduction in a MEC biocathode.

2.3 Bioelectrochemical CO_2 reduction

Anaerobic biocathode utilises a complex mixture of microbial species to perform reduction reactions aiming to product specific products (e.g. hydrogen and acetate). Production of these products no only depended on the microbial community but also the cathode potential and applied voltage. In standard condition, reduction potential of hydrogen is -0.41V (Chapter 1: Reaction 1.1) while acetate is -0.28V (Chapter 1: Reaction 1.2). As hydrogen production required lower potential than acetate or other compounds (e.g. methane and ethanol), other non-hydrogen products may have produced along with hydrogen evolution. Even though microbial electrolysis cell and microbial electrosynthesis cell are focused on different compound production depended on the applied voltage and cathode potential, both operating principle and conditions are similar. For the reason, this quick review is to understand the principle of biocathode in CO_2 reduction and how it may affect hydrogen production in MEC.

2.3.1. CO_2-reducing biocathode and microbial electrosynthesis cell (MSC)

As global greenhouse effect over the past decades is related to the unrestrained release of carbon dioxide (CO_2) into the atmosphere, one of the solution is to limit its emissions and capture/reuse it before it reaches the atmosphere. Inorganic carbon in the form of CO_2 is a useful resource for microbial ecosystem. Microbial electrosynthesis cells (MSC) are one of the BES that can use biocathodes to generate useful products such as acetate, hydrogen and methane from CO_2 reduction (Mohanakrishna *et al.*, 2015; van Eerten-Jansen *et al.*, 2015; LaBelle and May, 2017). The process of CO_2 reduction in biocathode MSC is commonly related to a metabolic process called acetogenesis and methanogenesis. Acetogenic bacteria or acetogens are anaerobic organisms able to assimilate CO_2 or CO via Wood-Ljungdahl pathway. The pathway is also known as acetyl-CoA pathway or carbonate respiration (Kracke *et al.*, 2015). *Clostridium* sp. and *Acetobacterium sp*. are two main species involved in the pathway and usually used as models to explain the CO_2 reduction process especially acetate production in biocathode (LaBelle and May, 2017). Meanwhile methanogenic bacteria and archaea or methanogens can produce methane via direct electron transfer or indirectly via hydrogen or acetate oxidations. It involved two major pathways: CO_2-reduction and aceticlastic methane-producing pathways (Ferry, 2011). Hydrogen is known acts as intermediate to produce methane under CO_2-reduction pathway (Wagner *et al.*, 2009; van Eerten-Jansen *et al.*, 2015). Under electrochemical condition, hydrogen is generated at low potentials and used by methanogens to produce

methane with available CO_2 in their growing environments (Villano *et al.*, 2010). Besides, methane can also be produced via different pathway where acetate or formate is available (Madigan *et al.*, 2014). However, CO_2 is produced as a by-product rather than being consumed in this pathway.

Up to date, most of the reduction processes involved in biocathodes are related with the reduction of CO_2 and proton into desired products such as CH_4, H_2, acetate, formate, ethanol, butanol, etc. (Zaybak *et al.*, 2013; Batlle-Vilanova *et al.*, 2014; Raes *et al.*, 2017; Vassilev *et al.*, 2017; Jourdin *et al.*, 2018). Theoretically, the reduction potentials for these products range from -0.24 to -0.41 V vs. SHE. For example, HCO_3^-/CH_4 (E_o' = -0.24 V; $8e^-$); H^+/H_2 (E_o' = -0.41V; $2e^-$); HCO_3^-/CH_3COOH (E_o' = -0.28V; $8e^-$); HCO_3^-/C_2H_5OH (E_o' = -0.31 V; $12e^-$); $HCO_3^-/HCOOH$ (E_o' = - 0.41V; $2e^-$) in standard conditions of 1 M reactant in water pH 7.0 at 1 atm and 25°C (Rabaey and Rozendal, 2010; Choi and Sang, 2016; Zhen *et al.*, 2017). In real conditions, parameters like pH, conductivity and temperature could further increase the potential threshold required. In the case of protons reduction to hydrogen, the potential varies between 0.00 to -0.83 V depending on the solution pH (H^+/H_2 acidic: 0.00V; neutral: -0.41 V; alkaline: -0.83 V) causing the increase of the energy input required. Both Rozendal *et al.* (2008) and Jeremiasse *et al.* (2010) regulated pH at neutral in their hydrogen-producing biocathode under a pH controlled system and managed to reduce proton reduction potential to at least -0.5 V which was determined by chronoamperometry method. Without a stable neutral pH control, the reduction potential could move to more negative than -0.5 V (up to -0.8 V or more) proportional to the shift of catholyte pH in which may require extra input of external power supply (Aulenta *et al.*, 2012; Batlle-Vilanova *et al.*, 2014; Lim *et al.*, 2017). Apart from the proton reduction, CO_2 reduction is also affected by pH when the value is higher than 7.0. However, the minimum reduction potential is slightly lower than the hydrogen evolution potential which lay between -0.5 and -0.6 V (Bajracharya *et al.*, 2017b; Jourdin *et al.*, 2018).

2.3.2. Chain elongation to high-value products in MSC

Production of organic compounds in MSC is generally considered more complex than simple organic reactions as multistep reactions may preferably be accomplished by microbial cathodes. Even though simpler organic compounds such as formate or acetate is desired and easier to obtain at the end of the cathodic reactions, it always ends up in producing various organic compounds (Zaybak *et al.*, 2013; Bajracharya *et al.*, 2017b; Wenzel *et al.*, 2018). The diversity of the microbial community and the complexity of its metabolic pathways have made the

production of specific compounds difficult to accomplish (Modestra and Mohan, 2017). In the case of acetate production, either the hydrogen is produced abiotically first and then consumed by acetogens to produce acetate or direct acetate production is still debatable. Nevertheless, both pathways involve the reduction of proton which might have related to hydrogen production.

Very recently it has been demonstrated, on the example of obtaining high valuable organic compounds through chain elongation process, simpler organic compounds which were formed initially can be used as carbon backbones gone through further reductive 'upgrading' reactions to form longer organic chains such as butyrate and caproate (Raes *et al.*, 2017; Jourdin *et al.*, 2018). Nevertheless, the formation of longer chain compounds such as caproate could only be produced under high applied current (-175 A/m^2) and higher concentration of short chain compounds (9.2 g acetate/L/day). The authors applied higher current in their system may decrease the biocathode potential to the lowest point which abiotic hydrogen is actively generated. In turn, the accumulated hydrogen under a low potential condition in biocathode inducing the production of acetate and longer chain products.

2.3.3. Future outlook of bioelectrochemical CO_2 reduction process

So far, the electrochemical CO_2 reduction process of producing biofuels is demonstrated in small scale reactors under laboratory-controlled conditions. The process is proven a viable alternative to produce renewable biofuels such as volatile fatty acids and alcohols to replace conventional fossil fuel in the future. Low carbon compounds (C1-C2) like acetate and formate are easier and simpler to form and mostly found under the CO_2 reduction process (Mohanakrishna *et al.*, 2015; LaBelle and May, 2017). However, higher carbon compounds (C3-C6) is formed in conjugation with the low carbon compounds (Raes *et al.*, 2017; Jourdin *et al.*, 2018; Wenzel *et al.*, 2018). The main challenges in the large scale bioelectrochemical CO_2 reduction to produce valuable biofuels is the cost and production efficiency. The process requires a large amount of electrical energy input and long operation time to accumulate the products up to a certain concentration. For example, acetate production required weeks of accumulation and reaction time under specific applied potential or current. (Mohanakrishna *et al.*, 2015; Bajracharya *et al.*, 2017b; LaBelle and May, 2017; Wenzel *et al.*, 2018). In other words, to replace the current conventional fuels, the process should be cheaper which could be an arduous effort to meet the market requirement in term of quantity. As a result, strategies to increase the productivity of the process should be focused to make the technology feasible and applicable in the future.

2.4 Utilisation of bioanode and biocathode in single BES

Bioelectrochemical system (BES) fully catalysed by microorganisms is not uncommon reactor setup in this research especially in the field of MFC (Milner *et al.*, 2016; Yuan *et al.*, 2016). In MEC or MSC, however, most of the study has been focused on half-cell experiments to have better control on the abiotic counter electrode rather than using living microorganisms. There is a lack of insight information about how both bioanode and biocathode interacted in one single system. In this review, the benefit, problems and possibilities of large scale application that may face in using solely bioelectrodes in a MEC or MSC system will be discussed.

2.4.1. Advantages of using of both bioanode and biocathode in BES

The usage of bioelectrodes is attractive due to a few advantages over their abiotic counterparts. Firstly, the bioelectrodes consist of living microorganisms which attached on the surface of a supporting electrode (Logan *et al.*, 2006; Torres *et al.*, 2009). This means the organisms are worked as biocatalysts and can be self-generated as long as substrate is continuously supplied to the bioelectrode (Lee and Rittmann, 2010; Rahimnejad *et al.*, 2012; Schneider *et al.*, 2016). Meanwhile, abiotic electrode uses non-viable catalysts which cannot be generated by itself and could be worn out and required replacement after long term operation (Kundu *et al.*, 2013). Secondly, the biocatalysts based on microorganisms are more robust to surrounding environments and resisted to sulphite or organic poisoning compared to abiotic catalysts (Kim *et al.*, 2015). Thirdly, the biocatalysts can be obtained from natural environments which is less expensive than abiotic electrodes especially when precise metals such as platinum are used as catalysts (Kim *et al.*, 2004; Mohanakrishna *et al.*, 2015; Patil *et al.*, 2015; Modestra and Mohan, 2017). Lastly, the bioelectrodes are sensitive to electrolytes in a highly specific manner (Schneider *et al.*, 2016). Therefore, it is also ideal for environmental applications like pre-screening specific wastewaters whether it is suitable for further BES process since the microbes have the ability to sense both the presence and toxicity of chemical species.

Regardless, comprehensive information of bioelectrodes interaction in BES is limited especially between electricity-generating bioanode and product-inducing biocathode. To understand the interaction, microbiology knowledge is important and system management is required for the effective scale-up process. Ineffectual biocathode performance has been reported when coupled with electricity-generating bioanode showing the necessity of understanding each electrodes' requirements (Jeremiasse *et al.*, 2010). It involved the

investigations of electrode reactions, electro-kinetic, reactants, and external energy input between the anode and cathode.

2.4.2. Bottlenecks of using both bioanode and biocathode in a single MEC or MSC

As mentioned in section 2.4.1, performance and reaction efficiency in BES fully catalysed by microorganisms are depended on its bioelectrode interactions. Ideally, at least 0.13 V extra voltage is required between the acetate-oxidising bioanode and hydrogen-producing biocathode to drive a minimum oxidation-reduction process in a BES. In spite of that, applied voltages higher than 0.5 V was used in most studies considering overpotentials caused by the system and energy losses due to microorganism metabolic activities (Geelhoed *et al.*, 2010; Jeremiasse *et al.*, 2010). Various cell configurations have been tested and used in laboratory for biocathode-driven processes, especially hydrogen production. The technology has advanced from half-cell to full cell configuration, two chambers to single chamber, batch to continuous tubular mode, and laboratory to large scale (Jafary *et al.*, 2015; Zhen *et al.*, 2017). Studies aim in reducing overpotentials and cutting down operation cost and development time (Escapa *et al.*, 2016; Kadier *et al.*, 2016; Zhen *et al.*, 2017). Nonetheless some questions still remain unanswered in these systems including the optimum operational environments for bioelectrodes (e.g. pH, conductivity, cell voltage), time of growth for both bioanode and biocathode (e.g. 1 vs. 4 weeks), optimum reducing power or potential required by biocathodes to produce certain products (e.g. HCO_3^-/CH_3COO^- E_o' = -0.28V vs. H^+/H^2 E_o' = -0.41V) when coupled with bioanode for wastewater treatment and the most important how the bioanode and biocathode interact in a single cell system (e.g. current response and how biofilms evolve) even during the beginning of the enrichment? A microbial electrolysis cell fully catalysed by microorganisms for the purpose of hydrogen production and wastewater treatment was demonstrated by Jeremiasse *et al.* (2010) for the first time. Even the current density was increase during enrichment and maintained at significant level (1.9 - 3.3 A/m^2) but still the whole system suffered from the low hydrogen recovery in cathode (17 - 21%) at cathode potential of -0.7 V. In additional to the problem, the authors also addressed other issues in the system included longer biocathode start-up time compared to usual platinised cathode, slow deteriorating effect of calcium phosphate precipitation under low reduction potential and methane production after long term operation. However, no further experiment was conducted to study the issues. Meanwhile, Kumar *et al.* (2017) discussed the efficiency of biocathode hydrogen production through a start-up viewpoint. In the review, they surveyed the main influencing factors and methods from literature included

the selection of inoculum, bioelectrode enrichments and acclimations, operating conditions and cell architectures. They concluded that proper start-up factors and methods are the keys for long-term viability and effectiveness of a MEC. In fact, the usage of microorganisms as biocatalyst in the system can reduce the cost of investment because they can multiply as long as the environment is favoured for growth.

Similar to the MEC system mentioned above, Coma *et al.* (2013) and Luo *et al.* (2014), in different studies, showed that biocathode for the purpose of sulphate removal can be enriched and acclimatised simultaneously with an electricity-generating bioanode in a single MEC. In Coma *et al.* (2013)'s results, the interaction of the bioelectrodes and their potentials and electrolyte evolvements based on applied voltage were presented. They also found the anodic potentials were gradually increased throughout the study with no substrate oxidation in the anode. The phenomena raised the suspicion of weak bioanode performance or abiotic instead of biotic reaction has occurred. In addition to Coma *et al.* (2013)'s work, Luo *et al.* (2014) improved the system by imposing pH control and feeding mode in the cathode. Even though the sulphate removal increased, they did not study the involvement or role of bioanode to the whole system. Besides, both studies focused on sulphate removal rather than hydrogen production in the cathode. Information regarding the interactions between biocathode and bioanode is important. Meanwhile MSC system and its reactions is highly closed to the MEC except the cathode reductive reaction is meant to produce organic compounds or reductive carbon matters such as acetate and formate instead of generating hydrogen. In comparison to the MEC, there is no study showing a MSC fully catalysed by microorganisms or use bioanode as the counter electrode in to support the biocathode CO_2 reduction reaction.

2.4.3. Scale up of CO_2- or/and H^+-reducing biocathode(s) with an electricity-generating bioanode

Combining a CO_2- and H^+-reducing biocathode with an electron-generating bioanode into a BES, not only reduces the requirement of external power input for the generation of valuable bioproducts but also acts as a potential technology for wastewater treatment (Jeremiasse *et al.*, 2010; Lim *et al.*, 2017). MSC technologies with combined bioanode and biocathode are attractive due to the sustainability and low-cost maintenance associated with the use of microorganisms as biocatalysts (Rabaey and Rozendal, 2010; Choi and Sang, 2016). It makes the technologies become feasible for scale up and real applications while offset operation costs (Escapa *et al.*, 2016; Kadier *et al.*, 2016). However, it is hard to maintain the scale-up system

without elucidated knowledge about how these bioelectrodes evolved and reacted to each other to accomplish the desired treatment or produce specific products in a single cell.

In most MEC system, anode and cathode are divided by a separator which might increase overall internal resistance and complexity for scaling up. Nevertheless, there were few studies operated both electrodes in a same solution without a separator which is good for scale-up application. The system was reported providing better ion transport between anode and cathode while reducing overall internal resistance as overpotentials decreased (Rozendal *et al.*, 2007; Call and Logan, 2008; Wagner *et al.*, 2009; Wang *et al.*, 2010; Foad Marashi and Kariminia, 2015). However, cross contamination of reactant and exposure of products to opposite electrodes could reduce electricity generation or hydrogen and bioproduct recoveries.

Additionally, knowledge of electron transport is important in designing large scale BES. However, controlling electron transfer within microbial cells is not easy due to natural biotic activity except providing a suitable transfer condition such as pH and temperature (Kracke *et al.*, 2015). A controllable parameter of electron transfer is considered between outer microbial membrane and electrode or within extracellular environments (Rosenbaum *et al.*, 2011). Wide electrode gap and large surface area can also undermine the function of the bioelectrodes. More information and careful design are required to study the limitations related to the increase in reactor size which is not as simpler as proportionally scale up from original laboratory scale (Ewing *et al.*, 2014; Santoro *et al.*, 2017). This is because potential energy is consumed during the transfer of the electrons to its final destination throughout the wide surface area. (Li *et al.*, 2011; Rivera *et al.*, 2017).

2.5 Conclusion

From the literature survey, it is found that electricity-generating bioanode is an important component to BES functioning as biocatalysts to recover potential energy from treating organic matters in wastewaters. Meanwhile, hydrogen-producing biocathode is attracting due to its self-sustainable and robustness in producing hydrogen from wastewaters. A study of using and combining both bioelectrodes in a single MEC has been done before, however, there is still a lack of information of how these bioelectrodes can be perfectly integrated. In order to maintain their oxidation and reduction activities, they could only operate at certain conditions and required specific environments. These limitations have created a bottleneck to the usage of bioelectrodes the MEC, thus, understanding the limitations and optimising them in a single

MEC is essential. The review not only has given the necessary idea of integrating and optimising these bioelectrodes in one system but also requires control strategies to improve the MEC performance in terms of hydrogen production and wastewater treatment. During the review, it is also discovered that MSC posted the same functionality to MEC when CO_2 is available in cathode under less minimum potential condition. There is still lack of information on the microbial electrosynthesis cell deploying both bioanode and biocathode in a single system apart from half-cell experiments.

Chapter 3. Materials and methods

3.0. Chapter summary

The purpose of this study is to develop self-sustained biocatalyst and deploy them in a single MEC. The biocatalysed-electrodes, both bioanode and biocathode, was studied separately at the beginning before integrating them into the MEC in the to treat wastewater (anode part) and produce hydrogen (cathode part). Once the bioelectrode was successfully integrated, optimisation process and strategies were aimed in order to upgrade the system performance. Step-by-step methods and procedures were designed to pursue systematic examinations in this study. This chapter is focused on the materials and methods used in (1) preparing certain experiments, (2) operating or maintaining bioelectrochemical cells, (3) conducting desired tests and (4) analysing collected samples and calculating energy efficiencies. To start with, cell designs are introduced with the detail of the materials, components, size, volume and other necessary information used to build complete and functional cells. The composition of media or electrolytes used in each chamber and experiment where a specific solution is needed is clarified. Start-up procedures are mentioned and explained why certain operating conditions are required. This includes the general equipment used to collect and record specific data like electrode potential and cell current. General electrochemical methods are also mentioned in this chapter. They are used as fundamental techniques to check the cell performances practically bioelectrode behaviours and bioelectrochemical properties. Besides, analytical methods dedicated to gas and liquid sample quantifications are described. Those analytical results together with the electrochemical outcomes serve as principal information to calculate overall energy efficiency.

3.1. Cell design and experimental setup

3.1.1 Two- and three-chamber bioelectrochemical cells

Two-chamber microbial fuel cells (MFCs) were constructed from two pieces of polyacrylic blocks size 7 cm (length) × 7 cm (wide) × 2 cm (depth). The polyacrylic blocks were fabricated with a 5 cm (length) × 5 cm (wide) × 1 cm (depth) compartment with a final operational volume of 25 mL. Two ports with thread size 1/8" NPT were drilled at each rear side of the plate in order to fit a straight male hose coupling fitting (RS Components, UK). The ports were served as electrolyte inlet and outlet. Meanwhile, on the top of the plate, a same hole was drilled to fit a pneumatic straight threaded-to-tube adapter (RS Components, UK) to locate Ag/AgCl reference electrode (RE-5B, BASi, USA). Plain carbon felt (RVG-2000, Mersen, USA) was trimmed into a size of 5 cm × 5 cm × 0.3 cm as an anode. The same size of carbon felt was used as a cathode with additional 0.5mg Pt/cm^2 coated on the projected surface facing anode. A small piece of a titanium plate (Ti-shop.com, William Gregor Ltd, UK) was used to connect the electrodes to an external circuit. Once the electrodes were placed inside the compartments, both identical blocks were clamped together with four pieces of M5 screws (RS Components, UK) at its diagonal. Cation exchange membrane (CMI-7000, Membrane International Inc., USA) was placed between these compartments and sealed by two pieces of silicone gaskets (SILEX Ltd, UK). Figure 3.1 (a) shown the schematic of the MFC and a lab-scale MFC.

Two-chamber microbial electrolysis cells (2cMECs) were set up as same as MFCs mentioned above except both anode and cathode were plain carbon felts. In addition, on the top of the cathodic chamber, another 1/8" NPT port was prepared to fit a second pneumatic straight threaded-to-tube adapter. A custom-made 80 mL cylinder (Ø 30 mm × L 150 mm) was used as gas collector attached directly to the top of cathode compartment through the pneumatic adaptor. A septum was sealed on the top of the gas collector for gas sampling purpose. A side outlet was extended near the bottom end of the gas collector for waste discharge and pressure balancing purposes when hydrogen gas was produced in the cathode chamber. Both the cathode chamber and gas collector were totally filled with catholyte at the beginning of each experiment. Hydrogen produced from cathode was captured on the top of the gas collector while used catholyte was discharged through the side outlet. Figure 3.1 (b) displays the schematic of the 2cMEC and a lab-scale 2cMEC where the structure of the gas collector is clearly shown.

Three-chamber microbial electrolysis cells (3cMECs) were constructed from polyacrylic sheet and Nylon 6 rod (RS Components, UK). Anodic and cathodic chambers were

made from the rod with an internal diameter of 4 cm and length of 2 cm. Each cylinder had a working volume of 50 mL. These chambers were fixed with inlet and outlet fittings to facilitate the medium or gas replacement. The purpose of the gas chamber was to contain CO_2 or other CO_2 based gas mixtures. Cation exchange membrane (CMI-7000, Membrane International Inc, USA) was used to separate each chamber. Carbon cloth (HCP330, Hesen, China) was used as anode and cathode. Small pieces of a thin titanium plate (Titanium Grade 1 Sheet 0.5mm Thick, Ti-Shop.com, William Gregor Ltd, UK) were used as current collectors. Reference electrodes (RE-5B Ag/AgCl, BASi, USA) were installed into the anode and cathode chamber for potential monitoring purpose. A same size of the gas collector with the same purpose was connected on the top of cathode chamber as described in the previous paragraph for the 2cMEC system. A gas reservoir was also installed on the top of the gas compartment using water displacement method. The function of the reservoir is to balance the gas compartment with atmospheric pressure and determine the total volume of gas diffused into catholyte. A sampling port was also installed next to the gas reservoir in order to collect gas samples for gas composition analysis. Figure 3.1 (c) shown the schematic of the 3cMEC and a lab-scale 3cMEC where the sampling port, gas reservoir and collector were clearly displayed. All reactors described above were operated under constant temperature at 26.5 ± 2.5 °C.

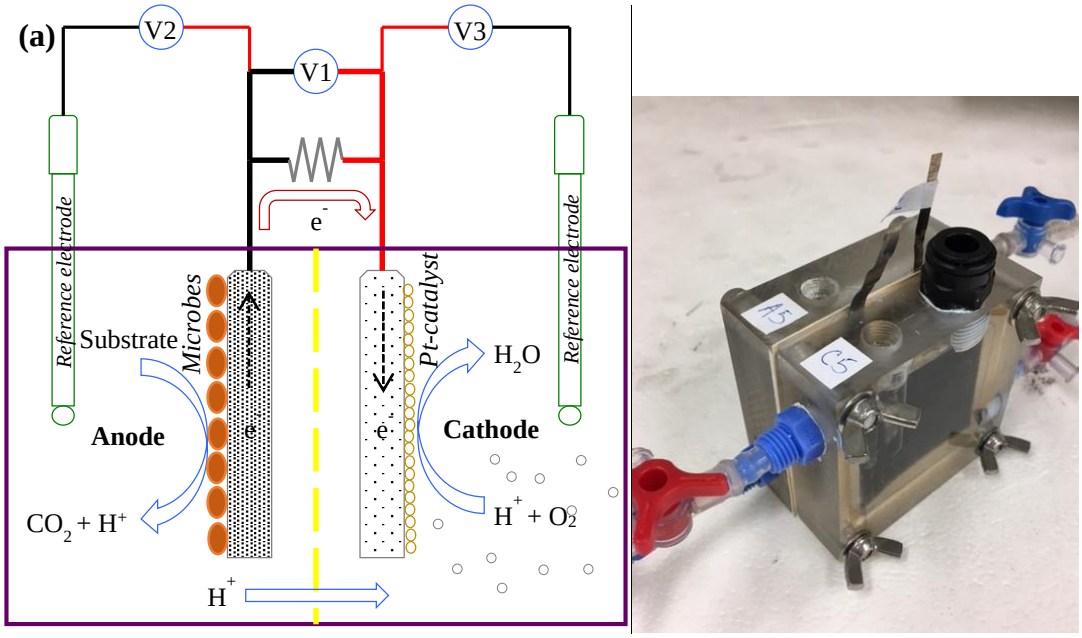

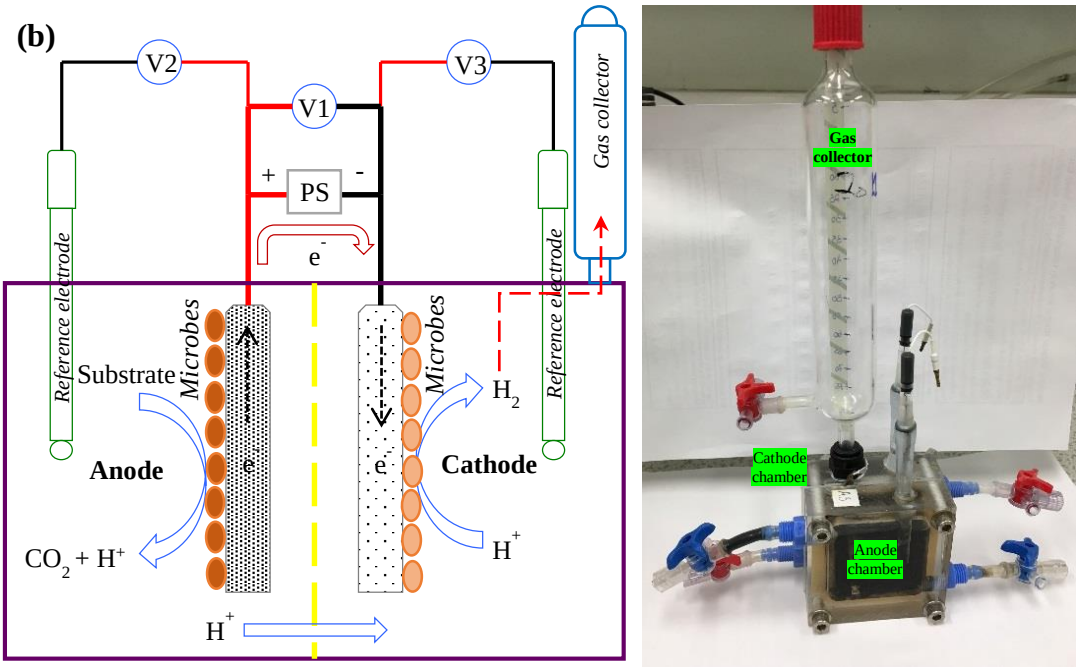

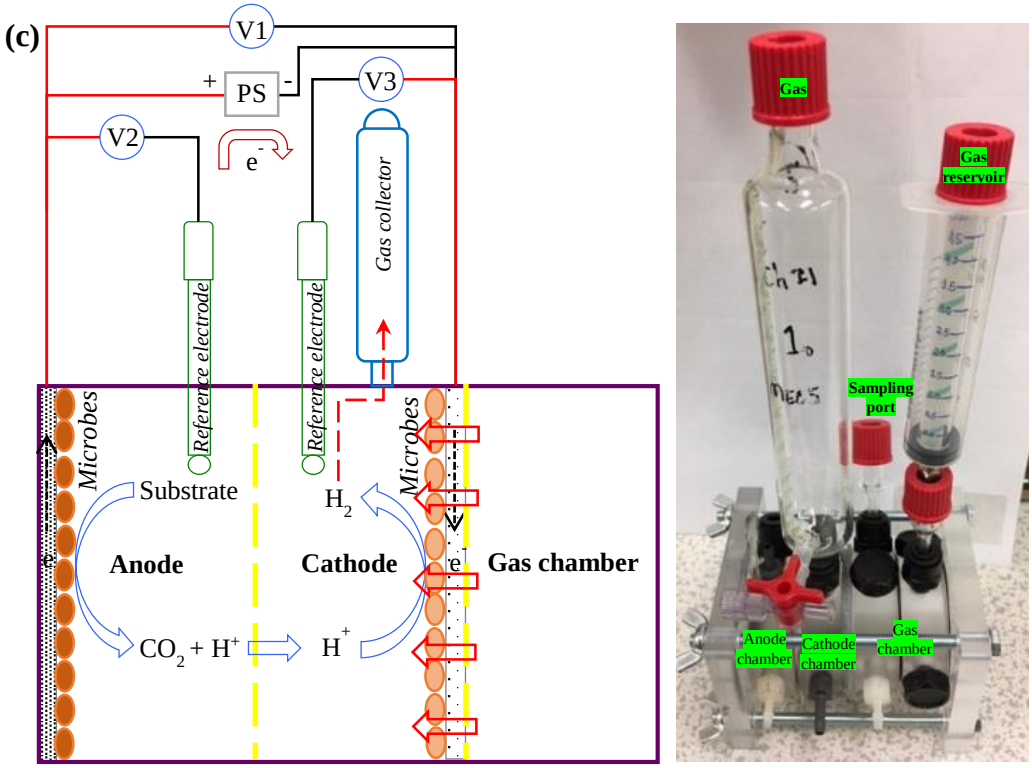

(c)

Figure 3.1 Schematic (on the left) and lab-scale bioelectrochemical system (BES) (on the right): (a) microbial fuel cell (MFC), (b) microbial electrolysis cell (MEC) and (c) three-chamber microbial electrolysis cell (3cMEC)

3.1.2 Media preparation

Anodic medium was prepared mainly based on Atlas (2010) with modification. The composition of anodic medium consisted (in g/L): CH_3COONa 0.82, NH_4Cl 0.54, $NaH_2PO_4 \cdot 2H_2O$ 3.30, $Na_2HPO_4 \cdot 2H_2O$ 5.14, Wolfe's vitamin and mineral solution 10mL/L (Lim *et al.*, 2017). First, the buffer solution contained $NaH_2PO_4 \cdot 2H_2O$ and $Na_2HPO_4 \cdot 2H_2O$ were prepared and autoclaved for 20 minutes at 15psi pressure 121˚C. All components were dissolved in deionised water and added to the autoclaved buffer by passing through a 0.2 μm polyethersulfone (PES) syringe filter. The vitamin solution consisted (in g/L): pyridoxine·HCl 0.01, *p*-aminobenzoic acid 0.005, lipoic acid 0.005, nicotinic acid 0.005, riboflavin 0.005, thiamine·HCl 0.005, calcium DL-pantothenate 0.005, biotin 0.002, folic acid 0.002 and vitamin B_{12} 0.0001. The solution was prepared by mixing all the components to deionised water and brought the volume to 1 L. After all the components were completely dissolved, the solution was vacuum filtered through a 5.0μm mixed cellulose ester membrane to eliminate microbes and undissolved particles prior store in refrigerator at +4˚C. Meanwhile, the mineral solution consisted (in g/L): $MgSO_4 \cdot 7H_2O$ 3.00, nitrilotriacetic acid 1.50, NaCl 1.00, $MnSO_4 \cdot H_2O$ 0.50, $CaCl_2$ 0.10, $CoCl_2 \cdot 6H_2O$ 0.10, $FeSO_4 \cdot 6H_2O$ 0.10, $ZnSO_4 \cdot 7H_2O$, 0.10, $AlK(SO_4)_2 \cdot 12H_2O$ 0.10, $CuSO_4 \cdot 5H_2O$ 0.10, H_3BO_3 0.10, $Na_2MoO_4 \cdot 2H_2O$ 0.10, Na_2SeO_3 0.10, $NaWO_4 \cdot 2H_2O$ 0.10 and $NiCl_2 \cdot 6H_2O$ 0.10. The nitrilotriacetic acid was first diluted in 0.5 L deionised water and the pH was adjusted to 6.5 with 1M KOH. After the acid was completely dissolved in the solution, the remaining components were added and the pH was once again adjusted to 6.8 before brought the final volume to 1 L. Finally, the solution was vacuum filtered through a 5.0μm mixed cellulose ester membrane prior store in refrigerator at +4˚C. This medium was mainly used in all BES contained bioanode unless stated otherwise.

Cathodic solution that used in Pt-coated cathode at pH 7.0 consisted buffer made from (in g/L): $NaH_2PO_4 \cdot 2H_2O$ 3.30, $Na_2HPO_4 \cdot 2H_2O$ 5.14 unless stated otherwise.

For cathodic medium, the formula used by Rozendal *et al.* (2008) was modified and consisted (in g/L): $KHCO_3$ 1.00, NH_4Cl 0.27, $MgSO_4 \cdot 7H_2O$ 0.10, $CaCl_2 \cdot 2H_2O$ 0.01, $Na_2S \cdot 9H_2O$ 1.0, $NaH_2PO_4 \cdot 2H_2O$ 3.30, $Na_2HPO_4 \cdot 2H_2O$ 5.14 and trace element mixture 1 mL/L. First, the $NaH_2PO_4 \cdot 2H_2O$, $Na_2HPO_4 \cdot 2H_2O$ and NH_4Cl were added into deionised water. Secondly, the $MgSO_4 \cdot 7H_2O$ and $CaCl_2 \cdot 2H_2O$ were added into the main solution once at a time after pre-dissolve them in a separate container and then the trace element mixture. The solution was then purged with N_2 for 10 min before adding $Na_2S \cdot 9H_2O$ and brought the final volume to 1L. The solution was stored under N_2 condition and kept in refrigerator at +4˚C prior use. The

trace element mixture consisted (in g/L): $FeCl_2 \cdot 4H_2O$ 2.00, H_3BO_3 0.05, $ZnCl_2$ 0.05, $CuCl_2 \cdot 2H2O$ 0.05, $MnCl_2 \cdot 4H_2O$ 0.05, $(NH_4)_6Mo_7O_{24} \cdot 4H_2O$ 0.05, $AlCl_3$ 0.05, $CoCl_2 \cdot 6H2O$ 0.05, $NiCl_2$ 0.05 and EDTA 0.50. First, the EDTA was dissolved in deionised water by adjusted the pH to 7.0 with 1M KOH. Once the EDTA was completely dissolved, all remaining components were added and mixed thoroughly before adjusting the pH again to 7.0. The mixture was vacuum filtered through a 5.0μm mixed cellulose ester membrane prior store in refrigerator at +4˚C. This medium was mainly used in two-chamber MECs unless stated otherwise.

For three-chamber MEC, CO_2 was used as a carbon source by the means of diffusion into catholyte. Therefore, the medium composition remained the same without adding $KHCO_3$ or stated otherwise.

3.1.3 Start-up and operational conditions

Inoculums were obtained from the effluent of an anode in a parent MFC and a control (cultivated without connecting an external circuit to cathode) which has been operated over a year (Spurr, 2016). Both cells were fed with glucose and glutamic acid as carbon sources and ammonium chloride as nitrogen source. Those electrodes had been identified as being colonised by dominating microorganism *Geobacter* sp. and *Desulfovibrio* sp., respectively (Spurr, 2016). In a two-chamber MFC using Pt-coated cathode, the inoculum was premixed with the anodic medium in a ratio of 1:1 v/v% and then purged with pure N_2 for 10 minutes before injecting it to the anode chamber. Meanwhile, the cathode chamber was filled with phosphate buffer solution at pH 7.0. After both chambers were filled with medium and buffer solution, the MFC was connected to a computer through a data logger (ADC-16, Pico Technology, UK). The half-cell and cell potentials were recorded via a controlling software provided by the manufacturer. The MFC was left for 24 hours in open circuit condition before the circuit was closed with a 25 Ω resistor. This is to create a lag time for microbes to integrate with new anode when they are introduced into a new environment and to ensure monitored condition such as potentials are corrected prior anode and cathode are connected. Alternatives to the usage of a resistor, a potentiostat (Quad Potentiostat, Whistonbrook Technologies, UK) was also used to set a specific potential on the anode to facilitate electrochemically-active microbes' growth. A common potential of +0.2 V vs. standard hydrogen electrode (SHE) was set at the anode during the enrichment process unless stated otherwise. After 48 hours, a peristaltic pump (120S, Watson-Marlow, UK) was activated to feed the anode medium continuously into anode

chamber while cathode solution was recycled from a 2 L reservoir where the solution was continuously saturated with air from an aquarium air pump.

There are two enrichment processes focused on enriching biocathode only and biocathode with bioanode using the reactors mentioned in section 3.1.1. For biocathode, a two-chamber MFC was converted to MEC by fixing the potential of the plain carbon felt working electrode (worked as anode in MFC) to -0.7V vs. SHE with a potentiostat and Pt-coated carbon felt (worked as cathode in MFC) as counter electrode. For biocathode with bioanode, bioanode was first enriched by coupled with Pt-coated cathode. Once the reactor produced a stable current, the Pt-coated cathode was replaced with a new plain graphite felt to start the enrichment of biocathode. All the enrichments were done by fixing the specific potential to the working electrode (anode or cathode). The strategy was performed for obtaining bioanode first and then biocathode in order to obtain both bioelectrochemically active electrodes in a MEC. A four-channel potentiostat (Quad Potentiostat, Whistonbrook Technologies, UK) was used in both enrichment processes. A fixed potential of +0.2V vs. standard hydrogen electrode (SHE) was first applied on the anode during bioanode enrichment before changing the fixed potential to -0.7V vs. SHE on biocathode while biocathode enrichment took place. At the initial stage of biocathode enrichment, the applied potential +0.2V vs. SHE was still fixed on the bioanode in order to protect the bioanode from losing its ability to produce a stable current. Once the Pt-coated cathodes were changed with the plain graphite felts, the cathodic chambers were injected with 25 mL inoculum 1:1 in the ratio as mentioned above. Hydrogen grade 99.99% was fed into cathode chamber once a day and recycled via a glass tube's headspace to encourage the growth of hydrogen-oxidising microorganisms for at least a week before switching the fixed potential from anode operation to cathodic operation (Rozendal *et al.*, 2008). A 40-channel data logger (NI USB-6225, National Instruments, UK) was also used in the experiments to record electrodes and cell potentials. Both anode and cathode media were fed continuously through their respective chambers at flow rates of 10 mL/hr using peristaltic pumps (120S, Watson-Marlow, UK). Control MFCs and MECs were setups in conjunction with the enrichment process of bioanode and biocathode. The same condition and media were used either without adding any inoculum into the reactors (mainly to create abiotic anode for comparison) or without electrical power supplied between anode and cathode (mainly for preparing control biocathode).

For direct enrichment of bioanode and biocathode simultaneously, both anode and cathode were assembled with plain carbon felts and fed with specific media and inoculum in the ratio of 1:1 as mentioned above. The cell was left overnight before a stable voltage of 0.3

V was applied between anode and cathode. In this method, potentials of anode and cathode were left uncontrolled and fluctuated according to their growth and enrichment process. The media of both anode and cathode were replaced when the current of the cells dropped to less than 20% of peak current. The same method was used in 3cMEC unless stated otherwise. All reactors described above were operated inside a polystyrene box and under constant temperature control at 26.5 ± 2.5 °C.

3.2. Electrochemical methods

The principle of how bioelectrode work is an important subject to understand the electricity generation process and later help to improve the performance of the whole system. Bioelectrochemical analysis is one of the ways to study the bioelectrode characterisation and properties. The most common electrochemical analysis used in the characterisation included electrochemical impedance spectroscopy (EIS), cyclic voltammetry (CV) and chronoamperometry method (CA) (Logan *et al.*, 2006; Fan *et al.*, 2008; Fricke *et al.*, 2008).

3.2.1. Potential monitoring

A multichannel data logger (NI-USB-6225, National Instruments, UK) was used to monitor the cell and electrode potentials throughout the experiments. Cell voltage was measured between anode and cathode while half-cell potentials were measured between the electrode and reference electrodes (RE-5B Ag/AgCl, BASi, USA) located in the same chamber. All potential values except applied cell voltage were reported as vs. SHE unless stated otherwise.

3.2.2. Electrochemical impedance spectroscopy (EIS)

Electrochemical impedance spectroscopy (EIS) was performed to obtained internal electrochemical information for each individual BES. A potentiostat (PGSTAT128N, Metrohm, The Netherlands) equipped with frequency response analyser (FRA32M module, Metrohm, The Netherlands) was used to acquire Nyquist, magnitude and phase Bode plots. The results were mainly used to calculate cell internal resistance and obtain equivalent circuit. The analysis was done under open circuit potential (OCP) condition by using 2-, 3- and 4-electrode configurations (Autolab, 2011b). The 2-electrode configuration was performed between anode and cathode to obtain whole cell information. The 3-electrode configuration was used when

only half-cell information was required. A reference electrode in the same solution with working electrode was required in this configuration. Meanwhile, the 4-electrode configuration was used to get electrochemical information of a separator inside a BES. The reference electrode was required in both the anode and cathode chamber to performed the analysis. The range of analysis frequency was varied between 10000000 to 0.01 Hz (10 points frequency distributed within every order of magnitude) depends on the real information that could be obtained from a single EIS analysis.

The EIS commonly used as a non-destructive tool to analyse electrochemical properties of whole cell system including its components like the bioanode. The information is mainly used to check the reliability of the connection to electrodes in term of internal resistance and conductivity of the solution between electrodes (Fan *et al.*, 2008; Zhang and Liu, 2010; Fan and Li, 2016). Internal resistance is caused by a phenomenon when electrical current passes through its components under operation process (Fan and Li, 2016). Similar to other types of electrochemical cell, the internal resistance which can be obtained from the EIS analysis consisted of three sub-resistances controlled by the components, materials and electrolytes used in the system. The sub-resistances are known as ohmic resistance, charge transfer resistance and mass transfer resistance (Hoogers, 2002). Ohmic resistance is normally dominated by electrolyte and separator present in the system. In spite of the sub-resistances category, the internal resistance is also categorised according to the components used to build a complete BES: (a) ohmic resistance, (b) anodic resistance and (c) cathodic resistance in most studies (Fan *et al.*, 2008; Manohar and Mansfeld, 2009; Zhang and Liu, 2010; Timmers *et al.*, 2012). Figure 3.2 shows the measurement setup for EIS analysis in a BES. Two-electrode configuration used to obtain whole system information by measuring the electrochemical impedance between anode and cathode included other elements laid between the electrodes such as electrolytes, biofilms and diffusion layers. Three-electrode setup is meant to check half-cell electrochemical properties especially of a specific interested electrode in the BES. A reference electrode is necessary for this analysis and should place close to the electrode surface to avoid possible interferences (Autolab, 2011b). Meanwhile, four-electrode configuration is used to obtained information of the processes occurred in the electrolyte and/or between separator. It is also useful to obtained electrochemical properties of the modified electrodes and its integration with electrolyte and reactants in the system (He and Mansfeld, 2009; Borole *et al.*, 2010; Dominguez-Benetton *et al.*, 2012; Sekar and Ramasamy, 2013).

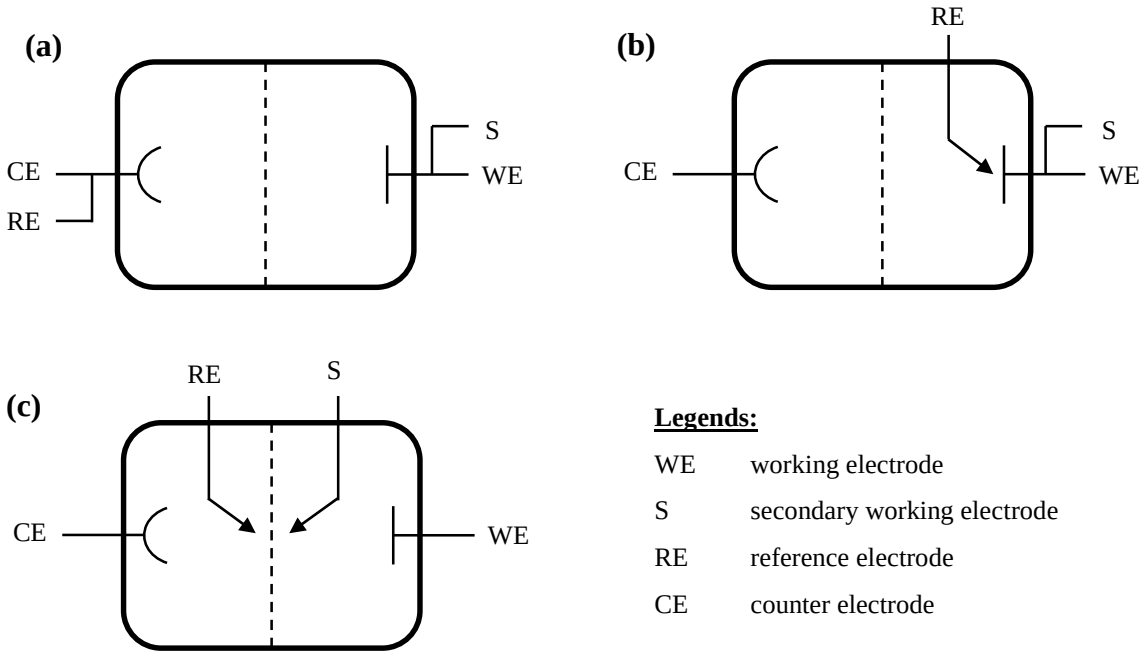

Figure 3.2 Experimental setup for EIS analysis in a bioelectrochemical cell: (a) two-electrode configuration for whole cell information, (b) three-electrode configuration for electrode spectrum, and (c) four-electrode configuration for separator analysis. Obtained and modified from (Autolab, 2011b).

In most BES, EIS spectrogram consists of a semicircle and a tail as shown in Figure 3.3. An initial semicircle indicated the resistances, semi-conductive and surface homogeneous behaviours of the system while latter part shows a tail conveyed information of mass transport between electrode and reactant in electrolyte (He and Mansfeld, 2009; Borole *et al.*, 2010). For a comprehensive study, individual half-cell measurements included in the whole system are required for every electrodes and membrane to obtain a complete set of information (Liang *et al.*, 2007). Based on the literature, the resistance between the electrodes and external connection maintained less than 10 ohm for better performance and avoid energy loss is achievable (Fan *et al.*, 2008; Borole *et al.*, 2010). The semicircle curve could decrease due to biofilm growth and reduce overpotentials activation as the electron transfer from outer membrane to electrode surface is thoroughly connected by the biofilm layer (Aulenta *et al.*, 2012; Sekar and Ramasamy, 2013). In contrast, the semicircle could increase as a result of non-electrochemically active microorganisms' growth or EPS thickening. Meanwhile, the diffusion tail changes when biofilm is growth on the electrode surface (Zhu *et al.*, 2013). Electrode like carbon felt and cloth posted finite-space diffusion impedance due to its porous materials flooded with electrolyte blocking outer interface with bulk solution (Macdonald, 2006). But, the changes of finite-space

diffusion, T to semi-infinite diffusion, W could happen when a layer of electrochemically-active biofilm is growth on the electrode surface. The diffusion behaviour is also depended on the biofilm thickness which some diffusion parameter can be calculated to predict the time of reactant transport through the layer. However, finite-length, O diffusion is rarely found in BES system worked using microorganisms as catalysts. As the older outer layer of biofilm could disintegrate from the newly formed layer underneath it, it is hard to have a thick biofilm layer which could exhibit finite-length diffusion behaviour (See Figure 3.3 for diffusion type).

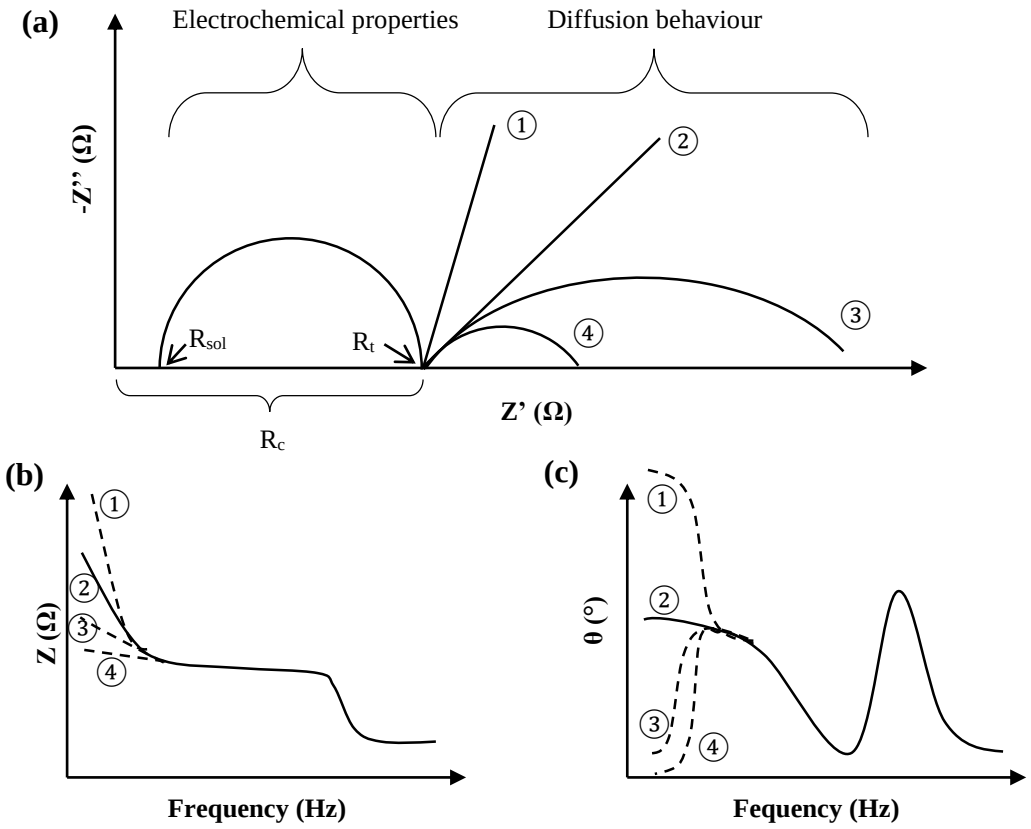

Legends:

R_{sol}	solution resistance
R_t	charge transfer resistance
R_c	total cell resistance
①	T, bounded Warburg, linear finite diffusion impedance (>45°)
②	W, Warburg semi-infinite linear diffusion impedance (45°)
③	G, Gerischer bulk chemical reaction impedance
④	O, finite-length diffusion impedance

Figure 3.3 Electrochemical impedance spectrogram: (a) Nyquist plot, (b) Bode modulus plot, and (c) Bode degree plot. The figures are obtained and modified after Dominguez-Benetton *et al.* (2012) and Sekar and Ramasamy (2013).

The results obtained from the EIS is usually used in fitting an equivalent electric circuit to find the detail of single parameter e.g. R_t. A most simple equivalent circuit is called Randles circuit (Figure 3.4 (a)) consisted four main parameters: R_s, R_t, CPE and D relative to electrolyte resistance, charge transfer resistance, constant phase element and diffusion properties. Combination of the information in cell configuration with EIS result is crucial to find the best fit equivalent circuit model. As BES normally consisted of both anode and cathode parts in one system, a modified Randle model (Figure 3.4 (b)) is recommended. However, there is more than one model that is currently used in BES depended on the study (Dominguez-Benetton *et al.*, 2012; Sekar and Ramasamy, 2013). Besides, some parameter in the circuit could be neglected due to the insignificant effect to the whole model. Therefore, individual analysis on electrode and separator included whole cell system are important in interpreting the results.

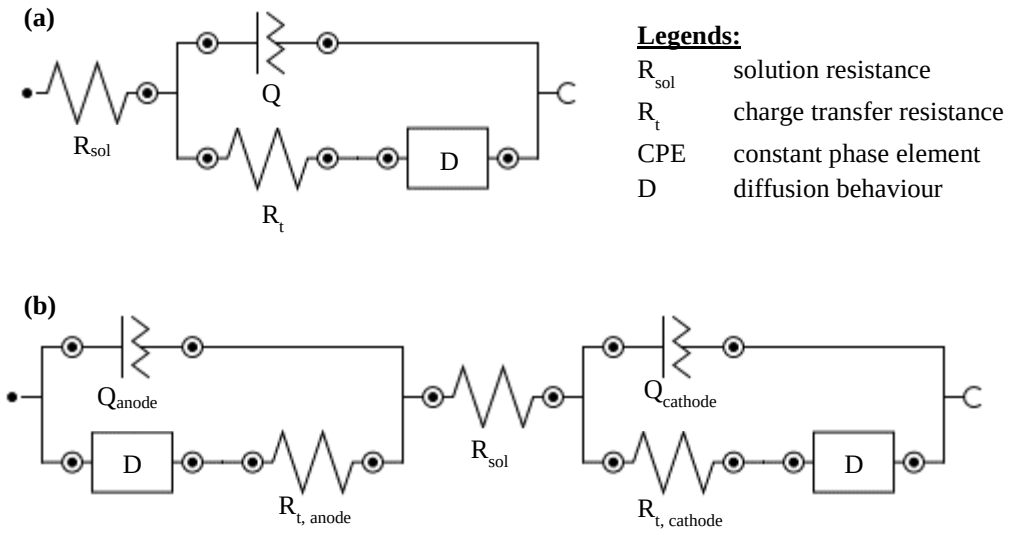

Figure 3.4 Electrochemical equivalent circuit: (a) simple Randle; (c) two-electrode BEC

3.2.3. Chronoamperometry method (CA)

All CA experiments were performed using a Quad potentiostat (Quad, Whistonbrook Technologies, UK) consisted of four channels which can run four parallel tests simultaneously. To fix the potential on an anode MFC, the anode was connected as a working electrode while a reference electrode located in the same solution with anode worked as a reference while a specific potential was fixed. Cathode worked as counter electrode where the potentiostat adjusts its potential in order to fix the anode potential to +0.2 V vs. SHE. After stable currents were obtained with applied potentials of +0.2 V vs. SHE, the bioanodes were subjected to a range of chronoamperometric test at -0.3, -0.2, 0, +0.2, +0.4, +0.6, +0.8 and 1.0 V vs. SHE. The same

principal connections were used to fix the potential of a cathode MEC to -0.7 V vs. SHE. However, the range of the analysis on biocathode was -0.5, -0.7, -0.8, -0.9 and -1.0V vs. SHE.

The CA method was also used to pursue the power and polarisation curve of an MFC. An applied potential was set starting from open circuit potential (OCP) down to 0V with a decrement of 0.05V every step. A fixed potential was applied to the MFC for at least 15 min before changing to the next step. Only a stable last point value of each step was taken as a result and incorporated into the power and polarisation graphs.

The Quad potentiostat (3-terminal) was converted to a simple power supply (2-terminal) by combining both reference and counter electrode terminals to a single terminal. The 2-terminal configuration was used in direct enrichment of bioanode and biocathode. Only specific voltage was applied between anode and cathode without considering each electrode potential requirements. The output voltage was set at 0.3 V during the enrichment period and the positive terminal was connected to the anode while the negative terminal to the cathode. During the period, cell performance was analysed with applied voltages ranging from 0 up to 2.5V with an increment of 0.2V every 10 min unless stated otherwise. The maximum applied voltage in each experiment was chosen based on the robustness of the bioelectrodes to performance oxidation-reduction reactions. No further voltage higher than before would be applied to the test cell if one of the electrodes, either bioanode or biocathode, failed to keep its potential at the consistent pattern (e.g. dropped or increased dramatically or significant fluctuation). All tests and analysis were carried out at controlled temperature at 26.5 ± 2.5°C.

The most crucial measurements of an EGB performance is the optimal current output and recovery efficiency from treating wastewater. Figure 3.5 shows a typical polarisation and power curves that could be obtained from a fuel cell system including microbial fuel cells. The fuel cell potential should be maintained at theoretical potential when electrical current is withdrawn from the system. Nonetheless, the potential dropped from maximum to zero proportional to the increasing current withdrawal. Three regions are identified where overpotential occurred and contributed to energy loses. They are activation, ohmic and mass transport loses regions. Activation losses are largely affected by the materials used to constructed electrodes and connections while mass transport losses are depended on reactor configuration and electrolytes' conductivity. Electrical energy is lost when the current is passed through a load or device through an external circuit and designated as ohmic losses. From Figure 3.5, potential dropped in ohmic losses region is less than activation/mass transport losses regions. This phenomenon explained that the energy losses, especially in activation/mass

transport losses regions, is higher than the ohmic losses region. Today, the EGB could achieve up to 1.0 kW/m^3 (working volume) or 6.9 W/m^2 (anode area) power output in laboratory scale and depending on the type of wastewaters and organic contents in the wastewaters (Logan, 2010). However, the output dropped significantly to about 0.01 kW/m^3 when the operational volume increased from 10 to 350 mL, which implies the extrapolation of the performance should be under caution (Premier *et al.*, 2016). Besides the power output, Coulombic efficiency (CE) use to determine the performance of the bioanode to recover electrical energy in term of electrical charges from organic matters in wastewaters. The CE calculation is devoted as total recovered electrical charge ($Q_{produced}$) divided by total charge possible produced by organic oxidation in wastewater ($Q_{oxidised}$). The CE varies through studies fairly depended on the types of wastewater, organic contents and reactor designs (Gil *et al.*, 2003; Kim *et al.*, 2011; Ahn and Logan, 2013; Lee and Huang, 2013; Foad Marashi and Kariminia, 2015; Moon *et al.*, 2015; Daud *et al.*, 2018). Nevertheless, up to 90% of the COD removal and 80% of CE performance are achievable using bioanode as biocatalysts in electricity generation (Kim *et al.*, 2005; Puig *et al.*, 2011a; Wang *et al.*, 2012). Real wastewaters tend to have low conductivity which could post a problem to the BES utilising bioanode as power source (Logan, 2010). Some studies add salt NaCl or decrease electrode spacing to increase conductivity and BES performance (Ahn and Logan, 2013; Lee and Huang, 2013). In designing pilot scale BES, the ratio of operational volume to electrode size is important and must be taken into consideration. The ratio is crucial to minimise overpotentials and internal resistance due to low conductivity and electrode spacing(Manohar and Mansfeld, 2009; Cheng and Logan, 2011). Practically, organic matter in wastewaters is oxidised by electrochemically-active microbes attached to anode surface. Larger operating volume in anodic chamber could decrease CE as a result of non-electrochemically-active microorganisms' activities. Thrive of the unwanted microorganisms in the bioanode is accelerated under high organic content wastewaters, i.e. chemical oxygen demand (COD) more than 1.0 g/L. The high organic strength wastewaters are not suitable for electricity generating bioanode-based system compared to fermentation or anaerobic digestion process and make them more uncompetitive in long-terms with non-electrochemically-active microorganisms' such as methanogens (Sleutels *et al.*, 2011).

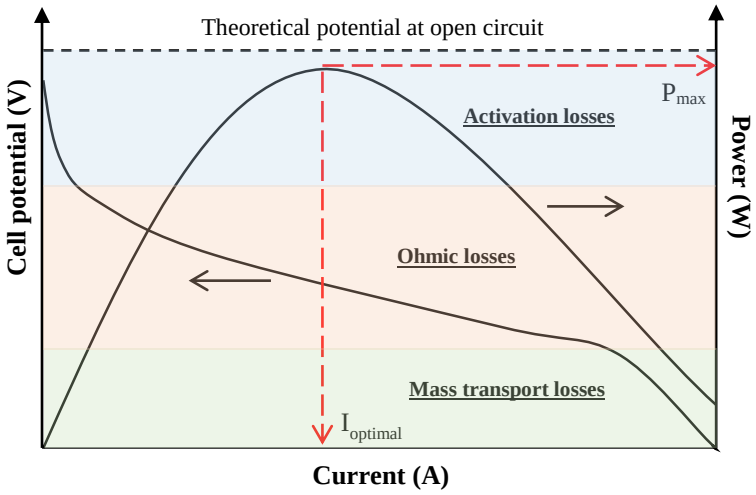

Figure 3.5 Polarisation and power curves in a fuel cell system

3.2.4. Cyclic voltammetry (CV)

All CV were performed either with Metrohm or Quad potentiostat (with available CV function). Bioanode CV was performed with applied potential ranged from -0.5 to +0.6V vs. SHE unless stated otherwise. At least 2 scan cycles were performed with a scan rate of 0.001 V/s unless stated otherwise and only the last scan was taken as a result. Meanwhile, biocathode CV was performed as same as mentioned above except the scan ranged between 0 and -1.0 V vs. SHE unless stated otherwise.

Electrons transferred from EGB microbes to electrodes involve series of reversible and irreversible enzymatic and electrochemical reactions in order to send the electrons to cell surface (Fricke *et al.*, 2008; LaBelle, 2009). Two main mechanisms of electron transfer (ET) are currently being recognised by the research community: meditated electron transfer (MET) and direct electron transfer (DET) (Kracke *et al.*, 2015). In MET, bacteria are not in direct contact with anode but with the assistance of special mediators. The mediators shuttled between the cell and electrode surface transferring the electron to anode. First, the mediators are reduced by receiving electrons from bacteria and then re-oxidised by releasing it to the anode. The oxidised mediators are recycled back to bacteria to receive new electron. In DET, bacteria are in direct contact with anode surface either via cytochromes or surface-associated structure called nanowires. These outer membrane-associated structures were found to efficiently transfer electrodes directly onto abiotic surface and also to other bacteria. For example, oxidation of acetate via TCA cycle to yield NADH and reduced proteins such as menaquinones (Kim and Gadd, 2008; Madigan *et al.*, 2014). The acetate is first diffused into the cell and

oxidised to extract the high energy electron through a series of chain reactions under the assistance of cytochromes, proteins, bound redox mediators or soluble mediators until they can reach the electrode surface (Jain *et al.*, 2012; Carmona-Martínez *et al.*, 2013; Kracke *et al.*, 2015). Cyclic voltammogram (CV) is one of the important technique to analyse those electron transfers between the cell surface and electrode. Similar three-electrode configuration as shown in Figure 3.2 (b) is used in this analysis. A range of potentials is swept through an electrode (WE) where a layer of electrochemically-active biofilm is attached with and in contact with outer membrane protein. The voltammogram is a response current curve corresponded to the potential sweep. A symmetrical peak current could be observed at certain potential points within the range indicated a maximum rate of reaction. Figure 3.6 (a) shows the reversible reaction of the bioanode in general which oxidation and reduction peaks were observed and the peak potentials are almost laid in the same line but the gap is relatively small. Usually, the cyclic voltammogram is converted to the first derivative of CV (Figure 3.6 (b)) for further investigation of any active redox potentials within the potential scanning range. It also implied a favourable potential for certain outer bound proteins to hop the electrons to electrode surface or vice versa (Kracke *et al.*, 2015). Aside from peak current potential, lower potential means the reaction is unfavourable as the diffusion rate is faster than the oxidation reaction while higher potential seems triggering excessive oxidation reaction until diffusion becomes a rate-limiting factor to block the current achieved higher peak (Fricke *et al.*, 2008). Most of the peak current in the voltammograms occurred at between -0.15 - -0.20 V vs. SHE for well-studied Fe(III)-reducing *Geobacter* species dominated bioanode using acetate as substrate (Bond and Lovley, 2003; Wei *et al.*, 2010). However, the peak current for *Shewanella* species, another common electrochemically-active strain, is slightly higher than *Geobacter* species (Kim *et al.*, 2002; Jain *et al.*, 2012; Carmona-Martínez *et al.*, 2013). Therefore, the goal of a good CV is at least ±0.10V vs, SHE above any peak current potential where a change is observed. The CV can be converted to first derivative for better detection of catalytic wave and favourable mid-point potential caused by maximum reaction rate (LaBelle, 2009).

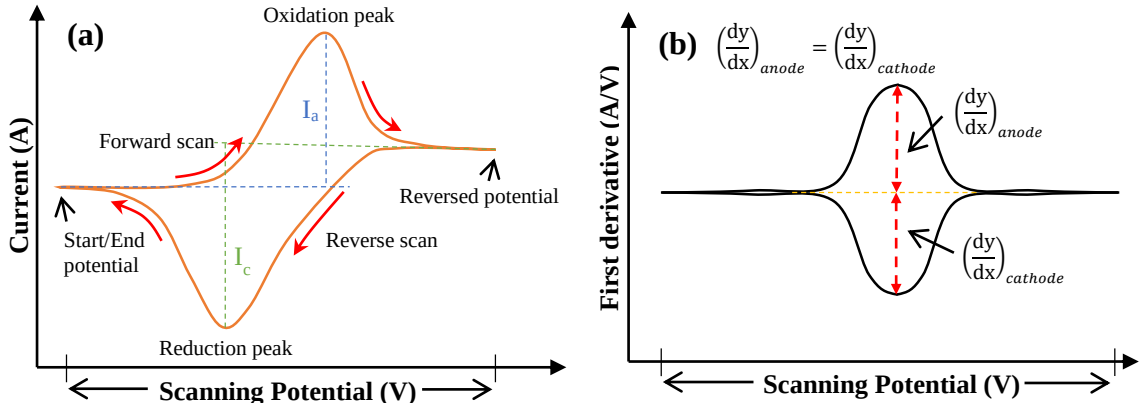

Figure 3.6 Common electricity-generating bioanode (a) cyclic voltammogram and (b) its first derivative. The figures are obtained and modified after LaBelle (2009).

3.3. Analytical methods

3.3.1. Gas sample

Gas evolution from the biocathode was measured using a water displacement method. The samples then were analysed using a gas chromatography (GC-8A, Shimadzu, UK). Two columns molecular sieve 5A (mesh range 40-60) and Chromosorb 101 (mesh range 80-100) were equipped and operated at isothermal temperature 40°C. The carrier gas was research grade 99.99% N_2 (BOC, UK) at a pressure of 100kPa. A thermal conductivity detector was used to detect the gas based on their retention times. The actual hydrogen volume was calculated as

$$V_{H2} = V_h \cdot X_{H2} \qquad \text{Equation 3.1}$$

Where V_{H2} is pure hydrogen volume, V_h is the headspace volume of the gas captured in the glass tube, X_{H2} is fraction of hydrogen in the gas samples. The pure hydrogen volume was then used to compute hydrogen production rate as

$$Q_{H2} = V_{H2} / (A_{cat} \cdot t_p) \qquad \text{Equation 3.2}$$

Where Q_{H2} (L H_2/m^2 cathode / day) is hydrogen production rate, A_{cat} (m^2) is cathode surface area and t_p (day) is production time.

3.3.2. Liquid sample

Influents and effluents were collected and filtered through 0.2µm PES membrane (VWR (514-0072), UK) prior analysis. pH (HI 9025 Microcomputer pH meter, Hanna Instruments, UK)

and conductivity (HI 8733 Conductivity meter, Hanna Instruments, UK) were measured before the samples were kept in refrigerator under 4°C.

Chemical oxygen demand (COD) was determined by using the cell test kits (114541: 25-1500 mg/L COD) supplied by Merck, UK. The samples were prepared and added into the reagent vials according to the manufacturer's procedures and then measured by a spectrophotometer (Spectroquant® Pharo 300, Merck, UK).

Ammonium (NH_4-N) content was determined by using the cell test kits (14559: 4.0 - 80.0 mg/L NH_4-N) supplied by Merck, UK. The samples were prepared and added into the reagent vials according to the manufacturer's procedures and then measured by a spectrophotometer (Spectroquant® Pharo 300, Merck, UK).

Anions compounds included sulphate (SO_4^{2-}) and phosphate (PO_4^{3-}) were determined by ion chromatography (Interrion HPIC, Dionex, USA) equipped with autosampler (AS-AP, Dionex, USA) while inorganic and organic carbon by total carbon analyser (TOC-5050A, Shimadzu, UK) equipped with autosampler (ASI-5000A, Shimadzu, UK). The pH of TOC samples was always maintained in 7.0 or above. The alkaline condition avoids dissolution of carbonate to CO_2 which could affect the results of total carbon.

The presence of fatty acids was analysed using a gas chromatography (Tracera GC-2010 Plus, Shimadzu, UK) equipped with Barrier Ionization Discharge (BID) detector (280°C) and autosampler (AOC-20i, Shimadzu, UK). A column (Zebron ZB-WAX-Plus capillary column 30m × 0.25mm × 0.25um, Phenomenex, UK) was used to separate the compounds and operated with a temperature profile: 50°C for 1 min to 180°C at 30°C/min to 180°C for 8 min. The injection port was set at 180°C with split ratio 10:1 under 1.0μL injection sample while the detector was maintained at 280°C. The carrier gas was high purity grade helium (99.999% BOC, UK) and was maintained at constant flow of 2.0 mL/min. All samples were filtered with 0.2μm syringe filter and then acidified with HCl 1.0 M under the ratio of 9:1 prior analysis. The values were reported in mg/L.

3.4. Energy recovery and contribution calculations

Energy consumed and recovered by bioanode or biocathode or both bioanode and biocathode were calculated to summarise the overall efficiency of the system used in each study. Anodic Columbic efficiency was obtained according to Logan *et al.* (2006) to determine the efficiency of any bioanode used in BES:

r_{CE} (%) = $Q_{produce}$ / $Q_{oxidise}$ × 100 % Equation 3.3

where $Q_{produce}$ (C) = ∫ I (t) dt, $Q_{oxidise}$ (C) = $\Delta S \cdot \upsilon \cdot F \cdot V_r$, ΔS is substrate consumed in term of acetate (mg Ac/L), υ is stoichiometric number of electron produced per mole of acetate oxidised (8 mol/e^-), F is Faraday constant (96485 C/mol) and V_r is anodic reactor volume (L).

Meanwhile, cathodic recovery was determined based on Faraday's law of electrolysis:

r_{cat} (%) = $Q_{recovery}$ / Q_{supply} × 100 % Equation 3.4

where $Q_{recovery}$ (C) = $n \cdot F \cdot z$ is the charge consumed to reduce proton and carbon dioxide to products, n is product recovery in mole, F is Faraday constant (96485 C/mol), z is the valency number of product formation (2 for hydrogen or 8 for acetate production). Meanwhile, Q_{supply} (C) = ∫ I (t) dt is total charge supplied from the power supply within the specified time of recovery.

The overall energy efficiency of MEC when both bioelectrodes were used is calculated based on Call and Logan (2008):

η_{e+s} (%) = W_h / (W_e + W_s)× 100 % Equation 3.5

where W_h, W_e, and W_s (J) are the energy contents of hydrogen, supplied electrical energy and energy released from substrate oxidation, respectively. The standard enthalpy of combustion for hydrogen and acetate are 285.83 kJ/mol and 870.28 kJ/mol, respectively. Therefore, W_h and W_s were calculated by multiplying the enthalpy values with total moles of hydrogen produced and acetate consumed. Meanwhile, W_e was computed by multiplying the applied voltage value with the total charge flow between the anode and cathode which is also equalled to $Q_{produce}$ or Q_{supply}.

The energy yield relative to the electrical input can be expressed as follows:

η_e (%) = W_h / W_e × 100 % Equation 3.6

and the energy yield relative to the substrate oxidation is:

η_s (%) = W_h / W_s × 100 % Equation 3.7

The energy contribution by external power input (e_e) and substrate (e_s) in the system at specific applied voltage were calculated as

e_e = W_e / (W_e + W_s) × 100 % Equation 3.8

e_s = W_s / (W_e + W_s) × 100 % Equation 3.9

Chapter 4. Bioanode as a limiting factor to a microbial electrolysis cell

4.0. Chapter summary

Bioelectrodes that could perform oxidation and reduction reaction were studied in this chapter. First, enriched electricity-generating bioanodes was studied to understand their characteristics under defined parameter or specific operating conditions. These included internal resistance, applied potential and substrate concentration. The effects of these parameters were then studied to determine the criteria of a healthy or best-performed bioanode. Secondly, similar tests were also done with hydrogen-producing biocathode to study its behaviours. Then after, both bioelectrodes were deployed in a single microbial electrolysis cell (MEC) to study their interactions and responses to each other.

*Part of this chapter has been published in *Bioresource Technology*, 238, pp. 313-324 in 2017 with the title 'Bioanode as a limiting factor to biocathode performance in microbial electrolysis cells'. All authors (Swee Su Lim, Eileen Hao Yu, Wan Ramli Wan Daud, Byung Hong Kim and Keith Scott) were equally contributed to the paper.

4.1. Introduction

Microbial fuel cell (MFC) is a device that converts chemical energy contained in organic matters into electric energy by the catalyst of microorganisms. It is considered as an alternative option to green energy in future compared to conventional fossil fuels. In recent years, the usage of the technology has widened in the field of wastewater treatment and sensor applications in conjunction with power generation (Schneider *et al.*, 2016; Spurr, 2016). As the technology received increasing attention in energy recovery from wastewaters, it still faces a great challenge in practical application. The bottlenecks included low power output, voltage reversal, complex biocatalyst activity and energy loss through poor configuration (Liang *et al.*, 2007; Manohar and Mansfeld, 2009; Yates *et al.*, 2012; An and Lee, 2014). Nevertheless, all these

issues have one common aspect which is related to internal resistance. Internal resistance plays an important role in affecting electron transfer mechanism and power output in bioelectrochemical system (BES). Due to the issue, many studies have been focused on seeking new strategies to keep the internal resistance as low as possible. This included the studies of cell design (Liang *et al.*, 2007), operating condition (Manohar and Mansfeld, 2009), long-term operation (Borole *et al.*, 2010) and distribution of internal resistance in the system (Zhang and Liu, 2010).

In recent years, BES others than MFC have been receiving increasing attention. Most of these cells consist of bioanode to work as a functional biocatalyst to perform substrate oxidation process. Those cell systems included microbial electrolysis cell (MEC), microbial electrosynthesis cell (MSC), microbial desalination cell (MDC) and etc. (Milner *et al.*, 2016; Vassilev *et al.*, 2017; Zhen *et al.*, 2017). The usage of bioanode in the system is inevitable crucial for the operation of the whole system. It may result in the fall of effectivity to the whole system when the bioanode was not performed in optimal condition. Jeremiasse *et al.* (2010) studied the first full biological MECs by combining both bioanode and biocathode in which both oxidation and reduction processes were performed by electrochemically active microorganisms. The same study was also performed by Liang *et al.* (2014) to test the effect of bicarbonate and cathode potential on a MEC. In their results, the study was focused on the hydrogen-producing biocathode and its performance based on a range of applied potentials providing little information on the bioanodes. It was assumed that the bioanode could supply sufficient current required for biocathodes to generate hydrogen. Some questions are still unanswered such as how the bioanode responds when the applied potential on the biocathode is changed, what is the limiting potential a bioanode can handle before it loses its ability to produce electrons and will it have the same performance when the set potential on the anode is high?

In this chapter, two main experiments were performed by focusing on the studies of electricity-generating bioanode behaviours and characteristics in specific operating conditions. In the initial study, three different internal resistance values were chosen to enrich electricity-generating bioanode over time. The aim was to determine the effect of the internal resistance to current output and internal electrochemical properties. During the enrichment process, microbial fuel cell performance in term of power outputs was recorded. In additional, cyclic voltammetry (CV) and electrochemical impedance spectroscopy (EIS) were also used to monitor and examine the microbial fuel cells and bioanode. After a stable current was obtained, the internal resistance and electrochemical behaviours of each component in the cells were

determined by polarisation equation and impedance spectrogram fitted under a suitable equivalent circuit. The information was then used to produce better bioanode to support hydrogen-producing biocathode in a microbial electrolysis cell.

In the second study, the main objective was to enrich the better bioanode according to the first study, test it at higher applied potential -1.0V before deploying it in MEC to assess its robustness. The anode should be able to supply the electrons to the cathode of MEC, therefore reduces the total electric energy required from hydrogen production. It was believed that sufficient electron supply from substrate oxidation by bioanode activity is vital to support the hydrogen evolution in a biocathode and therefore maintaining the energy demand from the external power supply as low as possible. In order to have an optimum hydrogen production rate from the biocathode, the anode plays an important role as a support to the biological MEC system. It may lower external energy supply to the system and increase energy recovery in term of hydrogen evolution on the one hand and it could be a limiting factor to the whole system together with other problems like substrate crossover and precipitation of mineral on the electrodes on the other (Jeremiasse *et al.,* 2010). Due to the fact that bio-catalysts will be used in both anode and cathode, double-chamber membrane-based MEC will be used for better environmental control in both chambers. Moreover, specified electrolytes to accommodate different reactions and end products are vital for the growth and regeneration of independent microbial dominated species in both separated chambers (Jafary *et al.,* 2015; Escapa *et al.,* 2016; Kadier *et al.,* 2016). The results collected from these experiments will be useful and could provide initial information for BES scaling and system feasibility in practical applications.

4.2. Experimental procedure

4.2.1. Experimental setup and operation

Two-chamber BECs as mentioned in Section 3.1.1 were used in these experiments. First experiment involved the enrichment of bioanode under different internal resistance by using two-chamber MFC. The experiment was started with preparing different internal resistance to be used in the bioanode enrichment process. Specific internal resistances (13, 61 and 164 Ω) were prepared by loosing the connection between carbon felt and titanium wire and only bioanode was enriched and focused in this experiment. Therefore, Pt-cathode was used as a counter electrode to enrich and maintain the bioanode. Media preparation and start-up operation

were similar to the procedures mentioned in Section 3.1.2 and 3.1.3. The bioanode performance was monitored continuously throughout the whole experiments.

Second experiment focused on the integration of the enriched bioanode from the first experiment into a two-chamber MEC. The bioanode was served as counter electrode to support biocathode during the enrichment process and hydrogen production. All experiments were conducted in duplicate.

4.2.2. Estimation of energy losses using polarisation equation

Polarisation equation is described as follow to explain energy losses when a specific current is withdrawn from a MFC (Hoogers, 2002):

$$V_{cell} = E_o - b \log I_D - RI_D - \gamma \exp(\omega I_D) \qquad \text{Equation 4.1}$$

where V_{cell} (V) is the final potential output considers the energy losses in the system, E_o is an open circuit potential (V) where there is no energy loss through the system, b is activation coefficient (V) due to the surface material of electrode that needs an initial potential energy to activate a redox reaction, I_D is current density (A/m^2), R is ohmic coefficient (Ω) considers the potential energy loss as a results of electron transportation between electrodes, and γ (V) and ω (m^2/A) are both diffusion coefficients. γ explains that potential energy is consumed in order to transfer the reactant from bulk solution to electrode's surface or vice versa and ω estimates the rate of current consumption per electrode surface area.

Data collected from polarisation test consisted of V-I results. The V-I data was then used to determine the coefficients' value in the polarisation equation. A statistic method called the sum of square residuals (SSR) was obtained to calculate the coefficient values. Four equations were derived to find the five main coefficients' value: E_o, b, R, γ and ω. The equations were

$$\sum V = nE_o - b\sum \log I_D - R\sum I_D - \gamma \sum \exp(\omega I_D) \qquad \text{Equation 4.2}$$

$$-\sum V \log I_D = -E_O \sum \log I_D + b\sum (\log I_D)(\log I_D) + R\sum I_D (\log I_D) + \gamma \sum \exp(\omega I_D)(\log I_D) \qquad \text{Equation 4.3}$$

$$-\sum V I_D = -E_o \sum I_D + b\sum \log I_D (I_D) + R\sum (I_D)(I_D) + \gamma \sum \exp(\omega I_D)(I_D) \qquad \text{Equation 4.4}$$

$$-\sum V \exp(\omega I_D) = -E_o \sum \exp(\omega I_D) + b\sum (\log I_D)\exp(\omega I_D) + R\sum (I_D)\exp(\omega I_D) + \gamma \sum \exp(\omega I_D)\exp(\omega I_D) \qquad \text{Equation 4.5}$$

To simplified the equations, alphabet representatives were used

$$Y_1 = \sum_{i=1}^{i=n} V_i \qquad Q_1 = n \qquad Q_6 = \sum_{i=1}^{i=n} I_D (\log I_D)$$

$$Y_2 = -\sum_{i=1}^{i=n} V_i \log I_D \qquad Q_2 = -\sum_{i=1}^{i=n} \log I_D \qquad Q_7 = \sum_{i=1}^{i=n} \exp(\omega I_D)(\log I_D)$$

$$Y_3 = -\sum_{i=1}^{i=n} V_i I_D \qquad Q_3 = -\sum_{i=1}^{i=n} I_D \qquad Q_8 = \sum_{i=1}^{i=n} (I_D)(I_D)$$

$$Y_4 = -\sum_{i=1}^{i=n} V_i \exp(\omega I_D) \qquad Q_4 = -\sum_{i=1}^{i=n} \exp(\omega I_D) \qquad Q_9 = \sum_{i=1}^{i=n} \exp(\omega I_D)(I_D)$$

$$Q_5 = \sum_{i=1}^{i=n} (\log I_D)(\log I_D) \qquad Q_{10} = \sum_{i=1}^{i=n} \exp(\omega I_D)\exp(\omega I_D)$$

These values were determined in MS Excel and substituted in a matrix equation to solve the coefficients. However, there was only four equation used to determine five coefficients. An initial value, ω_o was set at the beginning in order to calculate the remaining four coefficients. New V and I_D data were then calculated using the latest coefficient values and sum square error value, R^2 was recalculated. The R^2 value was set as close as to 1.0 for an ideal fit between calculated and raw V-I data. For this reason, a Goal Seek function in the MS Excel was used to adjust the ω_o value by getting R^2 closer to 1.0.

4.2.3. Determination of electrochemical properties through impedance analysis

The impedance data were collected as described in section 3.2.1. The equivalent circuit was build according to the cell configuration and materials presented in the measured system (He and Mansfeld, 2009; Dominguez-Benetton *et al.*, 2012; Sekar and Ramasamy, 2013). Normally the impedance results consisted a semicircle with a diffusion tail in Nyquist plot. Therefore, a suitable equivalent circuit that fitted the impedance data was constructed based on Randle circuit. NOVA 1.11 software was provided with the instrument used to measure the electrochemical impedance. The software consisted of a function to fit the data into an equivalent circuit and determined electrochemical coefficient values in the circuit. Before the circuit was run, initial resistance values of the semicircle were determined using 'Electrochemical circle fit' function before executing 'Fit and simulation' function for the entire equivalent circuit.

4.2.4. Experimental parameter and kinetic analysis for optimising bioanode

New MFCs were assembled under low internal resistance (< 10 Ω determined under EIS method). The MFCs were then started-up and inoculated under the same condition as previously described in section 3.1.3. After the MFCs had generated a stable current, the anodes were subjected to a series of experimental tests to check the bioanode catalytic activity and determine the optimal operating conditions. Three experimental parameter were tested (the tested range): applied potential (-0.3, -0.2, 0, +0.2, +0.4, +0.6, +0.8 and 1.0 V), phosphate (1, 5, 10, 20 and 50 mM), acetate (1, 5, 10 and 20 mM) and ammonium (1, 5, 10 and 20 mM) concentrations. The applied potential experiments were done using the chronoamperometry method by fixing the anode potential to certain potential under a specific period as mentioned in section 3.2.3. Meanwhile, phosphate, acetate and ammonium tests were done by alternating the concentrations in the medium that was continuously fed into the anode of the MFCs. The responses of the bioanode were recorded not only by the consumption rate of the compounds but also through the electrochemical activities. Therefore, analytical methods and electrochemical protocols as described in section 3.2 and 3.3.2 were followed. The experiments and analysis were performed in duplicates.

Energy recovery and energy yield were calculated based on the calculations in section 3.4. In addition, the modified Monod-type equation was used to estimate the anode current density related to substrate concentration as follows (Zhu *et al.*, 2013):

$$I_D = I_{D,max} \cdot S/(K_s + S) \qquad \text{Equation 4.6}$$

where I (A/m^2) is the current density generated from anode, I_{max} is maximum current density, S is substrate concentration and K_s is half-saturated substrate concentration.

4.3. Result and discussion

4.3.1. Low internal resistance ensures better bioanode oxidation efficiency

Three groups of MFC (with duplicates in each group) were prepared with different internal resistances: 13, 61 and 164 Ω were started-up and enriched with inoculum collect from a parent MFC (Spurr, 2016). The MFCs were subjected to polarisation test at the end of 100 days after a stable current (See Appendix A: Figure A.1). Current was withdrawn from the MFCs by using a potentiostat. Starting from the open circuit voltage of the cell, the voltage was reduced at a

decrement rate of 0.05V for every 15 min after a stable current was recorded. The results were plotted to show the power output performance of each MFCs and the initial internal resistance of each component as in Figure 4.1 (a) and (b). All MFCs posted OCP values around 0.75 V when external resistance was disconnected for more than an hour. Due to the effect from different internal resistance, MFC group 1 exhibited the best performance followed by MFC group 2 and 3 marking the peak power output of 0.093, 0.079 and 0.069 W/m^2, respectively. Meanwhile, the current densities at the peak power output were recorded as 0.237, 0.206 and 0.194 A/m^2 corresponding to external resistances of 414.0, 476.5 and 476.4 Ω (See Appendix A: Figure A.2) respectively to MFC group 1, 2 and 3. MFC performance acted even less efficient when both anode and cathode internal resistances were further increased as shown in MFC group 3. Cell voltage in MFC group 3 dropped significantly compared to group 1 and 2 when more current was withdrawn from the cell (Figure 4.1). The increase of anode and cathode internal resistances in MFC group 3 (Figure 4.2) not only causing the anode potential dropped faster but also increased the cathode potential in much faster rate (See Appendix A: Figure A.2). As a result, the electrons generated from anode were facing difficulties to channel them to cathode as internal resistance increased and less potential difference between anode and cathode. Moreover, it affected the anode and cathode in performing oxidation and reduction reactions (Liang *et al.*, 2007; Fan *et al.*, 2008; Manohar and Mansfeld, 2009).

To further investigate the effect of internal resistance relatively to overpotentials, polarisation equation was obtained and experimental data were fitted to the equation. The overpotential losses included activation, ohmic, and mass transfer were determined from the polarisation equation as shown in Equation 4.1. Open circuit potential for whole cell and electrodes were shown as E_o in the table. According to the fitted data, the coefficient value for cell ranged between 0.762 and 1.274 V while anode and cathode ranged from -0.256 to -0.274 V and 0.596 to 0.892 V. Surprisingly the anode potential was not changing a lot from the principal value of -0.260 V. Standard reduction potential of acetate in MFC has been reported as -0.290V and approximately 0.030 V potential lost could be due to microbial activity (Fricke *et al.*, 2008; LaBelle, 2009; Wang *et al.*, 2009; Zhu *et al.*, 2013). In contrast, the cathode potential was inconsistent and the value was much lower than the standard oxygen reduction potential (+1.23 V). The energy lost in cathode was inevitable using platinum catalysts according to real environmental conditions (Bajracharya *et al.*, 2016a; Burkitt *et al.*, 2016; Milner *et al.*, 2016). Optimised temperature, pH and abundant oxygen with continuous purging of air to saturate the solution was vital to keep the functionality of the catalyst. It has been reported cathode was a limiting factor to electricity-generating bioanode in MFC (Bajracharya

et al., 2016a; Burkitt *et al.*, 2016; Milner *et al.*, 2016). The drawback of the cathode halts the anode performance and limiting the improvement of the whole system. Alternative catalysts such as iron oxide and manganese oxide have proven posted equivalent functionality and achieved competitive performance compared to platinum (Burkitt *et al.*, 2016; Kodali *et al.*, 2017). Non-metallic catalysts were also used in cathode to reduce the cost of expensive platinum and economically reliable to scale-up while able to perform better oxygen reduction catalysis under mild environments (Rismani-Yazdi *et al.*, 2008; Yuan *et al.*, 2016).

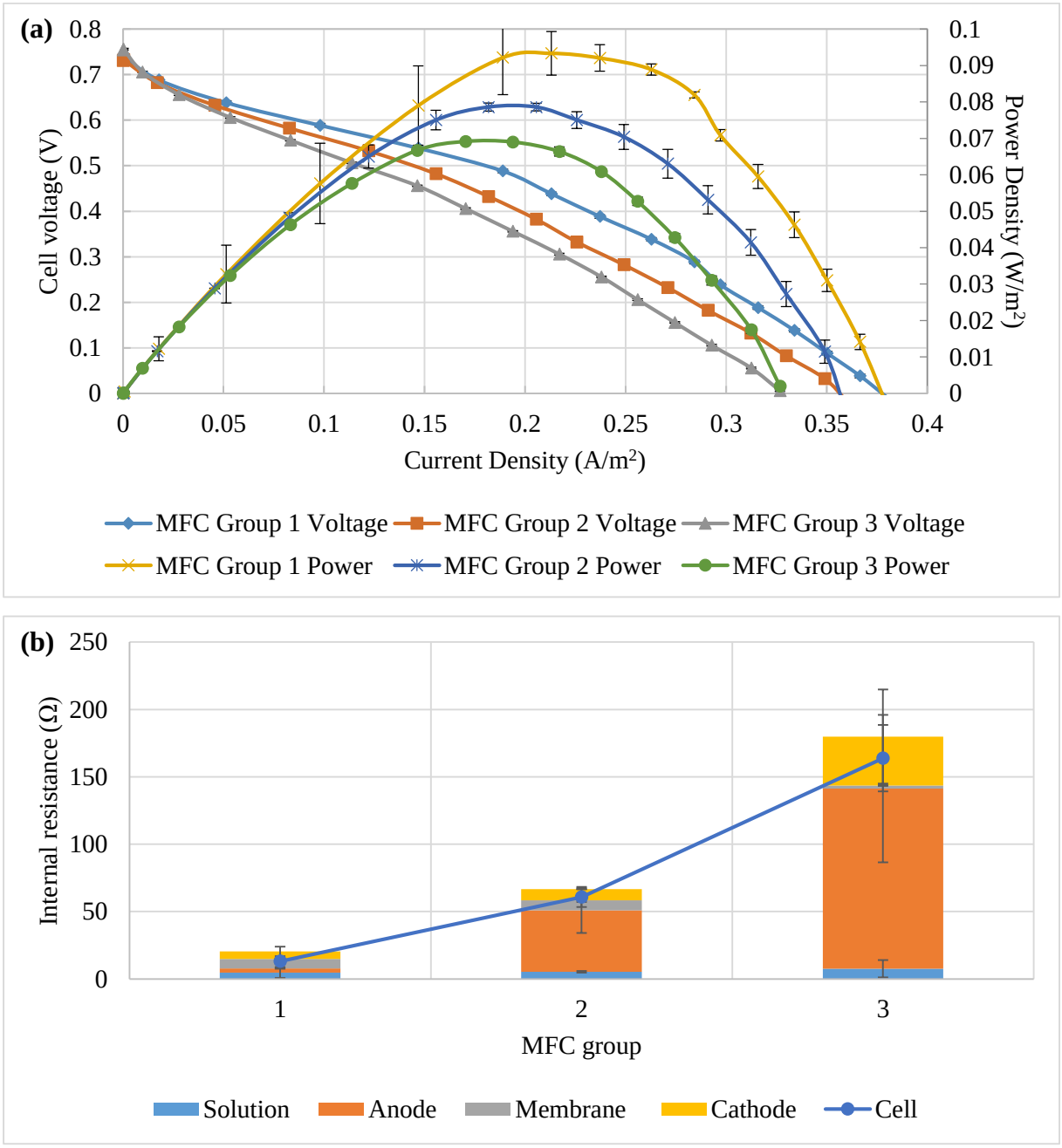

Figure 4.1 (a) Polarisation and power curves, and (b) initial internal resistance of the MFCs.

Second observation of the effect of internal resistance was the loss of energy through activation overpotential and ohmic represented by *b* coefficient in Table 4.1. The value increased from 0.027 to 0.037 and 0.041 V outlining the energy lost in term of reduction potential. Moreover, the ohmic energy lost was also noticed in the anode component starting from 0.390 to 0.433 and 0.745 Ω. High resistance value caused more energy lost in the anode. However, there was not consistent pattern observed from potential lost in electron transfer coefficient γ between bulk solution and electrode surface except ω for current consumption per electrode surface area. The ω explained the energy lost in term of current consumption per surface area and MFC group 1 posted the lowest current consumption rate in anode compared to group 2 and 3.

Table 4.1 Coefficients calculated from polarisation Equation 4.1 based on different internal resistance

Coefficient	MFC Group 1 (13 Ω)				MFC Group 2 (61 Ω)			
	Cell	Anode[1]	Cathode[1]	Sum[2]	Cell	Anode[1]	Cathode[1]	Sum[2]
E_o (V)	1.274	-0.256	0.892	1.148	0.762	-0.274	0.596	0.870
b (V)	0.027	0.187	0.219	0.032	0.037	0.190	0.220	0.030
R (Ω)	3.087	-0.390	2.481	2.871	2.250	-0.433	2.144	2.577
γ (V)	0.668	0.152	0.703	0.551	0.203	0.164	0.435	0.272
ω (m^2/A)	-4.937	-46.170	-5.802	-5.558[3]	-20.161	-7.698	-13.799	-8.200[3]

Coefficient	MFC Group 3 (164 Ω)			
	Cell	Anode[1]	Cathode[1]	Sum[2]
E_o (V)	0.923	-0.266	0.788	1.053
b (V)	0.041	0.188	0.223	0.035
R (Ω)	3.188	-0.745	2.691	3.436
γ (V)	0.355	0.156	0.609	0.453
ω (m^2/A)	-10.120	-7.321	-7.545	-6.971[3]

[1]Potential vs. SHE

[2]Equal to cell = (cathode-anode) potential value

[3]Value was calculated based on $\gamma_{sum} \exp(\omega_{sum}) = \gamma_{anode} \exp(\omega_{anode}) + \gamma_{cathode} \exp(\omega_{cathode})$

Electrochemical impedance spectroscopy (EIS) provides non-intrusive technique to examine the electrochemical properties or behaviour posted by MFCs under different internal resistances (Liang *et al.*, 2007; Fan *et al.*, 2008; Manohar and Mansfeld, 2009; Zhang and Liu, 2010). Figure 4.2 shows the spectrograms both taken under OCP and maximum power density conditions. EIS spectrogram consisted of a semicircle connected to a tail as shown in Figure

4.2 (a). Both semicircle and tail contained the electrochemical information of the MFCs especially internal resistance and mass transport properties (He and Mansfeld, 2009; Dominguez-Benetton *et al.*, 2012; Sekar and Ramasamy, 2013; Zhu *et al.*, 2013; Fan and Li, 2016). The first point at the left intercept with the x-axis is the resistance value of electrolyte measured between working and reference electrodes and in this case between anode and cathode. The resistance values of the electrolytes were laid between 5.6 and 8.2 Ω. Meanwhile, the second intercept at the right end of the semicircle is the resistance value of total internal resistance of the cell and the value varied between 13 and 164 Ω. The gap value of the semicircle along the x-axis is known as charge transfer resistance or resistance value without electrolyte where electron transfer across solid materials. Generally, it was understood that the growth of biofilm on the electrode surface contributed to the increases of the internal resistance value (Aulenta *et al.*, 2012; Dominguez-Benetton *et al.*, 2012; Timmers *et al.*, 2012). All MFCs showed the increases in internal resistance measurements after 21 weeks of operation (Figure 4.3). The difference of the internal resistance varied between 1 and 52 Ω and was proportional to initial internal resistance. For example, the maximum difference was 2 Ω for MFC group 1 but it could increase up 52 Ω for MFC group 3. Besides the internal resistance, another EIS was also performed at maximum power density where the current was continuously withdrawn from the MFCs. As oxidation and reduction reactions were continuously performed in the MFC system, mass transfer between bulk solution and biofilm was activated and triggered the instability to the EIS measurement particularly the tail in spectrograms. Nevertheless, MFC with the lowest internal resistance seemed to have less interruption when the current was withdrawn from the cell. The interruption had caused limitation in the reaction rate due to weak bioanode activity (Zhu *et al.*, 2013). This could be observed from Figure 4.2 (a) and (b) where a full semicircle and a half straight tail still could be identified near low frequency (<1 Hz). However, no clear diffusion tail could be identified from MFC group 2 and 3 except the initial semicircle.

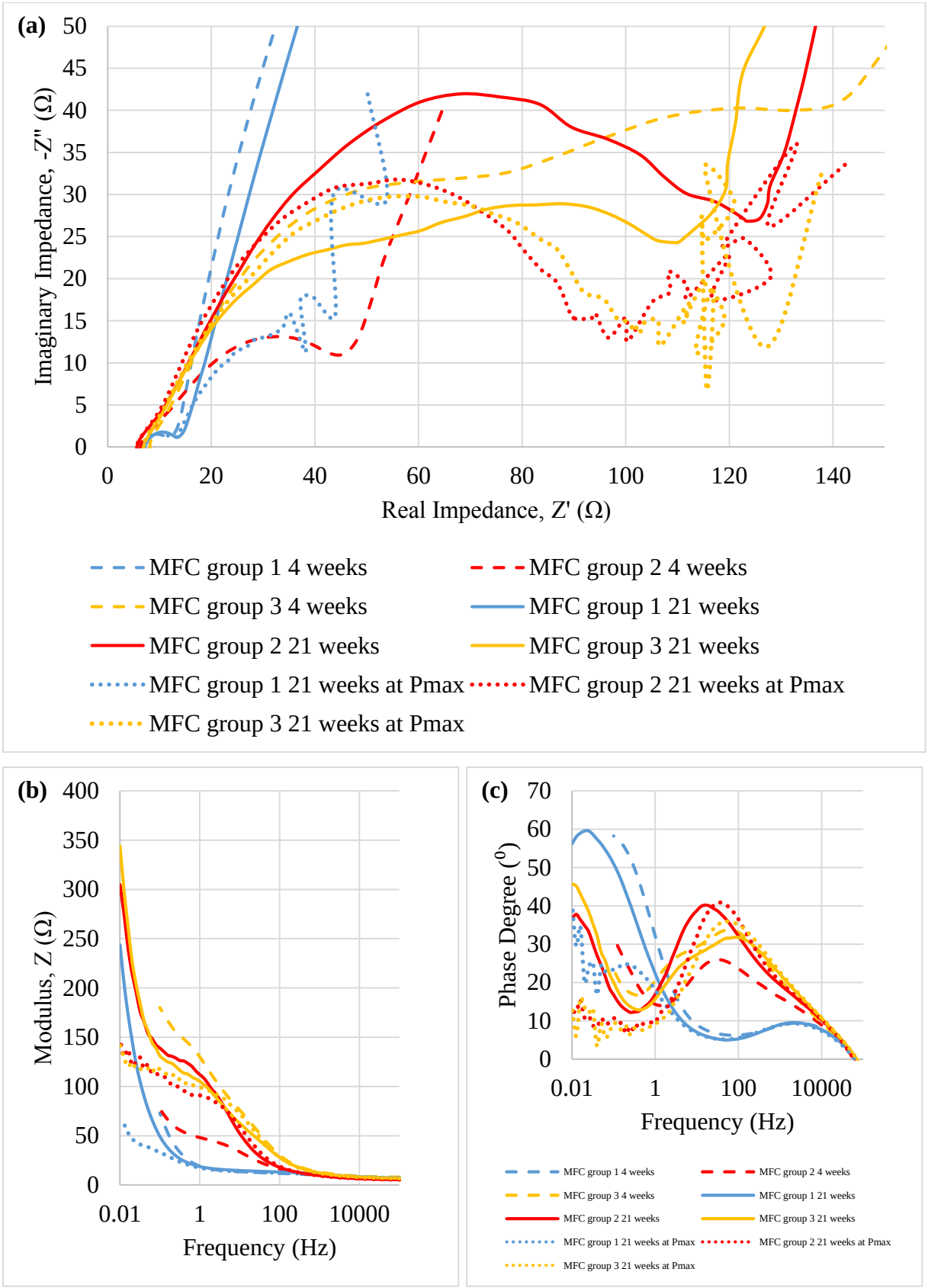

Figure 4.2 Electrochemical impedance spectrograms of MFC measured during and after the enrichment period at open circuit potential and maximum power density: (a) Nyquist (b) Bode magnitude and (c) Bode phase plots.

Next, the MFC component was measured separately and internal resistances were determined using proposed equivalent circuits based on component materials and cell configurations (See Appendix A: Figure A.3 and Table A.1). The data was then used to fit equivalent circuits represent the MFC electrode interfaces and the whole system. For internal resistance, the sum of R-value from each component (electrolyte, anode, cathode and membrane) is equal to the internal resistance of the whole cell. The initial internal resistance value are shown in Figure 4.1 (b) and the values after 21 weeks are shown in Figure 4.3. The internal resistances of MFC group 1, 2 and 3 after 21 weeks were marked as 16, 55 and 182 Ω which was expected slightly higher than the initial values (13, 61 and 164 Ω) due to bacteria attachment. Coefficients determined from the circuit is used to explain the electrochemical properties including resistance and diffusion behaviours in the measured system. Multiple parallel (RQ) group in the circuit displayed the non-ideal state of microbial-electrode interaction which is highly affected by biofilm thickness (Dominguez-Benetton *et al.*, 2012; Sekar and Ramasamy, 2013). The layer tends to act as a double layer capacitance between microbial-electrode interphase by influencing the electron transfer mechanism in the absence of mass transfer control. Nevertheless, each unit component in the equivalent circuit only displayed the dominant behaviour of anode and cathode combination (He and Mansfeld, 2009; Dominguez-Benetton *et al.*, 2012). Therefore, extra EIS measurement for each MFC components is vital to verify those recessive electrochemical properties. For instance, a layer of biofilm cover on anode could change the electrochemical properties due to limiting mass transport and electron transfer. By the time the biofilm growth older and thicker, the domination of the bioanode over metal-catalysed cathode electrochemical properties would take place. As a result, diffusion properties in anode was changed from T to W due to the nature of electrode materials at the beginning of enrichment and biofilm at a stable stage. There is one (RC) unit in the anode equivalent circuit explain the interphase interaction between biofilm and bulk solution and electrode. However, two parallel (RC) units were integrated into the equivalent circuit of membrane component to describe two different electrolytes used in the anode in one side and cathode in another side of the membrane. Meanwhile in cathode air was continuously purged into the catholyte and recycled from a 2L reservoir. Dissolution of oxygen into the catholyte had posted the T diffusion properties besides W which represented the kinetically determining mass transfer between bioanode and bulk solution. Finally, a cell equivalent circuit represented the general properties of all components in the MFC, however, the circuit only showed the master unit which had dominant or total effects to the whole system.

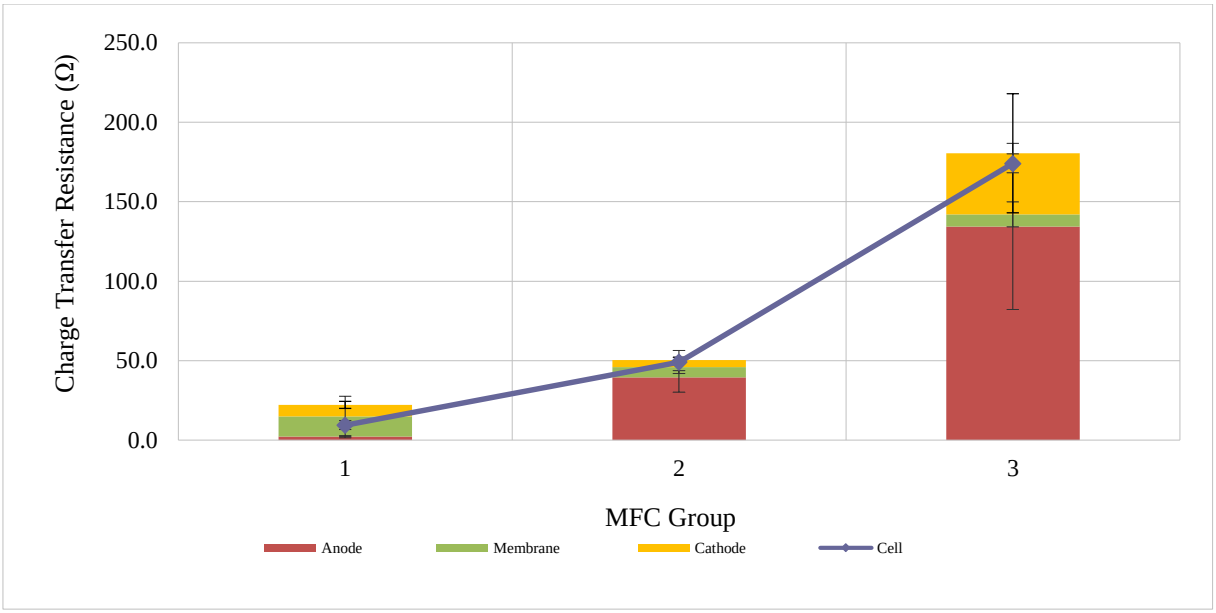

Figure 4.3 Internal resistance values (after 21 weeks of operation) obtained from the equivalent circuit with the best fitting to the spectrograms.

In additional to the EIS method, the bioanode was subjected to multiple cyclic voltammogram (CV) scan. The bioanodes were analysed under a range of scan rate starting from 0.0100 to 0.0005 V/s and then from 0.0005 to 0.0100 V/s. The multiple scans were performed to determine the diffusion properties of the bioanode. Figure 4.4 shows the voltammograms for all tested MECs according to different internal resistance. All of these CV showed the process of the bioanode reaction was irreversible with remarkable oxidation current peak. Even though the process was irreversible, it was noticed that the potential of peak current was maintained at a specific point when the internal resistance was low. At higher internal resistance, the potential tended to shift to more positive when the scan rate was slowly increased. In another word, the rate of peak current potential shifting was proportional to the internal resistance of anode. One of the reason could be the robustness of the enriched bioanode under different internal resistance. Lower internal resistance is good for growing stronger electrogenic microbes to perform substrate oxidation and transfer electrons to anode (Fan *et al.*, 2008; Zhang and Liu, 2010; Rago *et al.*, 2016). When the necessary condition was not optimised (e.g. pH, temperature, conductivity), in this case, the internal resistance, it could cause less electrogenic bacteria to grow and then lost the domination of population in the microbial community. Poor bioanode could be revived after optimised conditions were reintroduced to the system (Zhu *et al.*, 2013). Derivatives of the CVs showing similar interpretations are also attached in Appendix A: Figure A.4. The derivatives were used to check the bioanode oxidation or reactive region

under specific internal resistances. Bioanode enriched under low resistance presented a sharp symmetry peak within a narrow region. However, the peak became lower and border when the resistance was higher. The microbial community might have shifted from single dominated electrogen to more diversified culture as other non-electrogenic microorganisms were also able to grow on the electrode surface under higher resistance (Aelterman *et al.*, 2008; Rago *et al.*, 2016). In addition, a plot of peak current versus square root of scan rate was used to determine whether the oxidation reaction is controlled by diffusion or adsorption as in Appendix A: Figure A.5. The results clearly showed that the reaction was controlled by diffusion when a layer of biofilm established on the electrode surface.

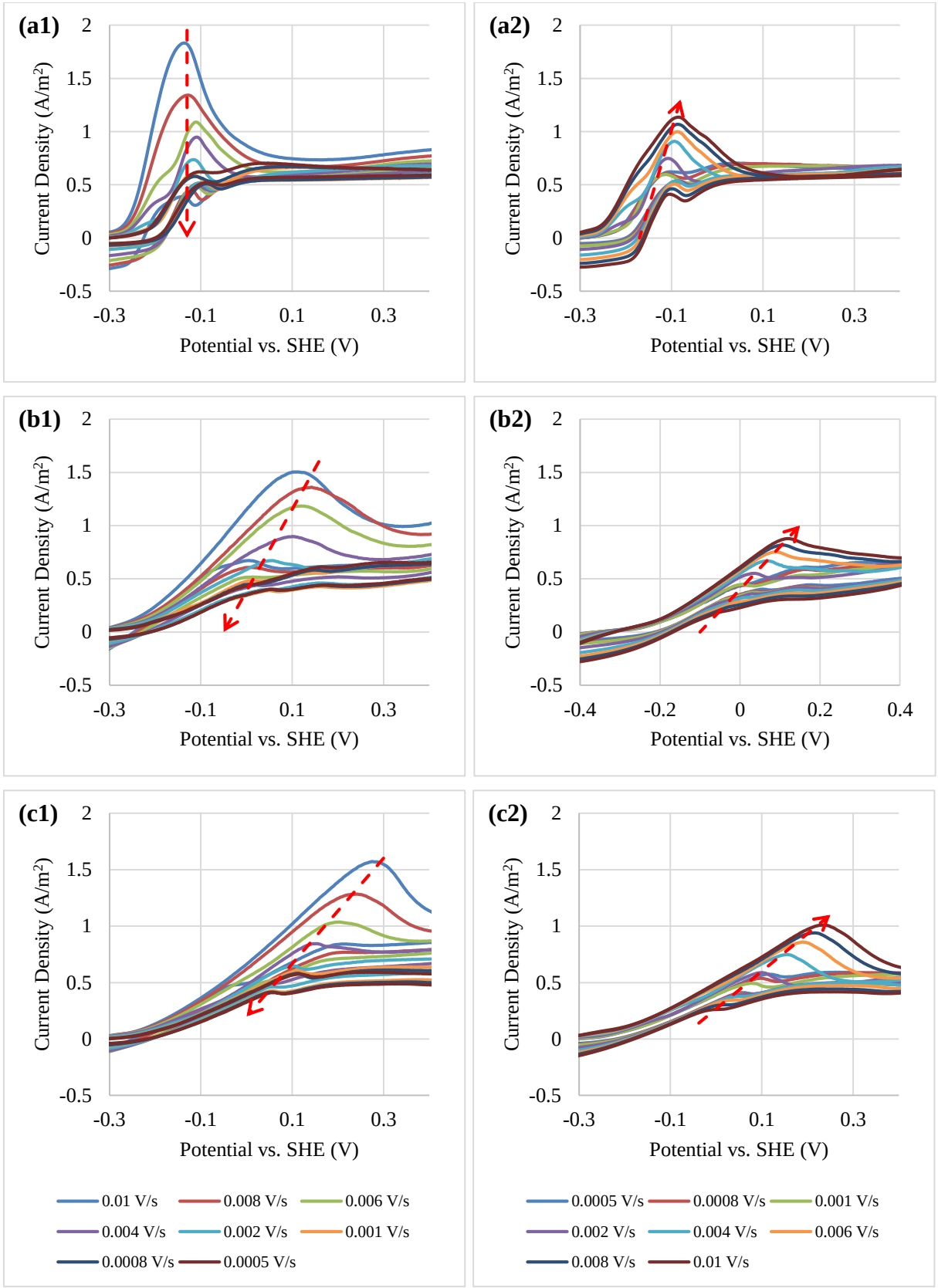

Figure 4.4 Cyclic voltammograms with increment scan rate ranged from 0.01 to 0.0005 V/s (x1) and decrement scan rate from 0.0005 to 0.01 V/s (x2) for MFC group 1 (a1 & a2) and 2 (b1 & b2) and 3 (c1 and c2).

4.3.2. Bioanode performance depends on applied potentials

Four new bioelectrochemical cells were set up in MFC mode, including two controls, with internal resistance in controlled less than 10 Ω. All the operating condition for the controls were the same with experimental bioelectrochemical cells without adding any sources of inoculum. First, the anode of the BECs was inoculated and a stable current was produced after a week of culturing under a fixed potential +0.20 V. Next, the bioanodes were subjected to chronoamperometry for at least a day before cyclic voltammetry analysis. The current density produced based on different applied potentials are shown in Figure 4.5 (a) as computed from the chronoamperometric results (See Appendix A: Figure A.6 (a)). There are two maximum current densities, 0.361 ± 0.034 A/m^2 and 0.372 ± 0.063 A/m^2, observed at 0 and +0.60 V, respectively, through a range of applied potential from -0.30 to +1.00 V. The first maximum current at 0 V was due to the contribution of electrogenic bacteria *Geobacter sp.* based on the inoculums added into the bioelectrochemical cells had been determined dominated by the species (Spurr, 2016). It is postulated that lower enrichment potential (-0.20 - +0.40 V) was the most suitable potential for the growth of dominating electrogenic species such as *Geobacter sp.* (Aelterman *et al.*, 2008; Busalmen *et al.*, 2008; Torres *et al.*, 2009; Ketep *et al.*, 2013; Zhu *et al.*, 2013). Meanwhile second higher current occurred at +0.60 V was suspected to either inducing dominating-electrogenic or non-electrogenic bacteria or both on the anode surface. Acetate-consuming bacteria or fermenters that can use highly poised electrode (e.g.+0.60 V) as electron sink instead of oxygen (O_2/H_2O $E_o{}' = +1.23$ V) might have survived and thrived on the electrode surface (Kiely *et al.*, 2011; Hari *et al.*, 2016). The electrogenic bacteria could also show lower acclimation rate than those acclimated near the potential of outer membrane cytochrome (normally around -0.20 V) (Wang *et al.*, 2009; Zhu *et al.*, 2013). New redox couples were detected which explained that new electron transfer mechanism might be used at this potential (Busalmen *et al.*, 2008). Intensive works have been done to study the effect of fixed potential used to enriched bioanode-respiring bacteria community (Aelterman *et al.*, 2008; Torres *et al.*, 2009; Wei *et al.*, 2010; Zhu *et al.*, 2013). The enriched bioanode posed different electrochemical behaviour and biofilm characteristic when a different potential was applied because of the divergence of bacteria community (Aelterman *et al.*, 2008; Cheng *et al.*, 2008). The lower the applied potential closed to the bioanode midpoint potential tended to suppress non-electrogenic microbes on the anode whilst favouring the electrogenic species and increasing the growth and portion of the electrogens such as *Geobacter sp.* in the bioanode community (Torres *et al.*, 2009; Ketep *et al.*, 2013). Another way of obtaining the highly pure

community is performing secondary enrichment using the culture from primary bioanode effluent (Liu *et al.*, 2008; Ketep *et al.*, 2013). Table 4.2 summarised the enrichment potentials which have been used in previous studies.

Table 4.2 Summary of enrichment parameter applied in chronoamperometry mode to enrich electrogenic consortia at anode. Current density can only be compared within the same study due to various system configurations and substrates were used. The community of microbes diverges as enrichment potential changed from one condition to another.

Enrichment Potential	**Current Density**	**Midpoint potential**	**Main Substrate**	**Microbial Community/Significant Observation**	**Reference**
V (vs. SHE)	**A/m^2**	**V (vs. SHE)**	**mM**		
+0.37	0.600	+0.15	15 (NaAc); 100 (PBS)	16% *Geobacter sp.*	Torres *et al.* (2009)
+0.02	2.000	+0.14		90% *Geobacter sp.*	
-0.09	6.000	-0.16		92% *Geobacter sp.*	
-0.15	10.300	-0.16		99% *Geobacter sp.*	
+0.70	0.046	-0.10	12 (NaAc); 50 (PBS)	Higher enrichment potential favoured bioanode electroactivity as electron transfer components increased	Zhu *et al.* (2013)
+0.20	0.047	-0.10		Power overshoot when higher potential was introduced due to the lack of sufficient electron transfer components to shuttle electrons	
-0.04	0.035	-0.10			
-0.26	0.005	-0.10			
+0.40	2.500	-0.10	10 (NaAc); 50 (PBS)	Dominated *Geobacter sp.*	Liu *et al.* (2008)
+0.40	5.000	-0.10		More dominated *Geobacter sp.* achieved through secondary enrichment	
+0.20	0.636	-0.20	18 (NaAc); 64 (PBS)	Same start-up time; lower respiration rate and highest biomass production at lower enrichment potential	Aelterman *et al.* (2008)
0.00	0.927	-0.20			
-0.20	0.817	-0.20			
0.00	0.600	N/A	10 (Glucose); 50 (PBS)	Lower charge transfer resistance; higher substrate	Wang *et al.* (2009)

				driving force; accelerated start-up time	
1000 Ω[1]	0.086	N/A		Higher charge transfer resistance; lower substrate driving force; slower start-up time	
+0.04	5.500	-0.16	5 (NaAc); 5 (PBS)	Primary enrichment; *Geobacter sp.* and *Desulfuromonas sp.* were dominating species on bioanodes	Ketep *et al.* (2013)
-0.16	6.000	-0.16		Secondary enrichment produced almost the same current as primary enrichment but can survive at lower enrichment potential; *Geobacter sp.* almost disappear	
-0.16	5.650	-0.16		*Desulfuromonas sp.* was the only dominating species after tertiary enrichment; Midpoint potential -0.16V almost disappears after tertiary enrichment.	
-0.16	<0.03	N/A		Primary enrichment produced no current due to low enrichment potential	
+0.40	1.035	-0.11	20 (NaAc); 47 (PBS)	A small amount of biomass was gained while the highest enrichment potential was used and substrate oxidation reduced significantly	Wei *et al.* (2010)
0.00	1.025	-0.11		Biomass was gained and power density was increased; Significant substrate oxidation; current generation was proportionated to biomass for all condition; single culture *Geobacter*	
-0.16	0.660	-0.11			

				sulfurreducens was used in the study	
500 Ω[1]	0.470	-0.11			
+0.40	1.143	-0.23	5 (NaAc); 5 (PBS)	Pure culture *Geobacter sulfurreducens* was used	Bond and Lovley (2003)
500 Ω[1]	0.065	N/A			
+0.8	2.400[2]	+0.70	5.5 (NaAc); 0.43 (PBS)	Pure culture *Geobacter sulfurreducens* was used; new redox couples were detected indicated new electron transfer mechanism was performed at higher enrichment potential	Busalmen *et al.* (2008)
+0.3	1.500[2]	+0.03			

[1] The potentiostat was replaced by a resistance load and the enrichment potential was depended on cathode performance
[2] Normalised current density (ratio value without unit)
[3] NaAc – sodium acetate; PBS – phosphate buffer solution

Chronoamperometric analysis revealed that the enriched bioanode could provide an almost similar current density at the anode potential over 0 V (Figure 4.5 (a)). Cyclic voltammogram (Figure 4.5 (b)) indicated that enriched bioanode from +0.2V can survive at higher poised potential up to 1.00 V. The bioanode enriched at +0.20 V produced two half wave with the midpoint potentials at -0.20 and +0.20 V as shown in Figure 4.5 (c) and probably resulted from different electron transfer mechanisms. A more positive applied potential may also have resulted in a larger current output, especially when the potential was increased more than + 0.40 V. New redox couples at the potential may indicate that new electron transfer mechanism could exist with more positive anode potential (Busalmen *et al.*, 2008). First derivative (Figure 4.5 (c)) analysis showed the first midpoint potential occurred at -0.20 V with both observable active oxidation and reduction activity, however, the second midpoint potential occurred at +0.20 V showed the catalytic activity was weaker compared to the first potential and favours oxidation rather than reduction activity. The - 0.20 V mid-point potential was mainly reported in the literature and confirmed that it was the activity of electrogenic microbes such as *Geobacter sp.* and *Shewanella sp*. (Liu *et al.*, 2008; Marsili *et al.*, 2008; Torres *et al.*, 2009). This could be either due to the multiple redox centres exposed on the surface of the microbes cells or redox–active mediators secreted by specific microbes which have the potential of - 0.20 V (Marsili *et al.*, 2008; Jain *et al.*, 2012; Carmona-Martínez *et al.*, 2013). Dark colour biofilm was found on the surface of the bioanode enriched at +0.20 V. The colour changes have been observed by other researchers as a change of biofilm community on the anode, for example

the colour of the biofilm changed from orange-brown to thinner and darker colour when the potential increase from -0.15 V to +0.37 V (Torres *et al.*, 2009). Based on this report, we suggest that a mixed community dominated by electrogens were grown simultaneously with non-electrogens at +0.20 V. Therefore, the community can survive at higher potential and posing the second catalytic activity on +0.20 V when bioanode potential was fixed >+0.40 V. Nonetheless, the bioanode behaviour fixed at potential more than +0.40 V only showed stronger oxidation activity rather than performing reduction reaction. Free flavins were normally secreted by the electrogen to facilitate the mediated electron transfer between outer membrane cytochromes and electrode (Jain *et al.*, 2012; Carmona-Martínez *et al.*, 2013). Once the flavins had been excreted from the electrogens, they start to accept electrons from cytochromes located at the outer membrane of electrogen and transfer electrons to the electrode in a reducing form. The reduced flavins were oxidised on the anode surface and probably washed out from the continuously-fed bioanode before they could actually recycle back to the electrogens again to transfer electrons.

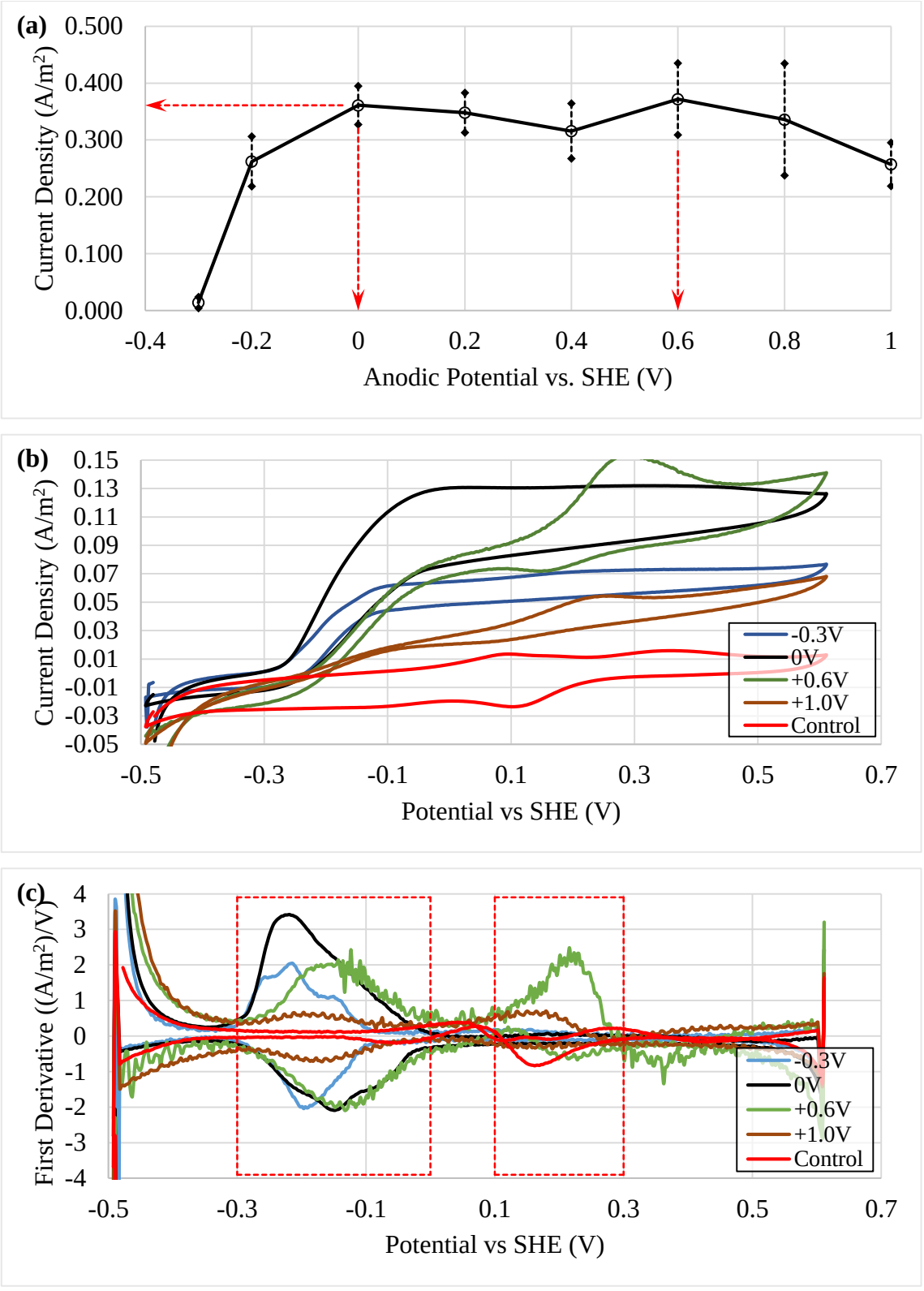

Figure 4.5 (a) Current density produced during bioanode chronoamperometry test at different applied potentials, (b) Response of the bioanode cyclic voltammogram fixed at selected applied potentials, and (c) First derivative of the cyclic voltammograms showing the bioanode active midpoint occurred at -0.20 V and +0.20 V.

Figure 4.6 (a) and (b) show the maximum/minimum point of catalytic waves in Figure 4.5 (b) versus a range of applied potentials. Figure 4.6 (a) revealed that the first electron transfer mechanism (deducted from the catalytic wave occurred at -0.20 V midpoint potential) was still active but exhibit low activity even when the poised potential was set near to the -0.20 V midpoint potential, e.g. -0.30 V. The catalytic wave was intensified while the poised potential was set more positive than -0.30 V. Therefore, more substrate could be converted to electrical current and more electron can be transferred to the electrode (LaBelle, 2009). Electrode with more positive poised potential was favourable for the electrogenic bacteria to discharge their used electron and conserve energy via direct electron transfer (DET) or mediated electron transfer (MET). The catalytic wave started to decrease after the poised potential was set more positive than 0 V. As observed from the first derivative in Figure 4.6 (b), a second catalytic wave started to appear at +0.20 V midpoint indicating that the bioanode could use other pathways to transfer the electron to the anode. Electrogenic bacteria were able to diverge its metabolic pathway to accommodate the changes of conditions for growth and survival, especially when the poised potential was changed from its original condition (Aelterman *et al.*, 2008; Busalmen *et al.*, 2008; Wang *et al.*, 2010; Ketep *et al.*, 2013). In addition to the divergent pathways, the changes of the microbial community that favour particular microbes but suppress the primary electrogenic microbes might be possible as the species can easily adapt to the changes of potential than the primary species in the community (Torres *et al.*, 2009). As a results, the second electron transfer mechanism (catalytic wave occurred at +0.20 V) started to appear when the poised potential was set more positive than +0.20 V. Figure 4.6 (b) shows the catalytic activity reached its maximum/minimum points when the potential was at +0.60 V, however, the catalytic wave decreased back to nearly zero after +0.60 V. There are two possible explanations on the second midpoint activity, either non-electrogen grew together side-by-side with the electrogen to create a robust biofilm that can use a wide range of high potential anode as electron acceptor or the electrogenic microbes had few electrons transfer pathways that could be switched among them when the surrounding environment changes, e.g. from +0.20 V to +0.60 V. Although the bioanode could survive in higher potential, toxic compounds and mineral deposition on the surface of the anode could cause the obstruction to the microbes to transfer electrons to anode surface (Torres *et al.*, 2009; Ketep *et al.*, 2013). Besides, the energy force that drives abiotic reaction, e.g. water electrolysis, was higher compared to biotic reaction when the potential was set more positive (> +0.60 V).

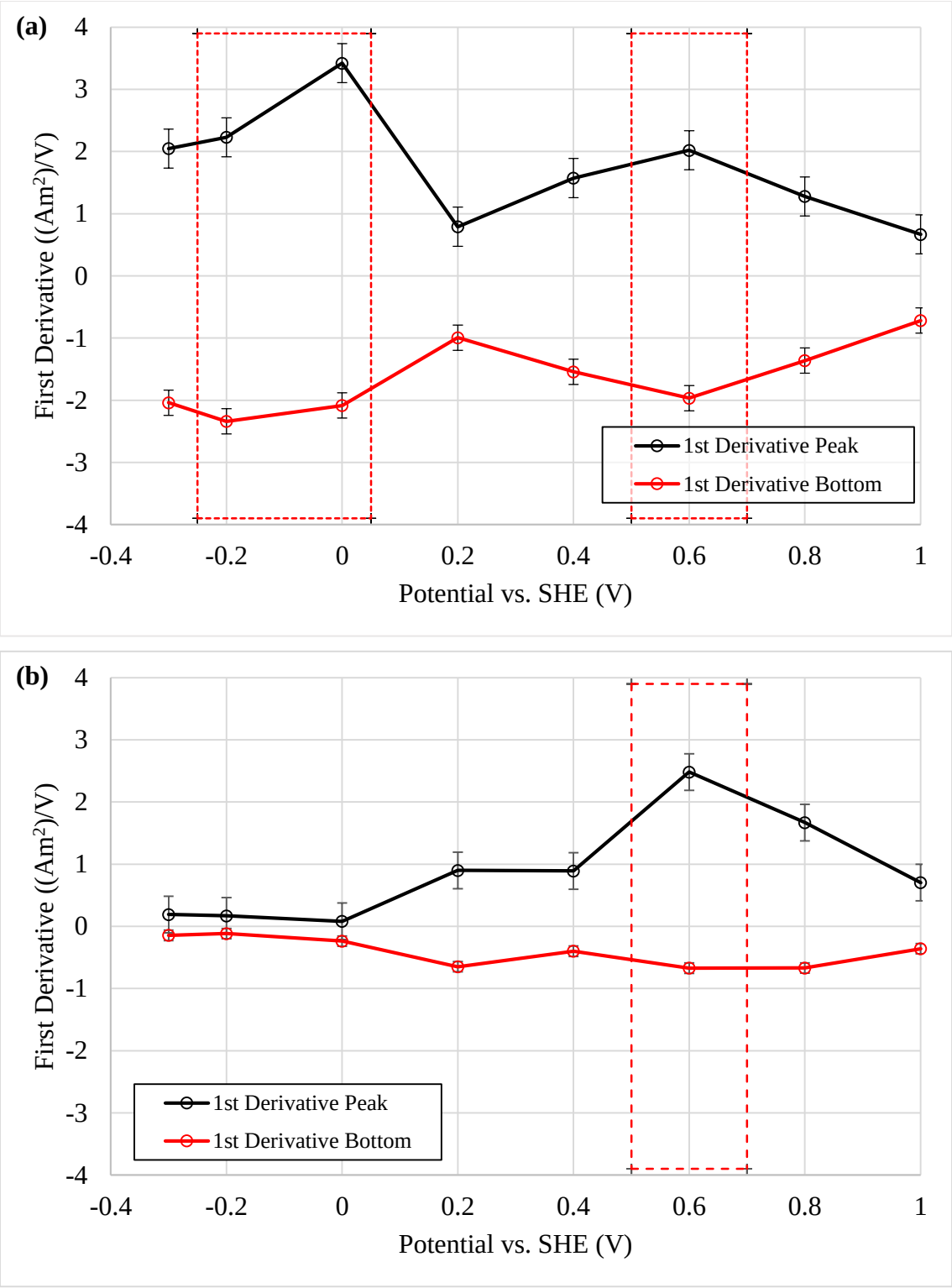

Figure 4.6 The response of peak and bottom values of the catalytic waves at (a) -0.2 V and (b) +0.2 V to different poised potentials derived from the first derivative (Figure 4.5 (c)). The red dash line box emphasises significant catalytic waves in the range of applied potentials.

4.3.3. The effect of buffer and substrate concentration to bioanode performance

Carbon (C), nitrogen (N) and phosphate (P) are three important components known to be essential for microorganism growth especially in wastewater treatment process. For aerobic growth, the required C:N:P ratio is 100:5:1, however, for anaerobic growth, the ratio can be varied from 250:5:1 to 500:5:1 (Thompson *et al.*, 2006). Even though bioanode oxidation activity is an anaerobic process, the required ratio might be different from the conventional wastewater treatment. Kim *et al.* (2004) performed experiments by adding nitrate, nitrite and sulphate to the enriched bioanode. The results demonstrated that nitrate and nitrite (worked as electron acceptors) was significantly affected current generation and COD removal compared to sulphate. Meanwhile, other studies only showed the attractive part of MFC in nitrate/sulphide removal in MFC rather than finding the optimum ratio of C:N:P (Lee *et al.*, 2012; Cai *et al.*, 2014). As phosphate buffer (PBS) was used in this experiment to control electrolyte pH, it should not be interpreted as phosphate source essential for bioanode growth. Meanwhile, C: N ratio was determined in this experiment but was mentioned as acetate (Ac) and nitrate (NH_4^+) to give a clearer definition.

Once the bioanodes were enriched with stable current output, they were tested in different substrate (acetate and nitrate) concentrations to observe the effect of the concentration in term of current density and Coulombic efficiency (CE). Figure 4.7 shows current density and CE plot pertaining to phosphate buffer, acetate and ammonium concentration. To check whether the control could act similar to the new MFC and produce the same current, the inoculum was injected into the control after 22 days of operation. The same behaviour was observed where the control followed the recovering MFC current output and reached maximum current after a week of enrichment (See Appendix A: Figure A.6 (b)). Optimal conditions which favoured the MFC are not only important to produce better current output but also shorten the process of recovery after serious disruption (Ketep *et al.*, 2013; Zhu *et al.*, 2013). First, a range of phosphate concentration was tested in the MFC followed by acetate and ammonium concentrations. It was found that current density and CE were increased when the phosphate concentration was adjusted from 1 to 50 mM (Figure 4.7 (a1)). In addition, different flowrates were applied to bioanode MFC to further check the effect to current density based on the range of phosphate concertation. Figure 4.7 (a2) shows the effect of the flowrates to current generation at specific phosphate concentrations. At low phosphate concentration (1-5 mM), lower current was generated and increased the flowrate of the feed did not improve the performance. However, the performance started to improve when higher phosphate concentration (10-20 mM) was used

in the flowrate tests. A significant current density increased from 0.8 to 1.3 A/m^2 when the flowrate was adjusted from 0 to 3.5 mL/min using the 20mM phosphate concentration. Phosphate buffer not only used to control pH in the solution but also contributed to the increases of the ion balances and conductivity (Fan *et al.*, 2007; Ahn and Logan, 2013). MFC exhibited better performance when more ions were available in the solution by increasing conductivity strength between anode and cathode.

Second, acetate and then ammonium was added into the bioanode MFC to determine the optimal concentrations. In both parameter tests, the optimal concentration for acetate was determined as 10 mM. Higher concentration than 10 mM did increase the current density but in a much slower rate than from 1 to 10 mM. In contrast to the current density, CE was decreased when acetate concentration was increased from 1 to 50 mM. Modified Monod equation was used to determine the Monod coefficient I_{max} and K_s as mentioned in Equation 6 (Zhu *et al.*, 2013; Foad Marashi and Kariminia, 2015). Based on the equation, I_{max} and K_s were determined as 0.5138 A/m^2 and 1.5163 mM. In this study, 10mM acetate concentration was used because it is the most applicable concentration which could sustain about 86.8% of I_{max} and 45 % Coulombic efficiency. Even higher acetate concentration (>10 mM) could bring up the current density (93.0 % of I_{max}), the CE dropped significantly to 15 % at 20 mM acetate concentration. Meanwhile, low acetate concentration (<10mM) generated a lower current which may jeopardise the whole MEC system in term of energy recovery. As a result, there would be not enough electrons to be supplied to the cathode for hydrogen evolution.

Thirdly, there was an insignificant effect on ammonium concentration in term of current density. When the concentration rose from 1 to 20 mM, the current density was almost remained at 0.5 A/m^2. A small raise in the electrical current output might be due to the increases of electrolyte conductivity when more ammonium ion was introduced (Shcherbakov *et al.*, 2009; Karthikeyan *et al.*, 2016). However, Coulombic efficiency was increased remarkably from 43 to 70 % indicating the importance of the nitrogen source to support the oxidation of carbon source, which is acetate in this study. While carbon source was used as energy source for the bioanode to grow and maintain metabolic activities, nitrogen source was used as important building block to construct cell components. Therefore, the ratio of carbon to nitrogen source is an important parameter to keep the bioanode healthy (Thompson *et al.*, 2006; Zhang *et al.*, 2013; Sawasdee and Pisutpaisal, 2015; Cerrillo *et al.*, 2017).

Lastly, the changes of pH and conductivity related to phosphate, acetate and ammonium concentration were recorded (See Appendix A: Figure A.7). The control of the pH to nearly neutral was possible when higher phosphate was contained in the medium. However, the pH of

the effluent was shifted away from neutral to nearly 6.0 with increased buffer concentration. It could be explained that higher phosphate content actually increased conductivity value by adding more ions to the medium (Fan *et al.*, 2007; Ahn and Logan, 2013). As a result, it improved acetate oxidation and the process released more proton that caused pH to drop even higher phosphate concentration could not control the pH at 7.0. For an estimation, 10 mM of acetate could produce 90 mM of proton according to the reaction formula: $CH_3COO^- + 4H_2O \rightarrow 2HCO_3^- + 9H^+ + 8e^-$ and the pH generated by the total released proton could be as lower as 1.0. The phosphate buffer used in the experiments consisted of Na_2HPO_4 and NaH_2PO_4 mixture. For preparing 50mM phosphate buffer, 29 mM of Na_2HPO_4 and 21 mM of NaH_2PO_4 are required to maintain the medium pH at 7.0. That means that the buffer is able to handle up to 29 mM of proton released from acetate oxidation or maximum 3.2 mM acetate concentration. Meanwhile, pH of fresh medium also increased proportionally to acetate concentration except for ammonium concentration. All conductivity figures showed increment value with increases concentration because more ions were available in the medium. By considering the current generation, Coulombic efficiency and pH shift by relating to the tested parameters: phosphate, acetate and ammonium concentrations, the optimum ratio was determined as PBS:Ac:NH_4^+ = 50:10:10 mM.

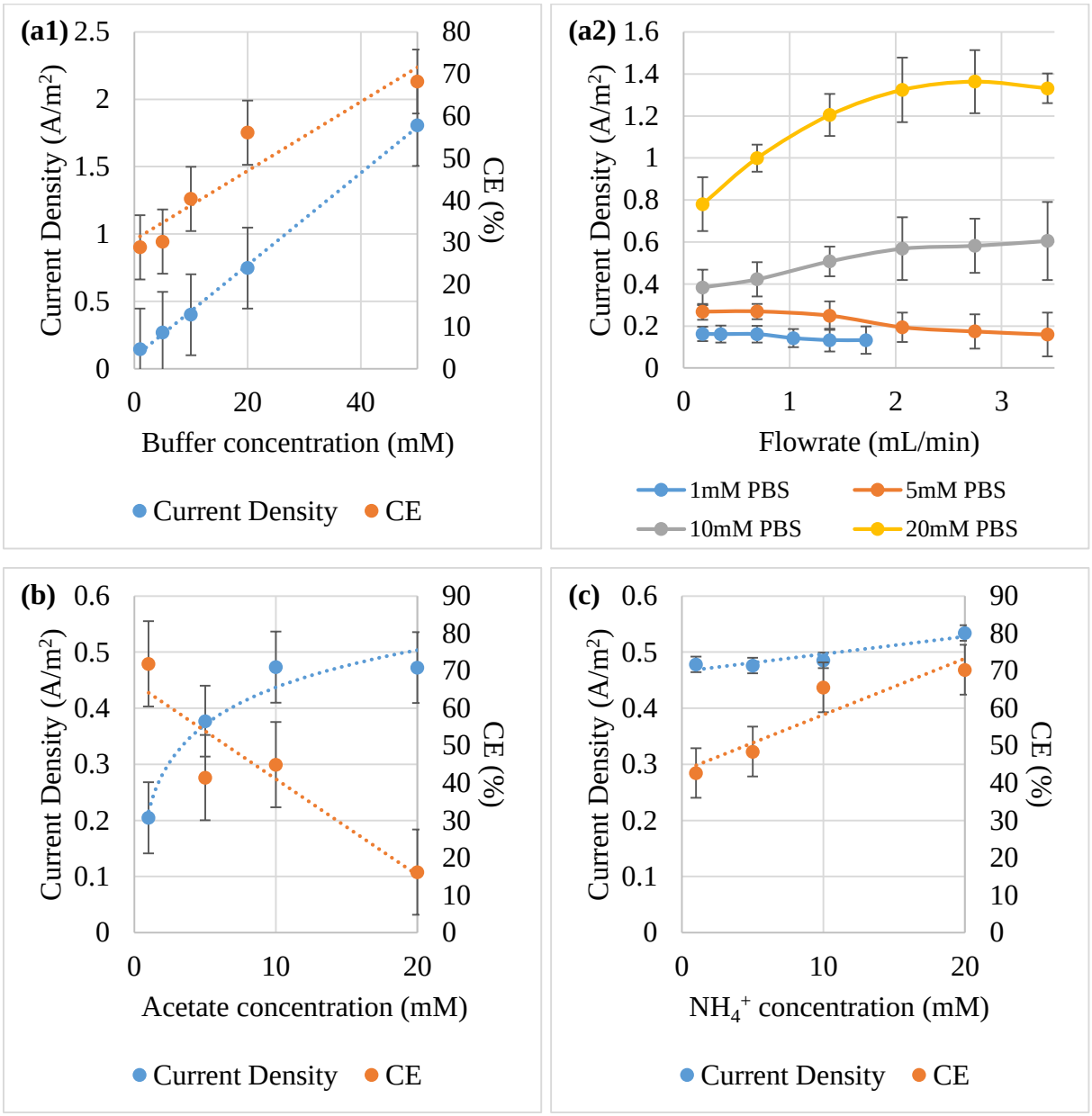

Figure 4.7 The effect of (a) phosphate buffer, (b) acetate and (c) ammonium concentration to current density and Coulombic efficiency (CE) of bioanode fixed at +0.20 V vs. SHE.

4.3.4. Bioanode limits biocathode performance in microbial electrolysis cell

All enriched bioanodes from the previous experiment were further deployed in dual-chamber MECs for examining biocathode performance. Figure 4.8 (a) shows the cell and electrode potentials of the control cathodes (without inoculum) and biological MECs recorded under

chronoamperometric tests. Interestingly, bioanode as a biocatalyst maintained its potential in between -0.30 ± 0.02 V when -0.50 to -0.80 V potentials were applied on the cathode. Even though the bioanode could maintain its potential when cathode was set as low as -0.8V, it started to lose its performance when more current was required to draw from the anode to support cathode at higher working potential more than -0.90 V. On the other hand, the control anode could maintain its potential until -0.90 V was applied to the cathode.

Cyclic voltammetry was performed on both bioanode and biocathode after each chronoamperometric test. Figure 4.8 (b) and (c) shows the voltammograms of the biocathode and bioanode, respectively. On the other hand, the relationship between hydrogen production and current density with cathodic potentials is shown in Figure 4.8 (d). By analysing the biocathode voltammogram, the first catalytic activity occurred at -0.35 V which is suspected to be the non-hydrogen-producing activity whilst the second catalytic activity started to occur at -0.80 V and below. A small hydrogen oxidation peak happened at -0.60 V proved the biocathode reversible catalysis activity accelerated by a specific enzyme called hydrogenase (Aulenta *et al.*, 2012; Batlle-Vilanova *et al.*, 2014). Meanwhile, based on Figure 4.8 (c), bioanodes which worked as counter electrode lost their ability to catalyse oxidation reaction after the chronoamperometric test. As per hypothesis mentioned in the introduction, the amount of electron consumed in cathode should be, at least, fulfilled by the electron produced by anode by substrate oxidation to balance and/or reduce energy demand from an external power supply, the bioanode no longer retain its bio-catalytic activity at the end. For instance, at cathodic potential -1.00 V, the current density was recorded as 0.99 A/m^2 but the maximum current density that the bioanode could produce was 0.36 A/m^2. The bioanode, at least, need to provide an extra 0.63 A/m^2 to close this energy gap. As a result, of they could not produce enough current to support the biocathodes, power supply forced anode potential to increase sharply (-0.28 to +1.26 V) to induce abiotic reaction e.g. water electrolysis or produce peroxides with the presence of oxygen. The growth of the bioanode was totally halted and probably killed by toxic products produced abiotically through a high potential. Moreover, oxygen may be produced from water electrolysis because more positive potential was applied to the anode after the biofilm could not keep up its oxidation activity to produce more electron. Additional oxygen contamination in the system would subsequently trigger the formation of peroxides and other inorganic anions which are toxic to the bioanode (Milner, 2015). The abiotic reactions were dominated in the anode as power supply had to withdraw high current from the anode to support the current consumed in the cathode. There was no considerable current flow or hydrogen production activity when applied potential was set from -0.50 V to -0.70 V as shown in Figure

4.8 (d). Although substantial current started flowing into the biocathode at -0.8V, the current yet favoured any hydrogen production in the biocathode unless more negative potentials (-0.90 to -1.00 V) were used. Cathodic overpotential could be the main reason why potentials lower than -0.80 V was required (Rozendal *et al.*, 2008; Jeremiasse *et al.*, 2010). Theoretically, hydrogen evolution potential is -0.42 V (Nernst equation, pH 7.0). That means at least -0.38V was lost in term of overpotential in this setup. The outcome is accordant to the previous study on a hydrogen-producing microorganism, *Desulfovibrio sp*., that equal or less reducing potential than -0.90 V is needed due to insufficient electron transfer above -0.80 V (Aulenta *et al.*, 2012). In contrary, mediators were used to reduce the overpotential between cathode and cell surface and facilitate electron transfer. Villano *et al.* (2011) tested methyl viologen in their study and proved that the mediator could effectively reduce the overpotential up to 0.30 V and brought the potential closed to -0.45 V, which is slightly lower than standard hydrogen reduction potential -0.41 V. However, the latter solution appears not suitable in practical application as mediator will be required most of the time.

Abiotic current flow became significant with an applied potential more negative than -0.90 V. However, the biocathode only consumed a significant amount of energy starting from -0.70 V and below as moderate current flow was observed at this point. Therefore, the working potential of biocathode in this system should be between -0.70 to -0.90 V. In order to protect the bioanode from losing its performance as a biocatalytic electrode, the maximum current that can be withdrawn from the bioanode is determined as 0.36 A/m^2 from Figure 4.5 (a). If the same amount of energy was required to support the biocathode then the maximum working potential that can be applied is about 0.84 V which is determined from Figure 4.8 (d) assuming that the same amount of current produced in anode was supplied to the cathode. This information is important to determine the optimum condition for the system to promote biohydrogen production and not water electrolysis. A significant amount of hydrogen production rate (2.05 L H_2/m^2 cathode/day) was recorded at -0.90 V even a reductive current (-0.19 A/m^2) was significant observed before this potential (-0.80 V). It seems that minimum energy is required to overcome the activation energy, which leads to overpotentials and activate microorganism's hydrogenase to produce hydrogen. A strategy to applied lower potentials in chronoamperometry form was used in a few studied to examine hydrogen production until a significant hydrogen volume was detected (Aulenta *et al.*, 2012; Batlle-Vilanova *et al.*, 2014). The reason why higher potential was required is to compensate for the hydrogen lost by diffusion and overpotentials such as higher pH electrolyte. Another strategy to promote hydrogen production is to keep hydrogen partial pressure as low as possible by continuously

removing it from the system and maintain the pH of the electrolyte at least around 7.0 (Rozendal *et al.*, 2008). The pH of the electrolyte is normally maintained between 6.5 to 7.5. If the value is lower than 6.0 or under acidic condition, less energy will be consumed and higher applied potential (>-0.7V) could be used when higher proton concentration is available in bulk solution (Batlle-Vilanova *et al.*, 2014; Kumar *et al.*, 2017). The latter strategy did increase the hydrogen yield, however, it also could increase the cost of investment and operation because of the complexity of the system configuration and control devices that had been used. Furthermore, a portion of hydrogen lost through the membrane depends on operating temperature. Higher temperature tends to increase the diffusion coefficient as reported in Rozendal *et al.* (2008). Besides, it also depends on the nature of the MEC either to produce hydrogen or clean inorganic matters. For instance, standard reduction potential of sulphate (SO_4^{2-}/HS^- -0.213V; SO_4^{2-}/S^0 -0.191V) is much lower than proton production (H^+/H_2 -0.414V) (Coma *et al.*, 2013; Luo *et al.*, 2014). If the MEC system was used to clean sulphate contaminates instead of hydrogen production, then slightly higher potential could be applied. Table 4.3 presents an overview of the usage of biocathode in hydrogen production and non-hydrogen producing purposes.

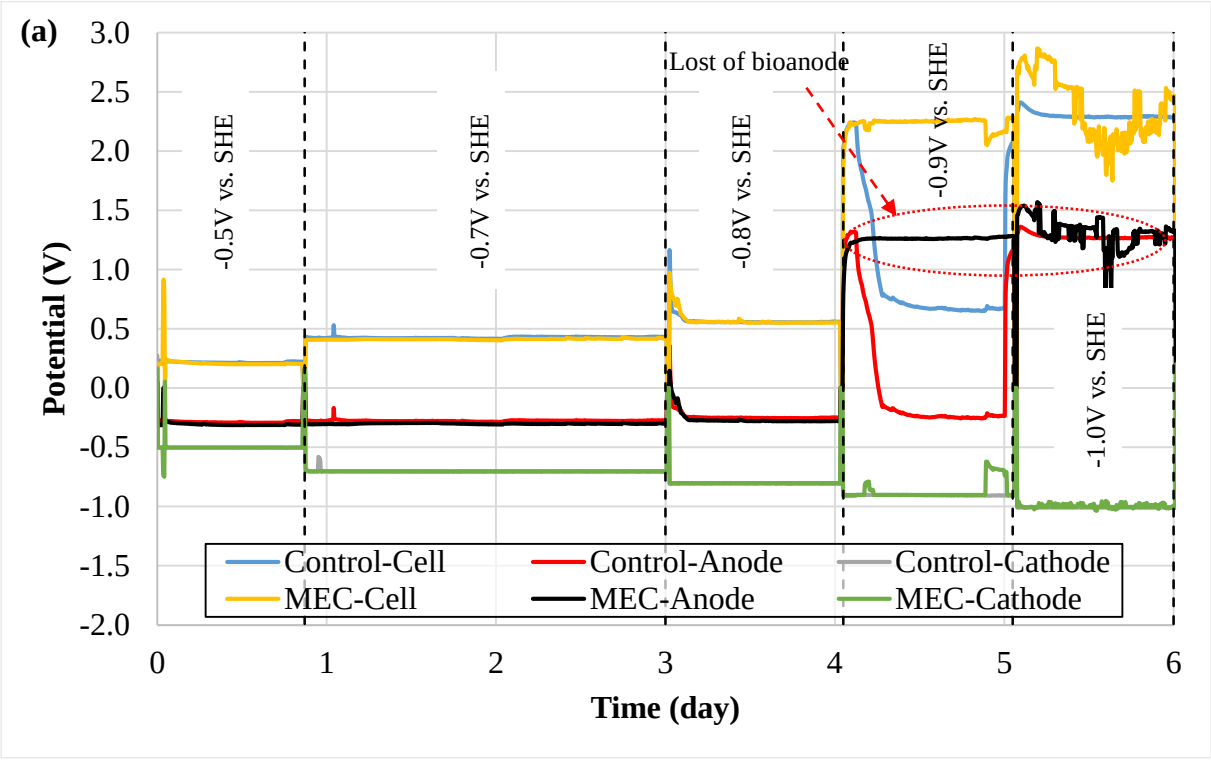

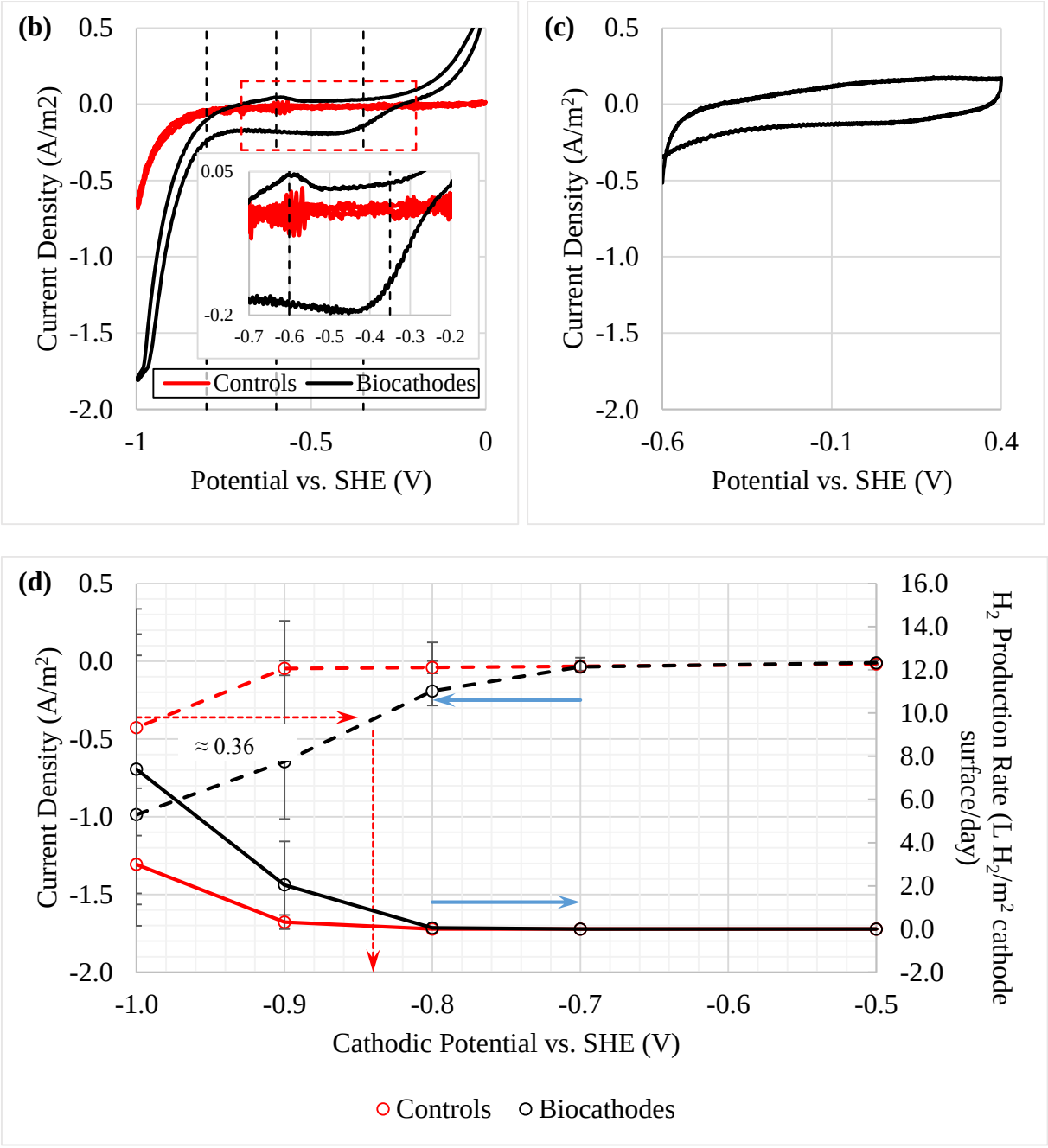

Figure 4.8 (a) Cell and half-cell potentials of control cells and full biological MECs; (b) cyclic voltammogram of biocathodes after chronoamperometric tests. A magnified graph is inserted showing a small active midpoint potential at -0.6V where hydrogen was oxidised; (c) cyclic voltammogram of bioanodes after biocathode chronoamperometric tests; (d) Current and hydrogen production across a range of applied potential. Noted that the red dash line was used to determine the upper limit potential that could be applied on the cathode assuming maximum current was produced at bioanode.

Table 4.3 Overview of the use of bioelectrodes reported in the literature

Cathodic potential	**Current Density**	**Hydrogen production rate**	**Hydrogen recovery**	**Vital ingredient in catholyte**	**Biocathode catalyst**	**Vital ingredient in anolyte**	**Bioanode catalyst**	**Mode of operation**	**Reference**
V (vs. SHE)	**A/m^2**	**m^3 H_2/m^3 reactor/day**	**%**						
Double-chamber MEC with both electrochemically active bioanode and biocathode									
-0.70	3.30	0.04	21	CO_2	Enriched electrochemically active culture from MEC	Acetate	Enriched electrochemically active culture from MEC	Continuous	(Jeremiasse *et al.*, 2010)
-0.75	4.40	0.01	-	CO_2	Hydrogenophilic dechlorinating culture	CO_2	Hydrogenophilic dechlorinating bacteria	Batch	(Villano *et al.*, 2011)
-1.00	0.99	0.17	96	CO_2	Enriched electrochemically active culture from MFC	Acetate	Enriched electrochemically active culture from MFC	Continuous	This study
Double-chamber Half-cell MEC focused on biocathode performance									
-0.70	1.20	0.63	49	CO_2	Effluent from an active bioelectrochemical cell	Ferricyanide/ferrocyanide	-	Continuous	(Rozendal *et al.*, 2008)
-0.70	0.60	2.20	-	Acetate then CO_2	Inoculum from UASB and enriched over 5 years in MECs	Ferrocyanide	-	Continuous	(Jeremiasse *et al.*, 2012)
-0.75	1.88	9.2 L H_2/m^2/day	-	CO_2	Mixed microbial consortia from pond sediments and WWTP anaerobic digester	Phosphate buffer	-	Batch	(Jourdin *et al.*, 2015)
-1.00	47 A/m^3	0.89	175	CO_2	Inoculum from urban WWTP and MFC treating WW	Same as catholyte	-	Batch	(Batlle-Vilanova *et al.*, 2014)
-0.90	3.00	8 mM/day	100	Lactate + SO_4^{2-}	*Desulfovibrio paquesii*	Same as catholyte without Lactate + SO_4^{2-}	-	Batch	(Aulenta *et al.*, 2012)
MEC with abiotic cathode									
0.8 [1]	11.00	1.54	54	Same as anolyte	Platinum-coated cathode	Acetate	Inoculum from previous working MFC	Single-chamber MEC; batch	(Rago *et al.*, 2016)
0.8 [1]	1.27	0.22	73	Same as anolyte	Type 304 Stainless steel mesh 60	Acetate	Pre-colonised bioanode in two-chamber MFC	Single-chamber MEC; batch	(Rivera *et al.*, 2017)
1.0 [1]	2.30	0.3	23	Gas collection chamber without solution	Platinum-plating cathode	Acetate	Effluent from an active bioelectrochemical cell	Double-chamber MEC; continuous	(Rozendal *et al.*, 2007)
3.0 [1]	7.50	0.38	49.5	Same as anolyte	Ti/RuO mesh cathode	Liquid fraction of pressed municipal solid waste (LPW) pH 5.5	MEC fed with grounded submerged aquatic plants	Single-chamber MEC; batch	(Zhen *et al.*, 2016)

0 [2]	-	-	-	Bicarbonate buffer	Platinum-coated cathode	Propionate	Camel manure and anaerobic digested sludge	Double-chamber MEC; batch	(Hari *et al.*, 2016)
-0.55 [3]	2.67	H_2 started to produced when anodic potential < -0.15	-	Phosphate buffer solution	Platinum-coated cathode	Acetate	Sewage sludge from municipal WWTP	Double-chamber MEC; batch	(Wang *et al.*, 2010)
-1.059	9.63	0.51	19.84	Same as anolyte	Activated sludge	Acetate	Activated sludge	Single-chamber MEC; batch	(Liang *et al.*, 2014)
MEC where the biocathode is not for hydrogen-producing purpose									
-0.2	+75 mA	Alkalinity produced from cathodic denitrification partially (19%) neutralised the acidity of the anodic reaction	85.3 [4]	Acetate	Activated sludge from municipal WWTP	same with catholyte without Ac or NO_3^-	-	Half-cell double-chamber MEC; continuous	(Cheng *et al.*, 2012b)
	-40 mA		87.3 [5]	NO_3^-					
-0.4	0.03	1.9g/L acetate; 2.09 g/L propionate; 2.25 g/L butyrate; 26.82 mg/L butanol; 16.04 mg/L ethanol; 0.16 mmol H2 (after 70 days operation)	-	CO_2	Pre-enriched culture from bog sediment	Same as catholyte	Pre-enriched culture from bog sediment	Double-chamber MEC; batch	(Zaybak *et al.*, 2013)
0.8 [1]	-	0.49 mg/day SO_4^{2-} removal	5.9 [6]	SO_4^{2-}	Pre-enriched domestic WW using 0.1 g/L SO_4^{2-}	Acetate	Enriched electrochemically active culture from previous MFC treating phenol	Double-chamber MEC; fed-batch	(Luo *et al.*, 2014)
	-	5.81 mg/day SO_4^{2-} removal	47.7 [6]					Double-chamber MEC; continuous	
-0.9	-	39 % SO_4^{2-} removal	27 [6]					Double-chamber MEC; fed-batch	

[1] Applied voltage between anode and cathode

[2] Anodic potential was controlled, no cathodic potential was recorded

[3] determined from graph at 0.6V applied voltage

[4] Coulombic efficiency for substrate oxidation

[5] Cathodic denitrification

[6] calculated based on electron recovery

4.3.5. Energy recovery and overall performance

Figure 4.9 (a1) and (a2) are summarised to show the reaction efficiency (in term of electron transfer) of a single electrode (anode or cathode). Hydrogen was produced in the cathode, therefore, the amount of electron required to produce certain amount of hydrogen was calculated and shown in Figure 4.9 (a1). In anode, electrogenic bacteria consumed acetate to produce electrons and use the anode as electron sink to dispose of the electrons. However, electron transfer was measured as current flow between anode and cathode. In addition, not all current was provided by substrate oxidation in the anode and a larger portion was supplied by an external power supply. As a result, the Coulombic efficiency as shown in Figure 4.9 (a2) experiencing spiked percentage (up to 9700 %) is due to the overestimation. Meanwhile, Figure 4.9 (b1), (b2) and (b3) are presenting the energy recoveries in term of hydrogen either provided by external power, bioanode or both external power and bioanode. On the one hand, energy recovery provided by external power (Figure 4.9 (b1)) was nearly 100% at applied potential -1.0 V. On the other hand, the same spiked percentage as observed in Figure 4.9 (a2) was appeared in Figure 4.9 (b2) while the recovery values were recalculated using the same hydrogen production values. It seems that external power supply plays an important role in driving hydrogen production in cathode rather than electron-producing bioanode. For instances, at cathodic potential -1.0 V, η_s biocathode was significantly high about 1317% and it means the larger portion (1317-100=1217%) of the hydrogen recovery was not mainly contributed by substrate oxidation in bioanode. However, it is quite opposite for η_e biocathode where the efficiency is 103% where the excessive 3% was not provided by the electrical energy (Call and Logan, 2008; Logan *et al.*, 2008). As hydrogen production was a joint contribution of external power and bioanode energy sources, Figure 4.9 (b3) is presented to show overall energy recovery which is more accurate than only considering one energy source. From the figure, overall energy recovery was first observed starting from -0.8 V while the control still remains zero. A remarkable overall recovery of nearly 96 % was recorded at -1.0 V.

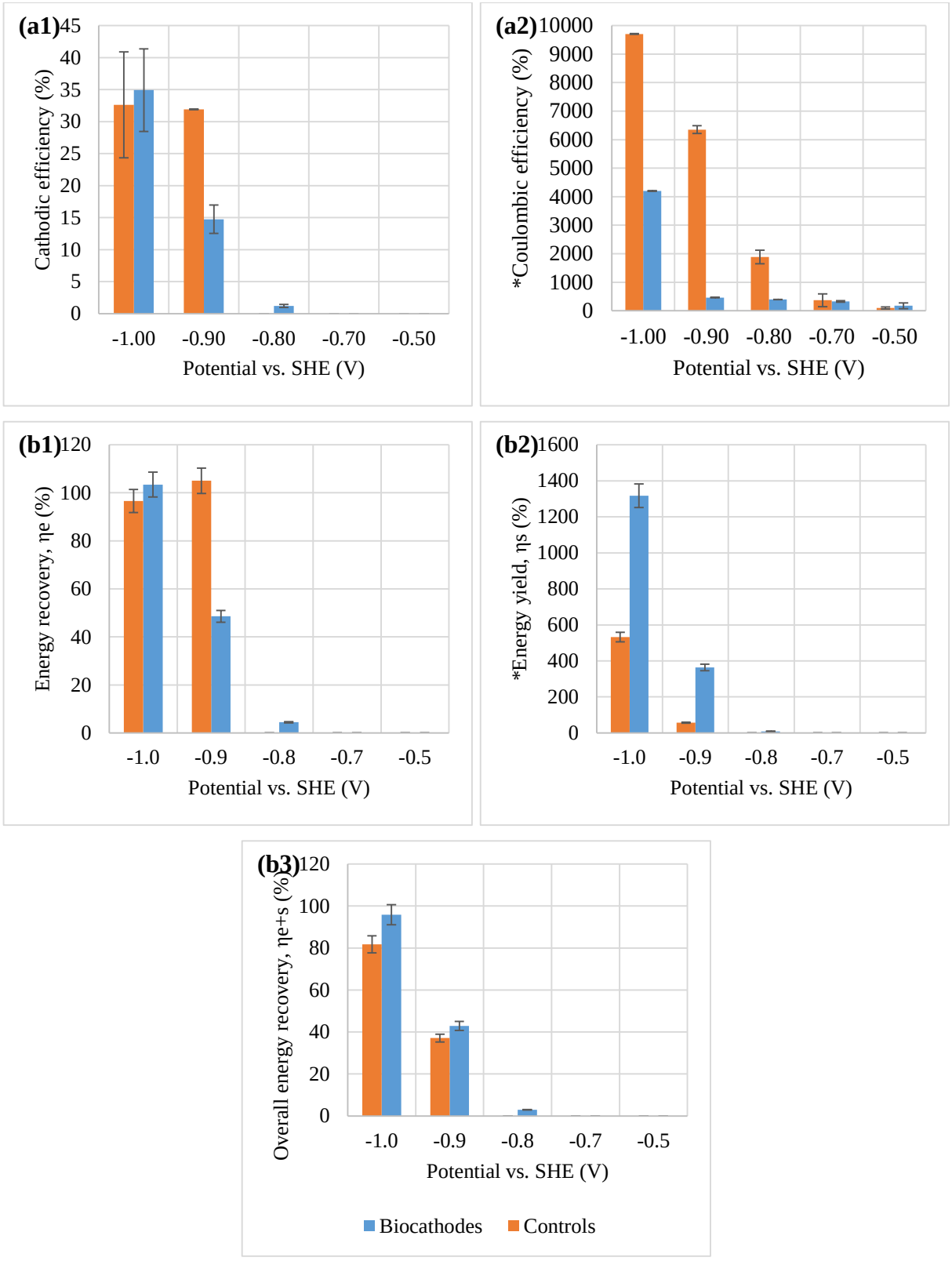

Figure 4.9 Cathodic (hydrogen production) efficiency (a), Coulombic (bioanode) efficiency (b), energy (external power) recovery (c), energy (bioanode) yield (d) and overall energy (external power and bioanode) recovery (e) from MECs at different applied cathodic potentials. *Calculated based on the maximum oxidation activity of bioanode at 0 V

4.4. Conclusion

This study demonstrated that the performance of bioanode can be a factor that can limit the biocathode in a MEC system. To provide a better bioanode, all condition must be considered included internal resistance, medium concentration and enriched condition. The internal resistance should be kept as low as possible to maintain maximum oxidation reaction in bioanode and decrease overpotential lost. Besides, the environment in the anode especially the medium should contain certain ratio of reactants that may increase electrogen metabolic activity and promote oxidation reactions. The effect of buffer (phosphate-based), reactants (acetate and ammonium) was studied. The optimal PBS:Ac:NH_4^+ ratio was found as 50:10:10 mM after considering the tested parameters' responses to the current output, Coulombic efficiency, pH and conductivity. Then after, bioanode enriched at -0.2V vs. SHE was discovered can survive at higher applied potential up to 1.0V and posted two significant catalytic activities at midpoint potentials -0.2V and +0.2V. The catalytic waves could be shifted between each other depending on the potentials fixed on the anode. This may due to community shifted or the changes in metabolic pathways of dominating microbes. Meanwhile, biocathode could produce hydrogen with applied potential lower than -0.8V. However, the applied potential -0.9V on biocathode killed the bioanode as it was not able to generate enough current to support the need of the biocathode. In the operation of a biocathode, the potential vs. current density behaviour for effective operation during hydrogen evolution may not be compatible with the effective operation of the bio-anode. The obtained current density may result in less than ideal anode potentials for effective anode biofilm operation at given cathode potential. Applied potential of 0.84V was determined as the maximum value that can be applied to biocathode without overloading the bioanode. The capability and robustness of bioanode are important to ameliorate the limitation to biocathode and the whole system.

Chapter 5. Operating conditions of a hydrogen-producing biocathode

5.0. Chapter summary

A comprehensive study of hydrogen-producing biocathode (HPB) was discussed in this chapter. Apart from enriching and confirming biotic cathode, the biocathode was also subject to applied potential and reactants tests. The biocathode behaviours were recorded and analysed through different electrochemical methods while its performance was determined hydrogen production rate and efficiency. Possible hydrogen producing mechanisms were also studied and proposed. In addition, the bottleneck of the usage of biocathode and long term operation were discussed.

*Part of this chapter has been published in *Frontiers in Chemistry*, 6, p. 318 in 2018 with the title 'Effects of Applied Potential and Reactants to Hydrogen-Producing Biocathode in a Microbial Electrolysis Cell'. Swee Su Lim carried out the experiment and wrote the manuscript with support from Eileen Hao Yu and Keith Scott. Byung Hong Kim conceived the original idea and suggested on the experiment framework. All authors provided critical feedback and helped shape the research, analysis and manuscript.

5.1. Introduction

Since hydrogen-producing biocathode was first introduced by Rozendal *et al.* (2008), biocathode activities in microbial electrolysis cells (MECs) were extensively studied. Combining wastewater treatment and production of hydrogen as an energy carrier makes MECs an attractive technology. As the catalysts used in the cathode are living microorganisms, the associated microbiological knowledge is important for systematic optimisation MECs (Kim *et al.*, 2015). Rozendal *et al.* (2008) used three phase start-up procedures to enrich hydrogen-producing biocathodes in a bioelectrochemical system (BES). A biocathode was obtained by reversing a bioanode. The whole process took less than a month to achieve a fully developed biocathode. Community analysis confirmed that sulphate-reducing bacteria (SRB) belonging to

the genus, *Desulfovibrio,* were the key players in the hydrogen-producing biocathode (Croese *et al.*, 2011; Croese *et al.*, 2014). *Desulfovibrio sp*. conserve energy through a hydrogen cycling mechanism, that involves different types of hydrogenases which are involved in hydrogen production and consumption. A decade after, Jourdin *et al.* (2015) successfully grew an autotrophic biocathode and operated it for nine months. They claimed that a sustainable autotrophic biocathode was involved in hydrogen evolution when suitable cathodic condition was applied with inorganic carbon as the carbon source. The bacteria communities on the biocathode changed over the biofilm enrichment period; a significant increase on *proteobacteria* distribution between initial inoculum and enriched biocathode from 10 to 57% at the end of the experiment. Initial *Archaea* distribution disappeared completely from 30.3% to less than 0.1% of the population. In additional to carbonates serving as the carbon source, both studies added a trace amount of sulphate into the catholyte to grow and maintain their biocathodes. SRB thrived and their domination could be due to the availability and quantity of sulphate present in the catholyte. It has also been showed that sulphate was an important final electron terminal accepter in SRB hydrogen cycling mechanism (Kim and Gadd, 2008; Keller and Wall, 2011; Madigan *et al.*, 2014). Nevertheless, hydrogen production in a SRB dominated biocathode was the main purpose of the studies. Considering the standard reduction potentials of hydrogen and sulphate, hydrogen ($E°$ $H+/H_2$ = -0.41V) requires more energy than sulphate reduction ($E°$ SO_4^{2-}/H_2S = -0.35V). Furthermore, as the reduction potentials are relatively close (-0.06 V), indicates that sulphate reduction could take place in conjunction with hydrogen evolution, and the concentration of sulphate present may impact hydrogen production. Regardless of the standard reduction potential, many studies used much lower potential than -0.41 V in practical condition for biological hydrogen evolution (Geelhoed *et al.*, 2010; Jeremiasse *et al.*, 2012; Batlle-Vilanova *et al.*, 2014; Jourdin *et al.*, 2015). If SRB play an important role in electrochemical hydrogen production, sulphate concentration and its availability should be taken consideration as it will not only affect the current density of BES but also the working potential applied to the cathode. Bicarbonate (carbon source) and ammonium (nitrogen source) were commonly used in the biocathode study which have a direct link to the growth of biocathode but not the case where sulphate is responsible as an electron acceptor and sulphur source. Therefore, sulphate could be the third important parameter after the carbon and nitrogen sources. Some studies presented results where additional acetate could enhance the start-up process of biocathode (Jeremiasse *et al.*, 2012) or by using lactate as organic carbon with high sulphate concentration in pure culture tests (Aulenta *et al.*, 2012). Due to the fact that SRB especially *Desulfovibrio sp.* cannot use inorganic carbon directly as a

carbon source, there must be an active interaction between the species and other autotrophic bacteria in the hydrogen-producing biocathode to use the inorganic carbon as organic carbon. The community interaction between SRB and autotroph acetogens actually happened where only inorganic carbon, such as carbonates were in the solution (Muyzer and Stams, 2008; Mand *et al.*, 2014). Even though SRB specifically *Desulfovibrio sp.* were found responsible for hydrogen production in BES biocathode, questions on optimum operational conditions and the feasibility of the biocathode in real applications still remain unanswered. The changes of influent content in vary inorganic carbon, nitrogen source and sulphate concentrations could shift microbial metabolism and the community and affect whole BES performance.

To fully understand the operational conditions of hydrogen-producing biocathode in a microbial electrolysis cell (MEC), the study of essential parameters and community interaction need to be integrated. Mand *et al.* (2014) proposed that sulphate-reducing bacteria and acetogen's interaction were responsible for steel pipe corrosion. However, other evidence showed that the form of ferrous sulphide layer on an iron sheet due to SRB corrosion was more severe without the sources of organic carbons or presence of acetogens (Venzlaff *et al.*, 2013). The deposited ferrous sulphide works as a semiconductor in anaerobic corrosion by mediating electron flow from metal to the cells and by by-passing the slow reduction of the proton to free hydrogen. The mechanisms of electron transfer are similar to a biocathode enriched from a mixed culture aimed for hydrogen production and could serve as a model for biocathode community interactions. Meanwhile Keller and Wall (2011) studied genetics and molecular level of electron flow in *Desulfovibrio sp.* for sulphate respiration. They reported how the respiration could assist in hydrogen production while reducing sulphate to sulphides. The results also inferred that periplasm hydrogenases play an important role in hydrogen evolution. However, no experiment has been conducted to further examine the hypothesis. In addition, Geelhoed *et al.* (2010) discussed how the key enzymes, [Fe-Fe]- and [NiFe]-hydrogenases, from *Desulfovibrio vulgaris* were involved in hydrogen production. They stressed that utilisation of immobilised whole cells was better and more robust than using only enzymes and therefore co-culture should be considered. As the whole cells and community should be focused, electron transfer within syntrophic partners become important and, from a thermodynamic point of view, hydrogen production via reduction of the proton has to be coupled with energy conservation from hydrogenases. The balance between the conservation energy and hydrogen production indicated that microbial communities in a biocathode are able to grow and maintain their catalytic activity. It was also suggested that studying the correct growth conditions with a carbon source and applied voltage, longevity of the biocathode could be the key issues for

further understanding the electron transport mechanism. Later, Rosenbaum *et al.* (2011) proposed possible direct and indirect electron transfer mechanisms by analysing the literature on hydrogen-producing biocathodes. On the one hand, direct mechanisms were involved in direct electron transfer through *c*-type cytochromes either coupled with or without hydrogenases. On the other hand, indirect electron transfer mechanism relied on natural redox mediators shuttling between cathode and hydrogenases. Surprisingly, they suggested that the biocatalysed reactions were not necessarily an energy conservation process for microorganisms (Rosenbaum *et al.*, 2011). Recently, Kim *et al.* (2015) proposed another electron transfer mechanism, similar to those in microbial influenced corrosion (MIC) and showed a sound reason that biocathode should conserve energy during electron consuming reactions, i.e. microbes performed proton reduction and should grow and be maintained under the given cathodic condition for sustainable function and thermodynamically balance.

The objective of the study was to re-culture biocathodes to optimise operational conditions and increase biocathode performance for hydrogen production, by manipulating the cathode potential, inorganic carbon and sulphate concentrations. The study will help to determine what kind of wastewaters will be suitable for the biocathode formation and assist in establishing potential electron transfer mechanisms. It will also indicate the possible wastewater treatments that could be performed using this technology.

5.2. Experimental procedure

5.2.1. Experimental setup and biocathode enrichment

Double-chamber electrochemical cells, 25 cm^3 (mL) in volume (each chamber) were used as described in section 3.1.1. The enrichment of hydrogen-producing biocathode was performed as stated in Rozendal *et al.* (2008). A three-step start-up procedure and polarity reversal method were exploited to obtain the desired biocathode. An abiotic anode (RVG-2000, Mersen, USA) coated with 0.5mg/cm^2 platinum catalyst was used. Anolyte was a mixture of sodium chloride and phosphate buffer consisted of (g/L): $NaH_2PO_4 \cdot 2H_2O$ 3.30; $Na_2HPO_4 \cdot 2H_2O$ 5.14; NaCl 2.92. The anolyte was circulated from a 250 mL reservoir to anodic chamber at flowrate 8.7 mL/min to minimise mass transport limitation possible caused by slow flowrate. Once a stable current was observed, the biocathode potential was further increased and fixed at -1.0 V versus standard hydrogen electrode (SHE) for all the experiments unless stated otherwise. The catholyte medium contained (g/L): $NaH_2PO_4 \cdot 2H_2O$ 0.66; $Na_2HPO_4 \cdot 2H_2O$ 1.03, $KHCO_3$ 1.0, NH4Cl 0.27,

$MgSO_4 \cdot 7H_2O$ 1.23, $CaCl_2 \cdot 2H_2O$ 0.01 and trace element mixture 1.0 mL/L (Rozendal *et al.*, 2008). The medium consisted of only phosphate buffer was first prepared and autoclaved. The remaining ingredients were filter-added then after. The amount of $KHCO_3$ and $MgSO_4 \cdot 7H_2O$ was added into the medium as stated above except if mentioned otherwise. The medium was then fed continuously into the cathodic chamber at 0.1 mL/min. The anolyte consisted of 5 times higher concentration of phosphate buffer than in catholyte when the solutions were prepared. It is to ensure anolyte pH was maintained in neutral under recycling condition. Ion balance could affect conductivity value in the electrolytes and performance of MEC due to different phosphate buffer concentration. However, the effect was insignificant in our study as small operation volume (25mL each chamber with half of the volume filled with carbon felt electrode) and a closer electrode gap (≤ 1.0 cm) was used. A control was prepared similar to the electrochemical cell mentioned above except without adding inoculum during the biocathode enrichment process. The electrochemical cell including the control were prepared in duplicates and placed inside a polystyrene box under a constant temperature of at 26.5 ± 2.5°C.

5.2.2. Experimental parameter

Enriched biocathodes were subjected to three main experiments to examine optimum conditions for better performance especially in producing hydrogen. The experiments include manipulating applied potentials and feeding different sulphate and bicarbonate concentrations to the cathodes. The applied potentials used in the first experiments were -0.5, -0.7, -0.8, -0.9 and -1.0 V. In the second experiment, sulphate concentrations fed into cathode were 0 (0), 48 (0.5), 96 (1), 288 (3), 480 (5) and 768 mg/L (8 mM). In the final experiment, bicarbonate concentration fed into the cathode were 0 (0), 61 (1), 183 (3), 305 (5), 610 (10) and 3051 mg/L (50 mM). The applied potential experiments were done using chronoamperometry to check the biocathode performance in term of hydrogen production and their energy requirement in term of current. All experiments were conducted in duplicates. The average values with the maximum and minimum are presented.

5.2.3. Electrochemical analysis

Cyclic voltammetry (CV) was carried out after each experiment to compile the information on how the catalytic activity responses to the experimental parameters. The analysis procedure was followed as section 3.2.4 with some adjustments on scan region and rate. Start and end

potentials were 0 and 1.0 V with scan rate of 0.001 V/s and repeated for at least 3 cycles to obtain a stable voltammogram. Only the last voltammograms from the last cycles of each experiment are reported in this study. All potential values were reported as vs. SHE unless stated otherwise.

5.2.4. Sample analysis

Influent and effluent samples were collected for each parameter test. pH and conductivity are the simpler indications of the change in liquid properties through bioelectrochemical reactions. For instance, substrate oxidation or proton reduction in anode or cathode could result in the decrease or increase of pH value. While ionic conductivity may influence the efficiency of the whole system when the reactant and product contents vary in electrolytes. Besides pH and conductivity, sulphate and total soluble carbon are the two main parameters in this study. It is important to monitor the changes of the sample contents and the effect of applied cathode potential. Additional analysis to determine ammonium concentration was also included in this study apart from the main parameter analysis. This is because of ammonium ion could contribute to the ionic strength of the medium while acted as a nitrogen source to bioanode. Please refer to section 3.3.2 for all the analysis detail mentioned above.

5.2.5. Gas composition

Hydrogen is the main product in this study. In order to calculate the hydrogen production rate, gas evolution from the biocathode was measured using a water replacement method. A gas collection tube with marked volume was placed on the top of the cathodic chamber and then filled with catholyte from the top opening. Gas bubble produced from cathodic was evolved to the top of the tube and replaced the catholyte by pushing it out from a side outlet. The effluent channel was filled with catholyte all the time to maintain anaerobic condition and atmospheric pressure inside the chamber (Lim *et al.*, 2017). The gas samples then were analysed according to the procedures mentioned in section 3.3.1. The hydrogen recovery efficiency and yield were calculated based on section 3.4.

5.3. Result and discussion

5.3.1. Enrichment of hydrogen-producing biocathode

The enrichment of the biocathodes in this study was performed by following the method reported in Rozendal *et al.* (2008). Figure 5.1 is the schematic of the experimental setup in this study. Cathode chamber was cultivated with inoculum collected from the effluent of bioanode operated in microbial fuel cell mode for over a year (Spurr, 2016). The inoculum was dominated by *Deltaproteobacteria* (~60%), followed by Clostridia (~20%) and *Bacteroidia* (~10%). The *Geobacter sp.* (~50%) was the dominated ribotype in *Deltaproteobacteria* cluster and sulphate-reducing bacteria only consisted of around 2%. A defined medium was prepared as described as in _ENREF_25Rozendal *et al.* (2008). The medium was fed continuously into the cathode at a flowrate of 0.2 mL/min. Meanwhile, anolyte consisted of 100 mM phosphate buffer at pH 7.0 and 100 mM NaCl as a background solution to increase solution conductivity. The anolyte was fed and recycled from a 2 L reservoir at a flowrate of 8.7 mL/min. During the enrichment process, hydrogen was filled in cathode headspace and recycled by a peristaltic pump into the cathode chamber bubbled through the catholyte. The headspace hydrogen was refilled every day.

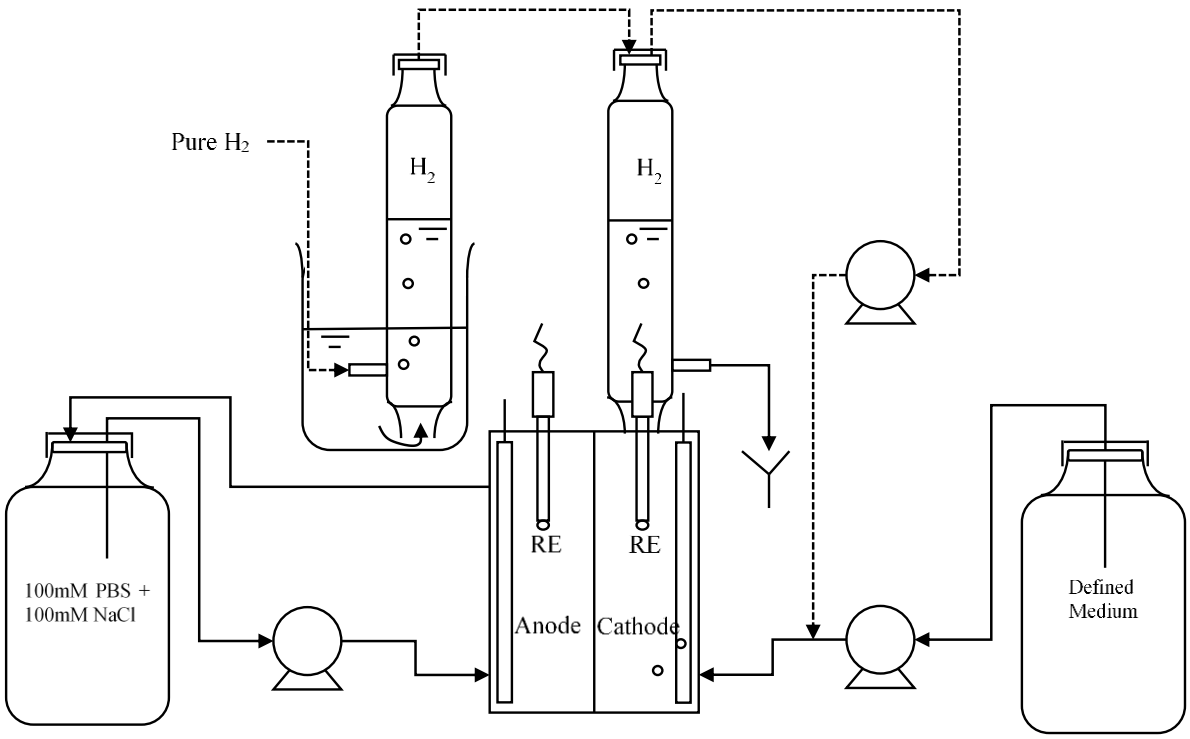

Figure 5.1 Schematic of the experimental setup

Figure 5.2 shows the monitored current density during the enrichment process. Targeted electrode (called 'cathode' after this) was fixed at -0.1 V and the cell was operated overnight without any inoculum added. The inoculum was added into the cathode after left overnight. Acetate was used as an electron donor to grow the bioelectrode and to produce significant amount of electrical current from its oxidation process. It reached a stable current after 4 days of enrichment. After 6.5 days, the potential was further reduced to -0.2 V and acetate was removed and replaced by hydrogen on the headspace. Hydrogen recycle rate was reduced and then increased in between 5.05 and 26.86 mL/min after 8 days of enrichment to check whether the bioelectrodes were actively growth under hydrogen as an electron donor. Meanwhile, Figure 5.3 shows the relationship between hydrogen consumption and the rate of recycling between headspace and bioelectrodes. The optimum recycle rate was determined as 13 mL/min and was used throughout the whole experiment. The biocathode test was continued by replacing hydrogen with nitrogen between day 12 and 13. This was to confirm that the biocathode relied and growth on hydrogen. After that, carbon dioxide was filled instead of hydrogen to check if the polarity of the bioelectrodes could be reversed. As positive current value changed from positive to negative between day 14 and 15.5, it justified that the polarity could be reversed from electron-producing to electron-accepting biocathode. A polarity reversal scan was performed at day 15.5 and the result is shown in Figure 5.4. Based on the graph, the minimum starting potential that could be applied to the bioelectrode was determined as -0.80 V. Therefore, -0.80 V was fixed for further enrichment of the electron-consuming bioelectrode. Bicarbonate was used as carbon source starting from day 16.5. A stable current was observed after day 23.5. Sulphate test was performed at day 26 to check whether the biocathode was dominated by sulphate-reducing bacteria and depending on the compound to perform anaerobic respiration (Jeremiasse *et al.*, 2012; Croese *et al.*, 2014). The results showed little or no significant effect of the sulphate when the concentration was reduced from 5 mM to zero. Therefore, the cathode potential was further reduced to -0.9 V and a remarkably current density dropped was noticed between day 32 and 34. The current was resumed after 5 mM SO_4^{2-} was reintroduced to the biocathode. The biocathode was put into maintaining mode or medium saver mode after day 37 before any further experiments (as stated in section 5.2.2).

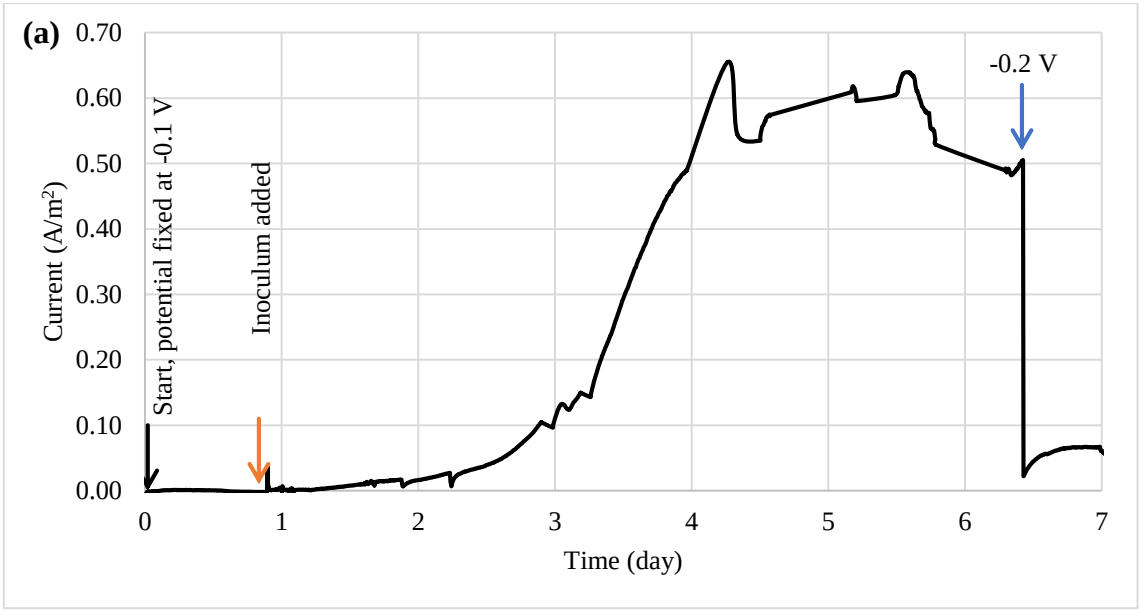
(a)
Current (A/m²)
Time (day)
Start, potential fixed at -0.1 V
Inoculum added
-0.2 V

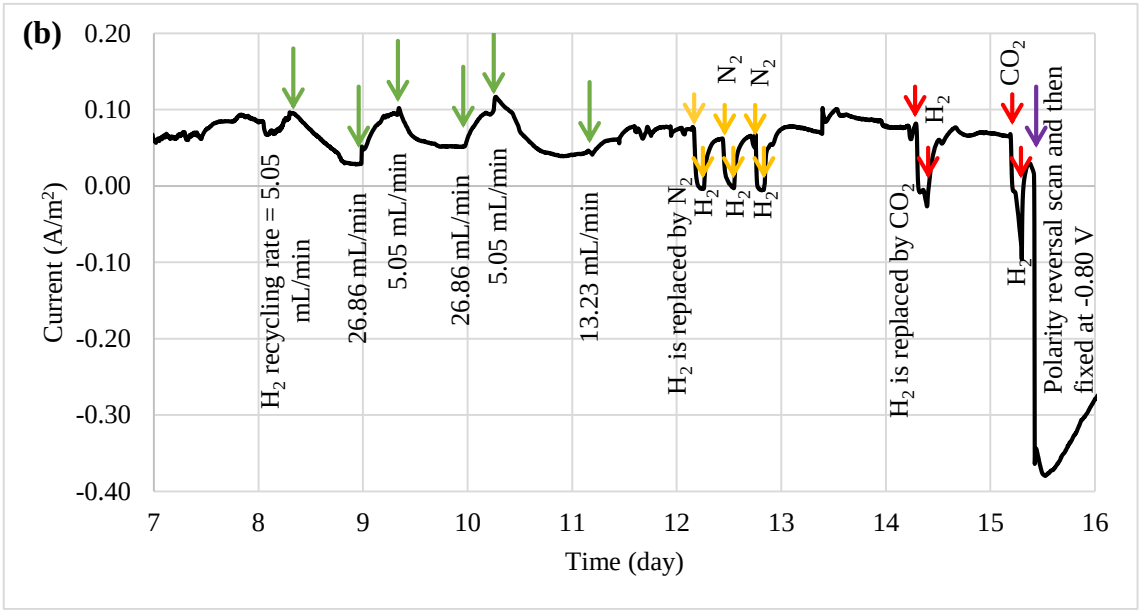
(b)
Current (A/m²)
Time (day)
H2 recycling rate = 5.05 mL/min
26.86 mL/min
5.05 mL/min
26.86 mL/min
5.05 mL/min
13.23 mL/min
H2 is replaced by N2
N2
N2
H2
H2
H2
H2 is replaced by CO2
H2
CO2
H2
Polarity reversal scan and then fixed at -0.80 V

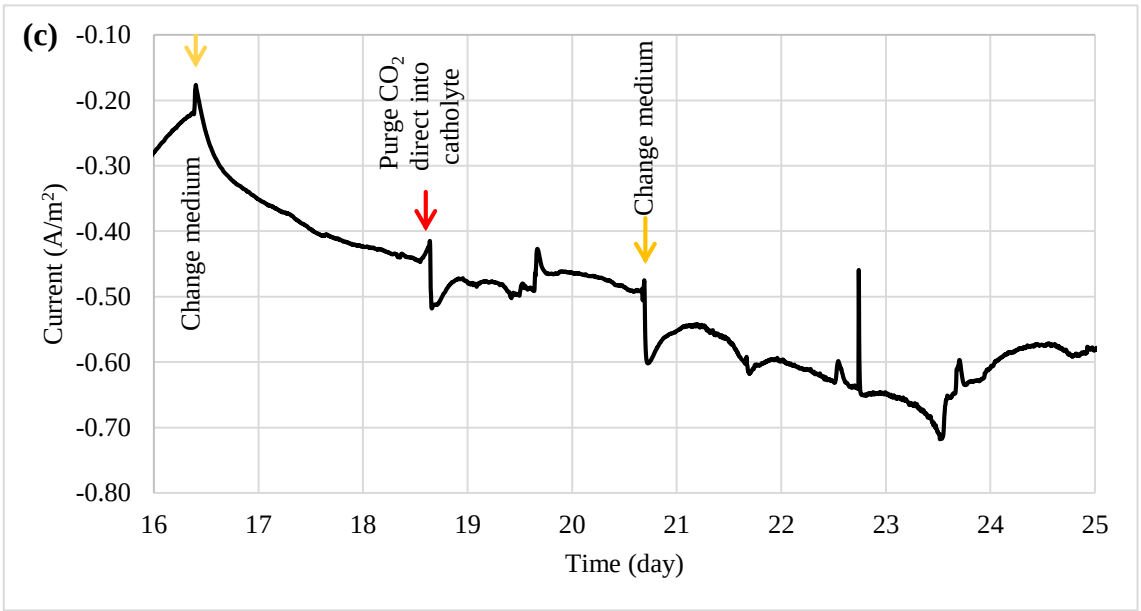
(c)
Current (A/m²)
Time (day)
Change medium
Purge CO2 direct into catholyte
Change medium

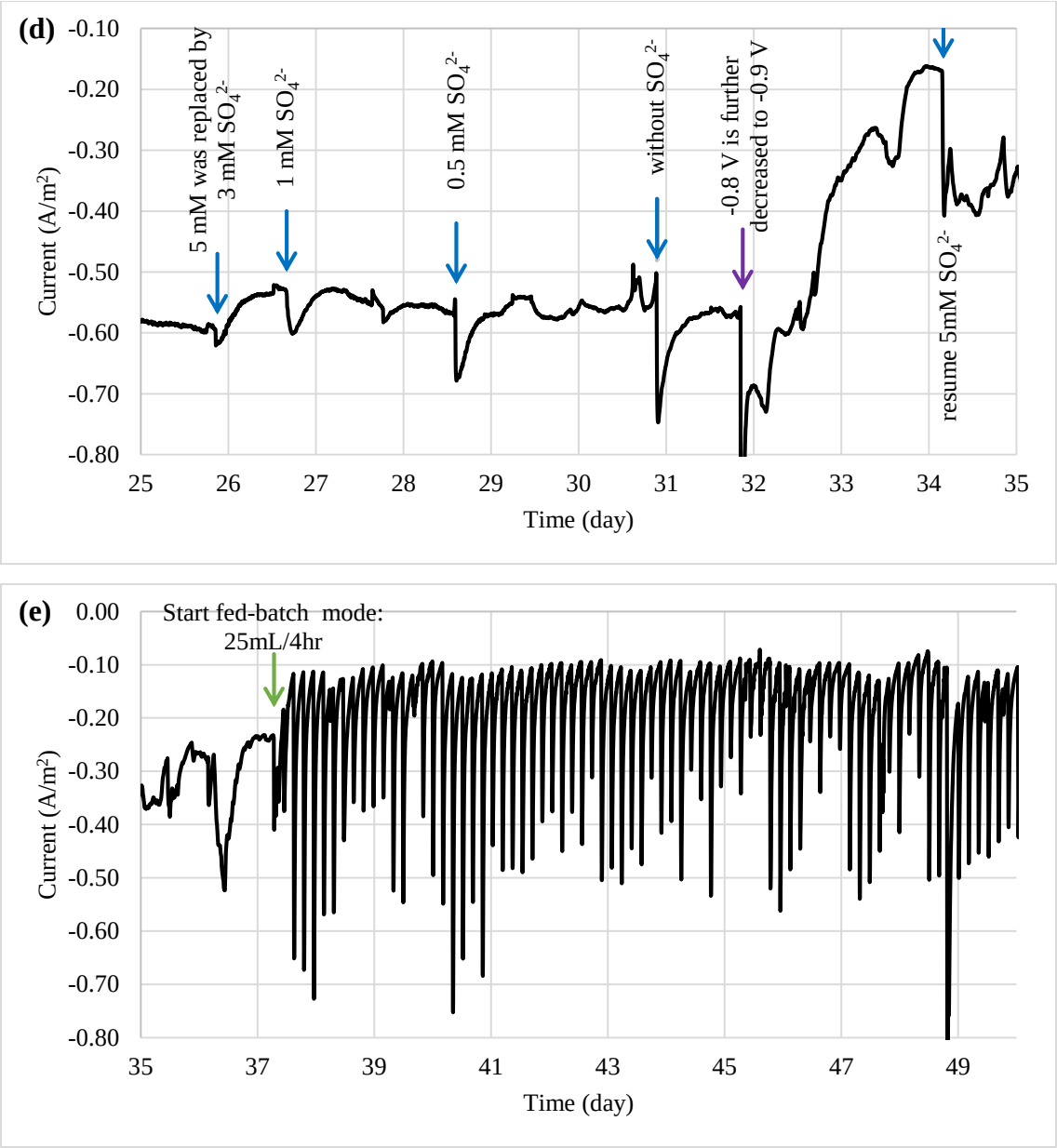

Figure 5.2 The bioelectrode profile of current density enriched using three-step start-up procedure and polarity reversal method.

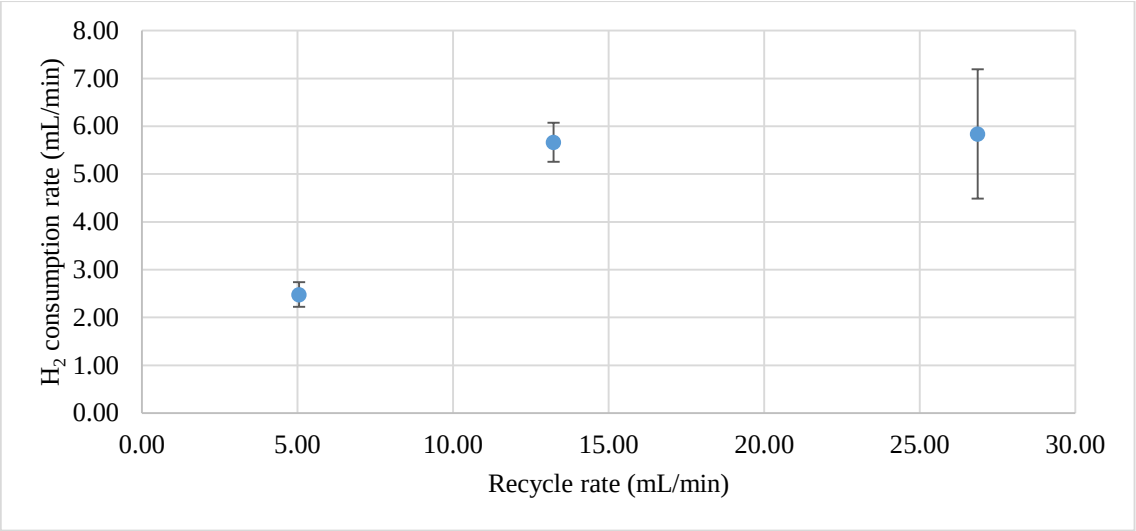

Figure 5.3 Hydrogen consumption rate based on hydrogen recycling rate from the headspace. The hydrogen consumption becomes saturated after the headspace recycling rate excess 13 mL/min.

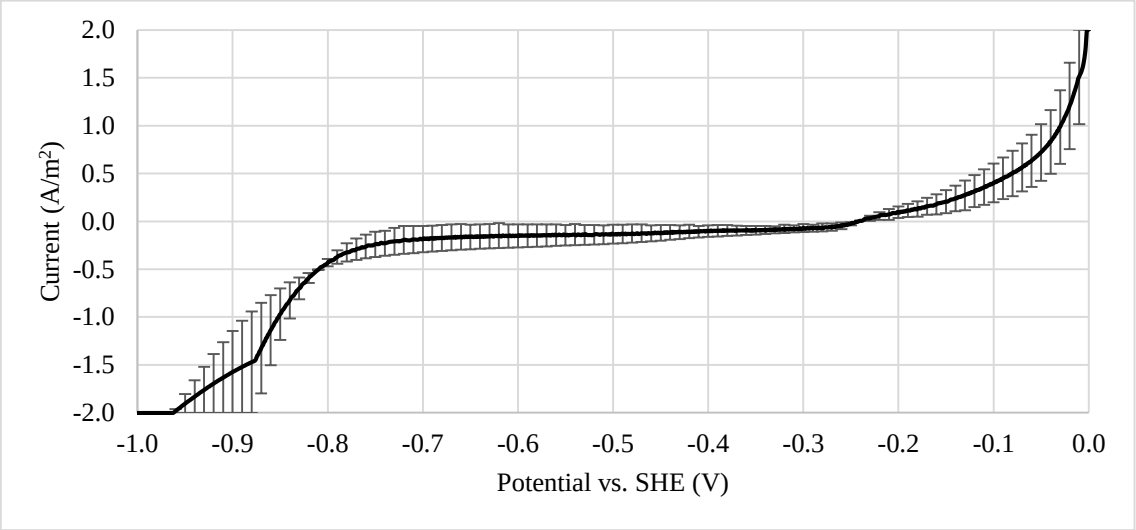

Figure 5.4 Polarity reversal scan from 0 to -1.0 V vs. SHE at a scan rate of 0.2 mV/s. The information was obtained to determine the potential to be fixed on the electrodes to produce hydrogen.

5.3.2. Effects of cathodic potentials on hydrogen production

The reactors were operated under different cathode conditions and performance between biocathode and abiotic cathode were compared. The cathode potentials were first fixed at -0.5V

before moving toward more negative potential until -1.0V where a significant amount of gas was collected in the headspace. Each applied potential was fixed and applied for at least 2 to 3 days to obtain a stable current and hydrogen production. Figure 5.5 (a) represents the current density and hydrogen production rate from both control and biocathode. As shown in Figure 5.5 (a), biocathode hydrogen production was higher than control when the cathode potential was fixed at -0.8V or below. No significant hydrogen production was observed in both biocathode and control when the potential was higher than -0.8 V. The biocathode produced almost 10 L/m^2/day compared with the control cathode production of 3 L/m^2/day at -1.0 V, evidencing biotic activity. The hydrogen production increased consistently with the external energy requirement for hydrogen evolution at lower potentials. The current density achieved was -1.10 A/m^2 for biocathode compared to -0.45 A/m^2 for the control, at a cathode potential of -1.0 V. Even though the reduction potential for hydrogen evolution from proton at standard condition is -0.41V, the real operational reduction potentials are much lower than the theoretical value (Lim *et al.*, 2017). Potentials as low as -0.7 V and below were used to produce hydrogen as a result of overcoming overpotentials during the electron transfer to microbes (Rozendal *et al.*, 2008; Jeremiasse *et al.*, 2012; Jourdin *et al.*, 2015). In addition, some studies applied even lower potentials than -0.7 V due to the different designs and configurations that possibly increased the overpotentials (Aulenta *et al.*, 2012; Batlle-Vilanova *et al.*, 2014; Liang *et al.*, 2014; Luo *et al.*, 2014; Lim *et al.*, 2017).

Figure 5.5 (b) shows the catalytic activity between biocathode and control (without inoculum) under the potential range of 0 to -1.0 V. Significant reduction activity was observed from -0.8 V and below. A small oxidation peak at -0.6 V was noticed when the voltammetry was scanned from -1.0 to 0 V. The peak was asserted as hydrogen oxidation reaction where the generated hydrogen (near -1.0 V) was re-oxidised under the outer membrane enzymes called hydrogenases (Aulenta *et al.*, 2012). Furthermore, a small reduction curve at -0.3V was also noticed and proved to be related to the process of inorganic to organic carbon conversion. Similar reduction peak was found in other CO_2 conversion studies especially those for acetate production at the range between -0.3 and -0.6 V (Marshall *et al.*, 2012; Blanchet *et al.*, 2015; Patil *et al.*, 2015; Bajracharya *et al.*, 2017a; Wenzel *et al.*, 2018). Meanwhile, the control only showed reduction activity at -0.8 V and below and the activity was significantly lower than the biocathode. The catalytic properties proved biocathode growth on the electrode surface (Aulenta *et al.*, 2012; Jourdin *et al.*, 2015). Data suggests that hydrogen production was significant after cathodic potentials more negative than -0.8 V.

Figure 5.5 (c) shows the variations in sulphate and ammonium contents at different applied potentials. The lower potential was not necessary to increase the sulphate removal rate as a fresh medium was continuously fed into the chamber (Jeremiasse *et al.*, 2012; Luo *et al.*, 2014). Sulphate concentration in biocathode effluents was lower than the control in general. There was a small removal of sulphate in biocathode (~20%) compared to the control. Ammonium removal in the biocathode was slightly increased after -0.7 V and lower. The ammonium acted as nitrogen source for the construction of microbial cell. When the biocathode received sufficient potential energy from external power source for growth, nitrogen source was required to build the cell components.

pH and conductivity are simpler indicators for biocathode activities. Figure 5.5 (d) presents the pH and conductivity according to cathodic applied potentials. The pH of catholyte in biocathode remained at 7.0 between -0.5 to -0.8 V but start to increase to 7.5 when the potential was further decreased to -1.0 V depending on hydrogen evolution. The rate of pH increases was disproportional to the applied potential. However, catholyte pH in control fluctuated slightly between 7.0 and 7.3. Conductivity for both biocathode and control was increased vaguely from 8.0 to 9.0 mS/m when the potential was dropped from -0.5 to -1.0 V. It is crucial to control the pH at neutral or slightly acidic to maintain the biocathode performance in producing hydrogen (Rozendal *et al.*, 2008; Jeremiasse *et al.*, 2010). This is because proton was continuously removed to produce hydrogen causing the increases of pH value.

Figure 5.5 (e) shows inorganic and organic carbon contents of biocathode and control effluents. Bicarbonate as an inorganic carbon can be converted to acetate by homoacetogens to generate energy for growth (Bar-Even, 2013; Schuchmann and Muller, 2014; Mohanakrishna *et al.*, 2015). Acetate was then could be used by SRB as the carbon source (Aulenta *et al.*, 2012; Jeremiasse *et al.*, 2012). This means that bicarbonate was converted to cell materials of homoacetogens and SRB, and to acetate. As observed from Figure 5.5 (e), inorganic carbon content went up faster than organic carbon when the more negative potential was applied to biocathode. External energy supply might shift the metabolic pathways from acetogenic energy conversion to direct electron uptake from a high potential cathode or because of the excessive external energy at lower potential was more favoured in SRB compared to acetate (Venzlaff *et al.*, 2013). As a result, inorganic carbon was not used causing the accumulation of inorganic carbon at lower applied potentials. However, cell yield is usually low in this system and the conversion to cell materials can be ignored. There was a 20-45 % increase of organic carbon compared to fresh medium indicating a formation of organic carbon was generated from the biocathode (data not shown). Interestingly organic carbon content from biocathode was higher

compared to control with the same applied potential. While the potentials were low, the differential of the content was significant but start to converge when reaching -1.0 V which showing the shift of CO_2 to electron uptake dependent and favoured the SRB instead of acetogens. However, there was no consistent pattern in inorganic carbon removal in controls. Standard reduction potential for hydrogen evolution at neutral pH is -0.41V while acetate is higher around -0.28 V (Geelhoed *et al.*, 2010; Rabaey and Rozendal, 2010; Lim *et al.*, 2017). Due to thermodynamic considerations, hydrogen-producing biocathode not only produce hydrogen but they could promote acetate production as well. In our experiments, more negative potentials were used starting from -0.5 to -1.0 V and not only inducing abiotic reduction of bicarbonate to organic carbon but also hydrogen evolution. Nevertheless, the reduction potentials favoured the biocathode compared to control because the rate of hydrogen production and current density were much higher in biocathode.

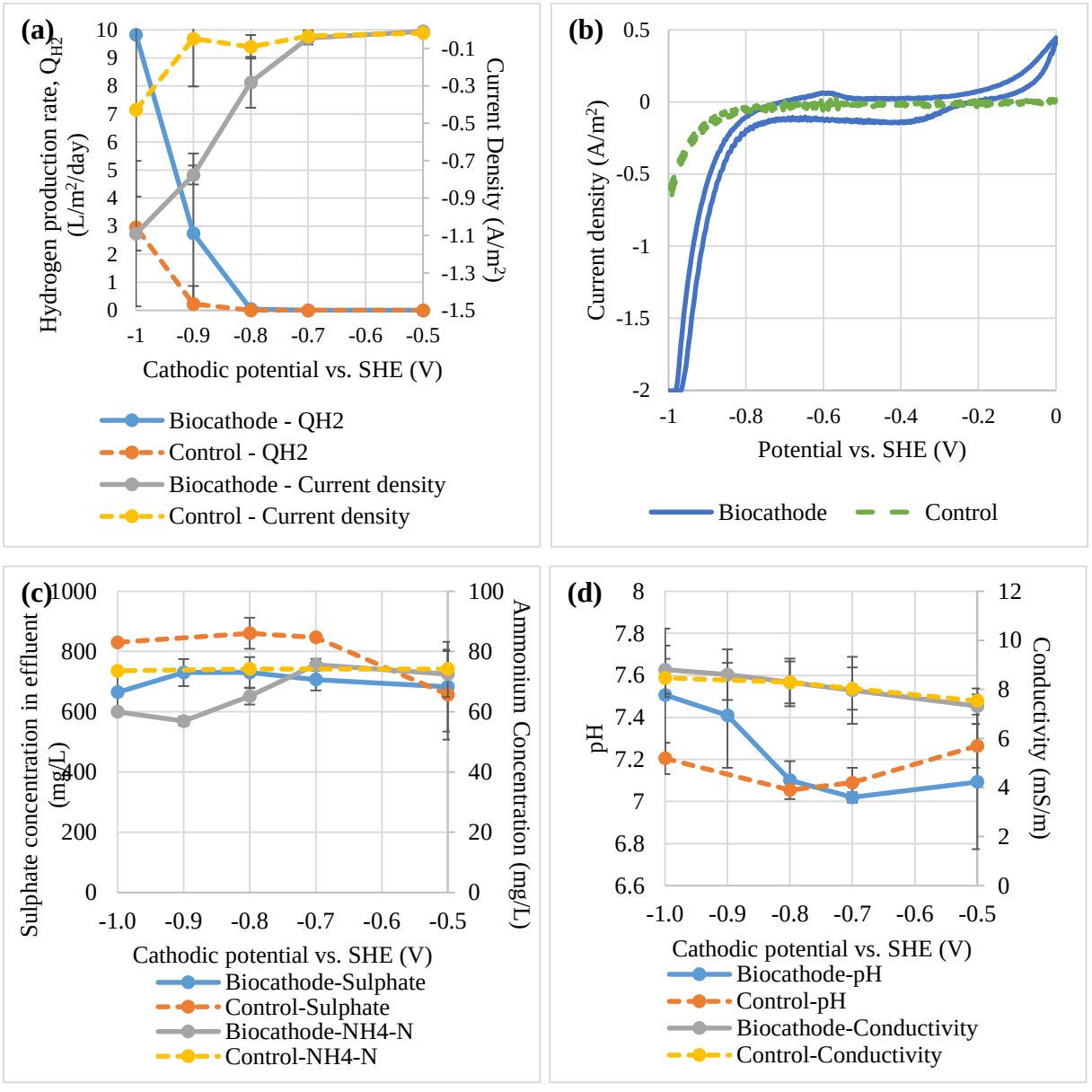

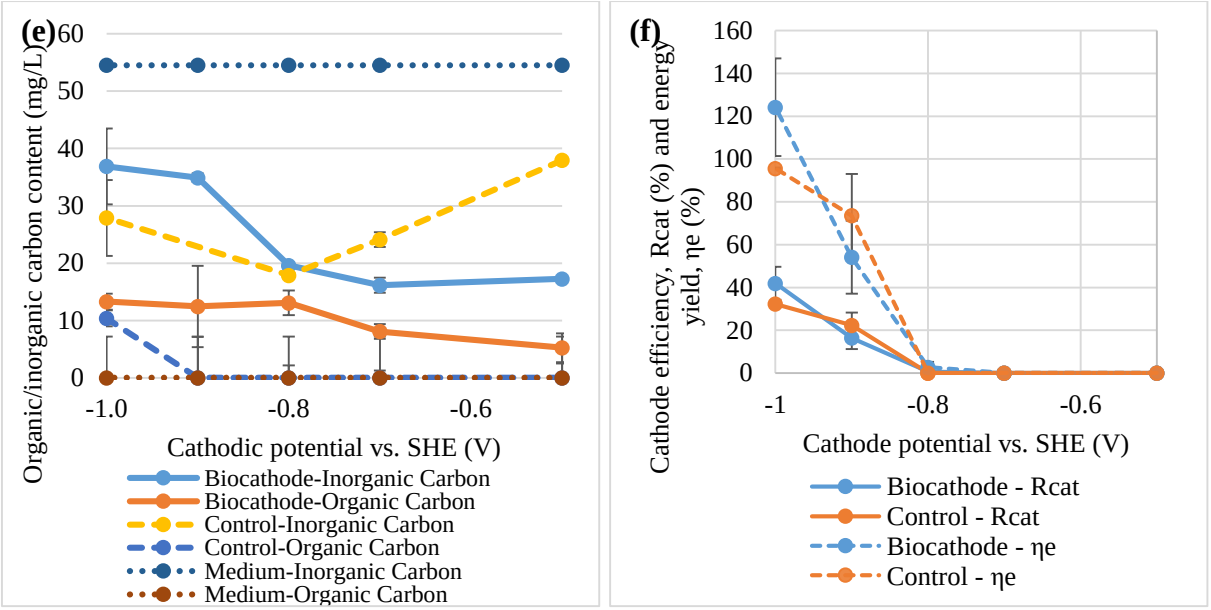

Figure 5.5 The effect of cathode potential on (a) hydrogen production rate and current density, (b) catalytic activity, (c) sulphate and ammonium contents, (d) pH and conductivity, (e) total carbon content, and (f) cathode efficiency and energy yield.

5.3.3. Effect of sulphate concentrations on hydrogen production

Figure 5.6 (a) shows the effect of sulphate concentration on current density and hydrogen production rate at the cathodic potential of -1.0 V. In the test, both peak hydrogen production rate and current density occurred at a sulphate concentration of 288 mg SO_4^{2-}/L. The peak hydrogen production rate and current density were 5.3 L/m^2/day and -0.81 A/m^2 respectively. Meanwhile, the control remained almost stagnant throughout this test. Hydrogen production rate could be highly depended on the sulphate concentration due to fact that the sulphate might favour certain microorganisms like SRB. It is commonly known that high substrate concentration could limit or saturate metabolic reactions in living cells. The sulphate reduction, in this case, was limited by low sulphate concertation (< 288 mg SO_4^{2-}/L). The effect of sulphate inhibition began to observe after 288 mg SO_4^{2-}/L where the current density and hydrogen production rate started to drop. At this stage, SRB would reduce sulphate preferentially over proton under unlimited bicarbonate source. Extra reducing power or lower cathodic potential was needed to support the reduction of sulphate. Therefore, the hydrogen production was disproportional to the sulphate concentration as more electrons are used to reduce sulphate rather than protons at high sulphate concentration. The presence of sulphate is important for SRB to outcompete other anaerobes, including methanogens and fermentative bacteria in the anaerobic environments (Muyzer and Stams, 2008; Madigan *et al.*, 2014). When the sulphate

is quantitatively low, methanogens could dominant in the community. However, SRB could survive at the very low amount of acetate as carbon source compared to the methanogens, and therefore, they will coexist with homoacetogens when acetate is not available (Odom and Singleton, 1993; Muyzer and Stams, 2008).

Figure 5.6 (b) shows the cyclic voltammograms of the biocathode on the sulphate concentration. Based on the results, we believe sulphate could be considered as one of the key parameters in this study. It can be seen from the figure that the evolvement of specific catalytic peaks at -0.6V and -1.0V was actually affected by the sulphate concentration. Both peaks were postulated catalysing hydrogen oxidation and hydrogen evolution related to the species of sulphate-reducing bacteria (Aulenta *et al.*, 2012; Lim *et al.*, 2017). Moreover, significant hydrogen oxidation and reduction peaks were observed at 288 mg SO_4^{2-}/L. The oxidation peak was believed to be related to reversible electrochemically active periplasm enzymes or proteins called hydrogenases. Hydrogenase can be found in many microorganisms included SRB, acetogens and methanogens and catalyse hydrogen production and/or utilisation. The higher oxidation peak at 288 mg SO_4^{2-}/L was due to the increased hydrogenase content on the biocathode. In the cyclic voltammogram, the hydrogenases performed instant hydrogen oxidation around -0.6 V which was generated at -1.0 V when the applied potential moved from -1.0 to 0 V. The increases in hydrogenase activity was also supported by the evidence that the maximum hydrogen production rate was at the same sulphate concentration. Even though hydrogen catalysis (by comparing the CV tails at -1.0 V) was slightly higher at 768 compared to 288 mg SO_4^{2-}/L, the hydrogen oxidation peak at -0.6 V was not as high as at 288 mg SO_4^{2-}/L. This could be due to the substrate inhibition on the hydrogenases (Aulenta *et al.*, 2012; Batlle-Vilanova *et al.*, 2014). It was believed that this enzyme posed an onset potential at least at -0.6 V while an extra -0.4 V (standard reduction potential for hydrogen evolution) should be invested to produce hydrogen (Lim *et al.*, 2017).

Figure 5.6 (c) exhibits sulphate and ammonium concentration in the effluent depend on initial sulphate concentrations. Sulphate concentration as low as 96 mg/L was actually good for ammonium removal. It means that sulphate and ammonium should be presented at the same time but not in high concentrations for a better biocathode reaction. Ammonium was depleting faster at 96 mg SO_4^{2-}/L that the other concentrations and became a limiting factor to block the current and hydrogen production as shown in Figure 5.6 (a). Surprisingly, the current and hydrogen production rate reached a peak at 288 mg SO_4^{2-}/L but decrease after higher sulphate concentration. Substrate inhibition could be the main factor restricting the activities and not

necessary for better hydrogen production as long as the sulphate was presented in the environments (Jeremiasse *et al.*, 2012).

pH and conductivity values were plotted relative to sulphate concentration in Figure 5.6 (d). The pH increased in biocathode explains protons were utilised and removed from the catholyte to produce hydrogen. The biocathode pH fluctuated between 8.9 and 9.3 which was higher than the initial medium pH around 7.0. However, the control pH was slightly lower than the biocathode pH with the value in between 7.7 and 8.6. The higher the pH values indicated that more protons were removed during the reduction process and biocathode activity. At this point, the pH values were increased remarkably from neutral to about 9.0. This means the added 50 mM phosphate buffer (PBS) in the medium wasn't the best option for controlling but managed to prevent dramatically changes of pH. LaBelle *et al.* (2014) lowered catholyte pH to around 5.0 in order to increase hydrogen production in acetogen and SRB dominated the mixed community. Acetogen domination in biocathode could be a problem as they ceased the production of hydrogen. Therefore, *Acetobacterium* dominated biocathode was controlled at a certain level in repeated exposure to acidic condition to increase hydrogen production rate (LaBelle *et al.*, 2014; LaBelle and May, 2017). Meanwhile, lower pH could also mean to provide more proton for hydrogen and acetate production. Surprisingly, conductivity values followed the trend of hydrogen production and current density. This is different from the effect of applied potentials where the conductivity and pH values did not change dramatically.

Figure 5.6 (e) shows the inorganic/organic content relatively to sulphate concentration. The organic carbon content in control and biocathode effluent remained almost the same without any significant difference when the sulphate concentration was increased. The main purpose of these results was to notice any relevant connection between bicarbonate and sulphate roles in the biocathode. From the results, there was no clear connection between the tested parameter. This may postulate that either bicarbonate or sulphate was required by two different communities and no competitions were existed between them for sulphate and bicarbonate at the same time. The evidence concretes the idea that bicarbonate was necessary for some autotroph community in biocathode to produce organic carbons (Mohanakrishna *et al.*, 2015). The organic carbons were then utilised by SRB to produce hydrogen with external reducing power for cathode (Jeremiasse *et al.*, 2012; Zaybak *et al.*, 2013).

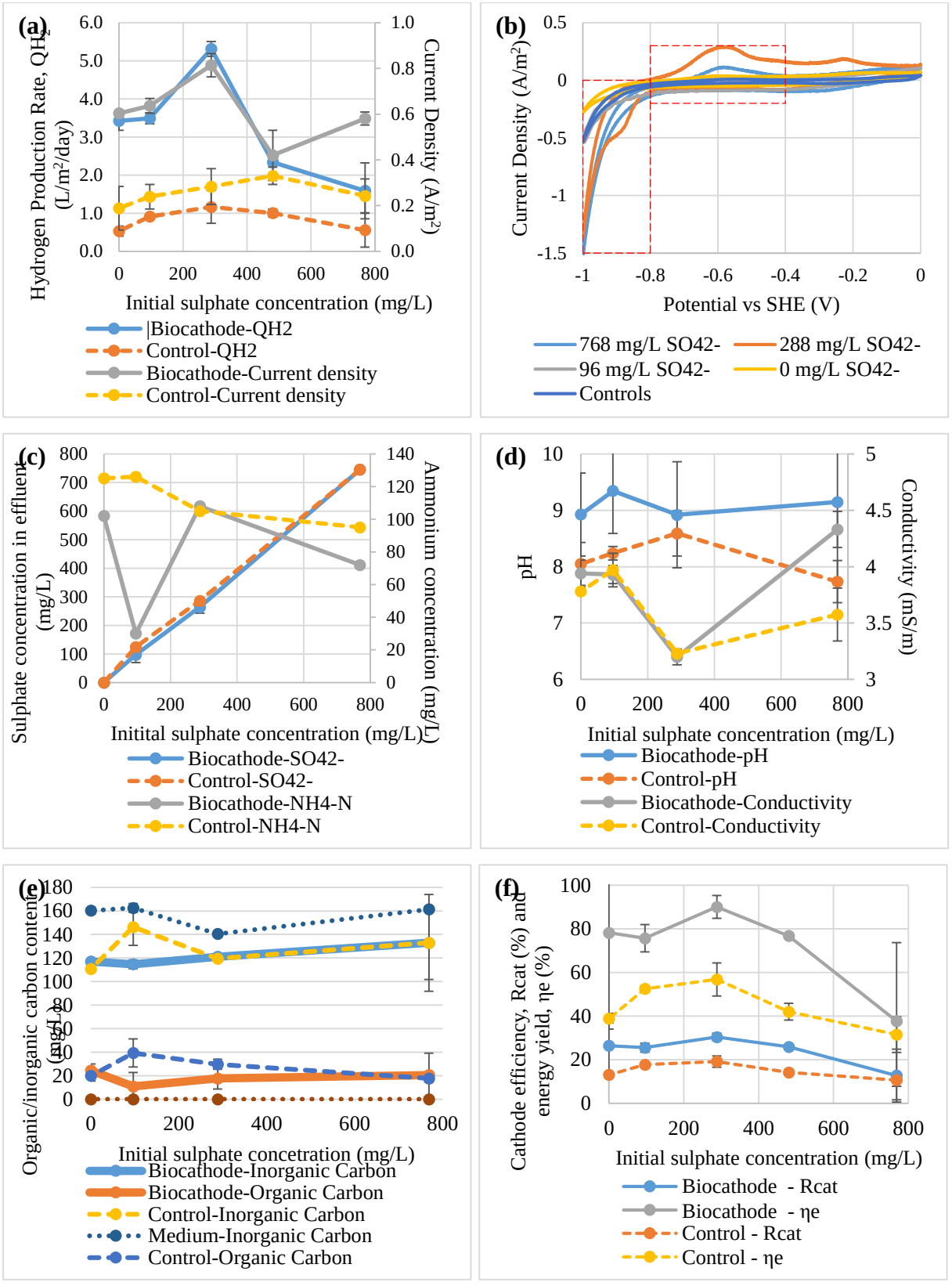

Figure 5.6 The effect of initial sulphate concentration on (a) hydrogen production rate and current density, (b) catalytic activity, (c) sulphate and ammonium contents, (d) pH and conductivity, (e) total carbon content, and (f) cathode efficiency and energy yield.

5.3.4. Effect of bicarbonate contents on hydrogen production

The effect of bicarbonate concentration on current density and hydrogen production rate is shown in Figure 5.7 (a). The bicarbonate test showed that a concentration of 610 mg HCO_3^-/L gave the maximum hydrogen production rate of 3.6 L/m^2/day and the maximum current density of -0.67 A/m^2. The control hydrogen production rate in this test was almost the same after 305 mg HCO_3^-/L. One of the speculations is that there is no biofilm was growth or attached on the surface of control cathode. Hence, the transportation of protons from the bulk solution to control cathode surface was faster than in biocathode. The abiotic hydrogen production rate was remained stagnant at 3.6 L/m^2/day after 305 mg HCO_3^-/L. Meanwhile, hydrogen production in biocathode peaked at 305 mg HCO_3^-/L with the production rate equal to 3.6 L/m^2/day.

Figure 5.7 (b) shows the cyclic voltammograms of the biocathode in different bicarbonate concentrations. Low bicarbonate concentration (61 and 183 mg HCO_3^-/L) was actually good for biocathode catalytic activity as they induced the highest hydrogen oxidation peak. However, only 610mg/L HCO_3^-/L promoted the highest hydrogen production rate and current density as shown in Figure 5.7 (a). If the interaction of microbial community in the biocathode was true, acetogens that produced short-chain fatty acids for the hydrogen-producing bacteria could be saturated with the inorganic carbon concentration at 610 mg HCO_3^-/L or higher (Su *et al.*, 2013; LaBelle and May, 2017). Maximum fatty acid was converted at this concentration. Thus, the hydrogen production rate and current density were the highest at this bicarbonate concentration. Higher catalytic activity at -0.6V did not necessary means it could promote high hydrogen evolution and the interaction of biocathode microbes should be taking into consideration.

Figure 5.7 (c) illustrates the profile of effluent sulphate and ammonium concentration to initial sulphate concentration. Bicarbonate worked as a carbon source is crucial to support biocathode growth. The quantity could affect sulphate and ammonium removal, especially at 610 mg HCO_3^-/L. The value is the optimum concentration because it gave the maximum current and hydrogen production. As we could see in Figure 5.7 (c) the sulphate removal in biocathode was gone up at low bicarbonate concentration but decreased after reaching the peak. It was revealed that either the fixed sulphate concentration was not sufficient to support the rate of biocathode activities when bicarbonate concentration was high. More sulphate was required for the reactions.

The effect of bicarbonate to pH and conductivity value is presented in Figure 5.7 (d). Carbonate species could act as a buffer system to maintain the pH as observed in control. The pH was maintained after 1831 mg HCO_3^-/L. For the biocathode, bacterial growth in biofilm usually is much lower than free-living bacteria and cell yield is low in anaerobic bacteria. These mean that the effects of carbonate might not be related to bacterial growth. Therefore, the hydrogen production rate between control and biocathode was not significantly different between each other. The only comparable performance was the current density where the biocathode required lower energy than the control. About 0.15 A/m^2 different between both control and biocathode after 305 mg HCO_3^-/L. The second explanation is that at least two biotic steps were need to produce hydrogen. As we know that SRB which responsible for the hydrogen production are chemoorganotrophs and could not use inorganic carbon to growth (Muyzer and Stams, 2008). Therefore, autotrophic acetogens become important to in the community to produce acetate from bicarbonate which in turn consumed by SRB. Some literature also suggested that the hydrogen and acetate production were coexistent in hydrogen-producing biocathode (Su *et al.*, 2013; LaBelle *et al.*, 2014; LaBelle and May, 2017). In addition to the PBS, Liang *et al.* (2014) suggested that bicarbonate could also enhance electric migration of proton when more H^+ was release from HCO_3^- and accelerated hydrogen evolution. This explained why the conductivity was getting lower at peak hydrogen production rate. Bicarbonate may contribute to the conductivity values. The catalytic activity of hydrogen production could actually utilise the proton and CO_2 derived from HCO_3^-, driving the conductivity value low as HCO_3^- was consumed.

Figure 5.7 (e) shows the inorganic/organic carbon conversion from different bicarbonate concentration. Bicarbonate concentration was increased constantly to monitor the effect on the biocathode. Organic carbon concentration increased until it reached a peak at 305mg HCO_3^-/L. The bicarbonate was essential in this study as a carbon source for microbial growth (Luo *et al.*, 2014; Jourdin *et al.*, 2015; Mohanakrishna *et al.*, 2016). Hydrogen production also reached a maximum point at this concentration. This postulated that possibly of carbonates consumed by autotrophs such as acetogens to produce organic carbons which in turn used by SRB to produce hydrogen. Once the bicarbonate concentration excess 305mg HCO_3^-/L, the hydrogen production rate dropped dramatically as shown in Figure 5.7 (a). Substrate inhibition may occur within the biofilm when acetogens produce excessive organics carbons and decrease hydrogen production in SRB (Croese *et al.*, 2014; Bajracharya *et al.*, 2017b; LaBelle and May, 2017). On the one hand, organic carbons content and removal in biocathode seems to peak at 305mg HCO_3^-/L which is proportional to hydrogen production rate. On the other hand, the organic

carbon content and removal in control were remarkably lower compared to the biocathode. The trend of changing was negligible and lightly shifted relative to the bicarbonate concentrations

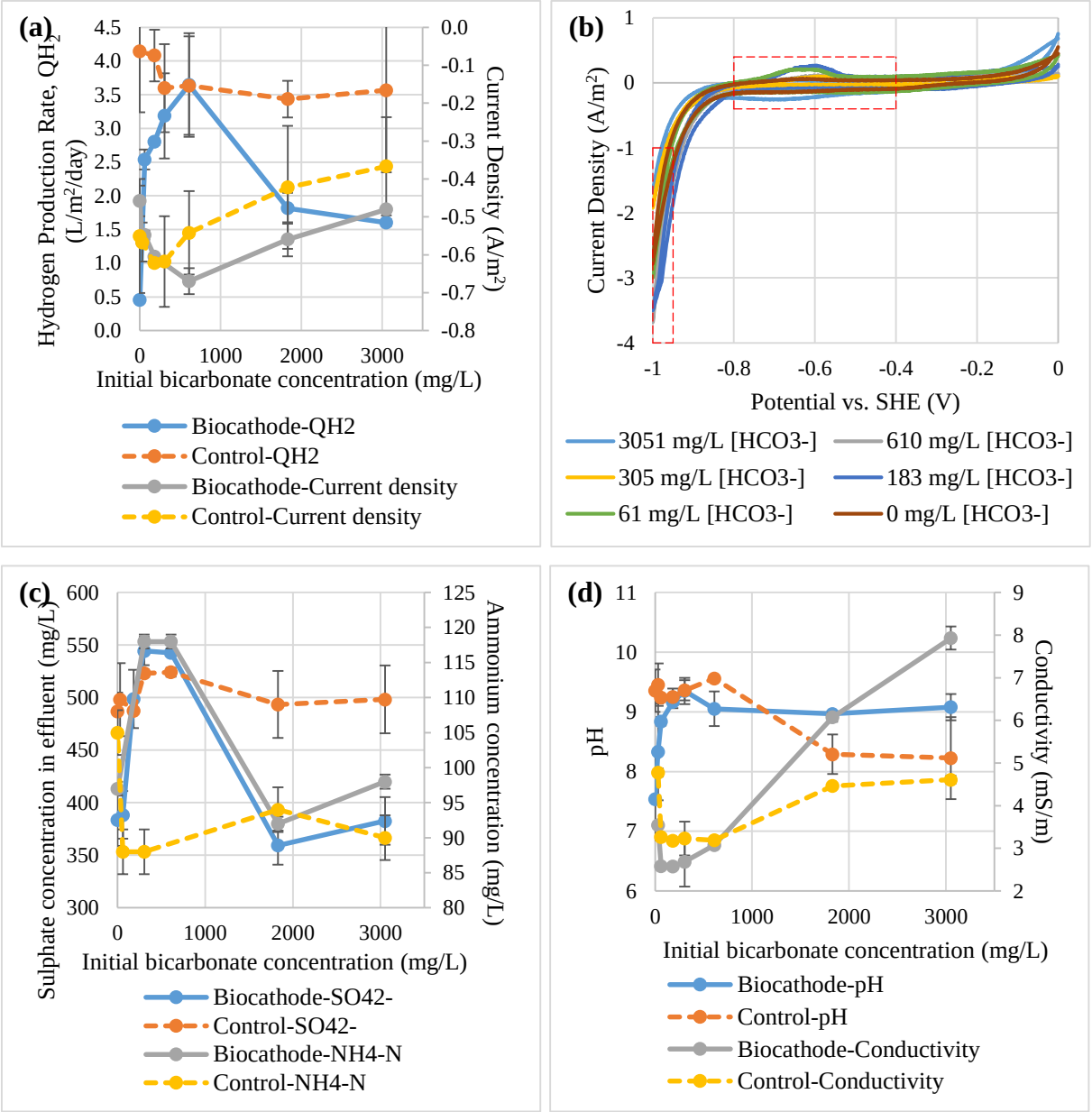

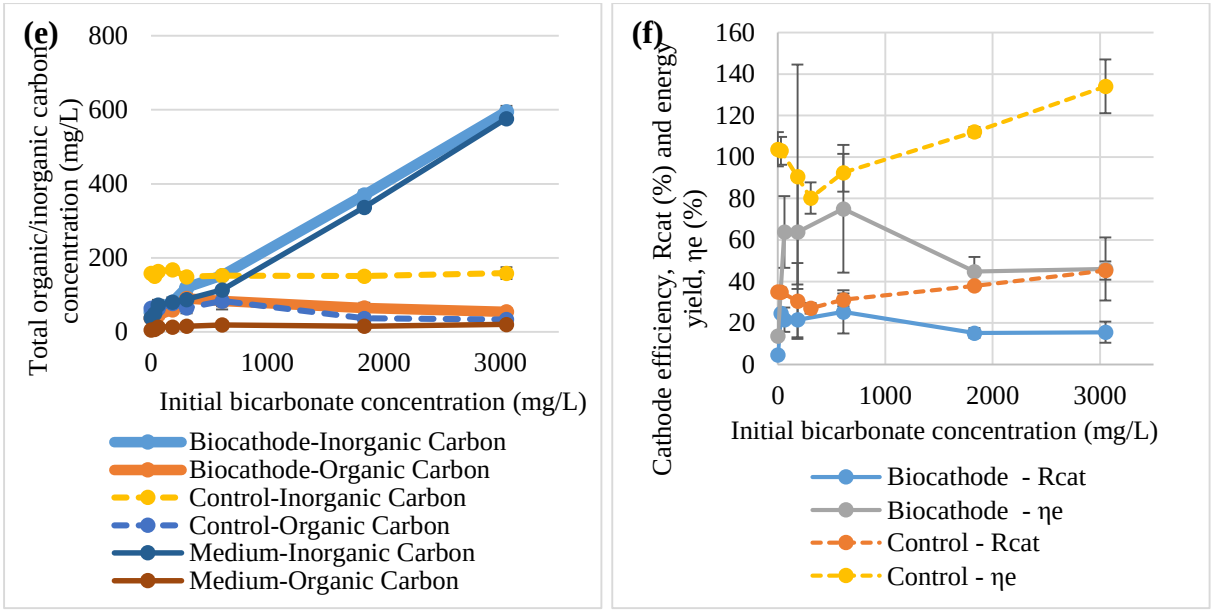

Figure 5.7 The effect of initial bicarbonate concentration on: (a) hydrogen production rate and current density, (b) catalytic activity, (c) sulphate and ammonium contents, (d) pH and conductivity, (e) total carbon content, and (e) cathode efficiency and energy yield.

5.3.5. Bottleneck and beneficial application of bioelectrochemical hydrogen production

It is believed that microbial community in hydrogen-producing biocathode should contain a key enzyme, hydrogenases in order to catalyst hydrogen evolution from protons (Geelhoed *et al.*, 2010; Croese *et al.*, 2011; Rosenbaum *et al.*, 2011; Jourdin *et al.*, 2015; Kim *et al.*, 2015). Sulphate-reducing bacteria (SRB) belong to *Desulfovibrio sp.* was then found abundant in the biocathode which contain active hydrogenase enzymes in its cytoplasm and periplasm (Croese *et al.*, 2014). According to the conventional information, SRB poses an energy conservation mechanism called hydrogen cycling mechanism in sulphate reduction (Kim and Gadd, 2008; Madigan *et al.*, 2014). The mechanism happens in anaerobic condition by oxidising organic compounds like lactate and ethanol as electron donors for sulphate reduction. However, there was no organic matter only inorganic carbon like carbonates introduced to hydrogen-producing biocathode. To replace the organic matter, an external energy source was required to provide the reducing power to the biocathode. In our study, it was found that at least -0.8 V vs. SHE was required to make the biocathode feasible for hydrogen evolution (Figure 5.5). The potentials provided sufficient exergonic energy to overcome overpotentials in the system and to facilitate electron transfer from the electrode to electrochemically-active microbes. These microbes normally contain membrane-bound complexes such as cytochrome C, Fe-S protein,

oxidoreductase and periplasm enzymes that could receive the electrons (Choi and Sang, 2016). As a result, the microbes could perform the metabolic process and initialise the electron transport-chain reactions and generate hydrogen included a trace amount of organic carbon.

From a thermodynamic point of view, standard reduction potential, E_o' for hydrogen evolution from proton, H^+/H_2 is -0.41 V at neutral pH. In real case scenario, potentials lower than this value were normally applied to biocathode to overcome overpotential and activation loss (Rozendal *et al.*, 2008; Aulenta *et al.*, 2012; Batlle-Vilanova *et al.*, 2014; Jourdin *et al.*, 2015; Lim *et al.*, 2017). In addition to the proton reduction under energy conserving hydrogenases in *Desulfovibrio sp.* respiration, sulphate is also an important element as a final terminal electron acceptor. The E_o' of SO_4^{2-}/H_2S is -0.35 V which the potential is slightly higher than the reduction of protons to hydrogen [E_o' SO_4^{2-}/H_2S -0.35 V is calculated based on E_o' SO_4^{2-}/HSO_3^- -0.52 V and E_o' SO_3^{2-}/H_2S -0.17 V (Madigan *et al.*, 2014)]. Sulphate reduction will be dominated in the presence of high sulphate concertation as less energy is required and causing less hydrogen evolution. Even in real environmental concentration is considered, the couple of H^+/H_2 is still more negative than SO_4^{2-}/HS^- (E_o' of H^+/H_2 is -0.27 V at 1 Pa of H_2 and SO_4^{2-}/HS^- is -0.20 V at 0.1 mM HS^-) (Keller and Wall, 2011). In a recent development, it has been proven that the potentials required of bioelectrochemically hydrogen evolution are lower than sulphate reduction (Luo *et al.*, 2014; Zheng *et al.*, 2014). Under fed-batch mode, the cathode potentials for sulphate reduction ranged between -0.6 to -1.0 V(Luo *et al.*, 2014). Meanwhile, significant hydrogen evolution potentials were around -0.8 to -1.2 V (Aulenta *et al.*, 2012; Batlle-Vilanova *et al.*, 2014; Lim *et al.*, 2017). Slightly more positive potential around -0.7 V was also used to generate hydrogen from biocathode but under a feed-controlled system in the anode and cathode. The purpose of the system is to eliminate mass transport limitation and overpotential losses that occurred in a batch system (Rozendal *et al.*, 2008; Jeremiasse *et al.*, 2010).

In this study, it is interesting to show that bioelectrochemically hydrogen production was sulphate-dependent. The hydrogen production rate was recorded by varying the cathode potentials, sulphate and bicarbonate concentrations as shown in this study. In spite of that, operational potentials have been well studied in hydrogen-producing biocathode and are predictable using the thermodynamic information (Geelhoed *et al.*, 2010; Keller and Wall, 2011; Jafary *et al.*, 2015; Choi and Sang, 2016). In addition to the potential, carbonate concentration might not be literally affected by the BES performance in this study. This is because of anaerobic bacteria normally grow slowly on biocathode compared to free-living bacteria or in aerobic condition (Kim and Gadd, 2008; Madigan *et al.*, 2014). SRB are chemoheterotrophic

bacteria that required organic matters like acetate to growth. Some studies reported the requirement of organic matter in hydrogen-producing biocathode by adding acetate in carbonate-containing medium (Liu *et al.*, 2005; Jeremiasse *et al.*, 2012; LaBelle *et al.*, 2014). It is suspected that these bacteria actually live syntrophically with acetogens which are autotrophs. The growth of these autotrophs was even lower if they involved in the biocathode activities such as acetogens and the accumulation of biomass would be redundant (Su *et al.*, 2013; Mand *et al.*, 2014). Jeremiasse *et al.* (2012) tried to test the acetate and sulphate effects on hydrogen-producing biocathode by feeding the medium with and without acetate or sulphate. It is interesting to point out that the current density supplied to the system was slightly lower at the beginning for sulphate-fed biocathode but overtook the control biocathode after 20 days (Jeremiasse *et al.*, 2012). Based on this reason, it is believed that electron bifurcation couple process occurred from both protons and sulphate reduction simultaneously. Electron bifurcation has been emerged and recognised as the third important biological energy conservation mechanism in the last decades after the two fundamental mechanisms, substrate level phosphorylation and electron transport-linked phosphorylation were unable to explain thermodynamically unfavourable reactions (Buckel and Thauer, 2013; Peters *et al.*, 2016).

In the review, Keller and Wall (2011) claimed that *Desulfovibrio sp.* produce hydrogen during sulphate reduction with ethanol. This involves electron bifurcation and *Desulfovibrio sp.* have energy conserving hydrogenases as *Desulfovibrio sp.* oxidise ethanol reducing NAD^+ to NADH (E_o'= -0.320V), NADH is bifurcated to reduce sulphate and proton (Ramos *et al.*, 2015). In the paper, Ramos *et al.* (2015) found hdrCBA-flxDCBA gene cluster is presented in many different phyla including electrochemically active microbes, *Desulfovibrio sp.* and *Geobacter sp.* This gene is responsible for transcribing flavin oxidoreductase (FlxABCD) and heterodisulfide reductase (HdrABC) to perform flavin-based electron bifurcation (FBEB). Both enzymes are involved in producing reducing carriers for hydrogen evolution and sulphate reduction. Proton reduction to hydrogen is catalysed by energy-conserving hydrogenase with the reducing carriers. It is hypothesized that at low cathode potential sulphate is reduced without hydrogen production, and if hydrogen is produced it is not sulphate-dependent. When the cathode potential was not low enough to reduce proton, electrons were bifurcated reducing both high and low redox potential electron carriers. The former is used to reduce sulphate and the latter to reduce proton conserving in both reduction reactions. Based on these facts, it is believed that hydrogen production would be inhibited in the presence of sulphate depended on its concentration. One of the reasons is because SRB is sulphate-dependent and conserves more energy by reducing sulphate (E_o'= -0.340 V) than reducing proton (E_o'= -0.410 V). As observed

in Figure 5.6 (a), overall hydrogen production rate in biocathode was higher than the control and peaked at 288 mg SO_4^{2-}/L. The rate started to decreased when higher sulphate concentration was introduced into the biocathode. However, there was only a small sulphate removal in biocathode compared to the control around the peak hydrogen production rate as shown in Figure 5.6 (c). Figure 5.8 describes the possible electron bifurcation flow for SRB growth on cathode used to reduce proton and sulphate. Lower sulphate concentration is actually good for SRB respiration (<288 mg/L) and promoted proton reduction. The hydrogen evolution decrease dramatically when more sulphate was added (>288 mg/L) as more electrons were utilised by reducing sulphate instead of protons.

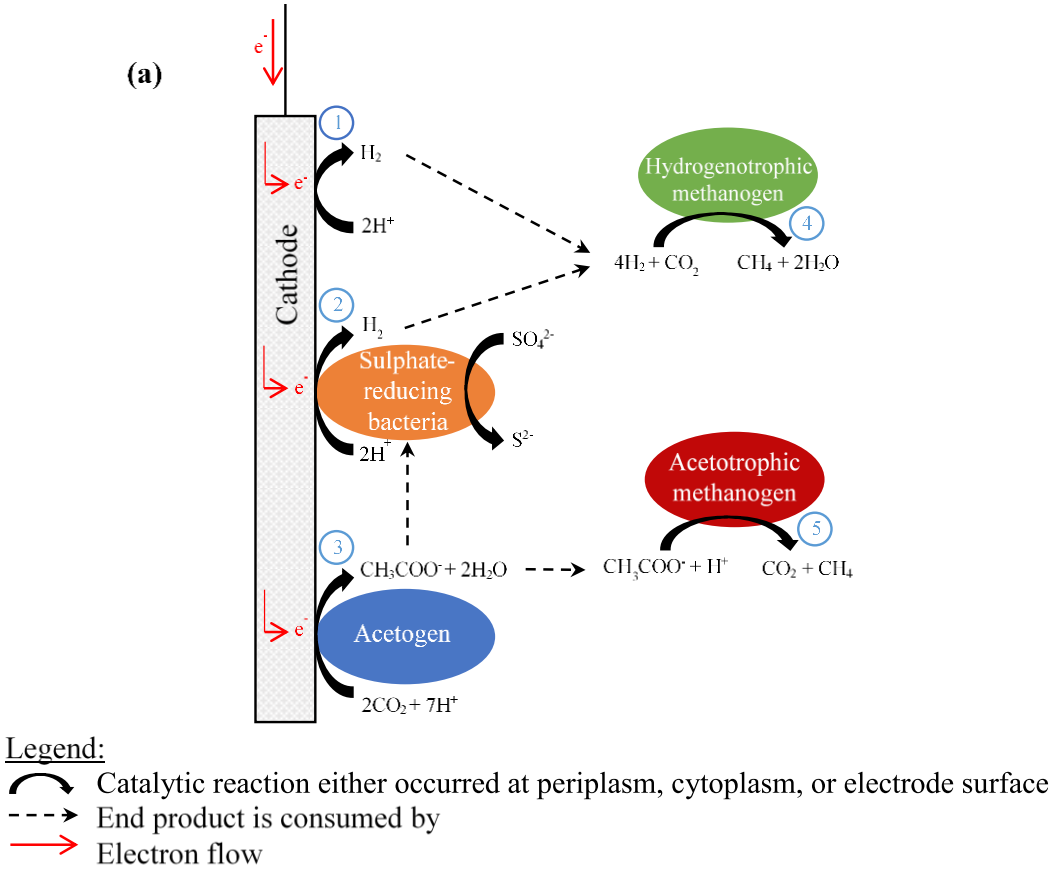

Mechanism	Mass balance	Potential vs. SHE (V)	Reaction type
1	$2H^+ + 2e^- \rightarrow H_2$	- 0.41	Electrochemical
2	$2H^+ + 2e^- \rightarrow H_2$ $CH_3COO^- + 4H_2O \rightarrow 2HCO_3^- + 9H^+ + 8e^-$ $SO_4^- + 6H^+ + 8e^- \rightarrow S^{2-} + 2OH^- + 2H_2O$	- 0.41 +0.28 - 0.34	Bioelectrochemical
3	$2HCO_3^- + 9H^+ + 8e^- \rightarrow CH_3COO^- + 4H_2O$	- 0.28	Bioelectrochemical
4	$HCO_3^- + 4H_2 + H^+ \rightarrow CH_4 + 3H_2O$	-	Biochemical

5	$CH_3COO^- + H_2O \rightarrow CH_4 + HCO_3^-$	-	Biochemical

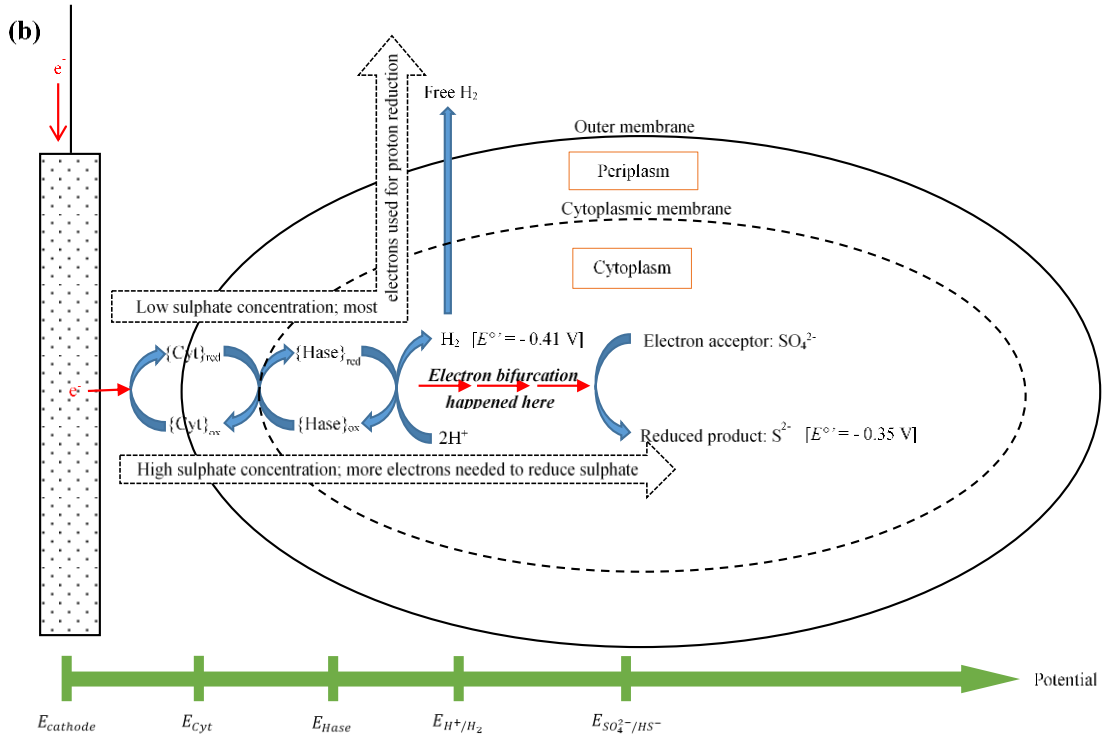

Figure 5.8 (a) Proposed electron flow and possible final destinations of the supplied electrons being utilised in producing various end products (modified after Mand *et al.* (2014), (b) description of electron bifurcation flow in sulphate-reducing bacteria-dominated biocathode to generate hydrogen and reduce sulphate.

Last but not least, the finding of the sulphate-dependent hydrogen-producing biocathode has raised the question; what type of wastewaters can be treated by using this technology? The sulphate dependency was due to the SRB domination in the biocathode and a specific range of sulphate concentration was required to maintain the balance and functionality of the biocathode to produce hydrogen while reducing sulphate. Domestic wastewater usually contains low amount of sulphate between 20 to 60 mg/L, although the concentration can be up to 500 mg/L for industrial wastewater (Lens *et al.*, 1998; Moussa *et al.*, 2006). Conventional sulphate removal technology benefits from the presence of SRB to treat domestic and industrial wastewaters. The benefits include reducing sludge accumulation and pathogen content (if present), removing heavy metals and as anaerobic digestion pre-treatment (van den Brand *et al.*, 2015). In the present study, an "optimum" sulphate concentration was 288 mg/L which

generated the maximum hydrogen volume. It is recommended to use domestic wastewater to enrich and maintain a hydrogen-producing biocathode because low amounts of organic compounds and sulphate make it a better medium to enhance the growth of SRB. (Jeremiasse *et al.*, 2012; Lee *et al.*, 2014).

5.3.6. Drawbacks on low potentials, mass transport limitation and long term operation

At the end of the experiments, white precipitation could be observed from the cathodic chamber as shown in Figure 5.9. The precipitated compounds were attaching along with biomass growth on the surface of the electrode and causing performance drop over time. It is believed that it was a form of crystallised phosphates due to the low applied potential (Jeremiasse *et al.*, 2010). Besides, a recycle flow was assisted by another peristaltic pump in order to reduce mass transport limitation and increase biomass accumulation in the chamber (Rozendal *et al.*, 2008). Figure 5.10 shows the relationship between the current density and the flow rate of the electrolyte recycle. Four flow rates were used to test the mass transport limitation: 0, 2.8, 7.1 and 11.4 mL/min. When zero flow rate was applied to the chamber, the current density reduced significantly. The flowrate of 7.1 mL/min was selected to use in the experiments as it generated almost similar current density compared to the higher flow rate at 11.4 mL/min.

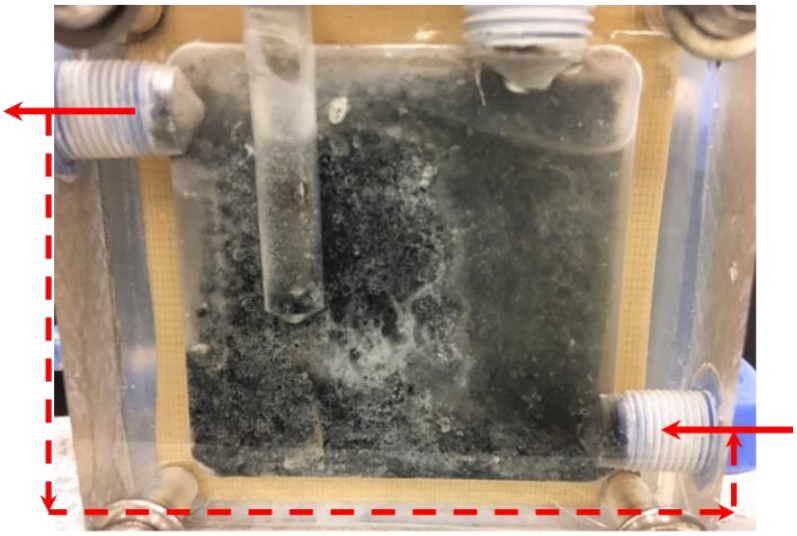

Figure 5.9 Biocathode after the experiments. White crystallisation and black biomass were appeared on the surface of the electrode causing current density dropped. Line arrows show inlet and outlet direction. Dash line arrows are recycling flows.

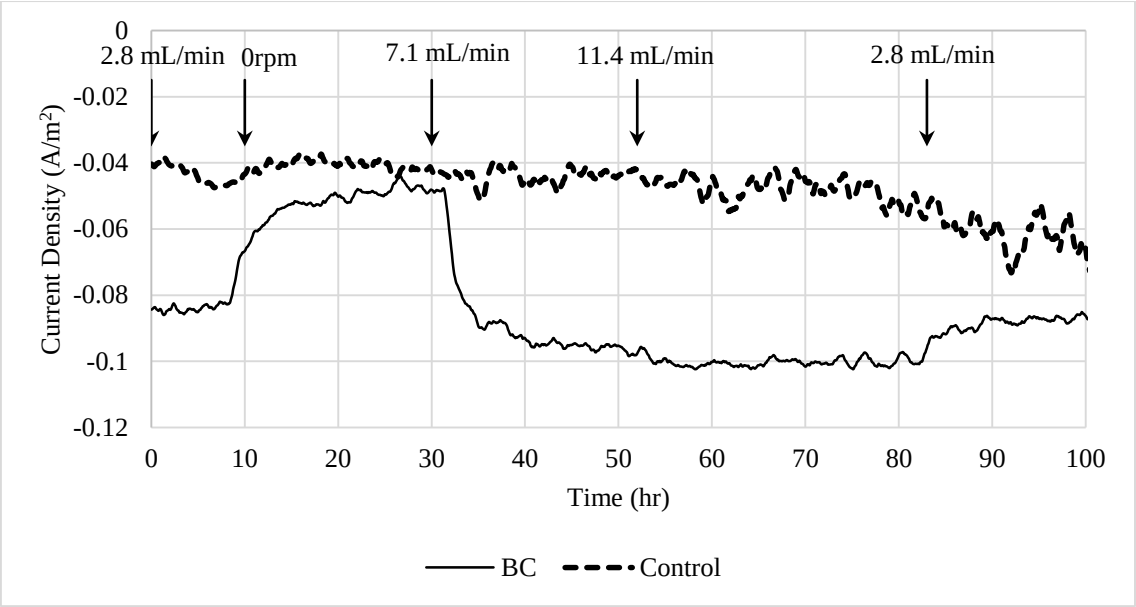

Figure 5.10 Current density affected by mass transport limitation. A flow line was connected between inlet and outlet to recycle catholyte in order to reduce the diffusion limitation. A control using 7.1 mL/min recycle flow rate was included in the figure for comparison purpose.

The risk of the enriched biocathode contaminated by methanogens under a hydrogen-rich environment after long time operation has been reported (Wagner *et al.*, 2009; Kyazze *et al.*, 2010; van Eerten-Jansen *et al.*, 2015; Bajracharya *et al.*, 2017b). Figure 5.11 (a1) and (a2) shows performance dropped when methane was first detected in the system after 120 days of operation (further data not shown). The timeline in x-axis was adjusted to zero for comparison purpose. Hydrogen production dropped remarkably after day 4 when methane content was detected in the biocathodes. A small amount of bicarbonate was probably released as CO_2 and could be also consumed by methanogens when they grew. Methane content at its highest point at day 6 and probably resulted the hydrogen production dropped significantly. Current demand was also increased as more energy was required to support both hydrogen and methane production. Figure 5.12 (a) shows the clean and normal recirculation tubes while Figure 5.12(b) compared the normal and methanogenic-contaminated recirculation tubes when methane was first detected.

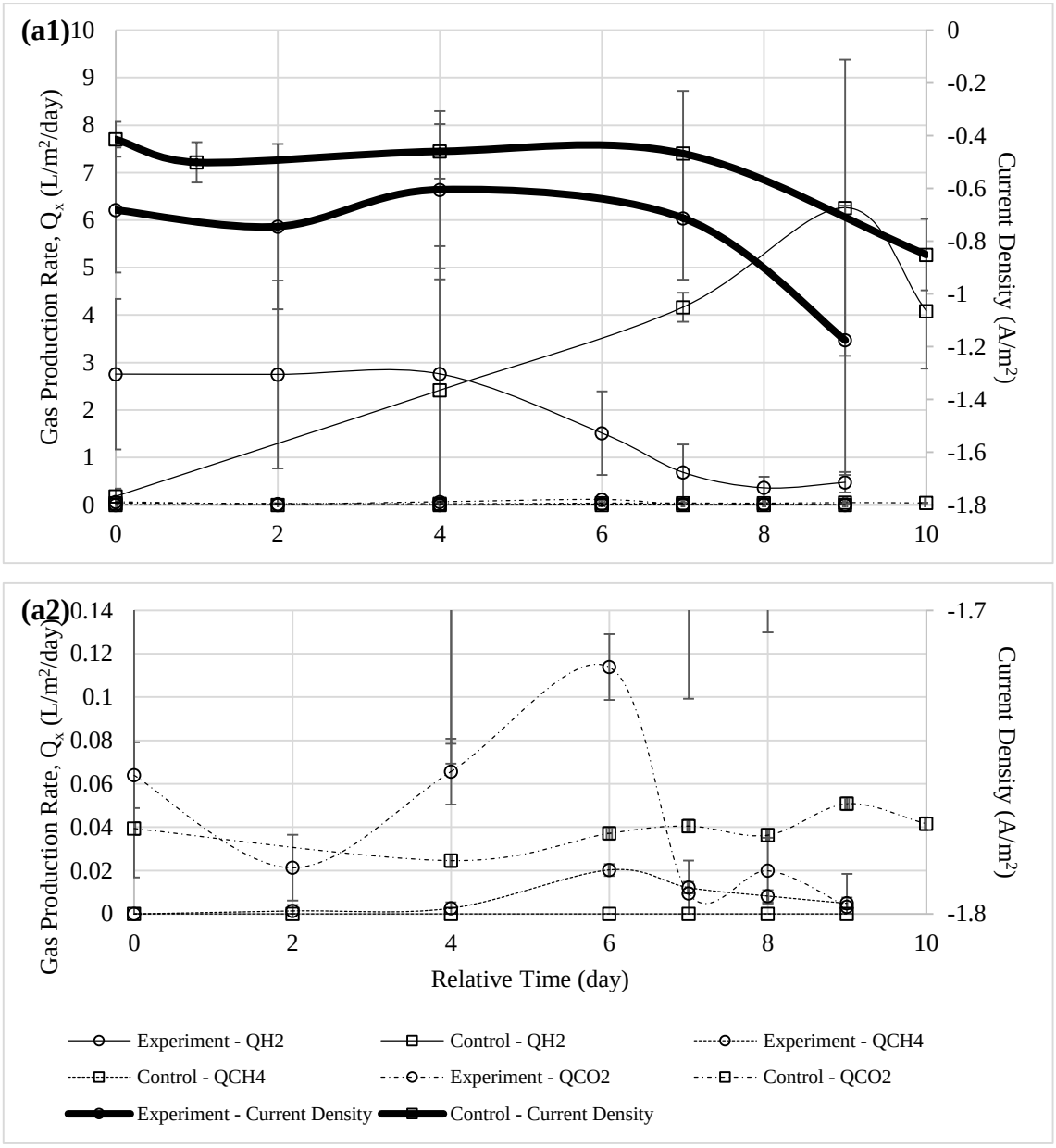

Figure 5.11 (a1) & (a2) Gas production rate of the defected MECs. Noted that the timeline is adjusted to zero adjusted for comparison purpose.

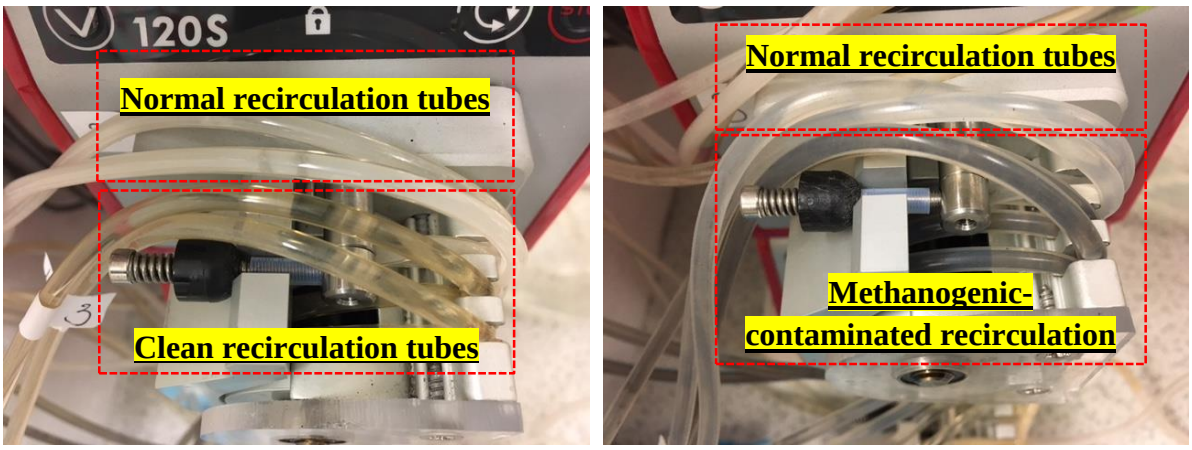

(a) (b)

Figure 5.12 (a) Upper tubes show white biofilm growth on the inner surface of the tubes while lower tubes were clear after cleaned and soaked with disinfectant, Virkon, and (b) upper tubes was the normal recirculation tubes while black colour biofilm in the lower tubes was observed when methane started to detect in gas samples.

5.4. Conclusion

Hydrogen-producing biocathode was successfully enriched as reported by the previous study. A series of confirmation tests reveal that hydrogen-producing biocathode was developed. Further study on the biocathode revealed that applied potential, sulphate and inorganic carbon are vital parameters to promote hydrogen production. The optimum ratio of PBS: HCO_3^-: NH_4^+: SO_4^{2-} in this study was determined as 950:610:90:288 mg/L (or 10:10:5:3 mM). The information provided the first insight of how much carbon, nitrogen and sulphate sources that must be presented in the influent in order to provide better operational conditions. Even though the ratio may slightly vary according to the size of the reactor, cell configuration and controlling system, the basic principle of how a biocathode catalyses hydrogen under the influences of those main sources would still remain the same. Besides the ratio, external power supply was required to provide initial energy under low potential electrons to start the biocathode catalytic activity while sulphate served as a final terminal electron acceptor to dispose of the exhausted electrons. It was found that applied potential to the biocathode should be at least -0.8 V or below to perform proton reduction reaction due to overpotentials. Inorganic carbon in the form of carbonates was added to the influent and worked as a carbon backbone to support the growth of the biocathode community. As organic carbon compounds were found in the biocathode effluents, it is believed that within the microbial community the inorganic carbon was consumed

by acetogens to produce organic carbons such as acetate and then consumed by SRB as a carbon source. Another significant finding is the present and quantity of sulphate did affect the hydrogen production in SRB-dominated biocathode. At high sulphate concentration, it could inhibit hydrogen production if the cathode potential was not low enough to reduce both sulphate and proton. The phenomenon is similar to electron bifurcation. After a long term operation (120 days), a small amount of methane was found in the biocathode headspace which gave a significant effect in reducing the hydrogen production. This is because four moles of hydrogen produced from biocathode was used to form one mole of methane under methanogenic condition.

Chapter 6. Operational applied voltage of microbial electrolysis cells

6.0. Chapter summary

The main focus of this chapter is the study of the applied voltage to a microbial electrolysis cell (MEC) fully catalysed by microorganisms. How bioanode and biocathode behave and interact with each other in a system during an enrichment process which were monitored using electrochemical methods. After a stable current was observed, the MEC was subjected to a range of applied voltage to study the bioelectrodes' responses. Moreover, oxidation-reduction reactions were also examined included the consumption of substrate in anode and production of certain products in cathode such as acetate and hydrogen. Any limitation to the bioelectrodes was clearly identified under the applied voltage range. Energy recovery and contribution for bioelectrode and whole system were determined at the end of the analysis. Besides two-chamber MEC, a three-chamber MEC was demonstrated to show the potential usage of the system in directly separating and dissolving CO_2 into catholyte.

6.1. Introduction

As global greenhouse effect over the past decades is related to the unrestrained release of carbon dioxide (CO_2) into the atmosphere, one of the solution is to limit its emissions and capture/reuse it before it reaches the atmosphere. Inorganic carbon in the form of CO_2 is a useful resource for the microbial ecosystem. It is believed that Bioelectrochemical systems (BES) could provide a solution to this problem. Microbial electrosynthesis cells (MSC) are one of the BES that can use biocathodes to generate useful products such as acetate, hydrogen and methane from CO_2 reduction (Mohanakrishna *et al.*, 2015; van Eerten-Jansen *et al.*, 2015; LaBelle and May, 2017). Combining a CO_2-reducing biocathode with an electron-generating bioanode into a MSC, not only reduces the requirement of external power input for the generation of valuable bioproducts but also acts as a potential technology for wastewater treatment (Jeremiasse *et al.*, 2010; Lim *et al.*, 2017). MSC technologies with combined bioanode and biocathode are attractive due to the sustainability and low-cost maintenance associated with the use of microorganisms as

biocatalysts (Rabaey and Rozendal, 2010; Choi and Sang, 2016). It makes the technologies become feasible for scale up and real applications while offset operation costs (Escapa *et al.*, 2016; Kadier *et al.*, 2016).

In a previous study, bioanode has been identified as a limiting factor capping the performance of microbial electrolysis cell (MEC) (Lim *et al.*, 2017). The results showed that to maintain a specific rate of hydrogen production, the biocathode required a certain amount of electron or current to operate. In an ideal condition, bioanode had to produce the same amount of electron in order to support biocathode reduction activity. Therefore, power supply was used to adjust the potentials of anode and cathode to favourable oxidation and reduction potentials. Nevertheless, the extra current was supplied by the power supply to compensate the energy gap in real condition due to the fact that overpotentials and difference rate of reactions between bioanode and biocathode. When the potential raised beyond the limit of bioanode, it lost its biotic function to perform substrate oxidation activity. An abiotic process started to dominate in the anode when bioanode could not provide sufficient electron to the system causing the overshoot of anode potential to more positive. Therefore, a deeper examination is needed to understand the behaviour of both bioelectrodes in terms of electrochemical properties and catalytic activities in a MEC. For instance, it is well known that the lowest bioanode potential that can be achieved is close to -0.20 V vs. SHE determined from the catalytic signal with a symmetric peak in the first derivative of cyclic voltammograms of electrochemical-active bioanode. The midpoint potential is believed to be associated with outer membrane cytochromes or free flavins secreted by cells (Bond and Lovley, 2003; LaBelle, 2009). Up to date, most of the reduction processes involved in biocathodes are related with the reduction of CO_2 and proton into desired products such as CH_4, H_2, acetate, formate, ethanol, butanol, etc.. Theoretically, the reduction potentials for these products range from -0.24 to -0.41 V vs. SHE (Rabaey and Rozendal, 2010; Bajracharya *et al.*, 2016a; Zhen *et al.*, 2017). For example, HCO_3^-/CH_4 (E_o' = -0.24 V; $8e^-$); H^+/H_2 (E_o' = - 0.41V; $2e^-$); HCO_3^-/CH_3COOH (E_o' = -0.28V; $8e^-$); HCO_3^-/C_2H_5OH (E_o' = -0.31 V; $12e^-$); HCO_3^-/HCOOH (E_o' = - 0.41V; $2e^-$) in standard conditions of 1 M reactant in water pH 7.0 at 1 atm and 25°C (Rabaey and Rozendal, 2010; Choi and Sang, 2016; Zhen *et al.*, 2017). As a result, at least 0.04 V is required by the bioelectrodes to drive the oxidation-reduction process in the BES. In spite of that, applied voltages higher than 0.5 V was used in most studies considering overpotentials caused by the system and energy losses due to microorganism metabolic activities (Geelhoed *et al.*, 2010; Choi and Sang, 2016).

Since then, various cell configurations have been tested and used in laboratory for biocathode-reduction processes, especially hydrogen production. Hydrogen is attractive as it is a clean energy source and a good energy carrier. The technology has advanced from half-cell to full cell configuration, two chambers to single chamber, batch to continuous tubular mode, and laboratory to large scale (Jafary *et al.*, 2015; Zhen *et al.*, 2017). Studies aim in reducing overpotentials and cutting down operation cost and development time (Escapa *et al.*, 2016; Kadier *et al.*, 2016; Zhen *et al.*, 2017). Nonetheless some questions still remain unanswered in full cell systems including the bioanode and biocathode interactions (e.g. current response and how biofilms evolve), optimum operational environments for bioelectrodes (e.g. pH, conductivity, cell voltage), time of growth for both bioanode and biocathode (e.g. 1 vs. 4 weeks), optimum reducing power or potential required by biocathodes to produce certain products (e.g. HCO_3^-/CH_3COO^- E_o'=-0.28V H^+/H^2 E_o'=-0.41V) when coupled with bioanode for wastewater treatment? In fact, the usage of microorganisms as biocatalyst in the system can reduce the cost of investment because they can multiply as long as the environment is favoured for growth. In this study, the bioanode and biocathode were enriched simultaneously in the same cell. The aim is to understand the impact of the cell voltage on the interactions between the bioanode and the biocathode and thus on the production of hydrogen and other products.

6.2. Experimental procedure

6.2.1. Preparation of microbial electrolysis cells

Two- and three-chamber microbial electrolysis cells (2c- & 3c-MECs) were assembled according to section 3.1.1.

6.2.2. Enrichment and operation

The detail of the media used in this study was collected and prepared as mentioned in section 3.1.2. Meanwhile, the MEC was started up and operated according to the procedure (direct enrichment of both bioanode and biocathode simultaneously) described in section 3.1.3 except the feed of anode was changed from batch to fed-batch mode using pre-set on-off timer (Electric Timer Switch ETU17, Timeguard, UK) and a peristaltic pump (Watson Marlow 120U/DM3, UK) once bioelectrodes were developed and a stable current was observed. The timer was set 'on' for 10min for every 6-hour gap and the peristaltic pump was set at flowrate of 3 mL/min

unless stated otherwise. A similar MEC was setup as control with added inoculum but without applying voltage between anode and cathode. The control was operated in such way due to the cross contamination issue found in previous experiments. It was difficult to maintain a sterile condition when the control was operated nearby the active cell. The cell and control were placed inside a polystyrene box to shield off from the daylight. All experiments were conducted in duplicates under a temperature controlled environment at 26.5 ± 2.5°C. The rest of the operational conditions are summarised in Table 6.1.

Table 6.1 Description of the experiments, tested conditions and adjustments for (a) 2cMEC and (b) 3cMEC.

Test number	Time (day)	Applied voltage (V)	Anode Feed control	Anode cycle	Cathode cycle	Note
1	0 - 10	0.3	No	Medium was replaced manually according to anode potential	Medium was replaced manually according to anode potential	Enrichment started, both anode and cathode were injected with 1:1 of inoculum: medium at the beginning
2	11 - 148	0.3	No	Medium was replaced manually according to anode potential	Medium was replaced manually according to anode potential	Enrichment process continued and media were replaced every 4-5 days
3	148 - 162	0.5	No	Medium was replaced manually according to anode potential	Medium was replaced manually according to anode potential	Increased applied voltage, no hydrogen was found
4	162 - 165	0.7	No	Medium was replaced manually according to anode potential	Medium was replaced manually according to anode potential	Increased applied voltage, no hydrogen was found
5	165 - 168	0.7	Yes	Medium was fed 4 times/day using pre-set timer and pump	Medium was replaced manually once/day	Found fed-batch mode in anode improved current density
6	168 - 178	0.3 - 1.6	Yes	Medium was fed 4 times/day using pre-set timer and pump	Medium was replaced manually once/day	First CA test, hydrogen was produced
7	178 - 212	0.5 - 0.9	Yes	Medium was fed 4 times/day using pre-set timer and pump	Medium was replaced manually once/day	Randomly applied voltage to find a significant hydrogen production condition
8	212 - 222	0.3 - 1.6	Yes	Medium was fed 4 times/day using pre-set timer and pump	Medium was replaced manually once/day	Repeat CA test, liquid samples were collected and analysed
9	222 - 264	0.9	Yes	Medium was fed in fed-batch and continuous mode	Medium was replaced manually once/day	Hydrogen production was slightly improved about 10%, continuous mode was not better than fed-batch mode in overall
10	239 - 248	0.9	Yes	Medium was fed 4 times/day using pre-set timer and pump	Medium was replaced manually once/day	Connection problem
11	264 - 286	0.3	Yes	Medium was fed 2 times/day using pre-set timer and pump	Medium was replaced manually at the end	Medium saver mode to keep bioanode active

12	286 - 319	0.3 - 2.0	Yes	Medium was replaced every day using pre-set timer and pump	Medium was replaced manually every two days	Two anode cycle was equal to one cathode cycle
13	319 - 322	0.3	Yes	Medium was replaced every day using pre-set timer and pump	Medium was replaced manually every 3-4 days	Bioanode recover

(a)

Test number	**Time (day)**	**Applied voltage (V)**	**Anode Feed control**	**Anode cycle**	**Cathode cycle**	**Note**
1	0 - 10	0.2 - 0.3	No	Medium was replaced manually according to anode potential	Medium was replaced manually according to anode potential	Enrichment started, both anode and cathode were injected with 1:1 of inoculum: medium at the beginning
2	11 - 100	0.3	No	Medium was replaced manually according to anode potential	Medium was replaced manually according to anode potential	Enrichment process continued and media were replaced every 4-5 days
3	100 - 115	0.3 - 1.1	No	Medium was replaced manually according to anode potential	Medium was replaced manually according to anode potential	First chronoamperometry test, no hydrogen was produced
4	115 - 118	0.3	No	Medium was replaced manually according to anode potential	Medium was replaced manually according to anode potential	Bioanode recover
5	160 - 180	0.3 - 1.6	Yes	Medium was fed 4 times/day using pre-set timer and pump	Medium was replaced manually once/day	Repeated CA test, found fed-batch mode in anode improved hydrogen production, the optimum applied voltage was 0.9V
6	210 - 225	0.3 - 1.6	Yes	Medium was fed 4 times/day using pre-set timer and pump	Medium was replaced manually once/day	Repeated CA test, liquid samples were collected and analysed
7	240 - 250	0.9	Yes	Medium was fed continuously	Medium was replaced manually once/day	Hydrogen production slightly improved about 20%, continuous mode was not better than fed-batch mode in overall
8	265 - 287	0.3	Yes	Medium was fed 2 times/day using pre-set timer and pump	Medium was replaced manually at the end	Medium saver mode to keep bioanode active
9	290 - 322	0.3 - 2.0	Yes	Medium was replaced every day using pre-set timer and pump	Medium was replaced manually every two days	Two anode cycle was equal to one cathode cycle
10	323 - 330	0.3	Yes	Medium was replaced every day using pre-set timer and pump	Medium was replaced manually every 3-4 days	Bioanode recover

(b)

6.2.3. CO_2 diffusion and calculation

In 3cMEC, CO_2 was contained in a gas chamber located next to cathode separated by a CEM. When the contained CO_2 diffused and dissolved into the catholyte, gas volume decreased and the volume was replaced by water using water displacement method. The pH of the water used in the displacement method was acidified with HCl to less than 2.0 to minimise the dissolution of CO_2 into the water and caused an unnecessary error. The difference volume in headspace before and after were recorded and converted to relative mass weight. The CO_2 mass transfer coefficient through CEM, k_o (cm/s) was then calculated according to:

$$k_o = -\frac{V_{gas}}{A_m t_d} \ln \frac{c_o - c}{c_o} \quad \text{Equation 6. 1}$$

where V_{gas} (cm^3) is total volume in gas chamber ($=\pi 2^2 \cdot 4$), A_m (cm^2) is membrane cross-sectional area ($=\pi 2^2$), t_d (s) is time required to diffusion c_o - c mole CO^2 through membrane, c_o (mole) initial CO_2 content in gas chamber, c (mole) final CO_2 content in gas chamber.

And, the CO_2 diffusion coefficient, D_o (cm^2/s) was computed by:

$$D_o = k_o L \quad \text{Equation 6. 2}$$

where L (cm) is membrane thickness (=0.045 cm).

6.2.4. Electrochemical methods

The potentials of the MECs were monitoring as described in section 3.2.1. Meanwhile, electrochemical impedance spectroscopy (EIS) and cyclic voltammetry (CV) analysis were carried out as mentioned in section 3.2.2 and 3.2.3 and chronoamperometry (CA) as in section 3.2.4.

6.2.5. Analytical methods

pH, conductivity, total organic/inorganic carbons (TOC) and short-chain fatty acids (SCFA) were measured and determined as described in section 3.2.3.

6.2.6. Overpotentials at high applied voltages

To further analyse electrical energy losses in the MECs, polarisation equation (as in Section 4.2.2) was modified as follows:

$$-V_{ap} = -E'_{Cell} + b \log I_D + RI_D + \gamma \exp(\omega I_D)$$ Equation 6. 3

where V_{ap} (V) is the applied voltage considers the energy losses in the system, $E_{Cell}^{'}$ is the standard cell voltage (V) where there is no energy loss or supply to the system (in this case, $E_{Cell}^{'}$ is -0.13 V. Cathode: H^+/H_2, $E_o^{'}$ = -0.41 V; Anode: HCO_3^-/CH_3COO^-, $E_o^{'}$ = -0.28 V), b is activation coefficient (V) due to the surface material of electrode that needs an initial potential energy to activate a redox reaction, I_D is current density (A/m^2), R is ohmic coefficient (Ω) considers the potential energy loss as a results of electron transportation between electrodes, and γ (V) and ω (m^2/A) are both diffusion coefficients. γ explains that potential energy is consumed in order to transfer the reactant from bulk solution to electrode's surface or vice versa and ω estimates the rate of current consumption per electrode surface area.

6.2.7. Energy recovery and contribution

The energy produced by the bioanode and consumed by the biocathode were calculated to evaluate the overall efficiency of the system used. The energy recovery and efficiency were determined based on acetate as a sole carbon source at the anode and hydrogen as the main product at the cathode. The calculations of the energy recovery and contribution were followed as described in section 3.4.

6.3. Result and discussion

Both 2cMEC and 3cMEC results are presented in this section to create a whole picture of how the operational voltage affected the performance of a MEC fully catalysed by microorganisms. Bioelectrode electrochemical behaviours and electrolyte properties are acted in the same principles between two cell configurations. Further discussions are included if there is any noteworthy to mention the differences.

6.3.1. Enrichment and operation of bioelectrodes

The cells were inoculated with inoculum collected from a parent microbial fuel cell fed with glucose and glutamic acid operated over a year. Both bioanodes and biocathodes were enriched simultaneously at a fix cell potential of 0.30V after being left for a few days at Open Cell Potential (OCP). Figure 6.1 (a1), (a2) and (a3) shows the potential profiles of anode and cathode during the enrichment period as well as the current density profile (b1), (b2) and (b3).

Biological cathodes producing hydrogen, methane, acetate, butanol or formate from CO_2 reduction have been reported (Rabaey and Rozendal, 2010; Choi and Sang, 2016; Zhen *et al.*, 2017). In real conditions, parameters like pH, conductivity and temperature could further increase the potential threshold required to more negative. In the case of protons reduction to hydrogen, the potential varies between 0.00 to -0.83 V depending on the solution pH (H^+/H_2 acidic: 0.00V; neutral: -0.41 V; alkaline: -0.83 V) causing the increase of the energy input required. Bioanodes in bioelectrochemical systems (BES) have been extensively studied and it was reported that negative potentials ranging from -0.28 to -0.41 V could be achieved, depending on the substrates and microbial communities (Wang *et al.*, 2009; Kim *et al.*, 2011; Lim *et al.*, 2012; Ketep *et al.*, 2013; Zhu *et al.*, 2013; Spurr, 2016). For instance, acetate- and glucose-fed bioanodes can reach -0.22 V and -0.43 V respectively, while OCPs for most bioanodes fed with real wastewaters were reported around -0.33 V (Bajracharya *et al.*, 2016a; Zhen *et al.*, 2017). In most of these studies, it was found that *Geobacter sp.* and *Shewanella sp.* were the electrochemical active microorganisms dominating the microbial communities (Kim *et al.*, 2002; Kim *et al.*, 2004). These strains can be easily enriched from natural environments in laboratory conditions, which make them versatile for BES technologies. However, part of the energy contained in electrons coming from the substrate oxidation (e.g. acetate or glucose) is used by microorganisms for growth and cell maintenance before they can reach the outer membrane surface for discharge to the anode. In order to act as an electron sink, the anode's potential should be slightly higher than the potential of outer membrane proteins or cytochromes to facilitate electron transportation. Even though such a potential gap enables the electron flow, energy loss can still occur when electrons travel between outer membrane proteins to an electrode. The overpotentials occur especially when the electrons hop across the space in extracellular matrix which links the microbial cell to the electrode. Energy is used to drive the electrons from the cell to the electrode, causing the anode potential to be higher than the standard oxidation potentials (LaBelle, 2009). For example, the lowest potential that most acetate-fed bioanode can reach is around -0.22V compared to standard reduction potential of acetate which is -0.28 V (Bond and Lovley, 2003; Lim *et al.*, 2017). Acetate-fed bioanodes are commonly used in laboratory conditions because of their stable and consistent current generation. In order to couple bioanodes and biocathodes reactions into a single cell, a minimum external power supply of [X - (-0.22)] V is required, where X is the reduction potential of the desired product. In this study, the objective is to develop a hydrogen-producing biocathode [H_2/H^+ $E_o^{'}$ = -0.41V] at neutral pH. According to the considerations explained above, the minimum theoretical applied cell voltage was determined as 0.19 V but 0.30 V was chosen as

a starting potential to take into account the energy losses and overpotentials at both electrodes. As can be seen in Figure 6.1 (a1), the anode potential was about + 0.20 V when 0.30 V was first applied (4.6 days) before starting to decrease within a day to -0.10 V (7.4 days) and reaching nearly -0.48V after the medium was replaced for the second time (8.3 days). On the other hand, the current density increased within 10 days of operation, confirming the growth of the bioanode. Meanwhile, the cathode potential followed the trend of the anode, reaching -0.76 V after the second cycle. The bioanode developed quicker and dragged the cathode potential down to more negative. This lower potential created more suitable conditions for the biocathode development which in turn favoured protons and CO_2 reduction. After then, both anode and cathode media were changed according to the bioanode cycle, i.e. every 3-4 days. It is believed that anode reaction was faster than cathode reaction as substrate is being oxidised at the anode, in opposition to products being generated at the cathode (e.g. fatty acids and hydrogen in this case) (Zaybak *et al.*, 2013; Jourdin *et al.*, 2015; Bajracharya *et al.*, 2017b; Raes *et al.*, 2017). A further small drop in cathode potential was observed at day 60 (Figure 6.1 (a1)) but no significant current increased until 130 days (Figure 6.1 (b1)). This increase was believed to be associated with the biocathode enrichment which requires a longer time to enrich than the bioanode (Zaybak *et al.*, 2013; Jourdin *et al.*, 2015). The rest of the operational conditions are summarised in Table 6.1 (a). For 3cMEC, the time of operation was in conjunction with the 2cMEC and similar to the interpretations of the results as discussed above. The results and figures are attached side by side with the 2cMEC main figures (Figure 6.1 (c1), (c2), (c3), (d1), (d2), (d3) and Table 6.1 (b)).

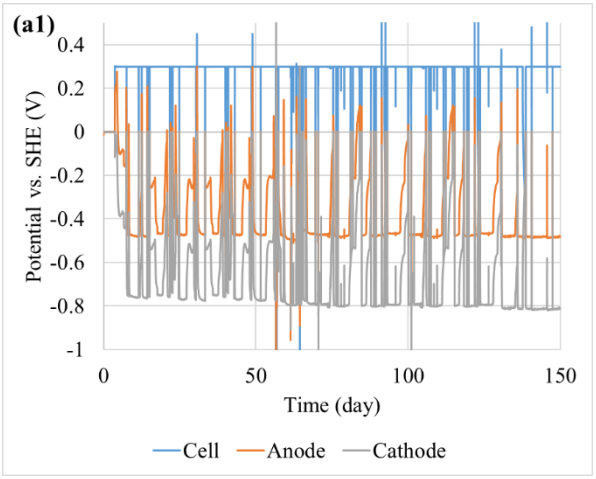
(a1)
Potential vs. SHE (V)
Time (day)
Cell
Anode
Cathode

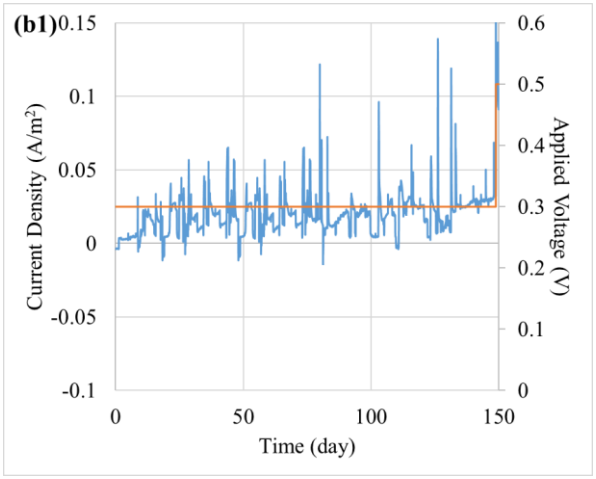
(b1)
Current Density (A/m²)
Applied Voltage (V)
Time (day)

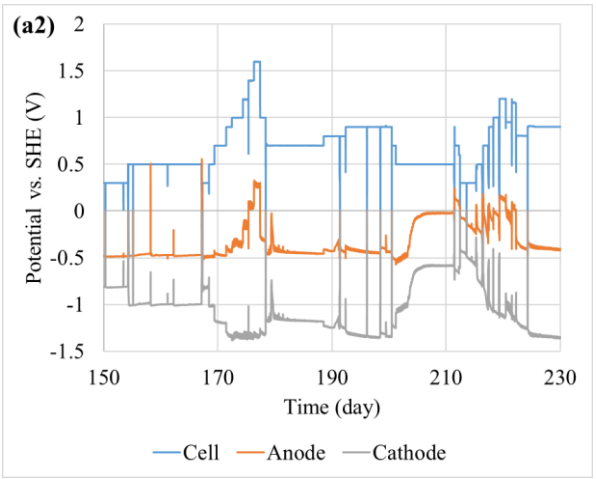
(a2)
Potential vs. SHE (V)
Time (day)
Cell
Anode
Cathode

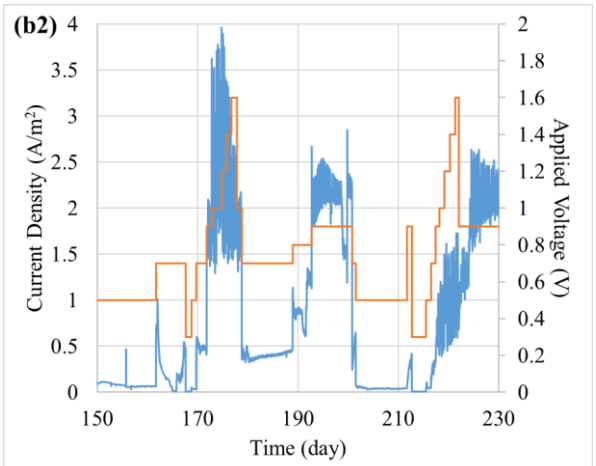
(b2)
Current Density (A/m²)
Applied Voltage (V)
Time (day)

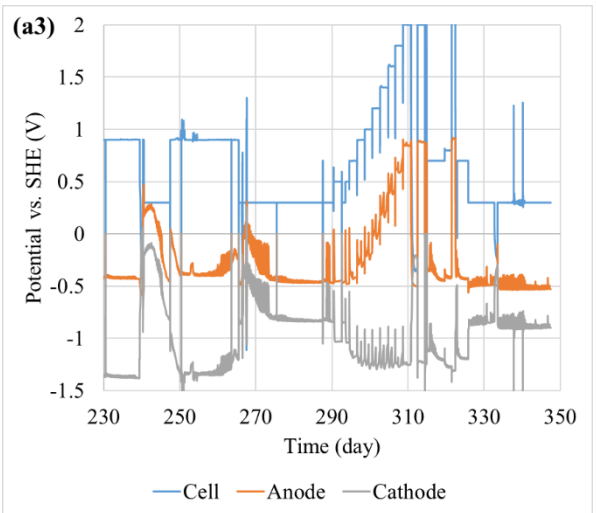
(a3)
Potential vs. SHE (V)
Time (day)
Cell
Anode
Cathode

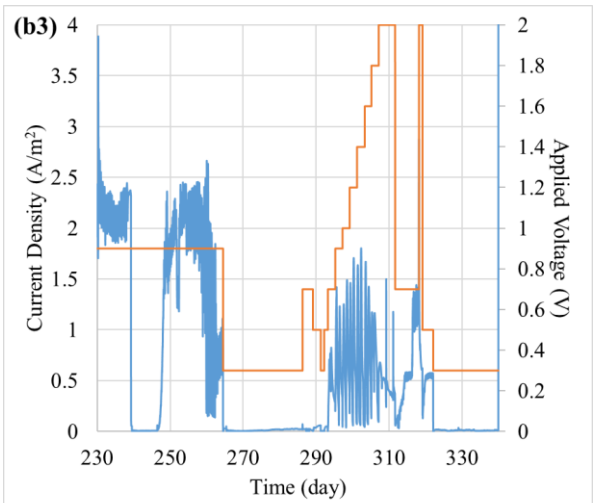
(b3)
Current Density (A/m²)
Applied Voltage (V)
Time (day)

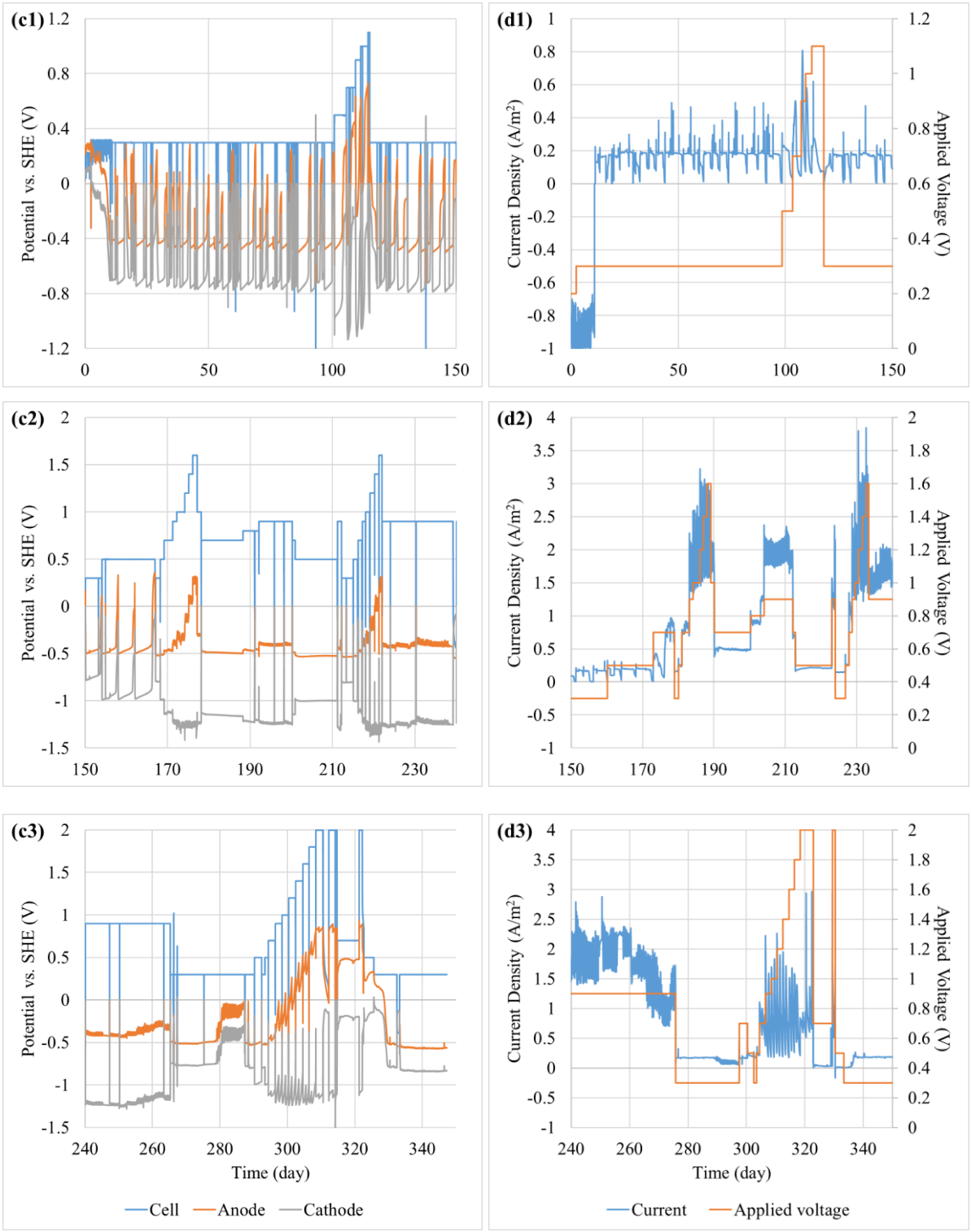

Figure 6.1 The profile of (a) electrode potentials and (b) current density for two-chambered microbial electrolysis cell (2cMEC) and the profile of (c) electrode potentials and (d) current density for three-chambered microbial electrolysis cell (3cMEC)

During the enrichment process, some electrochemical analysis was done to monitor and check the activity of the bioelectrodes over time. All monitoring and activity checking data

were showed and discussed in Appendix B. However, the important results were discussed in the following sections.

6.3.2. Chronoamperometry test and hydrogen production

The cells were subjected to a range of applied voltage from 0.3 to 2.0 V with a tested period of two days for each voltage between 286-319 days. Figure 6.2 shows the monitored voltage, potentials and current densities during the chronoamperometry experiments summarised in Table 6.1, whereas Figure 6.3 shows the corresponding hydrogen and other organics production rates in the cathodic compartment. Both the oxidation of acetate at the anode and the hydrogen production at the cathode were started when the applied voltage reached 0.7 V, as showed in Figure 6.2 and Figure 6.3. Below 0.7 V, the cathode potential was higher than -1.0 V, thus not low enough to support the biotic production of hydrogen. Below these applied voltages, excessive electrons were accumulated in bioanode instead of being sent out and used in biocathode. These observations are consistent with the very low H_2 concentration measured in the headspace for applied potentials below 0.7 V (Figure 6.3 (a) and (b1)). At 0.7 V and above, the oxidation potential at the anode increased thus inducing the reduction of protons and CO_2 at the cathode by supplying more electrons. At this point, the cathode potential reached almost -1.0 V with the lowest potential recorded as -1.1 V. It is believed that pH variation affected the cathode potential and performance, as will be discussed in the next section 6.3.3: electrolyte properties under different applied voltages. Aside from the headspace observation, anode and cathode potentials began to evolve according to the anodic cycle as observed. Due to the fact that bioanode growth faster than biocathode (weeks vs. months) and microbiology characteristics (organotrophs vs. chemoautotrophs) (Kim *et al.*, 2004; Wang *et al.*, 2009; Zaybak *et al.*, 2013; Jourdin *et al.*, 2015; Mohanakrishna *et al.*, 2015; Jourdin *et al.*, 2018), the catholyte was replaced according to two feed cycles of bioanode so more organic carbons could be accumulated. Since then the bioanode potential kept evolving and increasing according to its feed cycles at higher applied voltages. In contrast, for cell voltages higher than 0.7 V, the biocathode potential reached about -1.1 V and remained fairly constant until the end of the experiment. As shown in Figure 6.3 (a) and (b1), a cell voltage of 1.0 V (2cMEC) or 1.2 V (3cMEC) appeared as optimal range considering the volume of hydrogen measured, which was also consistent with other studies (Rozendal *et al.*, 2008; Batlle-Vilanova *et al.*, 2014; Jourdin *et al.*, 2015; Lim *et al.*, 2017). The test was carried out until the bioanode failed to oxidise substrate and produce electrons, which occurred at an applied voltage of 2.0 V where a decrease

in current density, lower hydrogen production and acetate removal rates were observed (see 'section 6.3.4: Bioelectrode limitations at high applied voltages'). It can be assumed that the higher oxidation potential induced abiotic reactions especially oxygen evolution which harming the anaerobic bioanode (Lim *et al.*, 2017). These results show that for cell potentials lower than 2.0 V, the role and performance of the bioanode are critical for the viability of the whole system. Indeed, as the catalytic activity of the bioanode collapses, the hydrogen generation rate drops. Although the cathode potential remained constant, the loss of the biocatalytic activity at the anode resulted in a lower current density. The current density profile in Figure 6.2 (b) indicated the rate of electrochemical reactions in the system where the optimised applied voltage should lay in between 0.7 to 1.8 V. Further investigation on the hydrogen evolution rate, acetate and carbonate removal narrowed down the applied voltage to a range from 0.9 and 1.2 V with a maximum hydrogen production rate at 1.0 V.

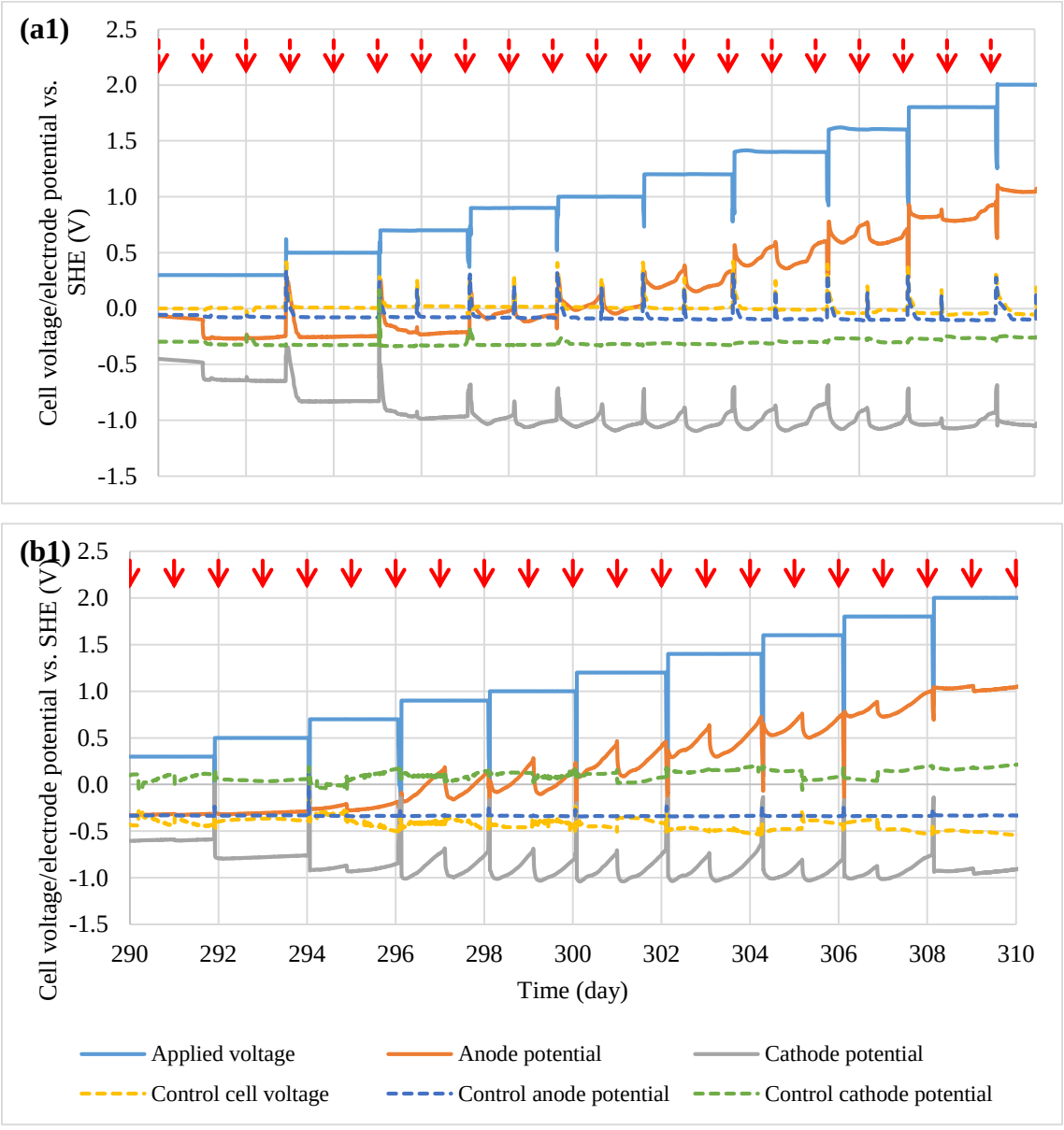

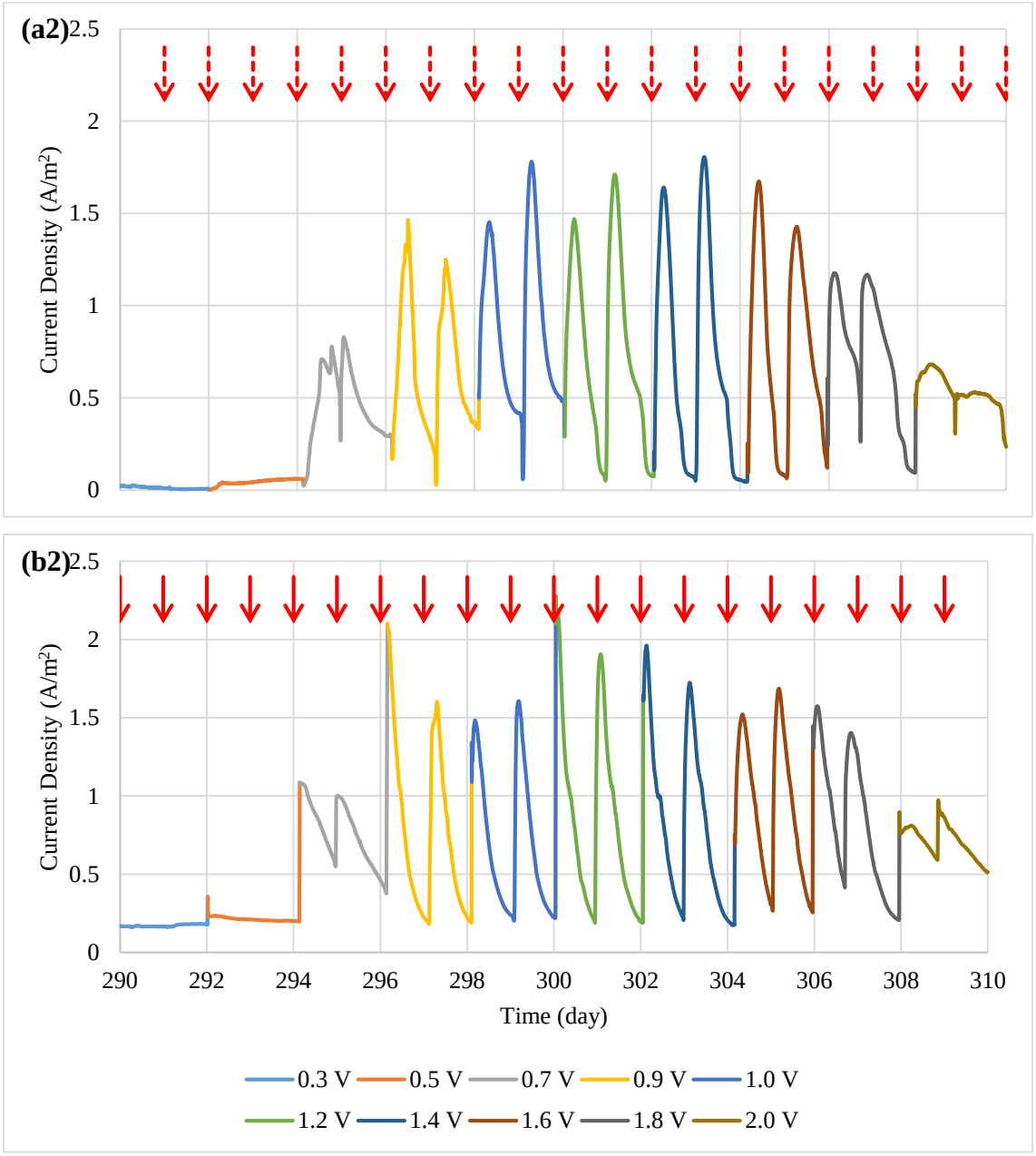

Figure 6.2 Applied voltage and electrode potential profiles for 2cMFC (a1) and 3cMEC (a2) and current density of external power supply to the 2cMFC (b1) and 3cMEC (b2) during the chronoamperometry test. Note: curves with the legend labelled as control are parallel test ran simultaneously during the experiments but without external power supply. The time was set to zero from the beginning of the CA test. The test was performed after 290 days of operation.

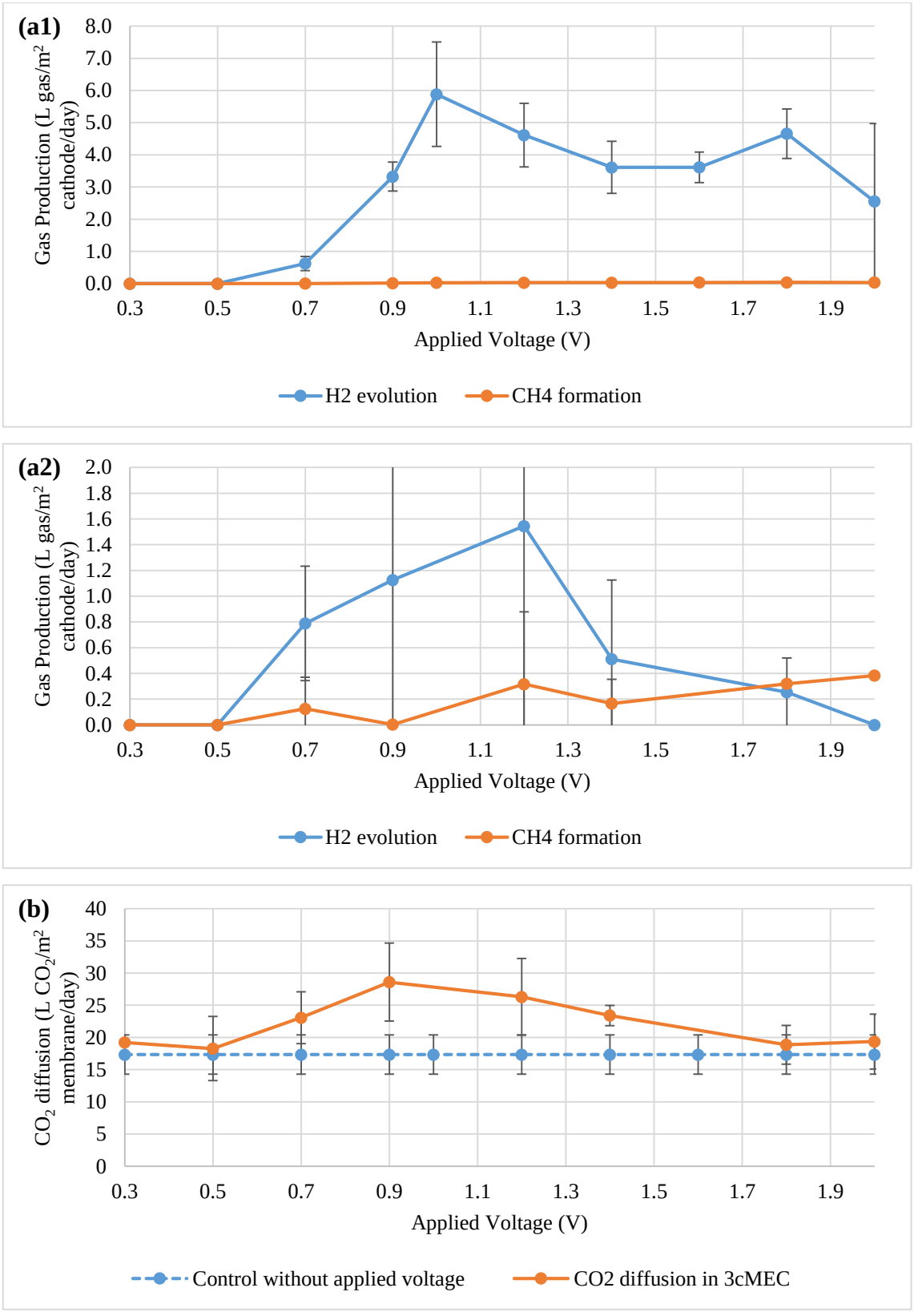

Figure 6.3 Hydrogen evolution and methane formation for 2cMEC (a1) and 3cMEC (a2) and carbon dioxide dissolution rate into catholyte through a CEM from gas chamber in 3cMEC (b).

6.3.3. Electrolyte properties under different applied voltages

Figure 6.4 displays the profile of pH and conductivity of the anodic and cathodic effluents based on applied voltages. Media used in the tests and control cell have been included in the same figure to facilitate comparisons. No significant change in pH and conductivity was observed for applied cell voltages between 0.3 and 0.5 V. The pH and conductivity values remained unchanged around 7.0 and 7.0 mS/m, respectively. Anyhow a significant shift of conductivity in anode and cathode effluent at the applied potential of 0.3 V from 7.0 to nearly 8.0 and 6.5 mS/m, respectively. On the one hand, the pH of anodic effluents decreased from 7.0 to 6.0 after 0.5 V. The conductivity value of the effluent was decreased on the same pattern as pH value from 6.7 to 5.5 mS/m. Both pH and conductivity values were maintained around 6.0 and 5.0 mS/m, respectively after 0.7 V. On the other hand, the pH and conductivity of cathodic effluents increased from 7.0 to 9.7 and 8.0 to 8.5 mS/m, respectively. The main difference between anode and cathode in the system is the power of oxidation and formation. In anode, the substrate undergoes a reaction to break intramolecular bonds in which electrons were lost to other species (Aelterman *et al.*, 2008; Kim *et al.*, 2011). These electrons were then collected by anode sent to the cathode through an external circuit. In cathode, carbon-based molecules undergo reduction reactions and were formed from the combination of carbon dioxide, protons and electrons (Mohanakrishna *et al.*, 2015; Choi and Sang, 2016; Raes *et al.*, 2017). The electrons supplied from anode served as an extra energy supply and reduce the reduction potential to favourable formation potential. In summary, the pH of anode decreased due to oxidation process or carbon-based molecular being broken down releasing protons into the solution (Kim *et al.*, 2011; Foad Marashi and Kariminia, 2015; Spurr, 2016). The reduction of the substrate to low weight compounds also reduce the ionic strength of the solution causing conductivity value to drop to a certain value. Meanwhile, the cathode pH increase as protons were constantly removed from the solution to form hydrocarbon compounds (Rozendal *et al.*, 2008; Mohanakrishna *et al.*, 2015; LaBelle and May, 2017; Raes *et al.*, 2017). Those soluble compounds were heavier than carbon dioxide and contributed to higher ionic strength compared to its counterpart. Therefore, the conductivity value went up at higher applied voltages.

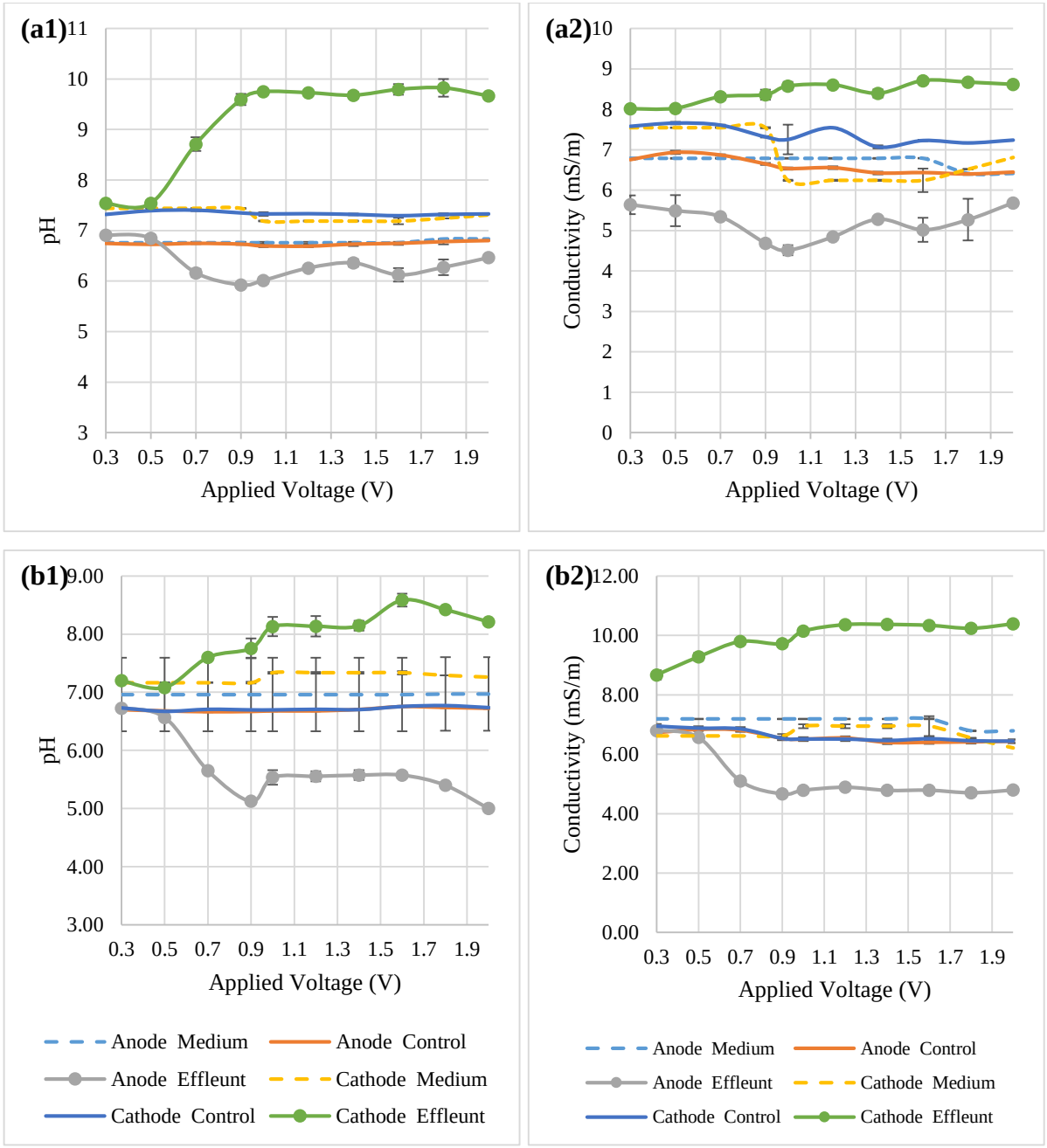

Figure 6.4 The profiles of pH for 2cMEC (a1) and 3cMEC (a2) and conductivity for 2cMEC (a1) and 3cMEC (a2) in anode medium and catholyte relatively to various applied voltages after 6 months. Note: All lines marked with medium and control are not subjected to chronoamperometry test. The samples were collected at the same time with effluents at specific applied voltages during the test. They are shown for comparison.

Figure 6.5 (a) and (b) presents the total organic/inorganic carbon concentrations in anode and cathode effluents and the organic compounds found in the catholyte at the end of

each chronoamperometry test. Sodium acetate was added into the anolyte as the main carbon source for electrochemically-active microbes to conserve energy and produce electrons. At the beginning of the enrichments, the anolyte and catholyte were replaced according to the cell current density and potential of the anode. As organic compounds were detected in very low concentrations in the cathode compartment, the catholyte was then replaced according to every two to four anode cycles before starting the chronoamperometry experiments. At the end of each cycle, effluents were collected and analysed to identify the content of short-chain fatty acids (SCFAs) and total carbon (TC) in the form of carbon dioxide equivalent. Short-chain fatty acids (SCFA) have been reported in biocathode studies included acetate (C2) and butyrate (C4) (Zaybak *et al.*, 2013; Choi and Sang, 2016). Recently, even longer chain fatty acids and alcohols such as caproate (C6) and butanol (C4) were synthesised from a biocathode (Raes *et al.*, 2017; Vassilev *et al.*, 2017; Jourdin *et al.*, 2018).

As shown in Figure 6.5 (a1) and (b1), the organic carbon removal was consistent with hydrogen production, pH and conductivity value shifts except at 2.0 V applied voltage. Extra energy was required to produce hydrogen when applied voltage was increased and higher potential was shifted in anode resulting in more acetate oxidation (Lim *et al.*, 2017). However, as discussed above, the biotic oxidation of acetate significantly dropped at 2.0 V applied voltage when the anode potential exceeded +1.0 V vs SHE, which is characterised by the accumulation of organic carbon in the anolyte, as depicted in Figure 6.5 (b). The accumulation of organic carbon in the catholyte was low (~40 mg CO_2/L) compared to inorganic carbon concentration but higher than in the control effluent sampled at the same time (10-30 % data not shown). The low concentrations measured can be associated with the slow kinetics of formation of organic carbon-based compounds at the cathode and slow development of the biocathodes which typically require weeks or months under low poised potentials (Zaybak *et al.*, 2013; Jourdin *et al.*, 2015; Mohanakrishna *et al.*, 2015; Bajracharya *et al.*, 2017b; Raes *et al.*, 2017; Jourdin *et al.*, 2018). However, in this experiment, cell potentials were only applied for two days, which does not allow the accumulation of significant amounts of organic compounds. The accumulation of hydrogen in the cathode environment could trigger the growth of methanogens which in turn produce methane and reduce hydrogen yield (van Eerten-Jansen *et al.*, 2015; Bajracharya *et al.*, 2017b). This phenomenon was somehow noticed in Figure 6.3 (a) and (b1), although methane concentrations detected in this experiment were very low (about 0.04 L CH_4/m^2/day). The organic carbon in fresh anode medium was higher at the beginning due to the added acetate, low concentration of organic and inorganic carbons was detected in the effluent of the anode. A small amount of CO_2 was generated through the oxidation of acetate

contributing to the inorganic value in the effluents (Kim *et al.*, 2004). In comparison with anode effluents, the trend of organic carbon of cathode showed almost the same values across the applied voltages with slightly higher than control (without applied voltage, data not shown). The accumulation of the organic compounds was not affected by the applied voltage used in this study as long as there was a voltage applied to the system. In contrast, inorganic carbon in the form of carbonates appeared significantly in cathode effluent indicated the CO_2 gas diffused through membrane from the gas chamber and accumulated in the catholyte.

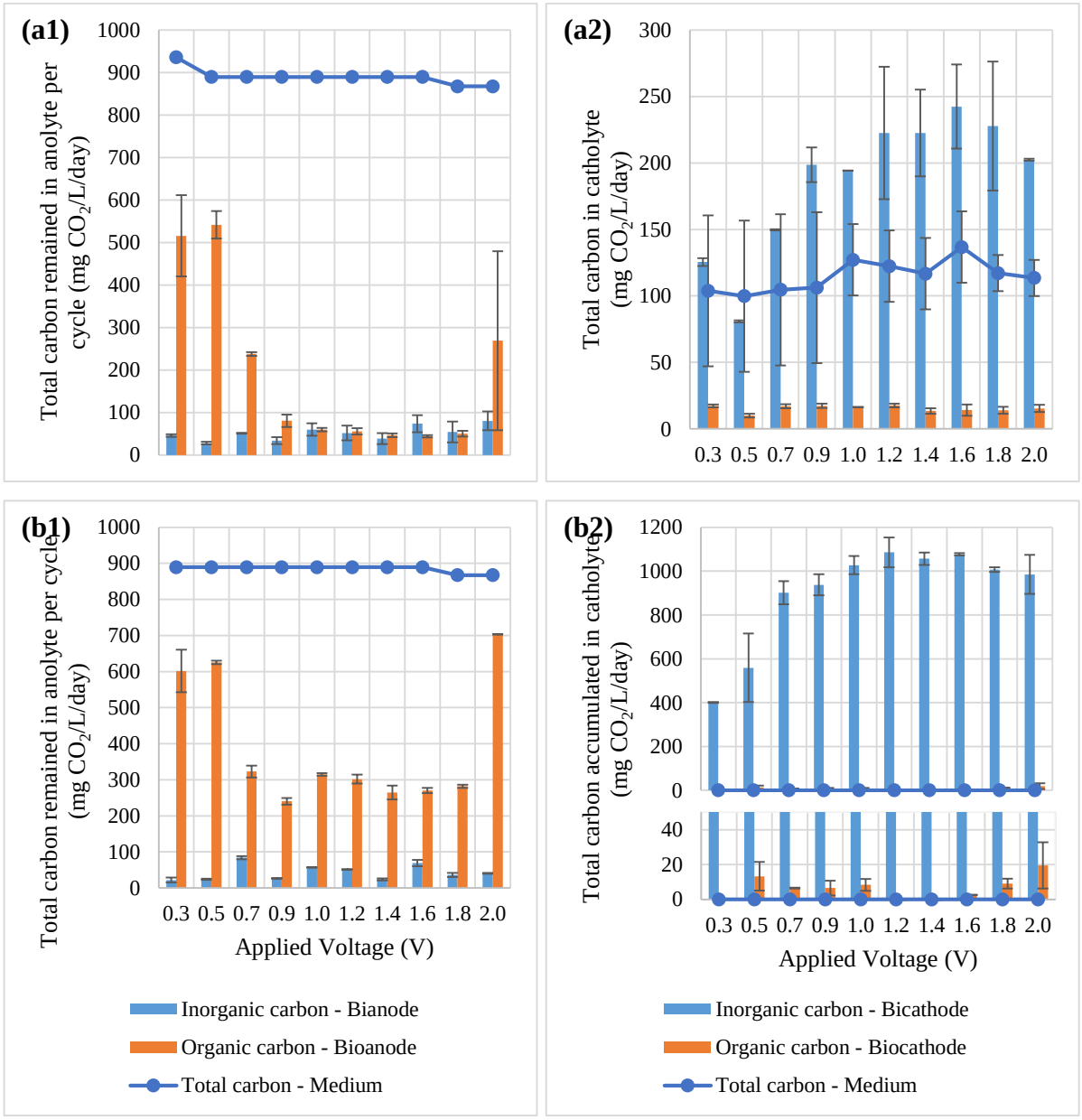

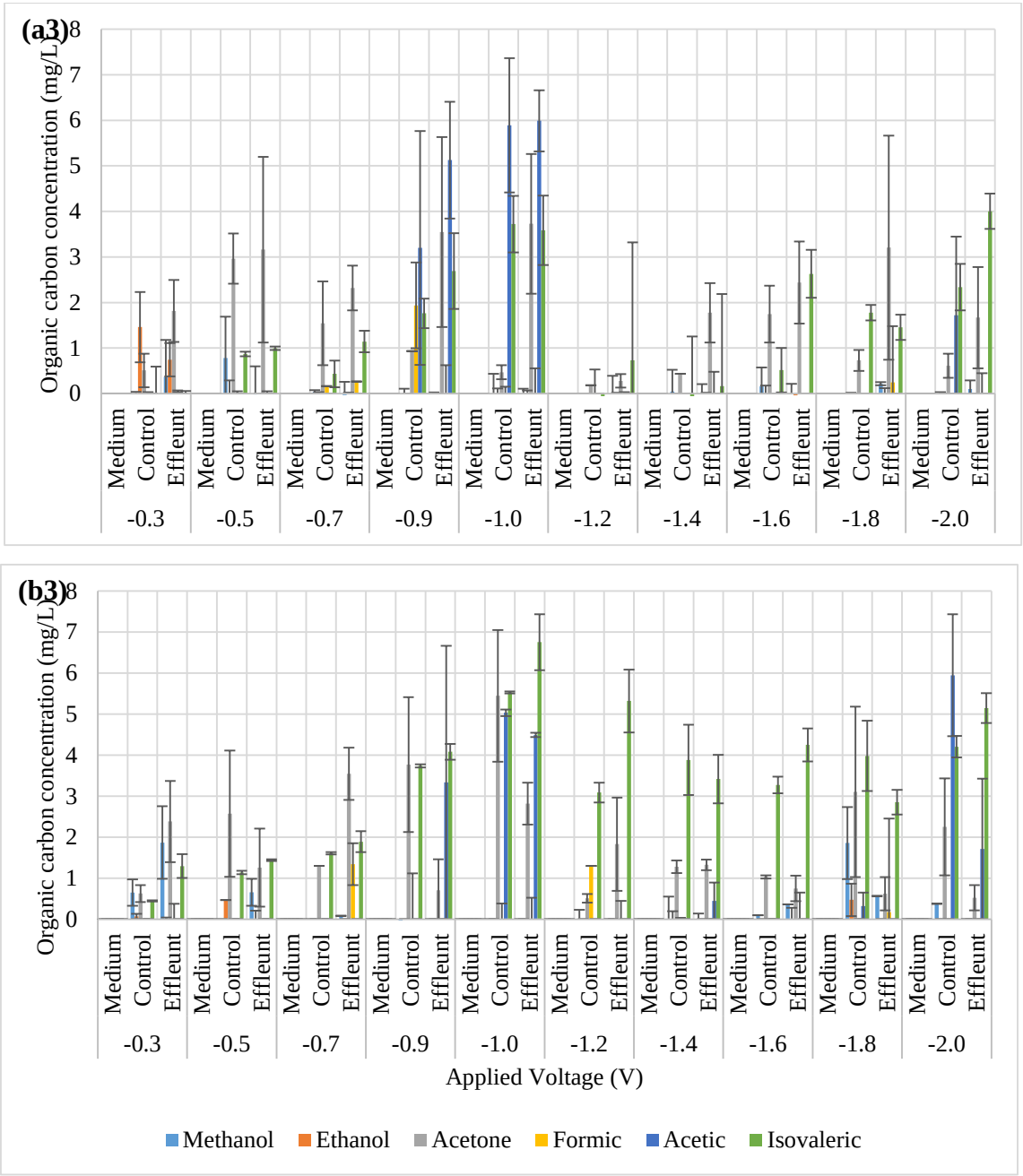

Figure 6.5 Total organic/inorganic carbon: (a) remained in anolyte, (b) accumulated in catholyte (in (b2), a small graph is inserted below as an enlarged figure to the top graph), and (c) percentage of difference in organic carbons by compared to control from the chronoamperometry test.

6.3.4. Bioelectrode limitations at high applied voltages

After the chronoamperometry tests, cyclic voltammograms and electrochemical impedance were recorded for the anode and cathode (Figure 6.6). As depicted in Figure 6.6 (a1) and (b1), there was a significant drop in the catalytic current associated with the oxidation of acetate by

the bioanode after the tests. The bioanode activity was clearly been suppressed which could be the result of toxic compounds being produced from abiotic oxidation. In addition, the anode potential reached 1.0 V when a 2.0 V cell voltage was applied, as can be seen in Figure 6.2 (a1) and (b1). At such a high potential, water hydrolysis is likely to occur, thus leading to oxygen and hydroxides which are harmful to anaerobic bioanodes. However, Figure 6.6 (a2) and (b2) shows that the biocathode maintained its catalytic activity and even better than before. It can be observed from the figure that reduction activity became more important in the region below -0.9 V. Furthermore, small oxidation and reduction peaks can also be noted around -0.7 and -0.3 V in the biocathode compared to the control. It was previously reported that the oxidation peak is associated with the hydrogen oxidation on the reverse scan of the hydrogen evolution reaction (Aulenta *et al.*, 2012; Batlle-Vilanova *et al.*, 2014; Lim *et al.*, 2017). This redox feature is attributed to the reversible catalytic activity of hydrogenase. On the other hand, the reduction peak is possibly due to non-hydrogen-producing activity and might be related to the formation of organic carbons such as acetate (Lim *et al.*, 2017).

The growth of biofilms on the surface of anodes and cathodes was supported by electrochemical impedance spectroscopy analysis. Figure 6.6 (a3), (b3), (a4) and (b4) present the spectrograms recorded for the cell (between anode and cathode). A semicircle continued with a tail in the spectrograms can be explained with an electrochemical equivalent circuit called Randles circuit (Macdonald, 2006; He and Mansfeld, 2009; Borole *et al.*, 2010; Dominguez-Benetton *et al.*, 2012; Sekar and Ramasamy, 2013). The modified circuit and its simplification form are shown in Figure 6.7 (a3) & (b3) and the coefficients from the fitted models are reported in Table 6.2. The former circuit represents every part in the cell including anode and cathode while the latter is simplified by combining similar behaviours in both anode and cathode to single elements (Dominguez-Benetton *et al.*, 2012; Sekar and Ramasamy, 2013). The simplified circuit consisted of two resistance values, R_1 and R_2, one constant phase element Q, and two diffusion properties W and T. R_1 represents the solution resistance and R_2 is the charge transfer resistance which is related to the conductivity of solid materials in the cell. CPE depicts the imperfect capacitance behaviour in the system. The imperfections are usually caused by the biofilm growth on the electrode surface and by the electrode material used in the system. Meanwhile, W is the Warburg diffusion, and T is the finite diffusion which represents the diffusion across the biofilm layers and porous electrodes (Macdonald, 2006). It is clear that the semicircle representing the internal resistance of the cell became slightly bigger than the control and initial results as layers of biofilm were actively growing and attaching onto the electrode's surface. The internal resistance value of 2cMEC was slightly higher (8.89 Ω vs. Control: 8.44

Ω) for the cell operated under applied voltage. The trend of total internal resistance for 3cMEC was the same, increased from 54.25 Ω (Control) to 66.55 Ω (cell operated under applied voltage). Initial values represented electrochemical property before a layer of biofilm grew or inoculum was introduced into the MECs. Meanwhile, the control was the MECs had similar operation condition with the experimental MECs but without external power supply. Both control and experimental results were compared to the initial value (effect of biofilm attachment) and the experimental results were compare to control (effect of the power supply) in order to perform a comprehensive analysis. As presented in Table 6.2, the charge transfer resistance for 2cMEC slightly decreased compared to initial value, which can be attributed to the attachment of electrochemically active microbes on the electrode, changing its surface morphology and electrochemical properties but this was not the case for 3cMEC system (Aulenta *et al.*, 2012). However, solution resistance decreased disproportionally to the charge transfer resistance in 2cMEC. Depletion of reactants and accumulation of products in the solutions were probably the main factors affecting the solution properties and the resistance. In contrast, constant phase element impedance value increased due to the increase of the biofilm thickness and the accumulation of older layers. Meanwhile, the tails of the spectrograms represent the diffusion behaviours W and T of the biofilms and porous electrodes. The angle of the tail remained slightly lower after the chronoamperometry test which means that the diffusion properties also slightly changed compared to the control and initial results (He and Mansfeld, 2009; Borole *et al.*, 2010; Dominguez-Benetton *et al.*, 2012; Sekar and Ramasamy, 2013).

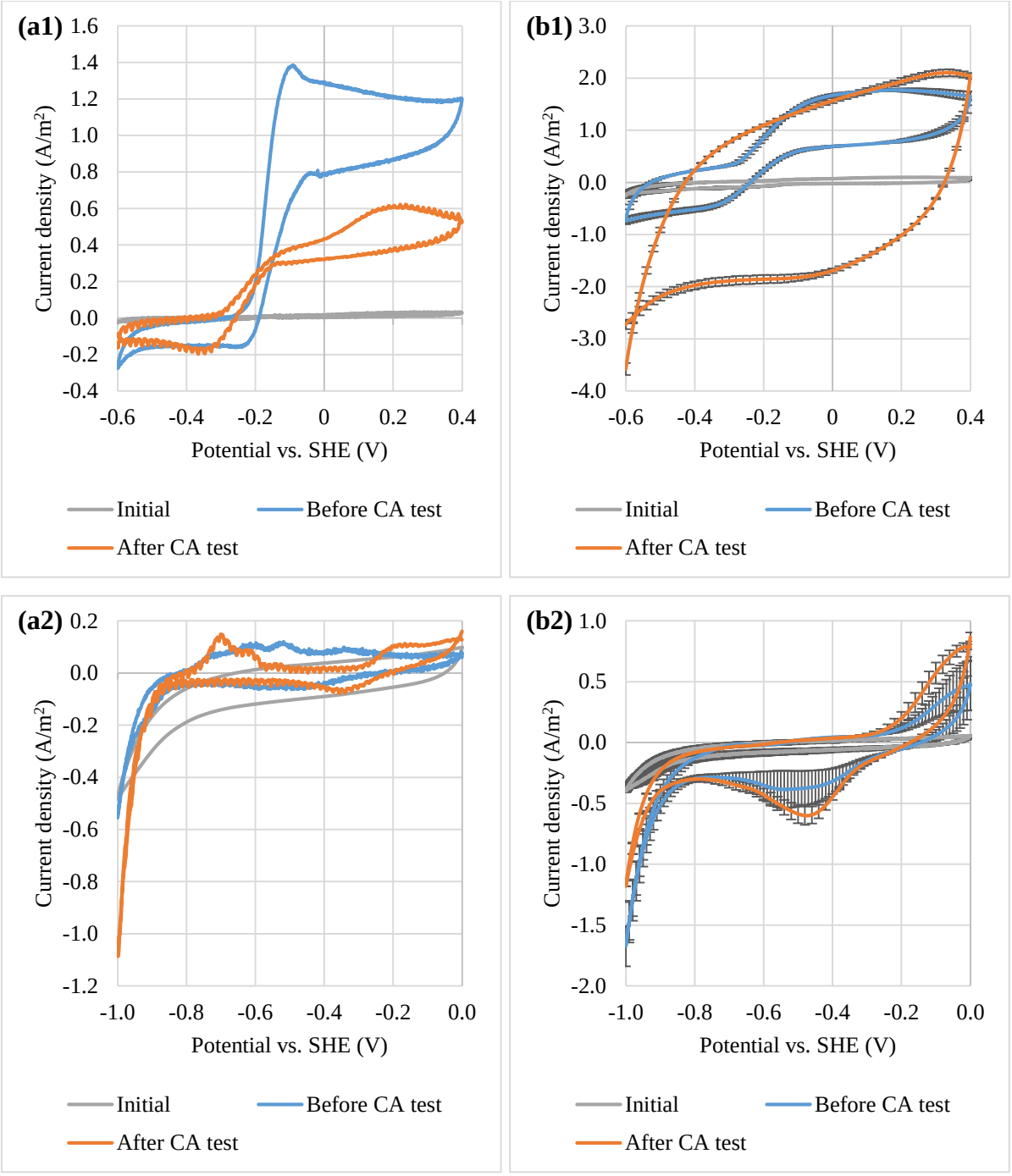
(a1)
Current density (A/m²)
Potential vs. SHE (V)
Initial
Before CA test
After CA test
(b1)
Current density (A/m²)
Potential vs. SHE (V)
Initial
Before CA test
After CA test
(a2)
Current density (A/m²)
Potential vs. SHE (V)
Initial
Before CA test
After CA test
(b2)
Current density (A/m²)
Potential vs. SHE (V)
Initial
Before CA test
After CA test

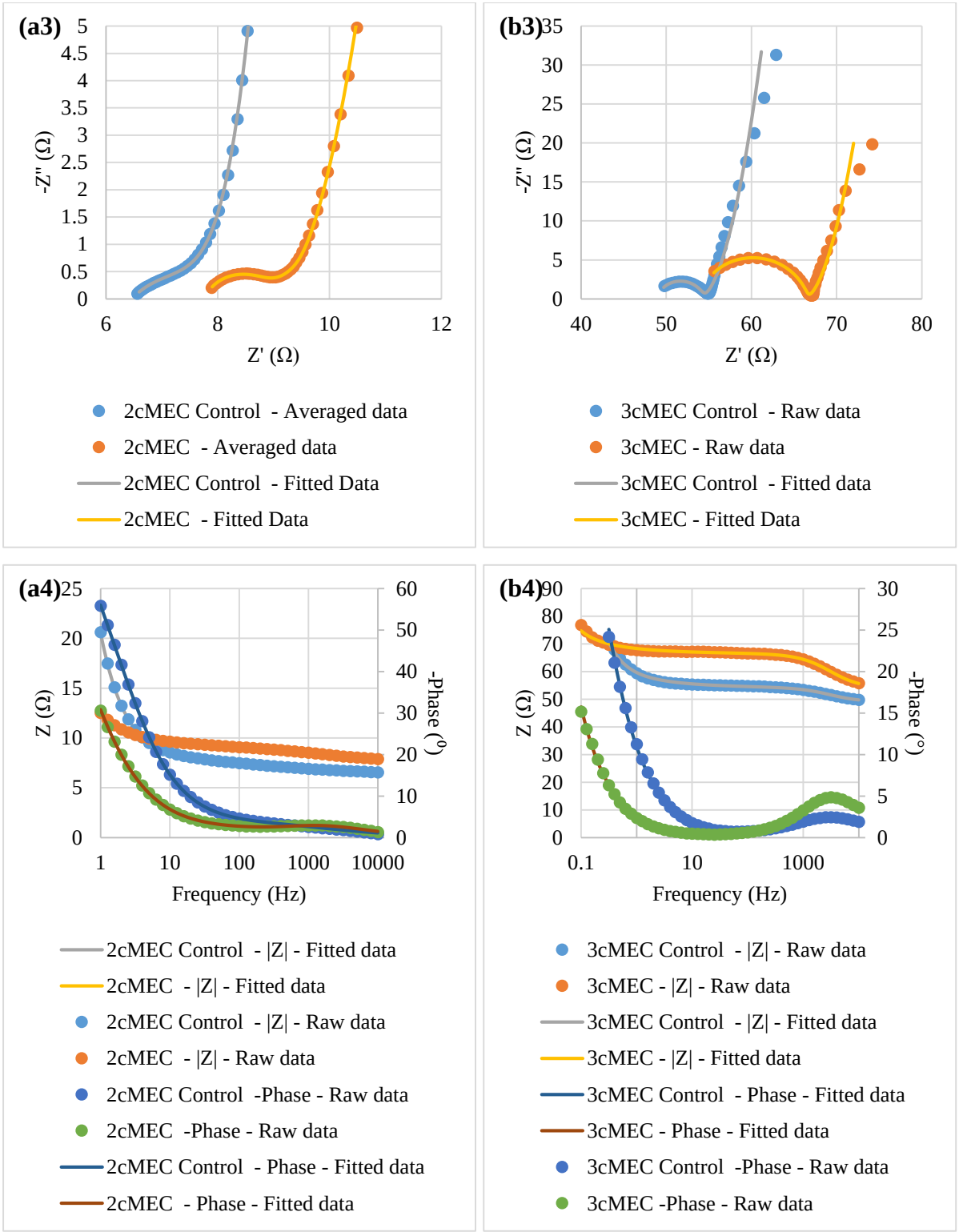

Figure 6.6 Catalytic activities of bioelectrodes in a bioelectrochemical cell: (a1) 2cMEC and (b1) 3cMEC bioanode cyclic voltammograms, (a2) 2cMEC and (b1) 3cMEC biocathode cyclic voltammograms and electrochemical impedance spectrograms: (a3) & (b3) Nyquist plot and (a4) & (b4) Bode modulus and phase after chronoamperometry test. Note: the Control is the cell operated under open circuit without applied voltage.

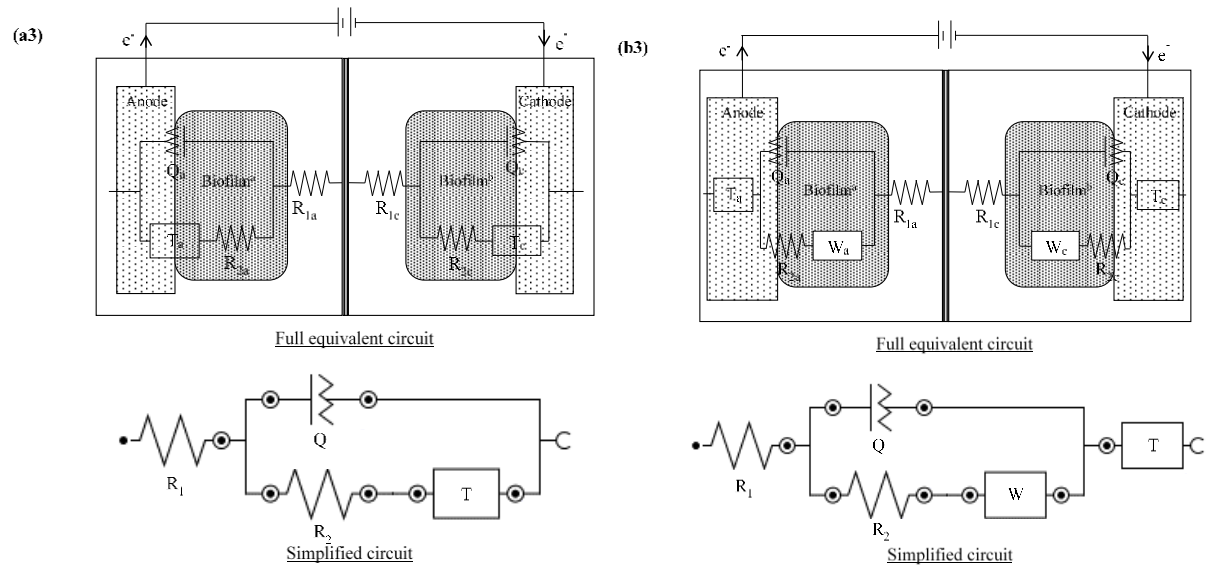

Figure 6.7 Electrochemical impedance spectrograms for the cells enriched at different stage (a) Nyquist plot, (b) Bode modulus and phase plots and (c) an overview of the full equivalent circuit with its simplified version: $[R_1(Q[R_2W])T]$ where R_1 = solution resistance, R_2 = charge transfer resistance, CPE = constant phase element, W = Warburg diffusion element, and T = finite diffusion element.

Table 6.2 Coefficient values determined from the equivalent circuit in Figure 6.6 (a3) & (b3) after chronoamperometry test

Cell	Solution resistance		Constant phase				Charge transfer resistance		Semi (Warburg)-diffusion		Finite diffusion				Internal Resistance	
			Impedance		Element constant				Impedance		Impedance		Time constant			
	R1		Q				R2		W		T				(R1 + R2)	
	Ω	±	Ω^{-1}	±	N	±	Ω	±	Ω^{-1}	±	Ω^{-1}	±	$s^{1/2}$	±	Ω	±
Initial	5.36	0.36	2.96E-02	2.79E-02	0.719	0.088	3.85	2.74	0.04	0.032	0.05	0.04	0.072	0.046	9.21	3.10
Control*	6.44	0.20	2.53E-02	2.04E-02	0.528	0.130	1.99	0.75	0.312	0.189	0.46	0.21	0.030	0.004	8.44	0.75
2cMEC*	7.76	2.07	8.82E-04	4.15E-04	0.783	0.013	1.14	0.62	0.218	0.081	0.22	0.01	0.173	0.048	8.89	2.07
Initial	35.54	1.62	4.09E-06	3.89E-06	0.913	0.187	4.13	0.92	0.007	0.001	0.02	0.01	0.028	0.011	39.67	1.62
Control*	48.89	0.52	3.75E-05	1.96E-05	0.879	0.062	5.36	0.06	0.114	0.068	0.40	0.13	0.073	0.026	54.25	0.52
3cMEC*	53.90	4.16	1.11E-05	1.99E-06	0.914	0.057	12.65	6.07	0.165	0.010	2.09	1.08	0.070	0.034	66.55	6.07

*EIS recorded after 6 month

Initial – Before the introduction of inoculum into the cell or the start of experiment

Control – Cell operated under open circuit

2c- or 3cMEC – Cell operated under a range of applied voltages (fixed at 0.3 V but varies between 0.3 and 2.5 V depended on the experiments)

Polarisation equation was used to analyse energy losses caused by overpotentials in the MECs. Figure 6.8 shows the original V-I curves with the calculated data. During the curve fittings, standard cell voltage, E_{cell}' was fixed at -0.13 V and the outcomes were done unless the regression value, R^2 (to check the level of fitting between the equation and data where 1.0 is the perfect fit) was higher than 0.9.

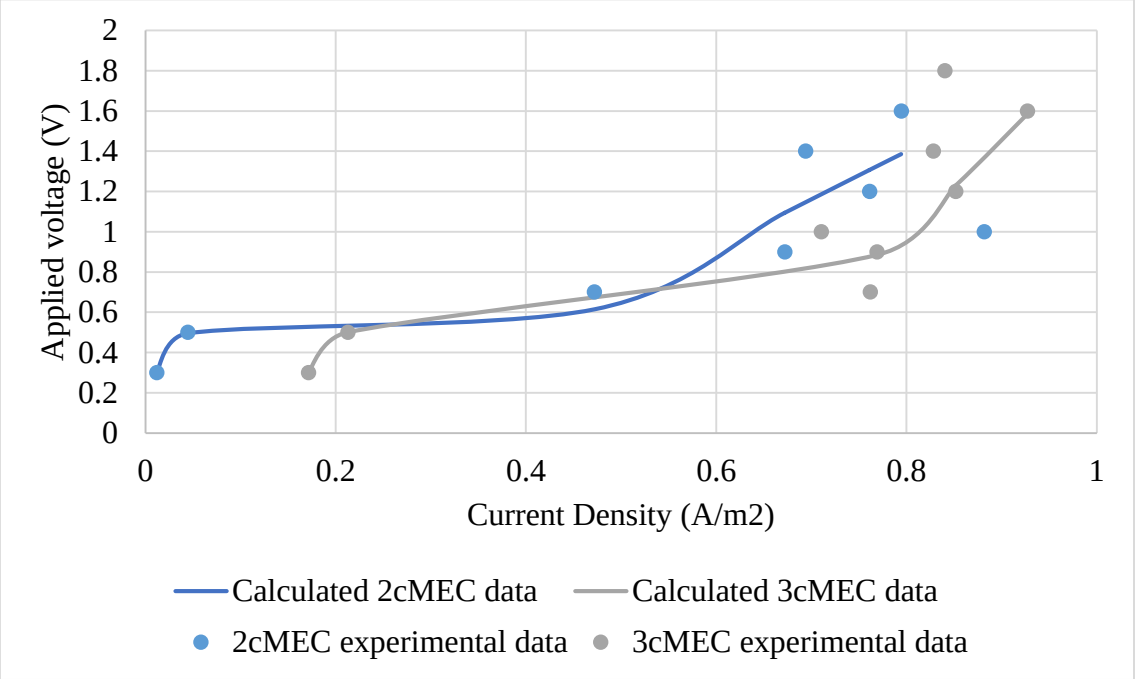

Figure 6.8 Original V-I curves with calculated data for the MECs.

Overpotential coefficients from the curve fitting are reported on Table 6.3. Based on the comparison between the coefficient values, 3cMEC had higher b and γ values (10-20 times) compared to 2cMEC which are devoted to activation and mass transfer energy losses. Higher activation energy was required in 3cMEC to initial the oxidation-reduction reactions. This may due to the different electrode materials used between the MECs (2cMEC used carbon felt while 3cMEC used carbon cloth as the electrodes). In addition, the cell configuration between the MECs were slightly different (because the gap between anode and cathode were estimated < 2 cm for 2cMEC and ~ 4 cm for 3cMEC) which may also increase the energy losses. Higher energy loss in mass transfer was expected as the purpose of 3cMEC was used to absorb CO_2 and turn it into soluble carbonates. Inside the 3cMEC, potential energy was not only used to transfer the proton from anode to cathode but also soluble CO_2 to cathode for further reactions.

Table 6.3 Overpotential coefficients determined from Equation 6.3.

Coefficient	2cMEC	3cMEC
E_{cell}' (V)	-0.1300	-0.1300
b (V)	1.2244	22.6552
R (Ω)	1.7271	0.1488
γ (V)	2.7545	28.4224
ω (m^2/A)	7.8377	2.8299
$1/\omega$ (A/m^2)	0.1276	0.3534

6.3.5. Energy recovery and contribution

Figure 6.9 presents the energy recovery, overall efficiency and energy contribution of this study. The Coulombic efficiency R_{CE}, and substrate oxidation energy yield η_s, were determined based on the acetate removal at the anode. From Figure 6.9 (a1), R_{CE} increased from 0% at 0.3 V to a peak value of 322% at 0.7 V before it dropped and reached a plateau of about 170% after 1.40V. The cathodic recovery $R_{cat,}$ and external input energy yield η_e were calculated based on hydrogen detected at the cathode. R_{cat} increased slower than R_{CE} from 0% at 0.3 V to 57% at 1.0 V and remained constant after 0.5 V. As can be seen in Figure 6.9 (a2), the trends of energy efficiencies η_e, η_s, and η_{e+s} were similar. However, η_s had the highest value compared to the other followed by η_e and η_{e+s}. All three efficiencies increased at 0.5 V and peaked at 1.0 V before decreasing until to 1.4 V to remain stable. A sudden drop at 2.0 V can also be noted in the figures due to the loss of the bioanode activity. Even though η_s was higher, overall efficiency, η_{s+e} was low as a result of low η_e value. The best η_{s+e} that could be achieved in this study is 29.4% at 1.0 V applied voltage. The difference in efficiencies at the anode and cathode is related to the different bacterial communities involved at each electrode (e.g. electrogens vs. lithotrophs) catalysing different reactions (oxidation vs. reduction) at different reaction rates (e.g. days vs. months). In addition, the consumption rate at the anode was higher than the production rate at the cathode. Another reason for the low efficiencies measured is the loss of energy to overpotentials due to system configuration and microbe's assimilation to maintain cell metabolism (Kim *et al.*, 2011; Nimje *et al.*, 2012). Energy efficiency from the external power supply, η_e was recorded as low as 42.2% compared to that from the anode 97.3% indicating that the substrate oxidation might play a bigger part in the energy contribution (Call and Logan, 2008; Logan *et al.*, 2008; Lim *et al.*, 2017). However, since the calculations were based on the energy in the hydrogen produced (see Equation 6 and 7), higher efficiency in η_s could be overestimated and low efficiency in η_e could be underestimated. The energy contribution from anode might be smaller than expected and vice versa. Since the current used

to produce a specific amount of hydrogen at the cathode was supplied by both anodic oxidation and external power, the determination of anode or cathode energy yield based on the total amount of hydrogen is not an accurate approach. Therefore, the overall energy yield η_{s+e}, (see Equation 8) was obtained because it is more accurate to estimate the efficiency of the whole system (combination of anode and cathode efficiencies). The η_{s+e} was 29.4% at 1.0 V, meaning that 29.4% of the total energy supplied by both the bioanode and the external power supply was harvested as hydrogen at the cathode. Finally, Figure 6.9 (a3) shows an overview of the energy contribution (break down of the overall efficiency) from the acetate-oxidising bioanode (e_s) and the external power supply (e_e) when applied voltage increased from 0.3 to 2.0 V. The energy contribution from the oxidation of acetate was as high as 99.2% at 0.30V, but it should also be kept in mind that at this potential the hydrogen production was very low. At the optimum hydrogen-producing applied voltage of 1.0 V, the energy contribution from the oxidation of acetate and external power supply was of 30.2% and 69.8% respectively, stressing out the importance of the bioanode to reduce the cost of external power supply. Finally, when the applied voltage reached 2.0 V, the contribution of the bioanode was only 22.5%, which is consistent with the progressive loss of its catalytic activity.

The typical direction of the energy recovery, overall efficiency and energy contribution of 3cMEC (Figure 6.9 (b1), (b2) and (b3)) are similar to those reported in 2cMEC. By comparing the energy recovery between those systems, the Coulombic efficiency in 3cMEC was higher than 2cMEC but for cathodic recovery, the trend was in the opposite way to 2cMEC. Apart from the overestimation or underestimation in the values of Coulombic or cathodic recovery calculation as mention above, the calculation represents the total estimation for a complete cell instead of a half-cell system. Overall, the efficiency values in 3cMEC were a little lower than the 2cMEC. Similar to 2cMEC, the 3cMEC peak efficiency occurred at 1.0 V. The maximum η_e, η_s, and η_{e+s} values were 46.5, 14.4 and 11.0 %, respectively. Moreover, the contribution of the electrical energy was higher at the low applied voltage condition. Starting from 0.3V, the electrical energy already supplied up to 30% of the total contribution. The contribution kept increased at a faster pace compared to the 2cMEC energy contribution. About up to 83 % (2cMEC was about 74%) was contributed by the electrical input at 1.8 V applied voltage before the bioanode fail at higher applied voltage of 2.0 V. Different cell configuration (2cMEC: 25 mL vs. 3cMEC: 50 mL) and electrode spacing (2cMEC: 1 cm vs. 3cMEC: 4 cm) might be the main reason the electrical energy contribution was slightly higher in the 3cMEC (Liang *et al.*, 2007; Kadier *et al.*, 2016).

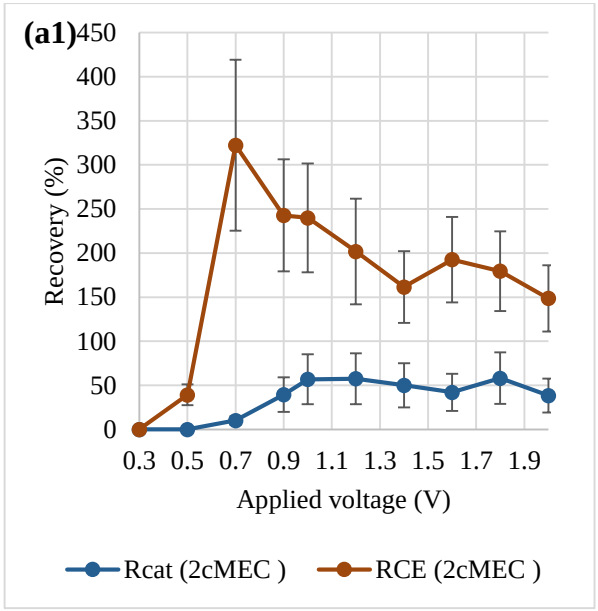
(a1)
Recovery (%)
Applied voltage (V)
Rcat (2cMEC)
RCE (2cMEC)

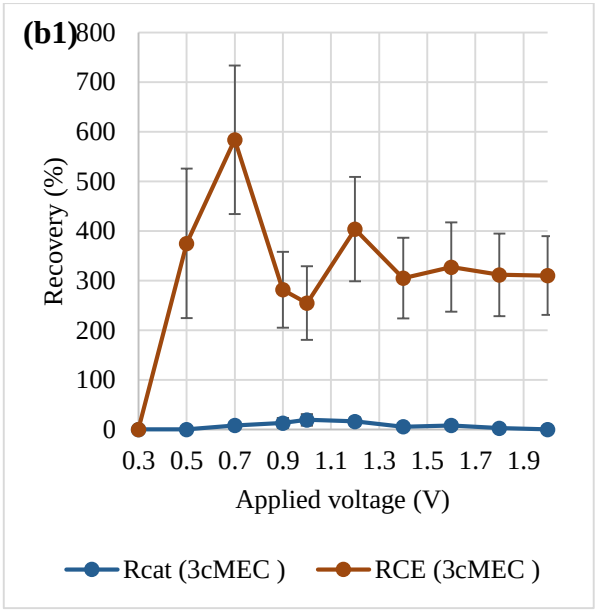
(b1)
Recovery (%)
Applied voltage (V)
Rcat (3cMEC)
RCE (3cMEC)

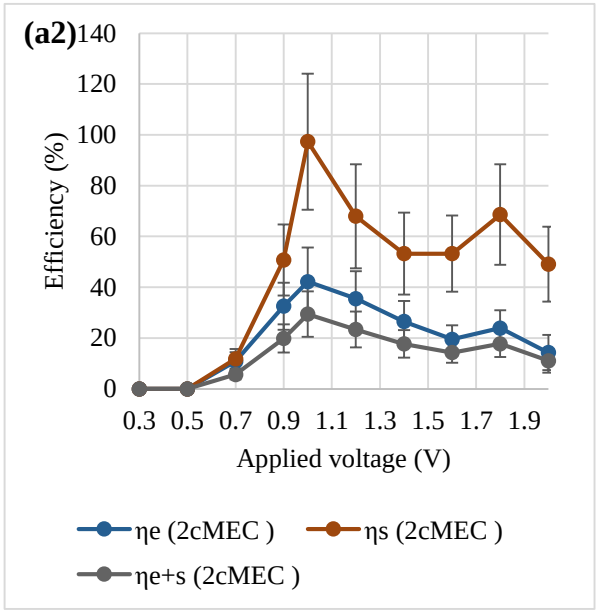
(a2)
Efficiency (%)
Applied voltage (V)
ηe (2cMEC)
ηs (2cMEC)
ηe+s (2cMEC)

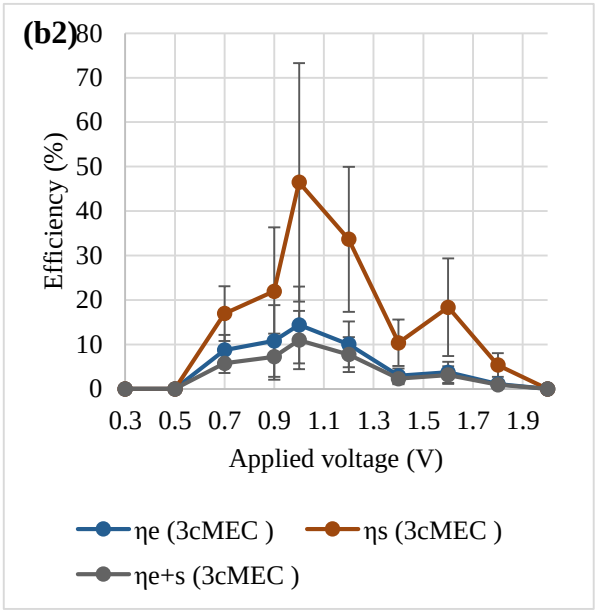
(b2)
Efficiency (%)
Applied voltage (V)
ηe (3cMEC)
ηs (3cMEC)
ηe+s (3cMEC)

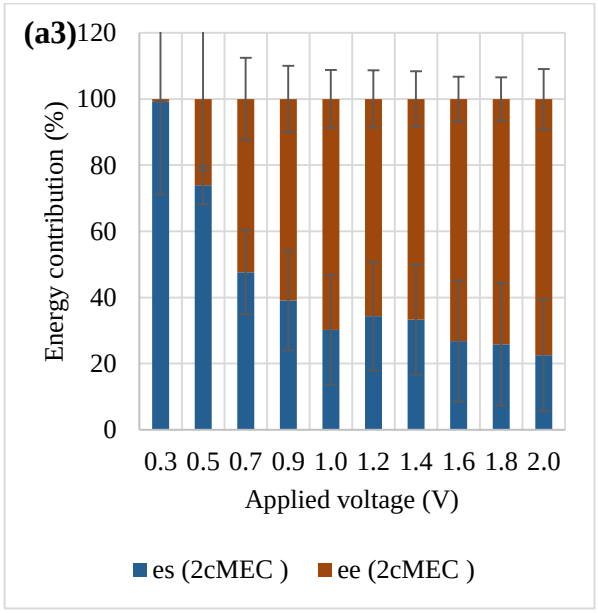
(a3)
Energy contribution (%)
Applied voltage (V)
es (2cMEC)
ee (2cMEC)

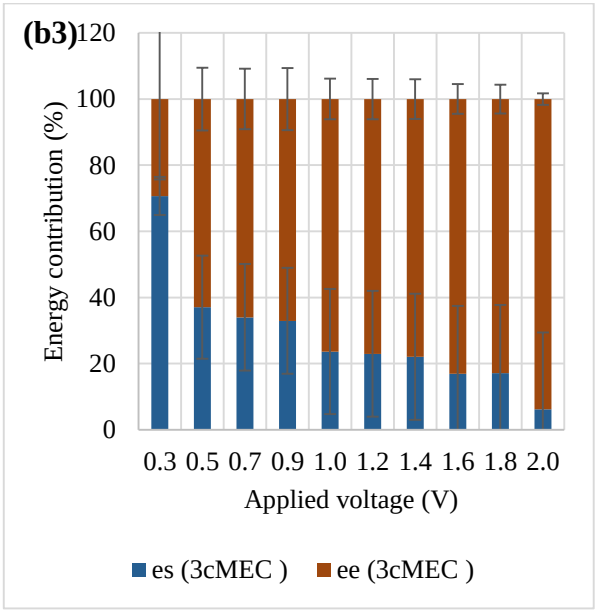
(b3)
Energy contribution (%)
Applied voltage (V)
es (3cMEC)
ee (3cMEC)

Figure 6.9 (a) Recovery yield, (b) energy efficiency and (c) energy contribution in the chronoamperometry test. Figure (a1), (a2) and (a3) are for 2cMEC while (b1), (b2) and (b3) are for 3cMEC. Note: the recovery (a1, b1), efficiency (a2, b2) and energy contribution (a3, b3) were calculated based on hydrogen production in cathode and acetate consumption in anode.

6.3.6. Extra chamber in 3cMEC alleviates pH shift and increases CO_2 accumulation

The usage of a third specific chamber (in addition to the anode and cathode chambers) is not a novel approach to improve the efficiency of bioelectrochemical systems (Luo *et al.*, 2012a; Luo *et al.*, 2012b; Liu *et al.*, 2015; Saeed *et al.*, 2015; Carmalin Sophia *et al.*, 2016). Normally the extra chamber was incorporated with the anode and/or cathode to form a functional and/or repeated units to enhance the reaction process (Carmalin Sophia *et al.*, 2016). A typical example is microbial desalination cell (MDC) which consists in an extra chamber placed between anode and cathode (Luo *et al.*, 2012a; Luo *et al.*, 2012b; Liu *et al.*, 2015; Saeed *et al.*, 2015; Carmalin Sophia *et al.*, 2016). The function of the extra chamber is to remove cations and anions from the solution. Another example is to create a better system configuration which allows multiunit to stack. A stacked MFC can be assembled using single unit (cathode-anode-cathode) and incorporate unit (anode) is used to connect the single units: (cathode-anode-cathode)-anode-(cathode-anode-cathode) (Rahimnejad *et al.*, 2012; An and Lee, 2014). Recently, a three-chamber system was also used as a microbial electrosynthesis cell to generate and extract target products (e.g. malic acid) formed in cathode (Liu *et al.*, 2015). The number of specific function chamber can be increased to more than one unit or in a stacking structure to improve the treatment efficiency (An and Lee, 2014; Carmalin Sophia *et al.*, 2016).

A gas chamber as a third compartment was also reported being utilised in bioelectrochemical system, especially in MEC and microbial electrosynthesis cell (MSC). Rozendal *et al.* (2007) reported in their MEC study using a gas chamber to separate the hydrogen from catholyte and avoid the hydrogen being used by microbial activity. In a recent study, the idea of dissolving CO_2 into the catholyte using a gas diffusion electrode was presented (Srikanth *et al.*, 2018). However, as part of this study, we assembled a simple version of gas diffusion layer by assembling a CEM and a cathode between cathode's and gas chamber as shown in section 3.1.1. It is well known that CO_2 has higher solubility in water compared to other permanent gasses such as nitrogen and oxygen in the atmosphere. Table 6.4 shows the solubility of common gases in water at standard condition. The solubility properties of CO_2 has

given the three-chambered MEC the advantage to separate the CO_2 from a certain type of mixed gases. The advantage of the solubility properties enables CO_2 to be easily separated and capture from the air under ambient temperature condition (Huang *et al.*, 2016). Huang *et al.* (2016) has demonstrated the capture and release of CO_2 from ambient air by using strong base ion exchange resin in a glass tube module. The CO_2 was concentrated under moisture-driven cycle and channelled into microbial electrochemical carbon capture (MECC) reactor for carbon sequestration and hydrogen production. Figure 6.10 (a) shows the comparison of the pH and conductivity values under chronoamperometry tests between 2cMEC and 3cMEC. The pH of catholyte increased proportionally with applied voltage, however, the pH value of 3cMEC shifted slower than the 2cMEC. Finally, the value reached a plateau at around 8.50 for 3cMEC and 9.75 for 2cMEC. In Figure 6.10 (b), inorganic/organic carbon content in term of CO_2 for 3cMEC is reported. The accumulation of inorganic carbon in the catholyte increased when the higher potential was applied which is correlated to the pH shift. As protons being used and removed from catholyte either in hydrogen evolution or to formed carbon-based organic compounds could cause the pH to rise. As the catholyte went to more alkaline conditions, the dissolution of CO_2 actually alleviates the pH shift by creating predominant species, HCO_3^- and H^+ (Snoeyink, 1980). The carbonates were used as building blocks for some short-chain fatty acids production while the protons increased the pH shift and could be used for hydrogen evolution in reduction process.

Table 6.4 Solubility of gases in water at 293 K, 1 atm (Croft, 1987)

Gas	Solubility (g/100 g water)
Hydrogen	0.00016
Nitrogen	0.0019
Methane	0.0023
Carbon monoxide	0.0028
Oxygen	0.0043
Carbon dioxide	0.169
Hydrogen sulphide	0.385
Chlorine	0.729
Sulphur dioxide	11.28
Ammonia	52.9

Figure 6.10 (c) is the proposed CO_2 transfer mechanism from gas chamber to catholyte separated by a cation exchange membrane. The membrane used is a cation permeable membrane having strong acidic sulphonyl group and theoretically will not allow anion species such as HCO_3^- or CO_3^- to pass through. However, the detection of high inorganic carbon concentration contradicted the hypothesis. The reason might be the gradient driven forces causing the carbonates species to migrate from the gas chamber to catholyte. The gas contained in the gas chamber was pure CO_2. Inside the gas chamber, a diffusion layer was formed on the membrane surface caused by the water from the cathode. CO_2 was then dissolute on the surface of the membrane resulting high concentration gradient of carbonates across the membrane. Even though the wet membrane surface facilitates the CO_2 dissolution and diffusion, water flooding in the gas chamber after long term operation remained as another major problem in this system.

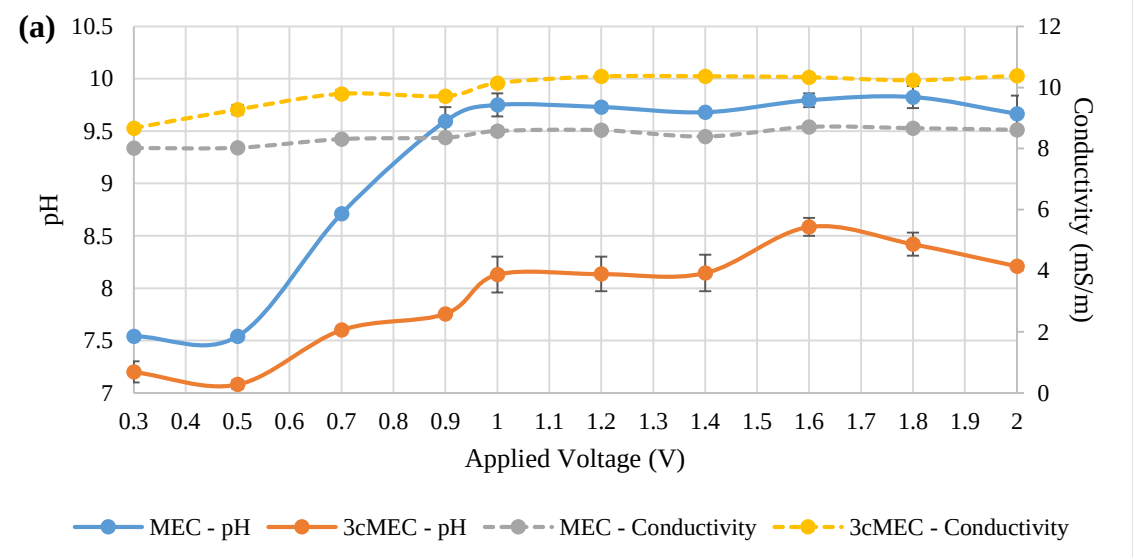

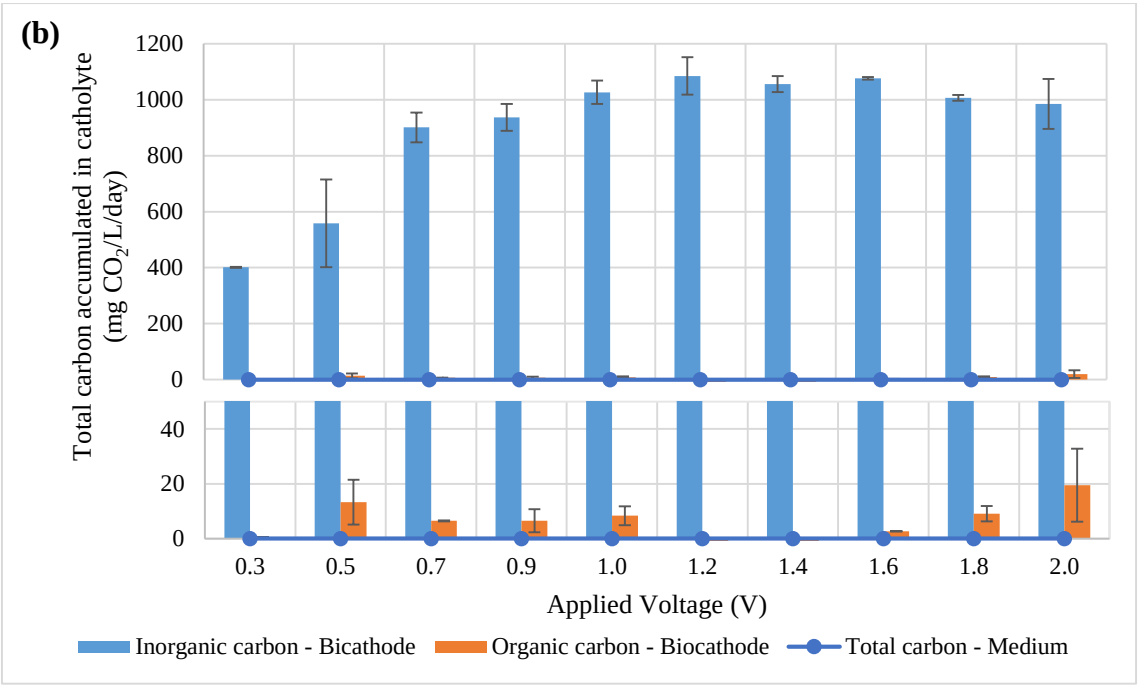

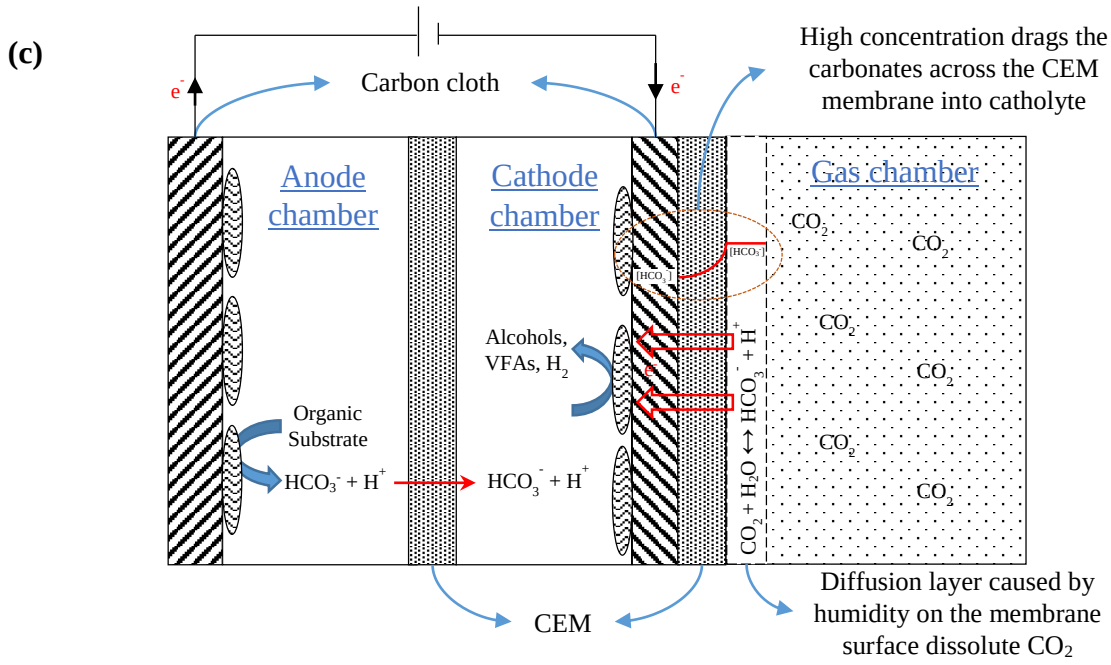

Figure 6.10 (a) The pH and conductivity profile compared to 3cMEC and (b) total carbon content in the cathode of 3cMEC (small figure is inserted below the original figure for showing the readable organic carbon values) and (c) proposed CO_2 dissolution and mass transfer behaviour

6.4. Conclusion and future study

1. The impact of operational voltage on the performance of a microbial electrolysis cell for hydrogen production was studied. A minimum cell voltage of 0.3 V was sufficient to promote the growth of biofilms on both electrodes' surfaces. The electrochemically-active biofilm grew faster at the anode than at the cathode.
2. The bioanode was first developed after one week of operation and was important to provide lower potential for enriching biocathode. A window of the applied voltage between 0.9 and 1.8 V was determined as the most relevant operational voltage to maintain the biocathode potential low enough for reduction reactions and at the same time protect the bioanode ability in oxidation reactions. The optimum applied voltage was determined as 1.0 V where the peak hydrogen evolution occurred with the production rate of nearly 6.0 L/m^2 cathode/day in 2cMEC.
3. Chronoamperometry tests suggested that the biocathode growth was much slower than the bioanode based on both half-cell potentials and current evolutions. It can be assumed that this is the reason why organics took a longer time to form from CO_2 than acetate to be consumed. Organic matters were found in catholyte after the tests included methanol, acetone, formate and acetate. Concentrations were very low because the test was done in a short period by following the bioanode growth cycle.
4. The shifts of pH and conductivity could cause serious problems to the system especially harming the bioanode at low pH (accumulation of protons) and blocking the hydrogen and organic carbon productions at high pH value (lack of protons). Malfunctioned bioanode might take time to recover and fail to provide enough reduction potential to the cathode. Sample analysis demonstrated that the values change was proportional to the anode and cathode reaction rates which were driven by applied voltage.
5. Energy recovery and efficiency calculations were used to understand the contribution of the energy between the anode and external power to support cathode. At the lowest applied voltage of 0.3 V, the anode contributed almost 99 % of the current. The external power began to dominate the contribution when higher applied potential was set in which favoured the cathode reduction reaction and at the same time reduce the gap of current shortage. At the optimum applied voltage of 1.0 V, the bioanode contributed for 32.4 % of the total energy, marking the important of bioanode to reduce external power cost.
6. A three-chamber MEC system was introduced at the end of this study to investigate the effect of direct CO_2 diffusion into catholyte. The CO_2 was initially contained in the third

chamber attached next to cathode separated by a CEM. The results showed that CO_2 accumulation in catholyte as carbonates was proportional to the applied voltage and hydrogen production rate. The study also suggested that dissolution of CO_2 into catholyte alleviated pH shifted while provided extra proton for hydrogen evolution.

Chapter 7. Improvement of hydrogen production in microbial electrolysis cells

7.0. Chapter summary

As found from the previous study, bioanode is not only the limiting factor in a microbial electrolysis cell (MEC) but posting different growing and reaction rates compared to biocathode. Therefore, a simpler but effective control of the bioanode reaction is required. In this chapter, the study is concentrated on improving and maintaining bioanode performance. Similar experiments and analysis were repeated as conducted in previous study/chapter except using specific feeding mode on the anode. The mode included batch, fed-batch and continuous feeding mode. The fed-batch mode is the feeding techniques laid between batch and continuous. It is distinguished from batch mode by the addition of a certain amount of fresh substrate and by the consequent withdrawal of a proportioned amount of broth within a specific time during the operations.

7.1. Introduction

Since the introduction of first BES in the past two decades, researchers have been trying different techniques and designs to improve the possibilities of fully deploying the system in real applications (Logan *et al.*, 2006; Jafary *et al.*, 2015; Kadier *et al.*, 2016). The techniques and designs are moved away from simple to complex methods in order to get better control on the oxidation-reduction reactions while enhancing the aims of higher current and process output. The methods included the use of monitoring devices to control pH, temperature, conductivity, dissolved oxygen, half-cell potentials and cell voltage (Tartakovsky *et al.*, 2009; Kyazze *et al.*, 2010). Data collected from the monitoring devices provides handful information to increase the BES performance, avoid malfunction and the collapse of the whole system. While complex methods such as the deployment of an electronic circuit for precisely and remotely control the external loads and potential polarity based on the organic levels of wastewater, multiple blocks of cell unit and design, merging of different BES technologies for multipurpose water treatment

have been reported. These methods tend to add complication to the system and increase the cost of operation (Call and Logan, 2011; Cusick *et al.*, 2011; Kim and Logan, 2011; Wang *et al.*, 2011a; Hussain *et al.*, 2018). Cell configuration optimisation and operational strategies such as automatic feeding system which have been demonstrated in some studies are one of the simplest methods and cost-effective way to improve BES (Tartakovsky *et al.*, 2009; Kyazze *et al.*, 2010; Cusick *et al.*, 2011).

The fact that bioanode could grow faster than biocathode has caused an imbalance in the reaction rates between anode and cathode. This is because bioanode not only provided electrons from substrate oxidation but also brought down the cathode potential when both of them were connected through a power supply. However, in real condition, the bioanode potential alone was insufficient to favour the reduction reactions in cathode. In standard condition, hydrogen evolution required at least -0.41 V and the best potential that bioanode could provide is -0.20 V (Rabaey and Rozendal, 2010; Choi and Sang, 2016). That means at least -0.21 V is still needed to drive the reduction activity. The purpose of the power supply is to provide a voltage differential between the anode and cathode and, therefore, increase their oxidation-reduction abilities at the same time. Besides, it also allocates extra current when the reaction activities were high and the bioanode could not supply enough current to the cathode. Hence, the bioanode must be robust and active with a consistent performance in the system to support the cathode (Wang *et al.*, 2010; Lim *et al.*, 2017). By keeping the bioanode in a good condition, it is crucial to reduce the cost of the extra power supply while maintaining the functionality of the whole system. In this study, bioanode was subjected to simple feeding mode in order to strengthen its performance in a MEC. The aim was to enhance the bioanode performance to support cathode in the reduction reaction. A pre-prepared fresh anodic medium was fed into the bioanode under batch, fed-batch and continuous mode. Under the tests, the potential of electrodes and current were monitored in conjunction with the hydrogen production, carbon dioxide dissolution rate and electrolyte properties. The objectives were to find the best feeding mode to enhance and maintain bioanode performance while comparing the difference between 2c- and 3cMEC. Apart from the wastewater treatment (anode) and hydrogen recovery (cathode) efficiencies, energy contribution was also calculated and studied to elucidate the importance of deploying bioanode in the system. In addition, integrated strategies were suggested for future study and improvement of the whole system in real applications.

7.2. Experimental procedure

Experiments were prepared mainly according to the procedure in Section 6.2. A peristaltic pump (Watson Marlow 120U/DM3, UK) was used to feed fresh medium into anodic chamber. The pump was connected to a power supply through a timer (Electric Timer Switch ETU17, Timeguard, UK) worked as an on-off switch for the pump under a specific time. For a batch mode experiment, the pump was switched 'on' manually for 10 min at the end of the anode cycle when the current was dropped and reached almost plateau. Under the fed-batch mode tests, the timer was set 'on' for 10 min for every 6hr or 12hr gap and the pump was set at flowrate of 3 mL/min unless stated otherwise. No timer was used to control the pump under a continuous mode test. The medium was continuously fed into the anodic chamber under the flow rate of 0.15 mL/min (hydraulic retention time = 2.8 hr). In addition, 50 mL of cathodic medium was either replaced or refilled every day from the top of the glass collector to replace the replenished catholyte due to hydrogen production and to maintain better cathode condition. All experiments were carried out in duplicates and under a constant temperature at 26.5 ± 2.5°C.

7.3. Result and discussion

7.3.1. Different growth cycle and catalytic properties trigger the need for feeding control

Electricity-generating bioanode and hydrogen-producing biocathode are two different bioelectrode catalysed by electroactive microorganisms (Kim *et al.*, 2004; Wang *et al.*, 2009; Jourdin *et al.*, 2015; Mohanakrishna *et al.*, 2015). Since they are dissimilar in catalytic activities and growth conditions, it is important to equalise both bioelectrode in order to match the rate of electron flow (in term of current density) while driving the electrodes to a favour condition (in term of potential or reducing power) which is necessary for redox reactions (e.g.CH_3COO^- /HCO_3^- and H^+/H_2). Figure 7.1 demonstrates the current and electrodes' potentials monitored under batch, fed-batch and continuous modes for anodic feeding. Figure 7.1 (a1) and (b1) show the results when the anodic feed was switched from batch to fed-batch mode. Meanwhile, Figure 7.1 (a2) and (b2) present the results when the anodic feed was switched from fed-batch to continuous mode. Two applied voltages (0.7 vs. 1.0 V) were used in Figure 7.1 (a1) and (b1) to show the amplified version of the current and potential responses when higher applied voltage (1.0 V) was used. In general, anode potentials began to decrease after the fresh medium was replaced. The potentials hit a minimum bottom point before they rose again. The drop and

rise of anode potentials after a fresh medium replacement depicts a single anodic cycle. Cathode potentials were technically followed the trend of the anode potential profiles under the tested conditions except for continuous mode. When the anode feeding mode changed from batch to fed-batch, anode performance was improved instantly because it could hold its potential in a more negative level. Besides it also shortened the time of cathode exposed to more positive potential when anode potential rose back to a more positive level. At higher applied voltage (1.0 vs. 0.7 V), the gap between anode and cathode potentials was slightly expanded improving both anode oxidation and cathode reduction abilities. The current density represented the total flow of electron from the anode to the cathode in the system. As observed from Figure 7.1 (b1), the current density was increased when the feeding was switched to fed-batch mode. The peak current rose from 1.5 to 2.5 A/m^2 which is about 67% rise of electron flow at 1.0 V applied voltage. Nevertheless, the percentage of the peak current (125%) even went up higher at 0.7 V applied voltage. At lower applied voltage, overpotentials and energy lost was less and could be the reason for higher percentage rise in peak current. However, the voltage might be not enough to drive the reduction reactions in cathode due to less electron flow or electrical current and overpotentials (Manohar and Mansfeld, 2009; Wang *et al.*, 2010). As studied from the fed-batch mode, significant enhancement of the anode performance was observed. The study was proceeded by switching fed-batch to a continuous mode in order to check whether continuous mode could further improve the anode performance. Based on Figure 7.1 (a2) and (b2), stable potentials and current were generated from the continuous mode. Anode potential in continuous mode almost retained the same minimum value and the generated current was almost reached the peak value as in fed-batch mode.

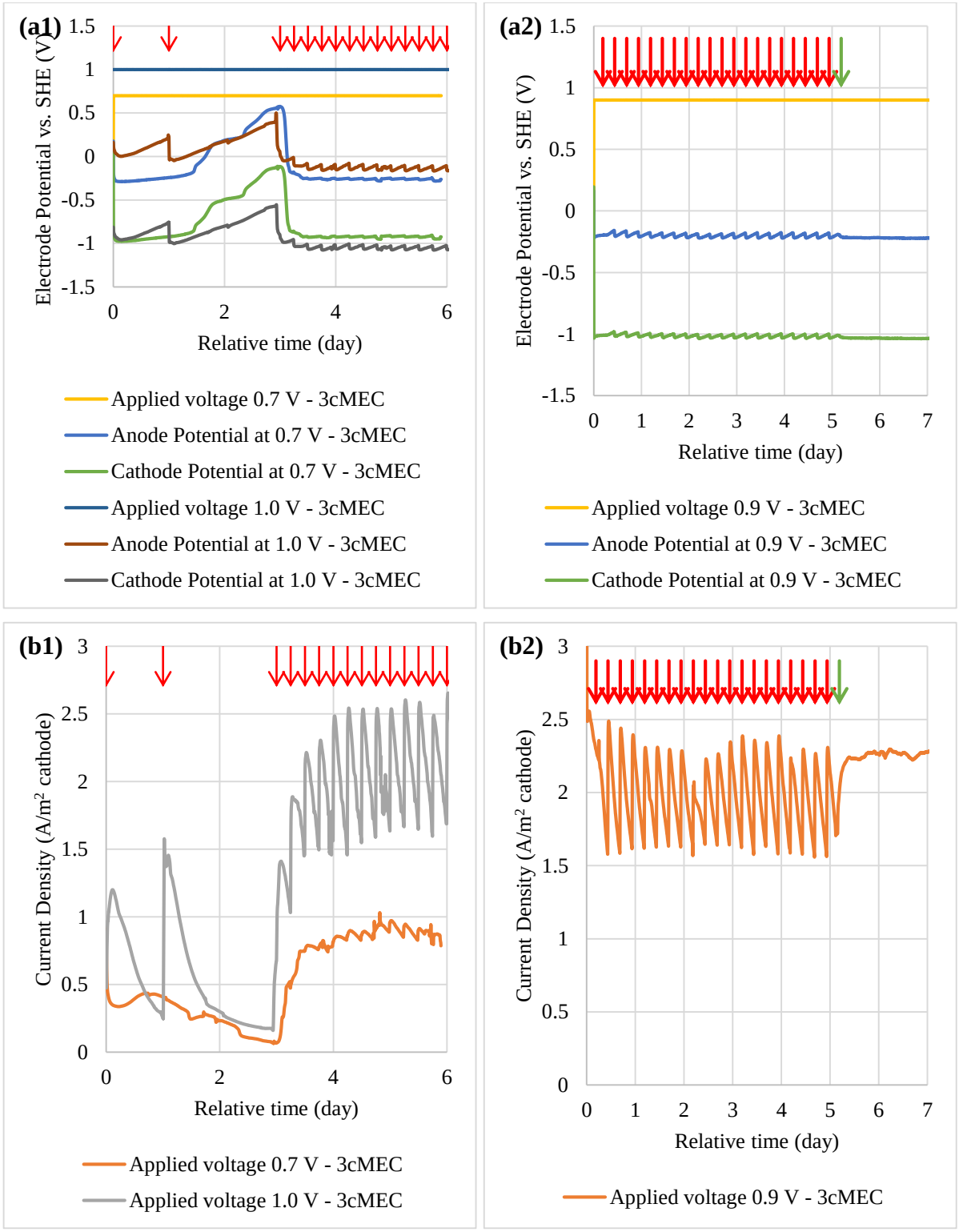

Figure 7.1 The profile of (a1) & (a2) applied voltage and electrodes' potential and (b1) & (b2) current density under the anode improvement tests by switching its feeding mode from batch to fed-batch, and fed-batch to continuous. Noted that red arrows indicated the feedings of fresh medium and green arrow showed the start of the continuous mode. The time was set to zero for comparison.

Figure 7.2 illustrates carbon dioxide diffusion and hydrogen production rate recorded under batch, fed-batch and continuous modes for anodic feeding. In overview, CO_2 diffusion under applied voltage was higher than the control (without applied voltage) (Figure 7.2 (a1) and (a2)). As reported in some studies, steady feeding approach normally improves the performance of MEC and provided a sustainable condition to produce hydrogen continuously (Tartakovsky *et al.*, 2009; Sleutels *et al.*, 2013). Switching of anodic feeding mode from batch to fed-batch and then continuous did increase the diffusion rate as more reactions occurred in the system. The previous study also found that catholyte pH was proportional to CO_2 diffusion and plateau when the applied voltage was increased until a certain value. The diffusion rate was slightly higher than the control at 0.7 V but more remarkable rose when the voltage of 1.0 V was applied. The trend was similar to that of hydrogen production in Figure 7.2 (b1) and (b2). However, significant hydrogen production was noticed on the second day after the mode was switched from batch to fed-batch. The hydrogen production rate was rising from about 1.6 to more than 15.0 L H_2/m^2 cathode/day at 1.0 V. Even though the continuous mode improved the cathodic potential by providing a steady reduction potential, the production of hydrogen was not enhanced as expected. The hydrogen production was slightly increased from about 14.0 to 16.0 L H_2/m^2 cathode/day or around 20% increase compared to the fed-batch mode. Besides, the continuous mode used larger amount of the influent compared to the fed-batch mode. In the fed-batch mode, 28 mL fresh medium was replaced every 6 hours which is equalled to 112 mL/day under 6 hour of hydraulic retention time (HRT). By comparing to the continuous mode, it required 212 mL/day under 2.82 hr of HRT which is nearly two times the fed-batch's influent volume. Perhaps the reason of low performance in continuous mode is due to the active microbes were being washed out, however, the cause might not be relevant because the bioanode was grown and attached on the surface of the electrode. Another explanation is the lack of electron shuttles secreted by electrochemically active microorganism when the fresh medium was continuously fed into the system causing the mediators being wash out. The electron shuttles are important to mediating the transfer the electrons between electrode and outer membrane cytochromes (Marsili *et al.*, 2008; LaBelle, 2009; Carmona-Martínez *et al.*, 2013). Therefore, the microorganisms under the continuous mode required a longer time to replenish the electron shuttles within the biofilm. In contrast, under the fed-batch mode, the bioanode was able to accumulate the mediators into a certain amount and boost the oxidation process by transfer more electrons to the electrode.

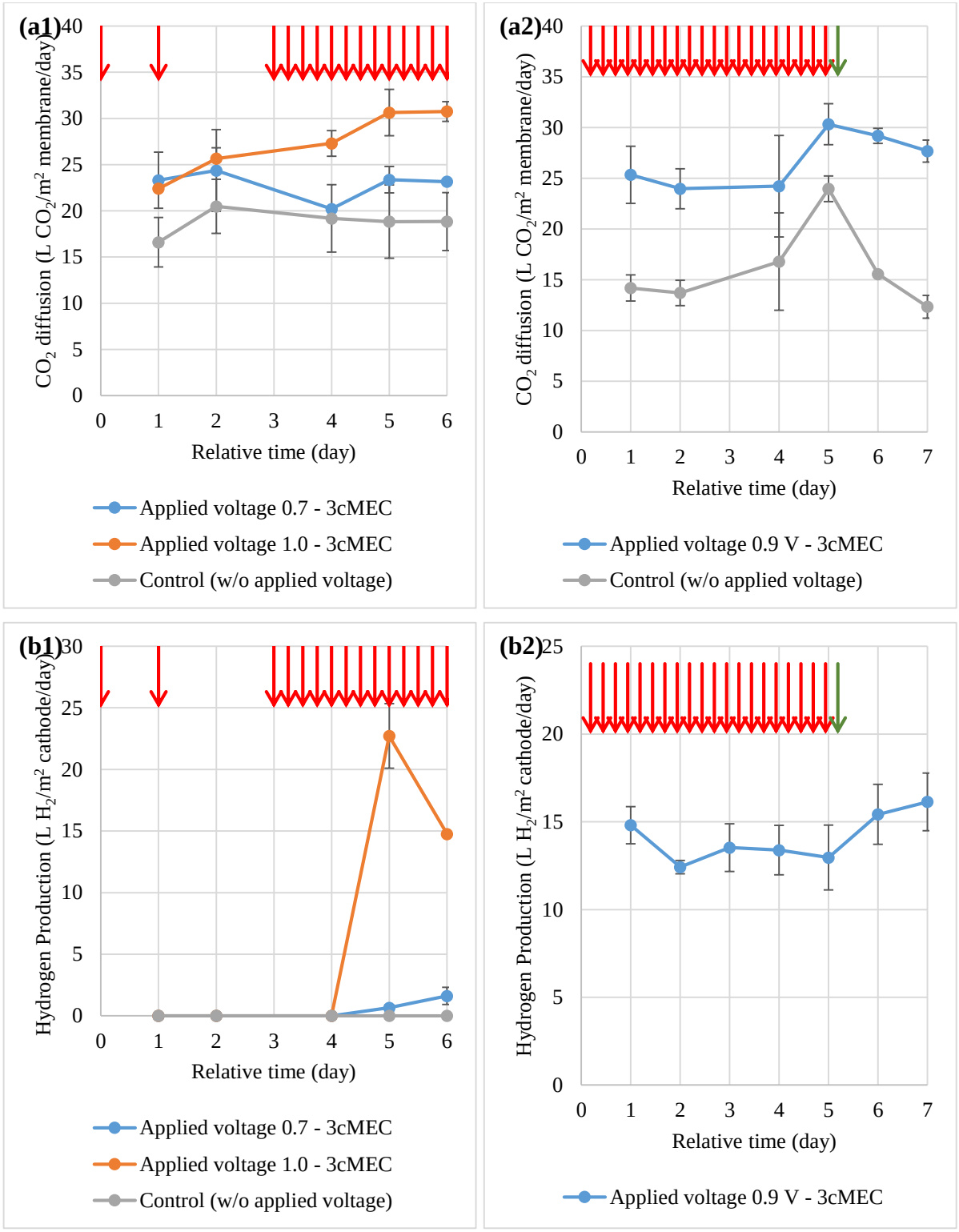

Figure 7.2 The profile of (a1) & (a2) CO_2 diffusion rate and (b1) & (b2) H_2 production rate under the anode improvement tests by switching its feeding mode from batch to fed-batch and fed-batch to continuous. Noted that red arrows indicated the feedings of fresh medium. In fed-batch mode, about 28 mL medium was replaced for every 6 hour gaps while in continuous mode, the medium was fed continuously at the flow rate of 8.854 mL/hr. Noted that the time was set to zero for comparison.

7.3.2. High rates of hydrogen production and CO_2 diffusion under anodic fed-batch mode

Figure 7.3 shows the hydrogen production and carbon dioxide diffusion rates under chronoamperometry tests. In the chronoamperometry tests, the anodic medium was replaced every 6 hours for a day before changing the applied voltage. From Figure 7.3 (a), significant hydrogen production was observed at 0.9 V and above. The production value about to plateau after 1.2 V. In comparison to 3cMEC, hydrogen production in 2cMEC was slightly higher (20 vs. 15 L H_2/m^2 cathode/day). This might due to the differential of cell configuration between those MECs. Two-chambered MEC has a closer gap between anode and cathode (1 cm) compared to 3cMEC (4 cm). The effect of electrode spacing between anode and cathode has been well documented in BES studies especially in MFC (Lee and Huang, 2013; Moon *et al.*, 2015; Rivera *et al.*, 2017). As the spacing between electrodes was reduced, the migration of ions from the anode to cathode and vice versa became easier. The conductivity between the electrodes was increased when the distance of travelling for the ions became shorter. No remarkable methane was observed in the systems. The present of methanogen could reduce the production of hydrogen as they use the hydrogen and available CO_2 to produce by-product, methane (Ruiz *et al.*, 2013; van Eerten-Jansen *et al.*, 2015; Bajracharya *et al.*, 2017b). Excessive protons were removed from catholyte when more hydrogen was produced under a higher applied voltage. pH value in catholyte increased when the protons were reduced to hydrogen. Higher pH value suppressed the methanogen growth and kept the methane production low in the system. A small increment of methane production was recorded between 0.7 and 1.0 V when the pH shifted from neutral was not as severe as above 1.0 V (Figure 7.5 (a)). Methanogens still could grow in mild alkaline condition, therefore increase the production increase in proportional to the growth. After 0.9 V, the methane production was decreased back to nearly zero resulting a small surge in hydrogen production at 1.0 V.

Meanwhile, averaged CO_2 diffusion from the gas chamber (Figure 7.3 (b)) was around 30 L CO_2/m^2 membrane/day, higher than the control about 20 L CO_2/m^2 membrane/day. Carbon dioxide is well known for its high solubility in water compared to other atmosphere gases (e.g.O_2, N_2). Since CO_2 can form carbonate compounds (H_2CO_3, HCO_3^- and CO_3^{2-}) with water in a wide range of pH (4-12), the properties have provided an alternative but easier technique to separate it from other gases (Huang *et al.*, 2016). In addition, the diffusion rate was depended on the solution pH. In 3cMEC catholyte, the pH was evolved from neutral to 10 (Figure 7.5 (a)) resulting in more dissolution of CO_2 into the solution.

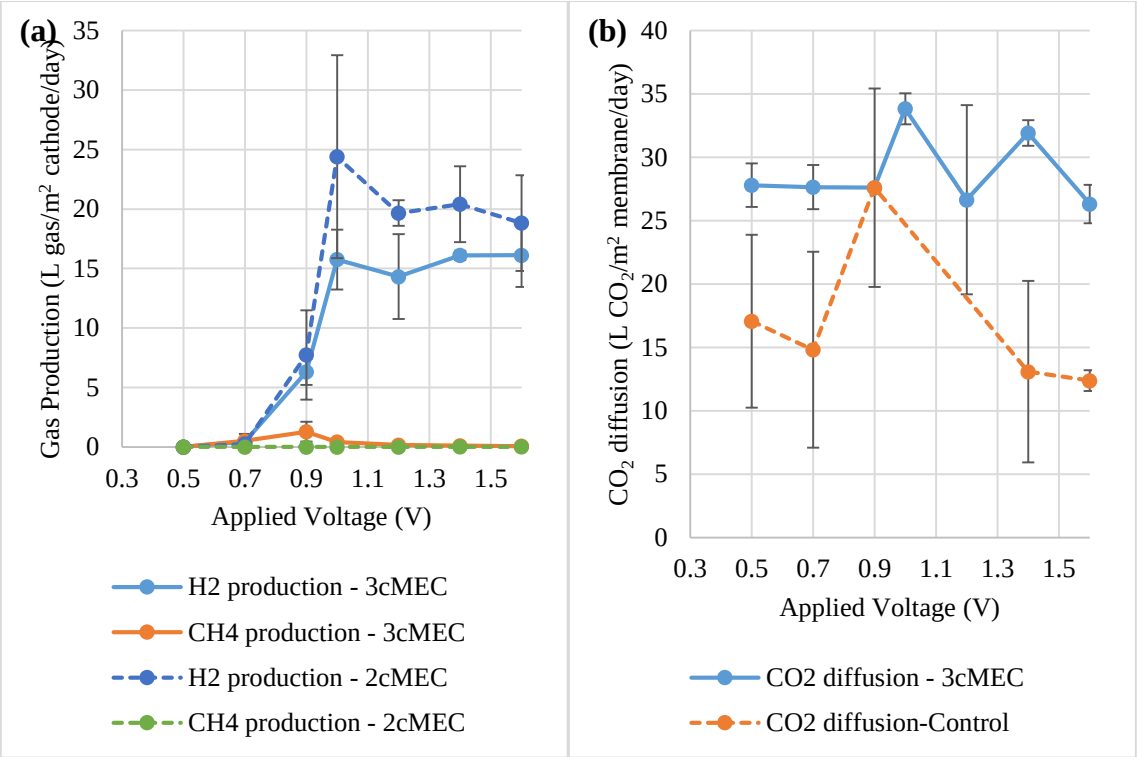

Figure 7.3 (a) Hydrogen production rate and (b) carbon dioxide diffusion rate under chronoamperometry tests. Anodic medium (28mL) was replaced under fed-batch mode in every 6 hours.

Figure 7.4 shows the profile of current density, applied voltage and electrode potentials under the chronoamperometry tests ranged from 0.3 to 1.6 V. The current record (Figure 7.4 (a)) was almost zero at 0.3-0.5 V. A notable current was observed started from 0.7 V. The zig-zag effect of the fed-batch mode in the anode was reflected on the current density record starting from 0.9 V and above. The peak current was plateau after 1.0 V. A detailed study on the electrode potentials (Figure 7.4 (b) and (c)) revealed the quantitative responses of the anode and cathode and its limitations in providing electrical energy. Between 0.3 and 0.7 V, anode potential was almost maintained at -0.3 V which was contradicted to cathode potential decreasing from -0.6 to -1.0 V. This means sufficient current was provided by anode at the beginning (0.3-0.9 V), however, cathode did not consume as much as anode supplied because its potential (< -1.0 V) was not in favour of reduction process. Therefore, the cathode potential dropped proportionally to the applied voltage at this stage. An opposite condition occurred in between 0.9 and 1.6 V where cathode potential was maintained at -1.1 V but anode potential shifted from -0.2 to +0.5 V. It implied the cathode potential had favoured the proton reduction but the anode had reached

a point where it could not provide the extra current required by the cathode. The imbalance of current requirement caused anode to raise its potential to oxidise more substrate.

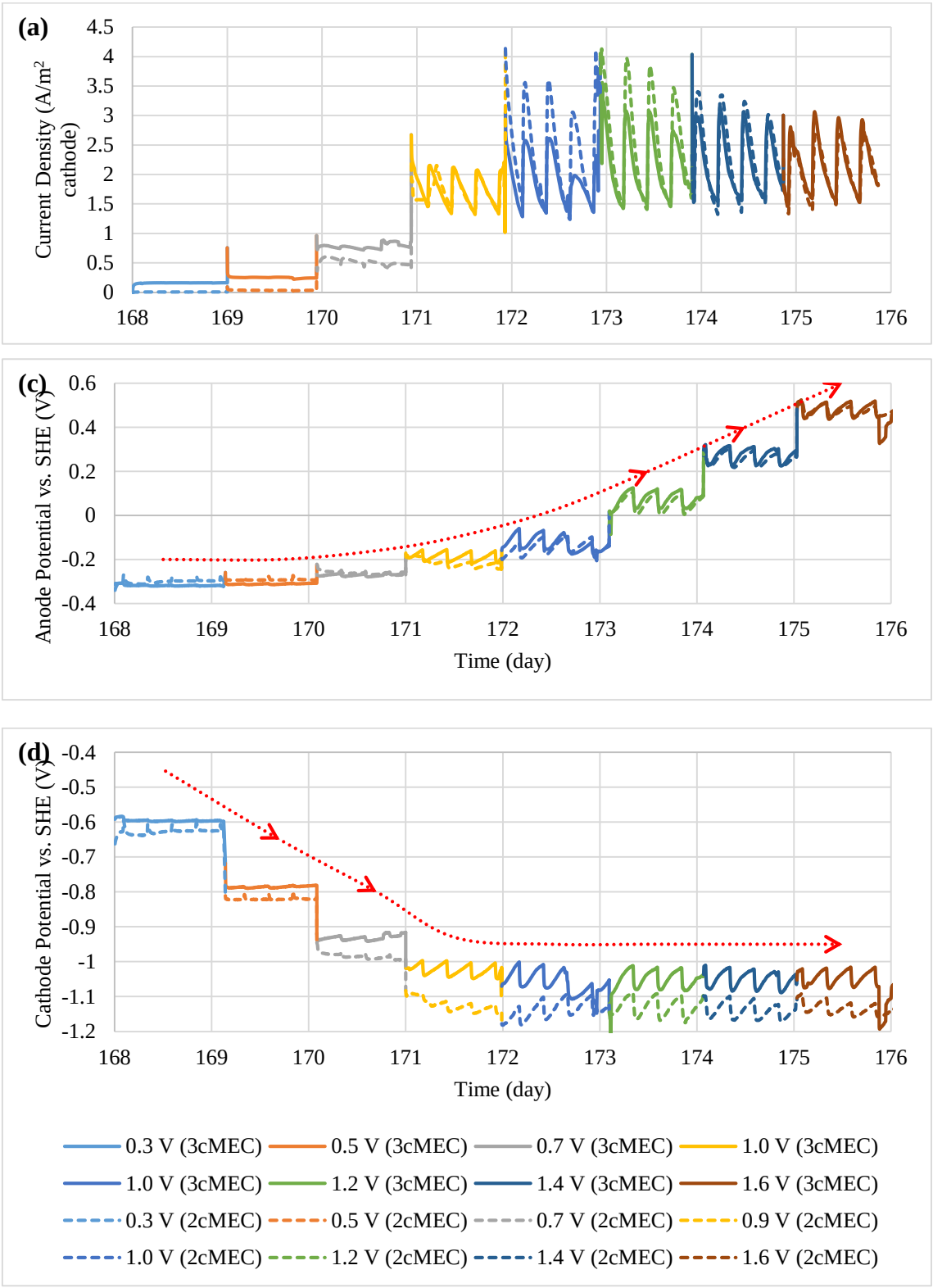

Figure 7.4 The profile of current density (a), applied voltage (b) anode potential (c), and cathode potential (d) responses to applied voltage ranged from 0.3 to 1.6V. Anodic medium (28mL) was replaced under fed-batch mode in every 6 hours.

7.3.3. Electrolytes' properties under the anodic fed-batch mode

Figure 7.5 exhibits the evolution of pH and conductivity values for both anolyte and catholyte in 2c- and 3cMECs. Apart from the current limitation in the anode, pH surged in cathode was also an negative effect on the system performance. The pH rose from 7.0 to 10 and 11 for 3cMEC and 2cMEC, respectively between the region of 0.5 and 1.0 V. Higher pH values (10-11) might kill or suppress the growth of hydrogen-producing bacteria and increase the domination of alkaliphiles in biocathode. Nevertheless, this is not always the case because other studies proved that alkaliphilic sulphate-reducing bacteria can survive in high pH up to 10.5 (Nielsen *et al.*, 1998; Sydow *et al.*, 2002). After 1.0 V, the pH was plateau which had the same profile hydrogen production rate (see Figure 7.3 (a)). High cathode pH could be a dominant factor to limit the MEC performance besides bioanode oxidation limitation (Kyazze *et al.*, 2010; Sleutels *et al.*, 2013; Lim *et al.*, 2017). As monitored between Figure 7.3 (a) and Figure 7.5 (b), hydrogen production slightly decreased or maintained after 1.0 V when the catholyte pH continued to increase and finally maintain at 10 or 11. Higher applied voltage did not further increase hydrogen production. It is postulated that the hydrogen production could be further increased by the control of the pH near neutral value (or 7.0) (Rozendal *et al.*, 2008). In the 3cMEC system, dissolute CO_2 can form carbonates compound under aqueous condition. While water molecules form carbonate compounds with CO_2 (H_2CO_3 in acidic condition; HCO_3^- at neutral pH; CO_3^- in alkaline condition) and leave protons behind, the protons not only serve as a reactant for hydrogen production but also mitigate the pH increase when more protons are reduced to hydrogen. In contrast, the pH of anode effluent was decreased from neutral to nearly 6.0 which was not as severe as in cathode. The anolyte might be used to alleviate the catholyte pH at higher applied voltage by feeding it into the cathode. However, the introducing of remaining organic matter from the anode could be a problem for the hydrogen-producing biocathode community.

The conductivity of a solution depended on the concentration of all the ions present, therefore, conductivity value changed according to the evolution of pH in the solution. However, pH only measures the concentration of proton could not represent the value of all active ions in the solution. Moreover, the ion concentrations changed depending on the oxidation and reduction reactions on the electrodes. Figure 7.5 (b) shows the catholyte conductivity value was increased, while in the opposite, the anolyte conductivity values decreased between 0.5-1.0 V. The oxidation or reduction reactions were changing the ion concentration by breaking or forming the compounds resulting in the change of conductivity. Furthermore, the accumulation

of proton in anode and consumption of proton in cathode also generated pH imbalance across the two chambers divided by a cation exchange membrane. Phosphate buffer was added into both electrolyte not only to control the pH but also increased the conductivity of the electrolytes. Some studies even added salts into the electrolyte to increase the overall conductivity and reduce internal resistance (Rozendal *et al.*, 2006; Ahn and Logan, 2013; Sleutels *et al.*, 2013). Maximum hydrogen production was observed at 1.0 V applied voltage. The conductivity value in catholyte was dramatically increased between 0.9 and 1.0 V. The increment implied the increases of ions composition and concentration were significant after 0.9 V where reduction reaction was the most active. This is the point where a significant amount of CO_2 ($\geq$ 1.0V: 33 L CO_2/m^2 membrane/day vs. < 0.9V: 27 L CO_2/m^2 membrane/day) was started to diffuse and dissociate into carbonates compounds. Meanwhile anolyte conductivity dropped and plateau starting at 0.9 V and above which is slightly earlier than catholyte that happened after 1.0 V. Oxidation of substrate at anode broke down the ion compounds such as CH_3COO^- (to CO_2) and NH_4^+ (to NO_3^-) (as discussed in section 4.3.3) which contributed to the decreases of conductivity (Shcherbakov *et al.*, 2009; Haynes, 2010). It suggested that bioanode current was first drawn to the maximum at 0.9 V before it can support the cathode at a maximum performance at 1.0 V.

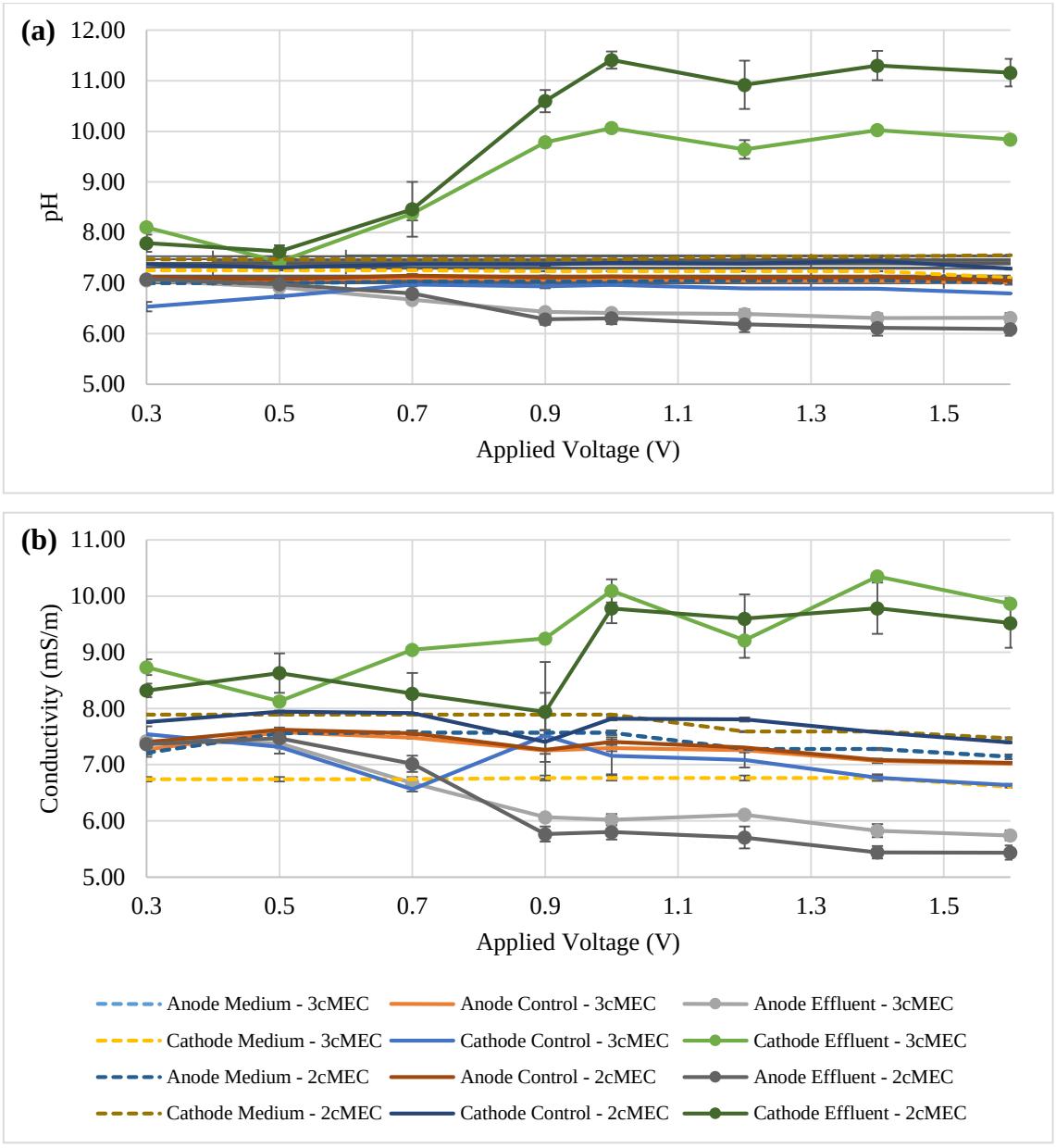

Figure 7.5 The evolution of pH (a) and conductivity (b) values under varies applied voltages

Figure 7.6 reveals the inorganic/organic carbon concentrations in anolyte and catholyte. The results of 2c- and 3cMEC are both included for comparison. From Figure 7.6 (a), removal of organic carbon in anode was almost similar to the control from 0.3 to 0.7 V. This is because the anode was not subjected to maximum oxidation reaction at this stage. However, there was still nearly 400 mg CO_2/L/cycle consumed by the bioanode metabolic activity. Further removal was observed when the applied voltage was further increased starting from 0.9 V. In overall, the removal rate in 2cMEC was better than 3cMEC. Small inorganic carbon concentration was also detected in the anolytes resulted from substrate oxidation. In Figure 7.6 (b), inorganic carbon in 3cMEC was higher than the 2cMEC. Gas chamber attached next to the cathode in 3cMEC

had provided an alternative to accumulate the carbonates from CO_2. In addition, the pH of cathode rose when the protons were reduced by the cathode to produce hydrogen increasing the CO_2 dissolution ability. About 800-1400 mg CO_2/L/day was accumulated in 3cMEC under applied voltage conditions. Another interesting observation is the increases of the inorganic carbon concentration in the effluent of 2cMEC when the applied voltage was more than 0.7 V. Supposedly the inorganic carbon concentration in Figure 7.6 (a) increased after the applied voltage more than 0.7 V as more substrate was oxidised. Nevertheless, the inorganic carbon concentration still remained very low (< 20 mg/L) in the anolyte. It is suspected that the inorganic carbon was transferred from anode to cathode under the concentration gradient. Besides, all the catholyte effluents contained higher inorganic carbon concentration than the control indicating the hydrogen production was not the only product of the biocathode reduction. From Figure 7.6 (c), formate, acetate and butyrate were found in catholyte for all the applied voltage region. The accumulation of butyrate in 2cMEC even went up to 15.8 from 6.9 mg/L compared to the control at 1.0 V applied voltage. However, only up to 10% butyrate accumulation was found in the catholyte of 3cMEC. Meanwhile, acetate remained low about 10 % or less was observed in both of the MEC systems especially in the condition where the butyrate concentration was high. Chain elongation of CO_2 to acetate and butyrate or multi-carbon based organic matters were observed in this study after nearly a year of operation of the MECs. In recent studies by other researchers, as long as six carbon-based organic carbon matters (caproate) was reported (Bajracharya *et al.*, 2017b; Raes *et al.*, 2017; Vassilev *et al.*, 2017; Jourdin *et al.*, 2018). The pre-condition to the chain elongation and produces higher value chemicals than acetate is the catholyte must accumulate up to certain amount of short-chain carbon-based organic matters (e.g. acetate (C2) and butyrate (C4)). This is to ensure the biocathode can further utilise the compounds to formed longer carbon chain organic compounds under the assistance of reducing power (reduction potential supplied from external power and/or bioanode).

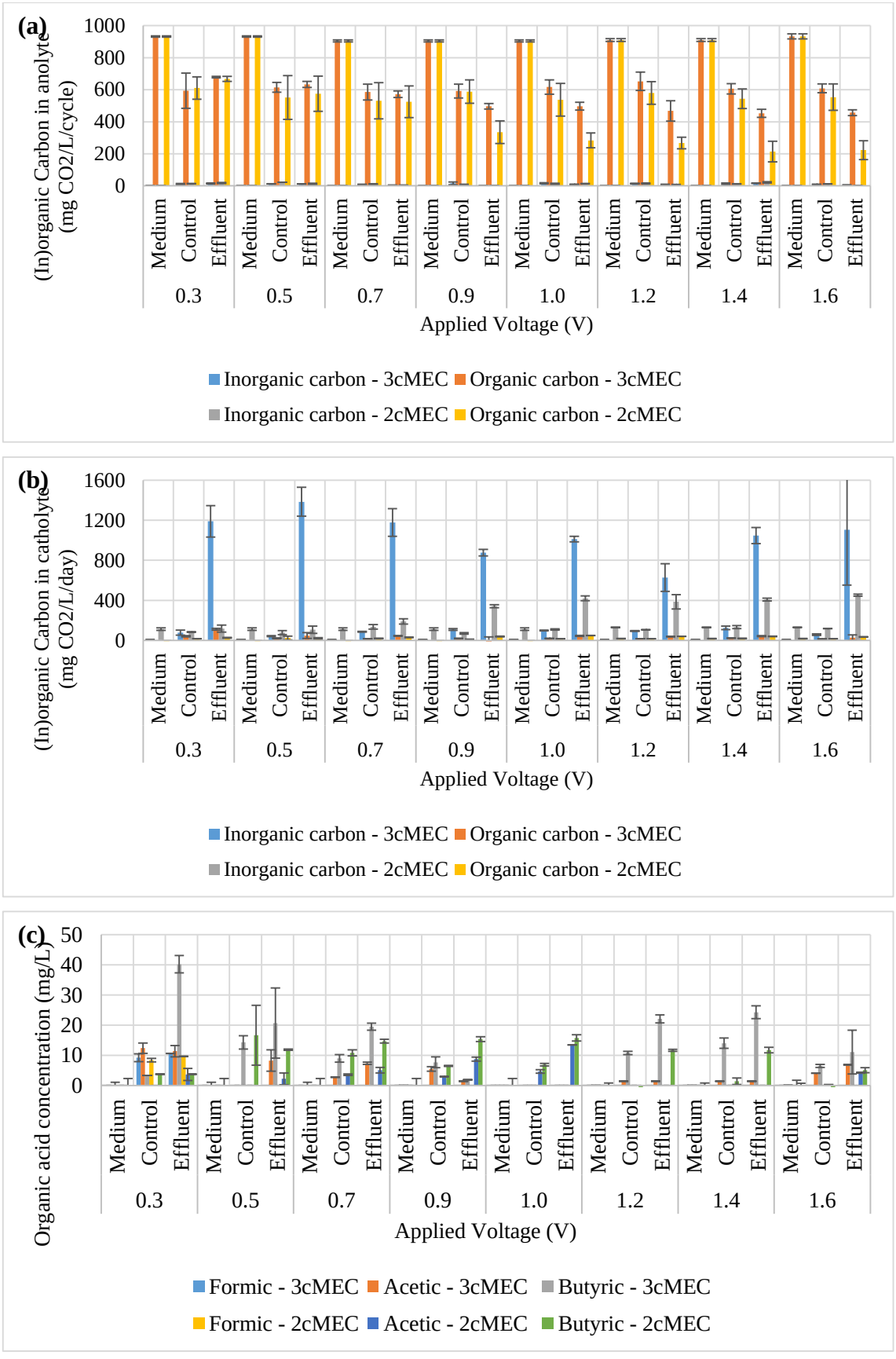

Figure 7.6 Total carbon content (a) remained in anolyte, (b) accumulated in catholyte, and (c) organic acid content under the chronoamperometry tests.

7.3.4. Energy recovery and system efficiency between 2c- and 3cMEC under anodic fed-batch mode

Figure 7.7 demonstrates energy recovery and efficiency in anode and cathode between 2c- and 3cMEC. There is a less significant difference in cathodic recovery between both cell configurations than in Coulombic efficiency (Figure 7.7 (a)). Small difference (< 20%) in the cathodic recovery was noticed within the range of 0.9 to 1.6 V between those cells. Meanwhile, huge difference (< 400%) in the Coulombic efficiency was observed especially between 0.5 and 0.9 V. Besides those differences, the peak values between cathodic recovery and Coulombic efficiency also occurred in different regions (0.7-0.9 V vs. 1.2-1.4 V). Again, it showed the evidence that the bioanode was first pushed to a maximum production of electrons to support biocathode before it could reach maximum performance under a transition region between 0.7-1.4 V or to be exactly between 0.9-1.4, and 0.7-1.2 V for 2cMEC and 3cMEC, respectively.

In Figure 7.7 (b), energy yields were not seen from 0.3 to 0.5 V except at 0.7 V and above. On the one hand, energy yields from substrate oxidation seem increased proportionally with the applied voltage and almost plateau after 1.4 V. On the other hand, energy yields from electrical input were peaked at 1.2 V before they started to decrease. In summary, the maximum overall energy yield was recorded at 1.2 V. They were about 40% and 62% for 2cMEC and 3cMEC, respectively. In additional to the 3cMEC exhibited better performance compared to 2cMEC, it also showed that it needs less potential (See Figure 7.7 (a): range between 0.9-1.4 V vs. 0.7-1.2 V) in the transition region as explained in the previous paragraph.

Further investigation on the overall energy yield revealed the percentage of energy contribution by substrate oxidation and external power. Figure 7.7 (c) shows the energy contributed by substrate oxidation decreased from 0.5 to 1.0 V for 2cMEC but the 3cMEC decrease slightly earlier from 0.3 to 0.7 V. After the decreases region, energy contribution was stable until 1.6 V. By considering the transition regions discovered in Figure 7.7 (a), the adjustment of the energy contribution actually happened before the region. Once again, it affirmed the energy from the bioanode was first withdrawn to a maximum point and then further assisted by external power to support the biocathode.

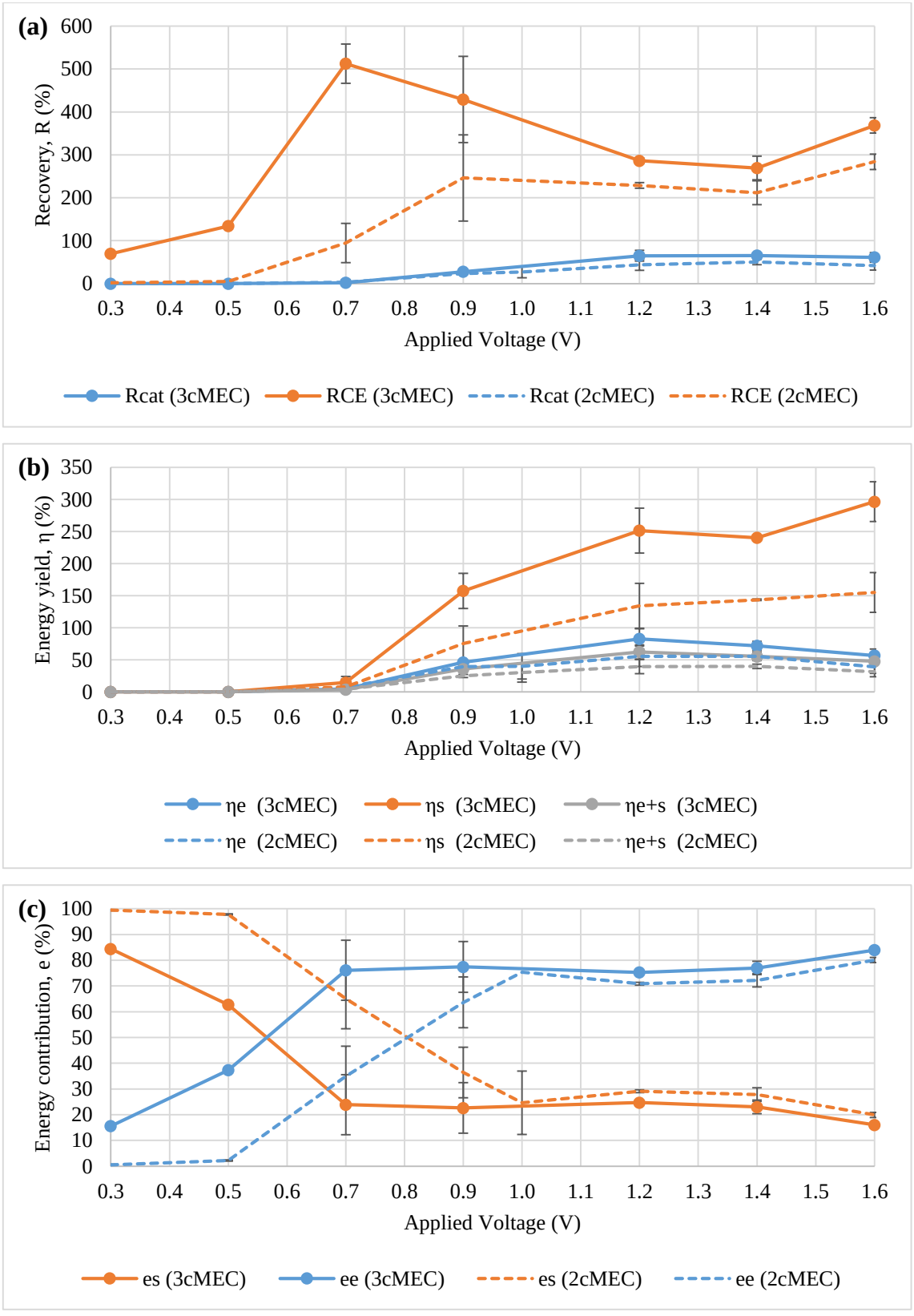

Figure 7.7 Cathodic hydrogen recovery and anodic Coulombic efficiency (a), electrical input, substrate oxidation and overall energy yields (b) and energy contribution (c) under different applied voltages.

7.3.5. Comparison of energy recovery, yield and contribution at different feeding gaps

To emphasise the usage of the fed-batch mode in anode, an experiment was conducted under a feeding gap of 12 hours and compared to the 6-hour gap results. Figure 7.8 shows the comparison of energy recovery, yield and contribution in 2c- and 3cMEC. The energy recovery results (Figure 7.8 (a1) and (b1)) in 2cMEC and 3cMEC showed some difference between the feeding gaps. In 2cMEC, cathodic and Coulombic efficiencies increased faster under longer feeding gap. Meanwhile in 3cMEC, there was indifferent and overlapped in Coulombic recovery, however, shorter feeding gap in anode increased the cathodic recovery at a higher applied voltage (>0.9 V). Figure 7.8 (a2) and (b2) presents the energy yields for 2cMEC and 3cMEC. Both energy yields based on substrate oxidation and electrical input were significantly increased at a higher applied voltage (>0.7 V) under the shorter feeding gap. Based on the energy contribution analysis (Figure 7.8 (a3) and (b3)), the shorter feeding gap did improve anode contribution to the system at the lower applied voltages (0.3-0.7 V). Nevertheless, the contribution from external supply still took over the big portion of the contribution at higher applied voltages (>0.7 V). Around 65-85% was contributed by the external power supply while the rest was from the anode.

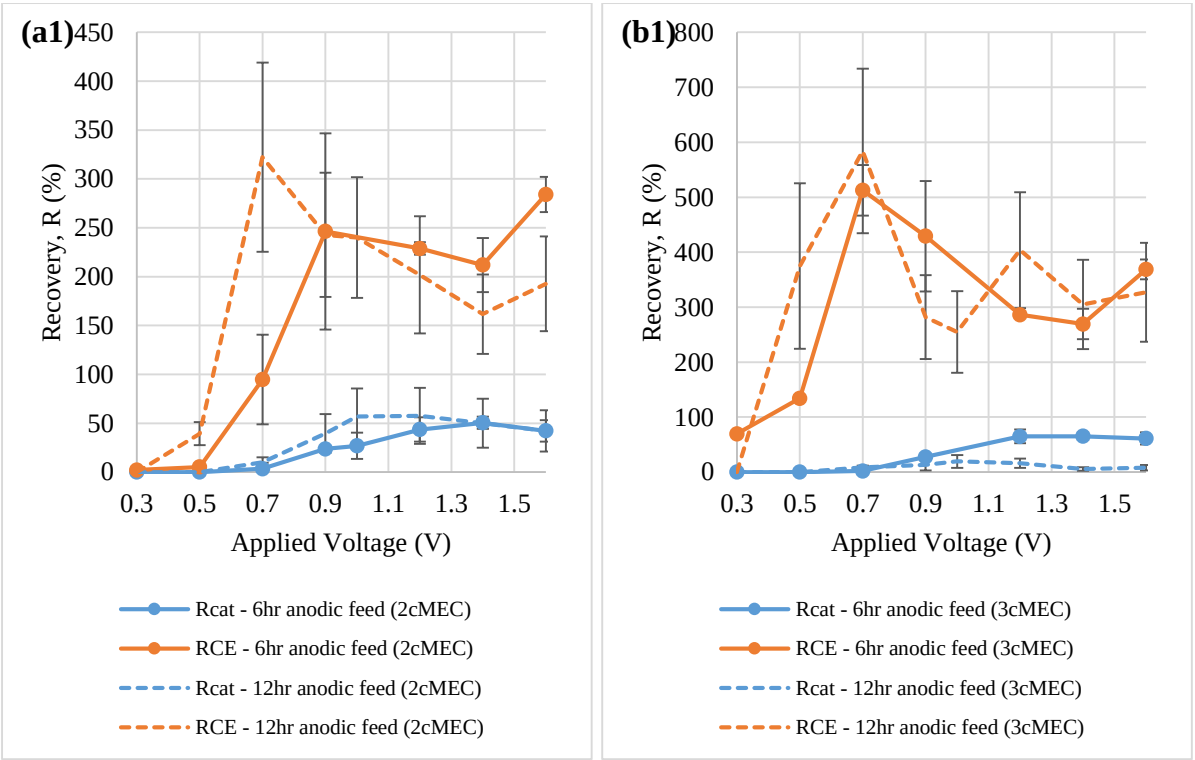

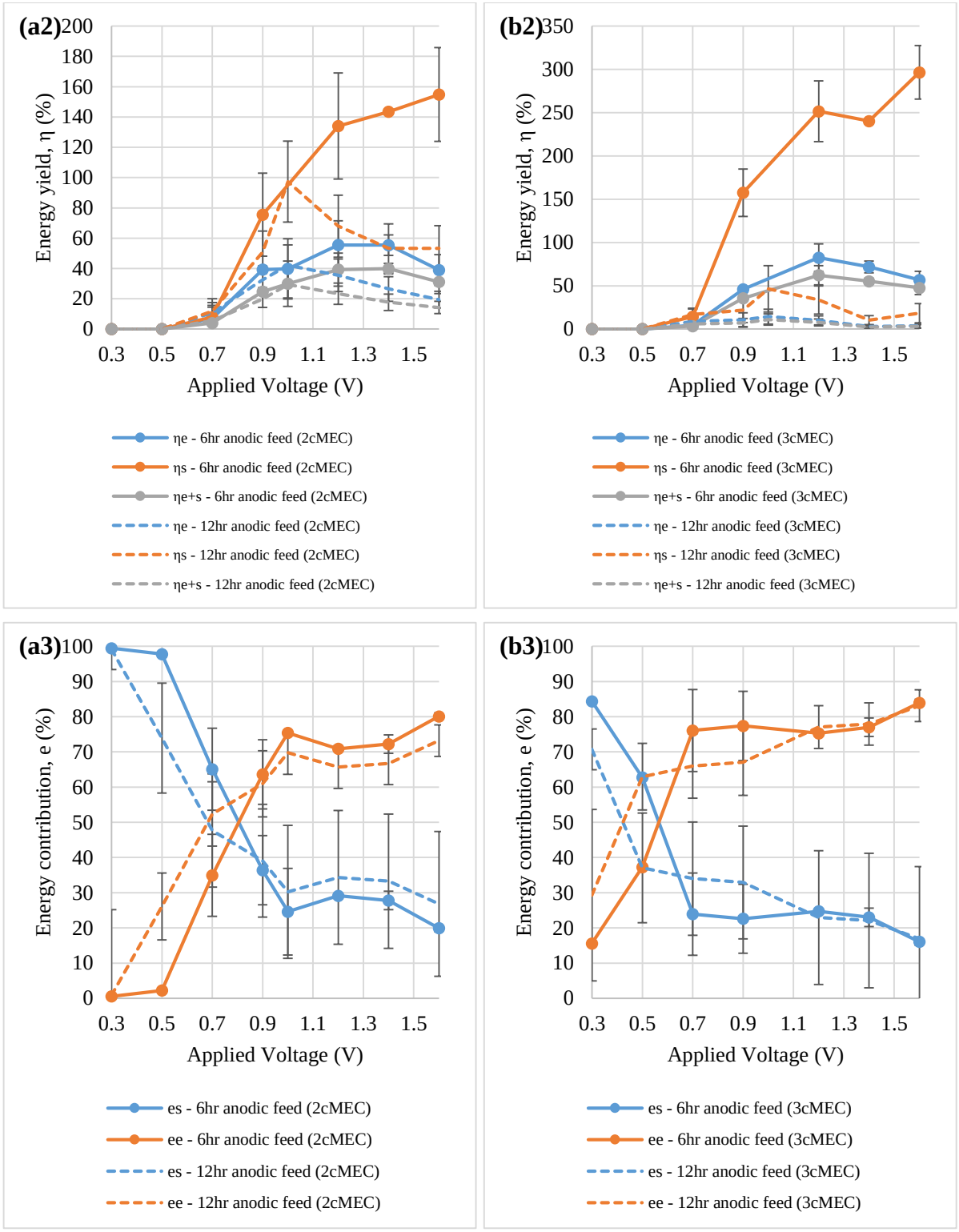

Figure 7.8 Comparison of the energy recovery (1), efficiency (2) and contribution (3) between 6- and 12-hour feeding gaps in the fed-batch mode: (a) 2cMEC and (b) 3cMEC.

7.4. Conclusion

In the study, bioanode performance was improved by changing its feeding mode from batch to fed-batch. However, the performance did not further increase when the feeding mode was switched from fed-batch to continuous mode. Under the chronoamperometry test, the maximum hydrogen production recorded between 0.9 and 1.2 V under the fed-batch mode was 10 times higher than the batch mode. Meanwhile, switching the mode to continuous did increase the hydrogen production but only a small increment or 1.24 times higher than the fed-batch mode. Moreover, the continuous mode also required a lot more influent than the fed-batch mode (212 vs. 112 mL/day). A detailed study of the half-cell potentials and current under varies applied voltages also gave extra insight to the bioelectrodes' properties. Based on the analysis, the bioelectrodes' behaviours could be divided into three main regions: cathode activation, transition and anode limitation regions relative to the lower applied voltage (< 0.7 V), optimal (0.7-1.2 V) and higher (> 1.2 V) applied voltages. The trend of the electrolyte pH and conductivity were also found following the applied voltage regions. Nevertheless, the trend was consistent at lower and higher voltage except at the optimal voltage conditions. Indeed, the finding of the energy recovery (R_{cat} and R_{CE}) peak values, at different applied voltage supported the claim of the transition region. The transition region suggested the energy from bioanode was being utilised first before it was further assisted by external power to support the biocathode. Even though shorter feeding gaps (6hr vs. 12hr) had a better advantage in the energy recoveries and energy yields, it still could not reduce the contribution of electrical energy to less than two-third of the total supplied energy.

Chapter 8. Conclusions and recommendation for future work

8.1. Conclusion

8.1.1. Defining the limitations of an electricity-generating bioanode

One of the main findings in this study is the limitation of bioanodes within a bioelectrochemical system (BES). An initial investigation looked at the enrichment and operation of bioanode and biocathode under different conditions (applied potentials). However, it was found that the bioanode did not perform as expected under the given conditions. Therefore, various electrochemical analysis was carried out to find the bioanode weaknesses including the determination of the bioanode's internal resistance. The resistance was considered as the simplest electrochemical and one indicator of bioanode robustness. The bioanode performance was determined under various operational conditions: poised potential, external resistance and influent properties including pH, carbon and nitrogen source concentrations. The study indicated that the increased of internal resistance value could affect the bioanode performance. The operational conditions and influent properties were also important in the enrichment and growth of the bioanode. The bioanode enriched at -0.2V vs. SHE was able to survive at higher applied potential up to 1.0V and had two significant catalytic activities at midpoint potentials: -0.2 V and +0.2 V. The catalytic waves could be shifted between each other depending on the potentials fixed on the anode. This may be due to the fact that the community shifted, or the changes in metabolic pathways of dominating microbes. In addition, the effects of buffer (phosphate-based), reactants (acetate and ammonium) to the current output, Coulombic efficiency, pH and conductivity were also studied. It was found that phosphate buffer: acetate: ammonium = 50:10:10 mM as optimal influent condition. The capability and robustness of bioanode are important to ameliorate the biocathode limitation and improve whole system efficiency.

8.1.2. Characterising the requirements of a hydrogen-producing biocathode

Important parameters affecting the hydrogen-producing biocathode was determined in this study. The experiments included the change of applied potential and the present of specific reactants (bicarbonate, sulphate and ammonium) in the biocathode environment. The optimum ratio of PBS: HCO_3^-: NH_4^+: SO_4^{2-} in this study was determined as 950:610:90:288 mg/L (10:10:5:3 mM) for a biocathode sized 0.005m^2, operation volume 0.0025 m^3 and applied potential 1.0 V vs. SHE in a continuous flow rate 0.1 mL/min. Besides the ratio, external power supply was required to provide initial energy under low potential electrons to start the biocathode catalytic activity while sulphate served as a final terminal electron acceptor to dispose of the exhausted electrons. As organic carbon compounds were found in the biocathode effluents, it is believed that within the microbial community the inorganic carbon was consumed by acetogens to produce organic carbons such as acetate and then consumed by SRB as a carbon source. Another significant finding is the presence and quantity of sulphate did affect the hydrogen production in SRB-dominated biocathode. Analysis of the results showed that community interaction occurred between sulphate-reducing bacteria and homoacetogens. In addition, the electron transfer pathway in SRB was affected by proton and sulphate concentrations under a specific applied potential. At high sulphate concentration, it could inhibit hydrogen production if the cathode potential was not low enough to reduce both sulphate and proton. The phenomena are similar to those electron bifurcations.

8.1.3. Characterising the interaction of bioelectrodes in a MEC

The evolvement of bioelectrodes' behaviour in MEC under the stress of applied voltages was studied. A minimum cell voltage of 0.3 V was sufficient to promote the simultaneous growth of the biofilms on both electrodes' surfaces. However, the electrochemically-active biofilm grew faster at the anode than at the cathode. Three main regions were identified under the tested range of voltages (0.3 to 2.0 V) where a significant change of behaviour or interaction of the bioelectrodes was observed. They are cathode activation (up to 0.9 V), transition (between 0.9 and 1.8 V) and anode limitation (more than 1.8 V) regions. Amongst those regions, the transition region was determined as the best applied voltage region because the highest hydrogen production rate was occurred at the range. A window of the applied voltage between 0.9 and 1.8 V was determined as the most relevant operational voltage to maintain the biocathode potential low enough for reduction reactions and at the same time protect the bioanode ability in oxidation reactions. At lower voltage region, cathode could not possess a

minimum potential to initiate hydrogen production while at higher voltage region, bioanode was overused and could risk of losing its biotic characteristic. Energy efficiency, and yield were also analysed in order to have an insight view of their energy contribution between bioanode and external electricity supply. At the lowest applied voltage of 0.3 V, the anode contributed almost 99 % of the current. The external power began to dominate the contribution when higher applied potential was set in which favoured the cathode reduction reaction and at the same time reduce the gap of the current shortage. At the optimum applied voltage of 1.0 V, the bioanode contributed for one-third of the total energy, marking the important of bioanode to reduce the cost of external power.

8.1.4. Improving the MEC performance by feed controlling to the bioelectrodes

Three feeding patterns named batch, fed-batch and continuous were applied to the MEC fully catalysed by microorganisms. The study found that fed-batch feeding is the best mode on improving the bioanode performance and significantly increasing hydrogen production in the biocathode up to 15.0 L H_2/m^2 cathode/day. Based on calculation, the value was 10 folds higher compared to batch mode and only 0.19 times less than continuous mode. This is due to the performance limitation in the bioanode causing the low efficiency of the biocathode. On the one hand, the bioanode took a longer time to recover if it was operated under the batch mode (1-2 days vs. 1-2 hours under fed-batch mode) which could affect the performance of the whole MEC system. On the other hand, the continuous mode slightly increased the bioanode performance and lead to a current rise from 2.0 to 2.3 A/m^2. Nevertheless, the mode required larger amount of influent or nearly two times compared to the fed-batch mode. When the fed-batch mode bioanode was studied under the chronoamperometry test, it revealed the same electrochemical behaviours as mentioned in the previous section. The behaviour was analysed and divided accordingly to the applied voltage condition named: cathode activation (< 0.7 V), transition or optimal (0.7-1.2 V) and anode limitation (> 1.2 V) regions. Interestingly, the finding of the energy recovery (R_{cat} and R_{CE}) peak values, at different applied voltage also supported the claim of the proposed transition and optimal regions. The transition region suggested the energy from bioanode was being utilised first before it was further assisted by external power to support the biocathode. However, the improved bioanode still could not reduce the contribution of electrical energy to less than two-third of the total energy.

8.1.5. Examining the effect of an extra gas chamber in MEC

A gas chamber was attached next to the cathode chamber in a two-chamber (2c-) MEC to form a three-chamber (3c-) MEC. The chamber was meant for examining the potential of the direct diffusion of CO_2 into nearby catholyte saperated by a CEM. The study was a proof-of-concept that CO_2 can be easily removed from the atmosphere without the input of external energy due to its high dissolution capability in water (solubility: carbon dioxide 0.169 vs. oxygen 0.0043, carbon monoxide 0.0028, nitrogen 0.0019, hydrogen 0.00016 g/100g water at 293 K, 1 atm). During the experiments, the accumulation of the CO_2 was proportional to the applied voltage and hydrogen production rate which was also associated to the change of pH and conductivity of the catholyte. In the MEC's cathode, protons were reduced to produce hydrogen. As a results, solution's pH was increased when more protons were removed from the catholyte. However, it was found that the pH increased relatively slow in 3cMEC (8.0) compared to 2cMEC (9.5). Aqueous CO_2 can react with water forming carbonic acid, H_2CO_3. The acid may lose protons to form bicarbonate, HCO^- and carbonate, CO^{2-} depended on the solution pH. A theory of CO_2 dissolution from the gas chamber to catholyte based on concentration gradient was elucidated. Carbonates were accumulated up to 550 mg CO_2/L catholyte/day in this study. In the meantime, the accumulation of CO_2 was also increased the catholyte conductivity from 8.0 to 10.0 mS/m. The dissolution of CO_2 not only accumulated carbonates and alleviate pH in the catholyte but also provided protons for hydrogen production.

8.2. Recommendation for future work

8.2.1. Minimising MEC internal resistance with a better cell design

As found in this study, pH shifts and conductivity drops in anode or cathode are serious problems in a separator-based MEC. To solve the problem, optimised and compact cell design should be considered. Feeding anodic effluent to cathode or vice versa might be a solution to the pH shift problem. The objectives are to find the optimal recirculation rate and periodic feeding time between anode and cathode. In addition to the pH shift, conductivity between electrodes can be achieved by determining the suitable electrode gap, size of the electrode (anode/cathode ratio) instead of adding chemicals and increase the cost of operation. In addition, some controlling strategy will also be studied during the scale-up process, e.g. periodic polarity reversal to stabilise the pH in two-chambered system (Jiang *et al.*, 2016), introducing a small

amount of seawater into the chamber to increase electrolyte conductivity etc. (Ahn and Logan, 2013) etc.

8.2.2. Real wastewater treatment and large scale applications

The study of MEC to treat wastewater and produce hydrogen can be initialised by using real wastewaters in laboratory. Results from this study could be used as basic information to scale up the process. In this stage, the study will involve designing a better system (e.g. Multiple electrode-tubes assembly, tubular-type MEC) to treat a large volume of wastewaters combines with the assistance of mathematic modelling to maximise whole system performance. Either direct scale up or multiple cell units, the best solution should be determined in this study.

8.2.3. Understanding electron transfer mechanism in biocathodes

It is important to understand the principle of how a hydrogen-producing or CO_2-reducing biocathodes works. There is a difference between hydrogen-producing and CO_2-reducing biocathode. While the first is meant to produce hydrogen as the main product, the latter is to utilise CO_2 to produce organic carbons (such as acetate, butyrate and even longer chain fatty acid like capriote (Jourdin *et al.*, 2018) depends on microbial community and operation conditions. In spite of the differential, the key species of producing hydrogen and organic carbon could be found in both biocathodes except the percentage of those species is varied according to the reduction process. For examples, sulphate-reducing bacteria was found dominating in a hydrogen-producing biocathode while acetogens were largely occupied in a CO_2-reducing biocathode (Croese *et al.*, 2011; Mohanakrishna *et al.*, 2015). Elucidated electron transfer mechanisms from the cathode to final products not only help to understand the biocathodes work but also to lay strategies to improve the production rate. In addition, it also assisted to comprehend the interaction relations between key species in biocathode. This can be done by using enriched and single culture biocathodes under the stress of specific inhibitor and final electron acceptor tests.

8.2.4. Selective separator/gas diffusion material selection for 3cMEC

Suitable materials that allow CO_2 to diffuse from gas chamber to athodic chamber but block the further transfer of CO_2 into anodic chamber should be sorted out properly. Water crossover into the gas chamber should also be considered when choosing the right separator. The study could

be started by selecting the available commercial membranes or thin film ion exchange membrane (Rozendal *et al.*, 2007) or ceramic filters (Winfield *et al.*, 2016) and tested them using the same 3cMEC setup. Based on the knowledge of the study, more suitable and effective separator/gas diffusion materials can be custom-made and check them in laboratory before any large scale testing.

Appendix A

A1. Enrichment of bioanode in microbial fuel cell with different internal resistances

Two-chambered MFCs were set up to enriched bioanodes under specific internal resistances. Each anode was operated under the assistance of a Pt-coated cathode and linked with 50 Ω external resistance. Figure A.1 shows the enrichment profile of the bioanode under the internal resistances. In the beginning, the internal resistances of the MFCs were determined as 13 Ω (MFC group 1), 61 Ω (MFC group 2) and 164 Ω (MFC group 3) under electrochemical impedance spectroscopy (EIS) method. The electrogenic bioanodes were first enriched by injecting 10 mL of inoculum collected from parent cell followed by 10 mL fresh medium. The fresh medium was continuously fed into the anodic chamber at a flow rate of 0.17 mL/min after the anode was left overnight. Current density rose instantly in the first 10 days for MFC group 1 and 2 except MFC group 3 picked up after 15 days. Since then the current density increased gradually until it reached a plateau around 0.3 A/m^2 after 50 days. This result was consistent to other studies using the same size of the reactor with a stable value of 0.04 A/m^2 within 30 days of operation (Kim *et al.*, 2004; Lim *et al.*, 2012).

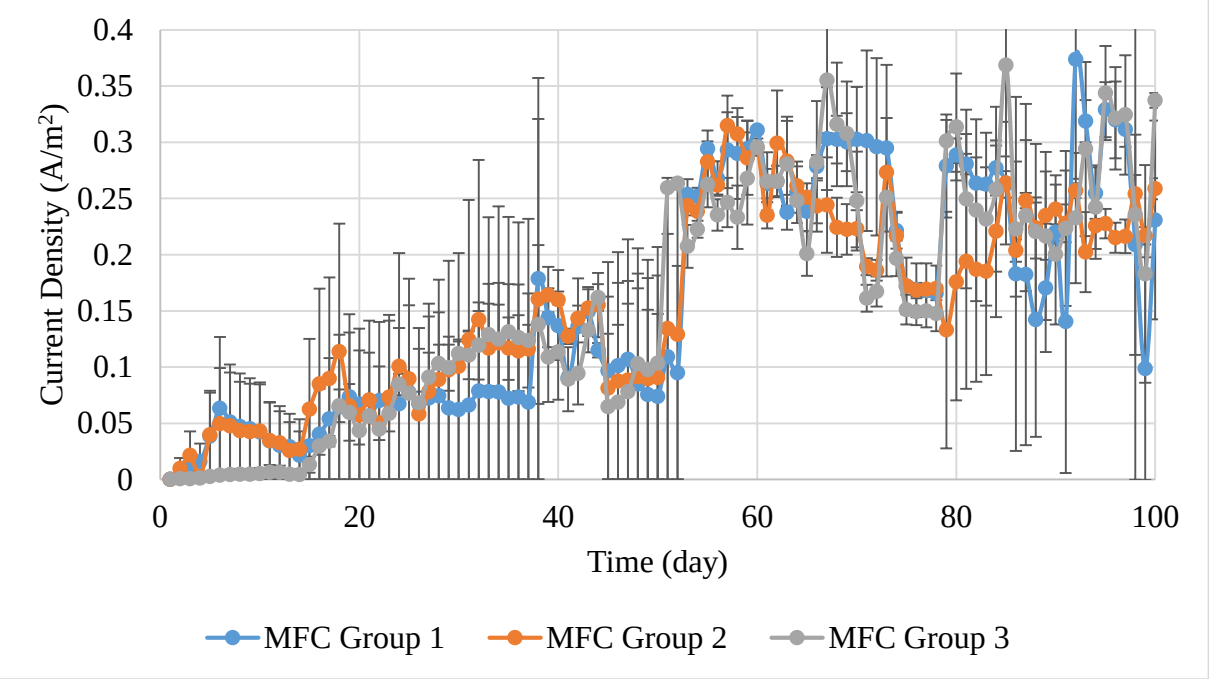

Figure A.1 Profile of current density for MFCs operated under different internal resistance. Note: Initial internal resistance of MFC determined from EIS method (Ω): MFC group 1 (13), MFC group 2 (61) and MFC group 3 (164)

Figure A.2 shows the calculated external resistance and potentials. One of the main observation from Figure A.2 (b) is the voltage decreased in a much faster rate when more current was withdrawn from the cell at higher internal resistance. The breakdown of cell voltage to half-cell potentials revealed the drawback of each electrode's internal resistance to whole cell performance (Liang *et al.*, 2007; Manohar and Mansfeld, 2009; Zhang and Liu, 2010). In Figure A.2 (b) the anode potential increased slightly faster in MFC group 3 compared to group 1 and 2. This is supported by the internal resistance values in Figure A.1 that anode resistances (in MFC group 2 and 3) and cathode resistance (in MFC group 3) were slightly higher than group 1.

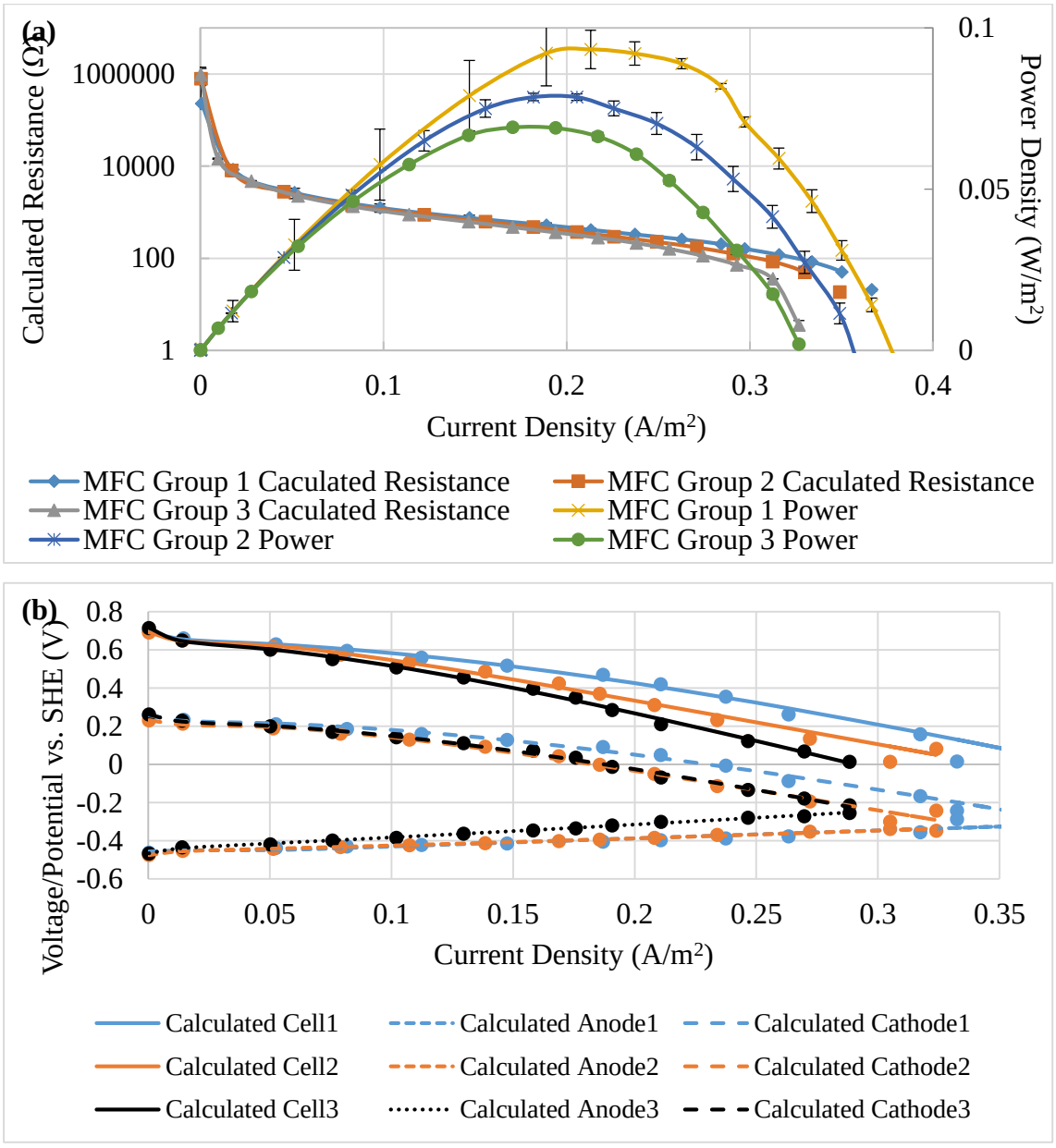

Figure A.2 (a) Calculated external resistance with power density, (b) cell voltage and half-cell potentials.

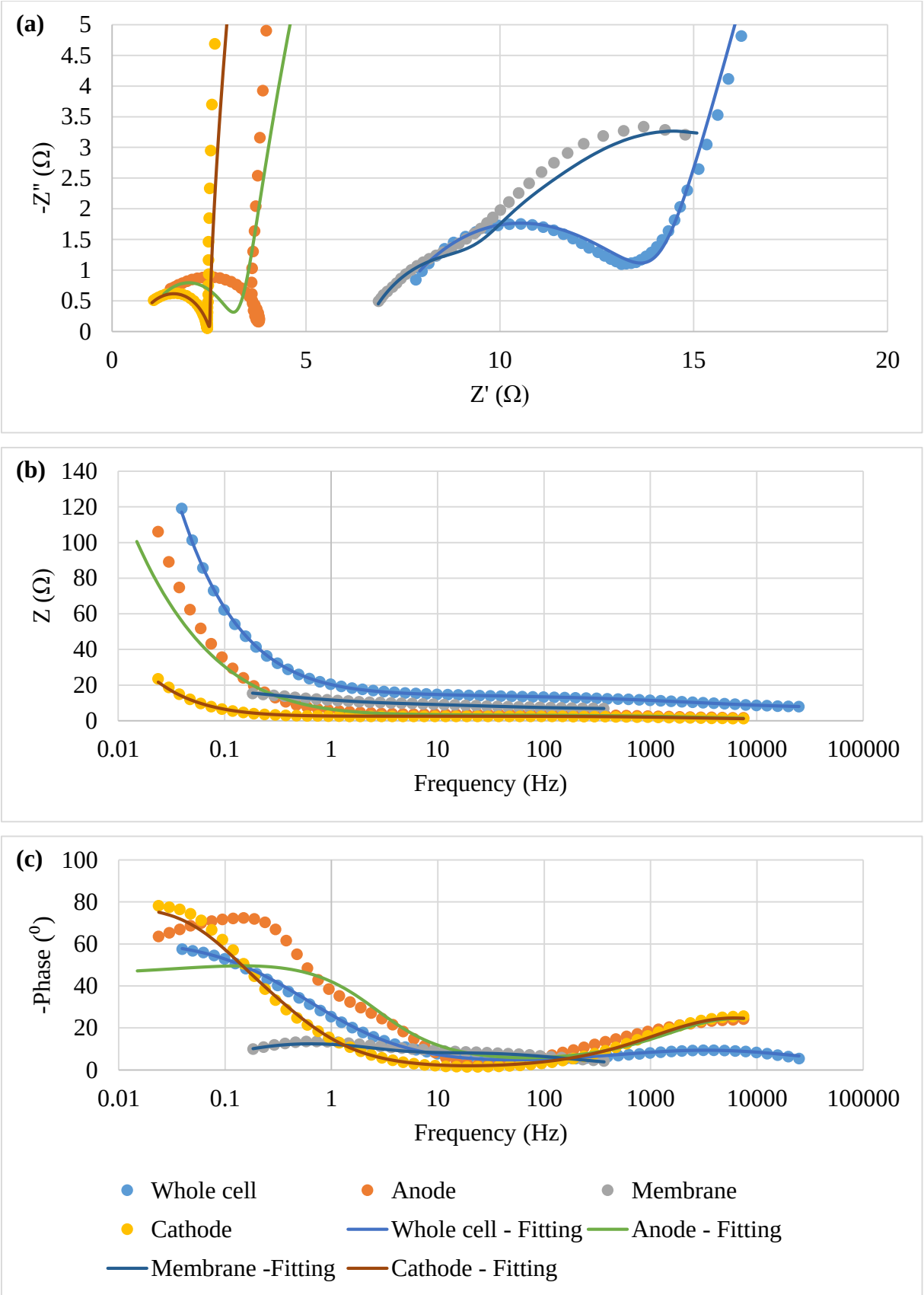

Figure A.3 Electrochemical impedance spectrograms of whole MFC and its components: anode, membrane and cathode. (a) Nyquist (b) Bode magnitude and (c) Bode phase plots.

Table A.1 Equivalent circuits used to fit the spectrograms in Figure A.3

(a) Component	Initial	During enrichment	Stable
Anode[1,3]	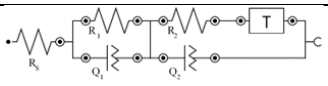	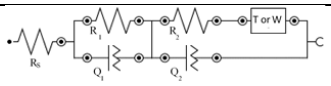	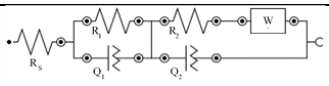
Membrane[1,2]	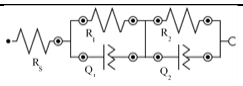	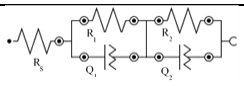	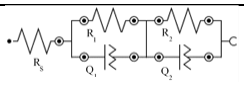
Cathode[1,4]	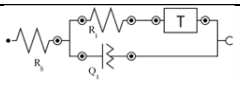	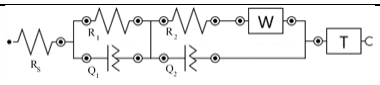	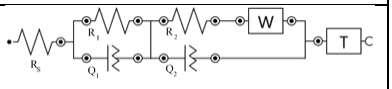
Cell[1,3]	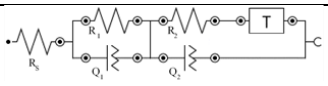	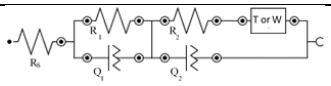	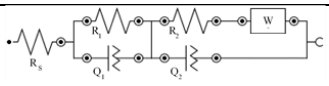

[1] R_S is solution resistance measured between RE and WE while R_1 and Q_1 are due to the material surface properties when in contact with electrolyte.

[2] R_2 and Q_2 are due to the material surface properties when in contact with electrolyte.

[3] R_2, Q_2 and T are because of the diffusion properties of the porous electrode layer while in the later T is replaced by W to represent diffusion behaviour of the integrated biofilm-electrode layer.

[4] R_2, Q_2 and W are because of the diffusion properties of the catalyst layer while T represents diffusion behaviour of the air-saturated electrolyte.

Figure A.4 shows the derivative graphs of CV derived from Figure 4.4. The purpose of the derivative plots is to narrow down mid-point potential where symmetric peak waves (oxidation and reduction reaction) occurred (Fricke *et al.*, 2008; LaBelle, 2009; Zhu *et al.*, 2013). The mid-point potential is well known related to the outer membrane cytochromes or protein potential which discharge the electrons from microbial cell to anode. Therefore the anode potential should be higher than this mid-point potential in order to transfer the electrons (Aelterman *et al.*, 2008; Torres *et al.*, 2009; Carmona-Martínez *et al.*, 2013; Ketep *et al.*, 2013; Zhu *et al.*, 2013). Under low internal resistance (Figure A.4 (a1 & a2)), the mid-point potential range was narrow (-0.3 - 0 V) but soon became more broad (-0.3 - +0.2V) when the internal resistance increased (Figure A.4 (b1 & b2) and (c1 & c2). Moreover, the peak value of the potential became weaker (from ±20 to ±6 and ±4 $(A/m^2)/V$) when the internal resistance increased (from 13, 61 and 164 Ω, respectively).

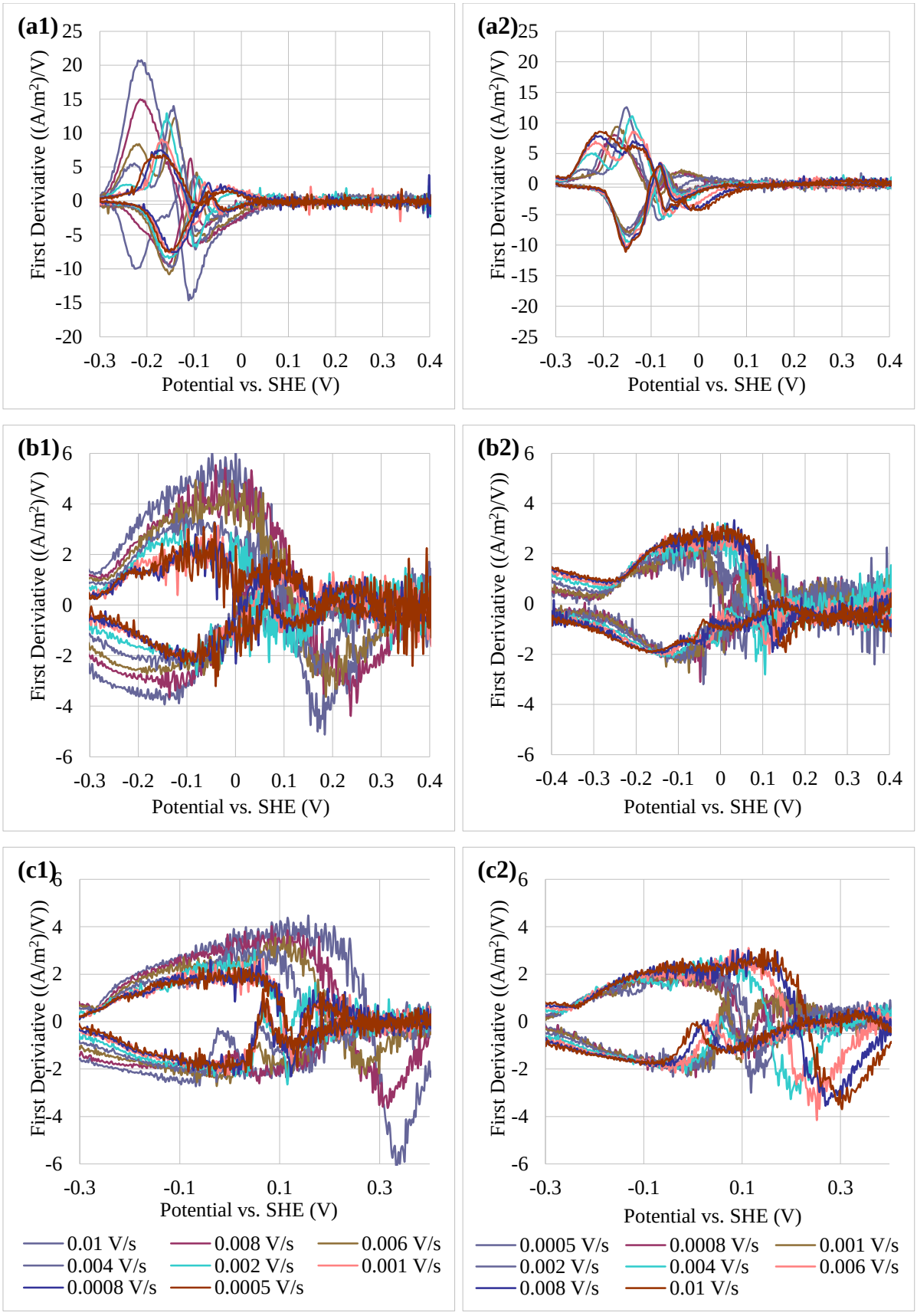

Figure A.4 First derivative of cyclic voltammograms with increment scan rate ranged from 0.01 to 0.0005 V/s (x1) and decrement scan rate from 0.0005 to 0.01 V/s (x2) for MFC group 1 (a1 & a2) and 2 (b1 & b2) and 3 (c1 and c2).

Figure A.5 is the plots of peak current versus square root of scan rate. Linear fitting to the points confirmed that the reaction was controlled by diffusion instead of adsorption (Milner *et al.*, 2016). A layer of biofilm growth on the electrode surface was limiting the mass transport of reactant and product in and out from the layer (LaBelle, 2009). Besides, the diffusion layer promoted by concentration gradient could also result in the diffusion limitation. Particularly under higher reaction rate when substrate replenished was kinetically surpassed by a thick diffusion layer formed on the electrode's surface. The layer obstructed the transportation of substrate or reactant from and products to bulk solution. Constant slope values between three set of tested MFCs confirmed that the diffusion limitation was caused by the same component or materials (biofilm and carbon felt). Nevertheless, the peak current value was remarkably different. MFC group 1 had the highest peak current values followed by group 2 and 3 as shown in Figure A.5 (a) where the scan rate was slightly reduced during the analysis.

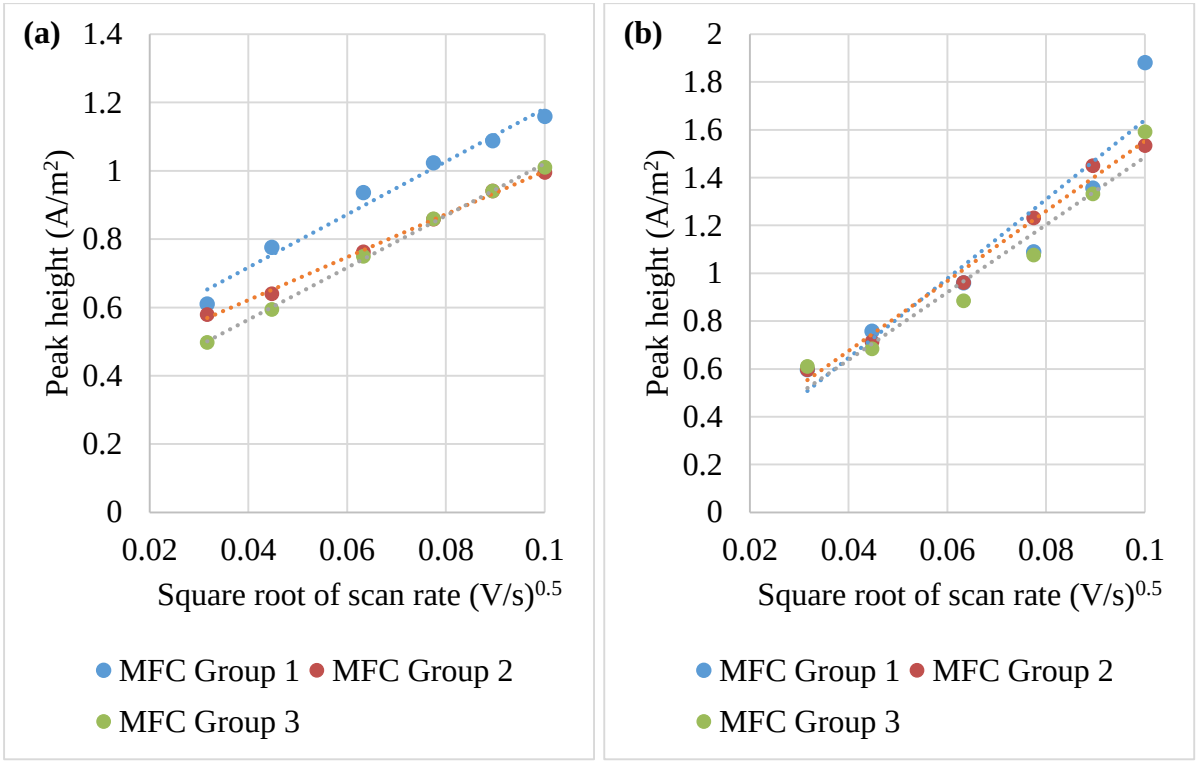

Figure A.5 The plotting of peak height versus square root of scan rate to determine the electrochemical properties controlled by anode biofilm.

A2. Effects of operating parameters to bioanode performance

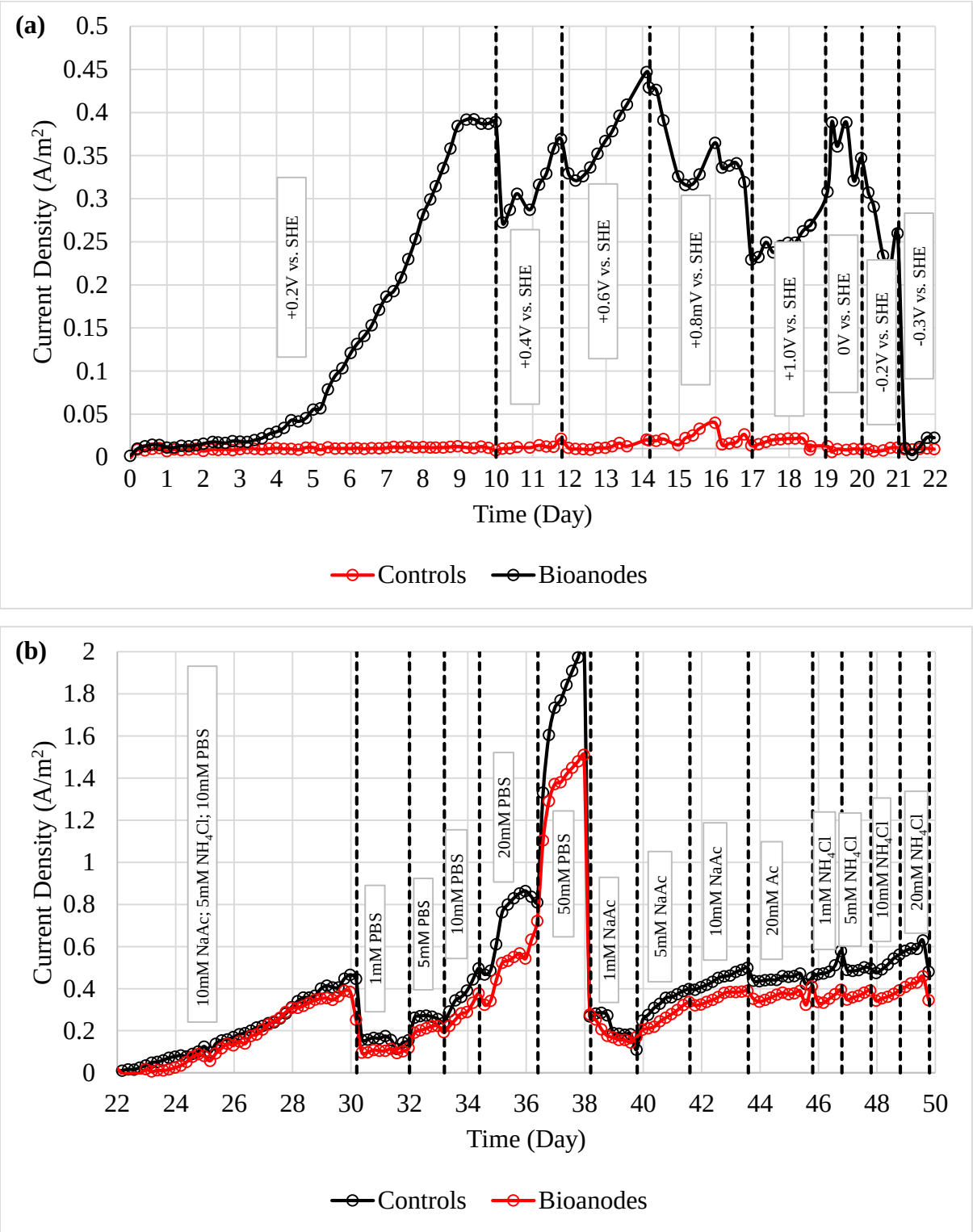

Figure A.6 Profile of current density for new MFC under low internal resistance (<10 Ω). Inoculum was injected into MFCs under the ratio of 1:1 inoculum at the beginning except control. Inoculum from the enriched MFC was injected into the control at 22 day.

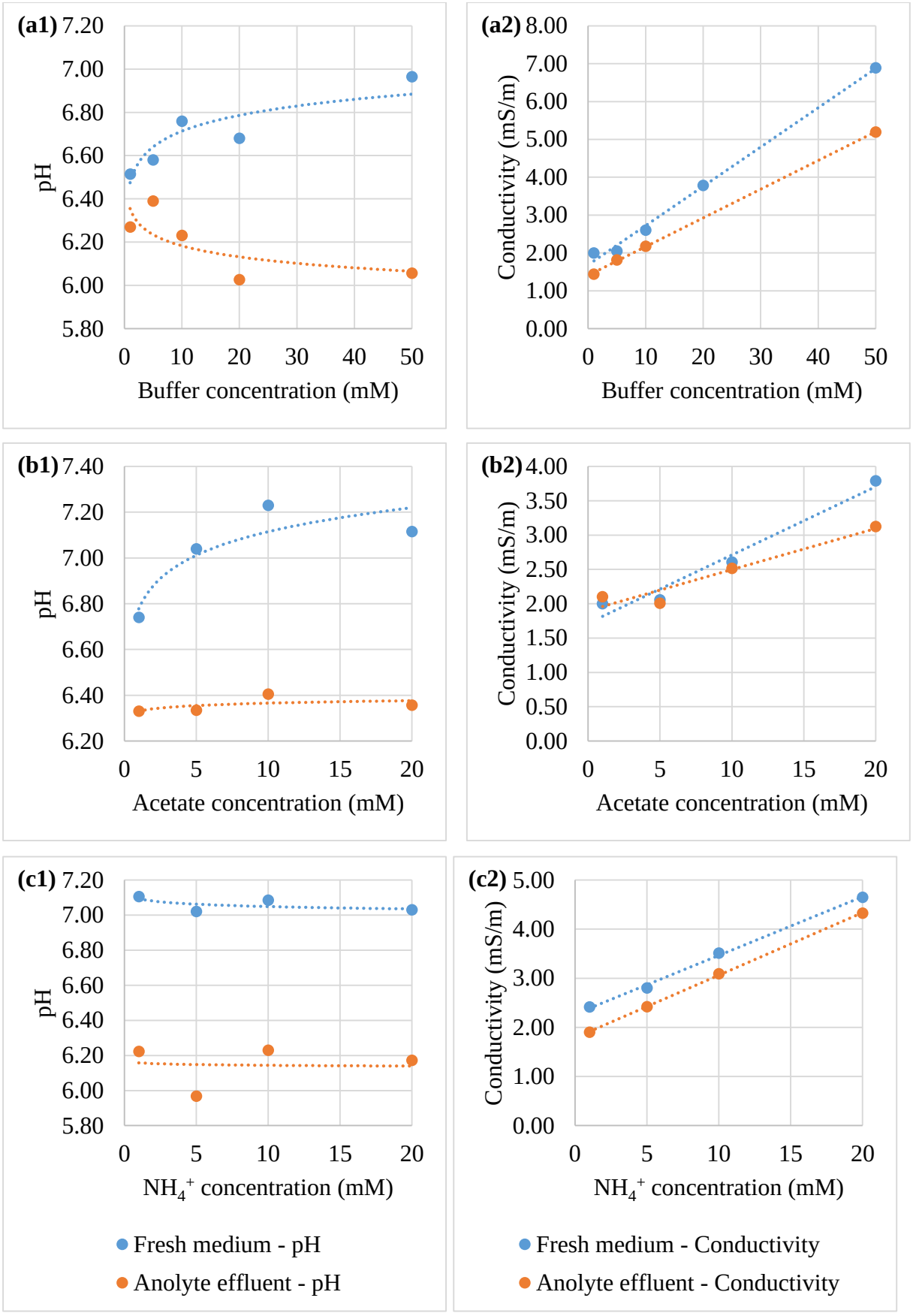

Figure A.7 The effect of (a) buffer, (b) acetate and (c) ammonium concentration to pH and conductivity of bioanode fixed at +0.2V vs. SHE

Appendix B

B1. Fast determination of bioelectrode activities at an early stage (0-60 days)

A range of voltage between 0 and 2.5V was applied to the cells to check the development of the bioelectrodes over time during the enrichment process. Chronoamperometry method was used in this analysis with the applying time of 10 minutes for each point from 0 to 2.5V. Figure B.1 (a1) and (b1) show the evolution of anode and cathode potentials according to the apply cell voltage and Figure B.1 (a2) and (b2) shows the current densities recorded from 2cMEC and 3cMEC, respectively. As the results from 3cMEC exhibited a complete evolvement of the bioelectrodes over time compared to 2cMEC, the explanations below are based on the 3cMEC to avoid confusion between the results obtained by different cell configurations while maintaining clear explanations under the same principles of how these bioelectrodes work. Few evolvements in the cell potentials were noticed as microbial growth on the electrodes. Firstly, the potential at the start point of 0 V was dropped from +0.40 V to -0.18 V during the enrichment process as shown in Figure B.1 (b1). Secondly, when it was developing (after 1 week), the bioanode potential remained constant at -0.20 V for a cell potential ranging from 0 to 1.0 V. This result indicates the domain of cell voltage for which the bioanode can sustain its catalytic activity. In this domain, the biocathode potential thus decreases progressively to reach about -1.0 V at a cell voltage of 1.0 V. As depicted in Figure B.1 (b1), when the applied cell voltage exceeds 1.0 V, the biocathode potential remains stable around -1.0 V whereas the bioanode potential increases to 1.2 V when the applied voltage reaches 2.5 V. When the applied voltage exceeded 2.0 V, both the bioanode and biocathode potential profiles converged with that of the respective controls. Abiotic reactions in the anode and cathode (i.e. OER and HER, respectively) might take over the biocatalytic reactions at the higher applied voltage. Standard reduction potential for water electrolysis (abiotic reactions) to oxygen and hydrogen are +1.23V ($O_2 + 4H^+ + 4e^- \rightarrow 2H_2O$) and -0.83V ($2H_2O + 2e^- \rightarrow H_2 + 2OH^-$). Therefore, abiotic reactions could happen when the potential of working electrodes was higher or lower than the standard reduction values (Lide, 2006).

Figure B.1 (b2) represents the evolution of the cell current along the times of enrichment. A current peak with the value of 0.50 A/m^2 at an applied voltage of 0.8 V started to appear after 3 weeks and increased to 1.68 A/m^2 and stable at an applied voltage of 1.2 V after 6 weeks. It revealed that applied voltages between 0.8 and 1.2 V were the maximum current that could be

produced biotically from the cell. Within the gap of these applied voltages ensured that the bioelectrodes were not overloaded under the higher current that causing the oxidation or reduction potential to shift further from its present threshold. Higher applied voltage actually increased the reaction processes in cathode when more electrons supplied from anode were able to be utilised by cathode under more negative reduction potential. However, when this happened, abiotic reactions could prevail and overtake the abiotic process. This phenomenon was seen at an applied voltage near 2.5 V where current density was increased dramatically and had a higher value than the first abiotic current peak. Meanwhile a second peak current was observed at some lines was probably due to biofilm thickness or diffusion layer that blocked the abiotic reactions which undergo water electrolysis process especially when the oxidation potential rose substantially over the standard value (the anode potential was nearly +1.3V at applied voltage of 2.5V observed from Figure B.1 (b1)).

In summary, the results show that there is an optimal range of cell voltage for which both the bioanode and biocathode were active and stable to operate. At low applied voltages (0-0.8 V), the bioanode potential remained constant at -0.2 V which is in agreement with most potent bioanodes reported in the literatures (Cheng *et al.*, 2008; LaBelle, 2009; Wang *et al.*, 2009; Wang *et al.*, 2010; Lim *et al.*, 2017). At such cell voltages, the cathode potential decreases from -0.25 to -1.0 V. an adequate and optimum applied voltage in this study is limited between 0.8 and 1.2 V considered both bioelectrodes operating conditions. On the one hand, at low applied voltages (0 - 1.0 V), cathode potential was still high even the bioanode worked effectively and potentially stay steadily at ~-0.2V as displayed by most potent bioanodes (Bond and Lovley, 2003; LaBelle, 2009; Lim *et al.*, 2017). On the other hand, the cathode potential was not suitable for reduction and at least -0.24V was required for CO_2 reduction without considering the plausible overpotentials in the system (Rabaey and Rozendal, 2010; Choi and Sang, 2016; Zhen *et al.*, 2017). Higher applied voltage especially when it over the current limit of anode could supply (> 1.2 V), the bioanode will lose its biocatalytic behaviour (Wang *et al.*, 2010; Lim *et al.*, 2017).

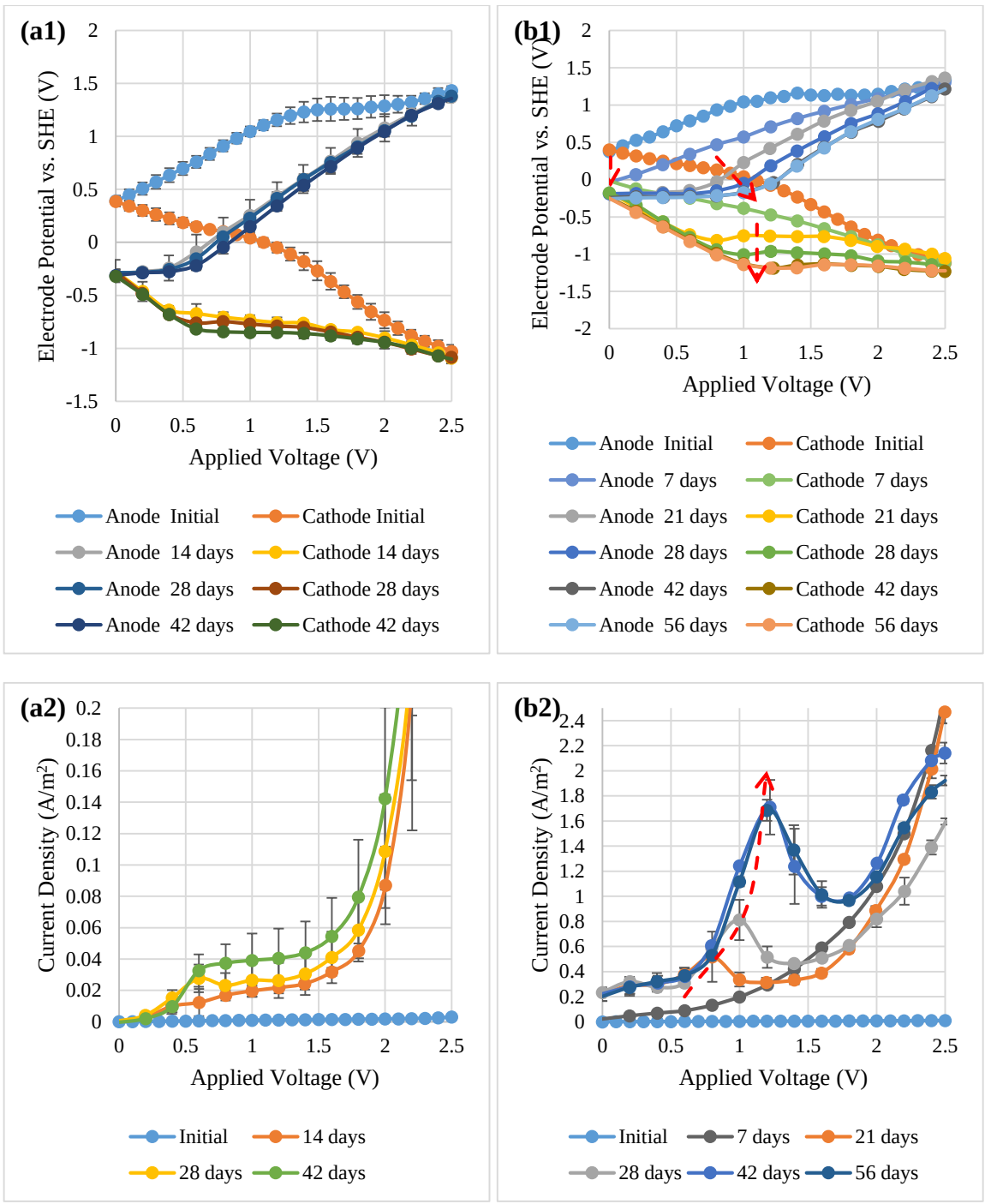

Figure B.1 The responses of (a) electrode potentials, and (b) current density to a range of applied voltage from 0 to 2.5 V. Figure (a1) and (a2) are for 2cMEC while (a1) and (a2) are for 3cMEC. Both results exhibit a similar principle on how the bioelectrodes response. The 3cMEC results consisted of better and complete results than 3cMEC. Red arrows show the evolution of bioelectrochemical properties over time.

B2. Bioelectrodes' catalytic activity and evolution over time

Figure B.2 shows the evolution of the cyclic voltammograms for bioanode and biocathode during their enrichment. The bioanode shows a significant catalytic activity between -0.30 and -0.05 V with a mid-point potential around -0.18 V as observed in both Figure B.2 (a1) and (b1). The oxidation rate grew steadily over time and became stable after 6 weeks of enrichment, which was consistent with the data reported in Figure B.1. An oxidation curve between -0.30 and -0.05 V was observed, thus demonstrating that the presence of a bioelectrochemically-active consortium generating current through substrate oxidation (Fricke *et al.*, 2008; LaBelle, 2009; Lim *et al.*, 2017). In addition, the consortium was highly dominated by electrochemically-active because there was the only oxidation curve in the measured range of -0.6 to +0.4 V. Some studies found that other non-electrochemically active microbes could growth simultaneously with electrochemically active microbes due to the high fixed potential in anode (Torres *et al.*, 2009; Lim *et al.*, 2017). Besides the potential condition, the used of the different substrate also affected the community diversity when one species favoured to the substrate outrun the others. For instance, both glucose and acetate can be the main carbon source for bioanode. The use of glucose could increase the number of fermentative bacteria and the diversify of other non-electrochemically-active bacteria like *Smithella* and *Syntrophobacter* promoting less electrochemically-active bacteria growth (Hari *et al.*, 2016; Spurr, 2016). In this case, multiple oxidation curves apart from -0.18V were observed.

On the cathode side, the development of the biofilm with time was characterised by a shift of the onset potential of the hydrogen evolution reaction (HER) towards less negative potentials. Indeed, the onset potential of HER shifted from about -1.0 V before enrichment to -0.7 V after 3 weeks. Similar results were reported previously in hydrogen-producing biocathodes (Aulenta *et al.*, 2012; Batlle-Vilanova *et al.*, 2014; Jourdin *et al.*, 2015; Lim *et al.*, 2017). In these previous studies, a small pseudo-reversible signal was observed around -0.45 V, which was attributed to the enzymes called hydrogenases performing the hydrogen oxidation and reduction activities. However, this signal was not detected in this study. In fact, the activity in this study was increased until 4 weeks and decreased afterwards as shown in Figure B.2 (a2) and (b2). In this study, cathode activity was basically depended on the anode activity as anode growth faster than cathode and depended on anode potential to bring down the cathode potential. The experiments were conducted mainly based on the cycle time of bioanode. As the cycle time did not match between anode and cathode, it means a cycle time for cathode would be few cycle time of anode, e.g.1 to 3. Most biocathode reduction processes took few days to weeks due to

the slow reaction of the biocathode building specific products like in well-known acetate production (Zaybak *et al.*, 2013; Jourdin *et al.*, 2015; Mohanakrishna *et al.*, 2015; Bajracharya *et al.*, 2017b; LaBelle and May, 2017). Another reason is species dependency in which one species growth relied on other species products. For examples the dependent of SRB and methanogens to acetogens to produce hydrogen and methane (Mand *et al.*, 2014; Kim *et al.*, 2015; van Eerten-Jansen *et al.*, 2015). When the inoculum was first injected to the cathode, glucose and glutamate originally brought together with the inoculum were still high. These organic carbons could result in a small increase of cathodic activity before it decreases back to the same level as initial cyclic voltammogram when all residues were consumed or replaced with a new medium.

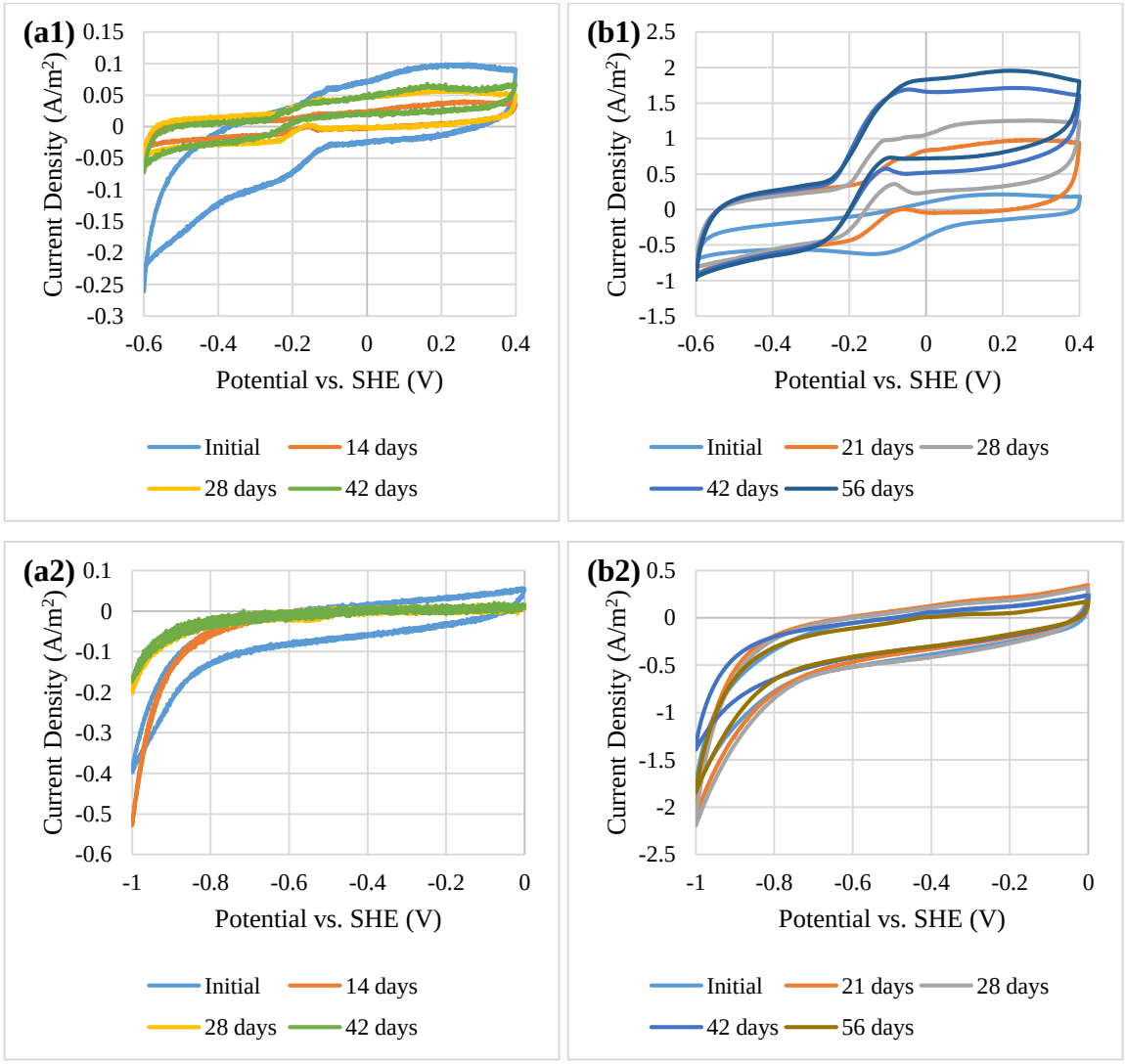

Figure B.2 Cyclic voltammograms of (a1) bioanode and (a2) biocathode in 2cMEC. The figures of (b1) bioanode and (b2) biocathode are for 3cMEC.

Figure B.3 (a1) & (a2) and (b1) & (b2) illustrate the electrochemical impedance spectrograms recorded for the entire 2cMEC and 3cMEC cell systems. Figure B.3 (a3) and (b3) presents the equivalent circuit reflecting the electrochemical properties in those systems while Table B.1 reports the best-fitted coefficient values from the equivalent circuit. Figure B.3 (a1) and (b1) suggests the formation of biofilms on the electrodes' surface over the weeks. Indeed, as can be seen from the high frequencies, the diameter of the semi-circle is increasing over the time, which implies an increase of the charge transfer resistance (Dominguez-Benetton *et al.*, 2012; Sekar and Ramasamy, 2013). In addition, the slope of the electrochemical tails that can be associated with diffusion properties decreased along time which indicated mass transport limitation from the bulk solution to microorganisms when biofilm layer growth thicker over time. The EIS semicircle not only suggests the growth of a biofilm layer on the electrode's surface but also records the improvement of the contact between the bulk solution and the electrode. As a result, the total solution conductivity reported as the first crossed point at x-axis decreased inversely proportional to the charge transfer resistance as shown in the spectrograms (Aulenta *et al.*, 2012). Lower frequencies between 100 000 and 0.01 Hz instead of 100 000 and 10 Hz were used to obtain the diffusion properties after the enrichments (Figure B.3 (a2) and (b2)). In addition, overall solution resistances also raised from around 36 - 37 Ω (0-2 weeks) to 43 - 53 Ω (3-8 weeks) which can be explained by the biofilms growth on the electrode's surface and suspended microbial cells in the electrolyte modifying the electrodes' and electrolytes' electrochemical properties. The equivalent circuit of the spectrograms was determined as $[R_1(Q[R_2W])T]$ modified after Dominguez-Benetton *et al.* (2012). Firstly, internal resistance R_{int} was determined as the sum $R_1 + R_2$ where R_1 is the total solution resistance measured between both electrodes and R_2 being the charge transfer resistance compiled of whole cell connection between electrodes included biofilm. In this case, the internal resistance ($R_1 + R_2$) slightly increased over time from about 5 and 40 at the beginning to around 6 and 78 Ω as reported in Table B.1. These results are in contradiction with previous studies in which the internal resistance decreased with the growth of the electrochemically-active biofilms (He and Mansfeld, 2009; Borole *et al.*, 2010; Aulenta *et al.*, 2012). The possible explanation to this disagreement was the poor contact between the electrode and external connection e.g.titanium wire or current collector. The weak and poor connection would not only increase the internal resistance but also decrease the current density. However, the poor contact improved when a layer of electrochemically-active biofilm growth on the electrode connecting the electrode surface to external connection resulting in low internal resistance (see section 4.3.1). Meanwhile, CPE is the constant phase element representing the characteristic of the electrode

material due to imperfect dielectric properties (Autolab, 2011a). Finally, W and T are the semi- and finite-diffusion elements representing the mass transfer behaviours occurring at the electrode surfaces. In this study, carbon cloth was used which is a porous material. It can be assumed that the interaction of the solution with the surface contributed to the T element (Macdonald, 2006; Borole *et al.*, 2010). In the meantime, the growth and thickness of biofilm mainly contributed to the W element (Dominguez-Benetton *et al.*, 2012; Sekar and Ramasamy, 2013). Both W and T impedances were nearly zero at the beginning of the experiment and increased as the biofilms developed, hence causing mass transfer limitations. However, the increment of the impedances values did not create significant drawback to the whole BES performance as reported by Sekar and Ramasamy (2013). Mass transport of reactants from the bulk solution to the biofilm and vice versa for the products remained relatively stable as observed from the time constant under the T element, which represents the time needed for the reactants to diffuse from one side of the biofilm layer to another layer and that is equal to $\delta/\sqrt{D}$ where δ is the thickness of the layer and D is the diffusion coefficient.

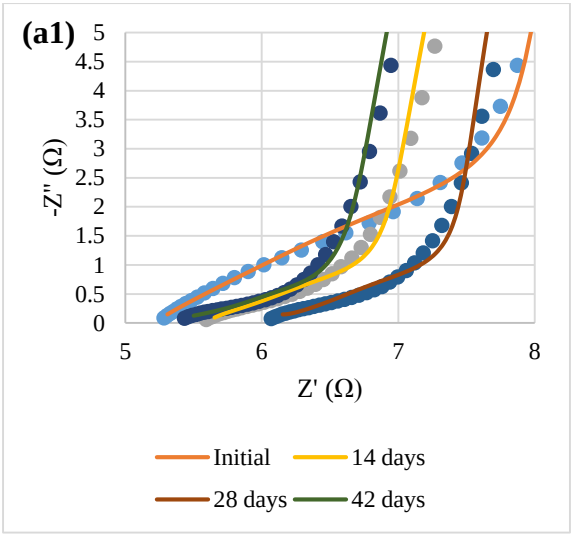
(a1)
-Z'' (Ω)
Z' (Ω)
Initial
14 days
28 days
42 days

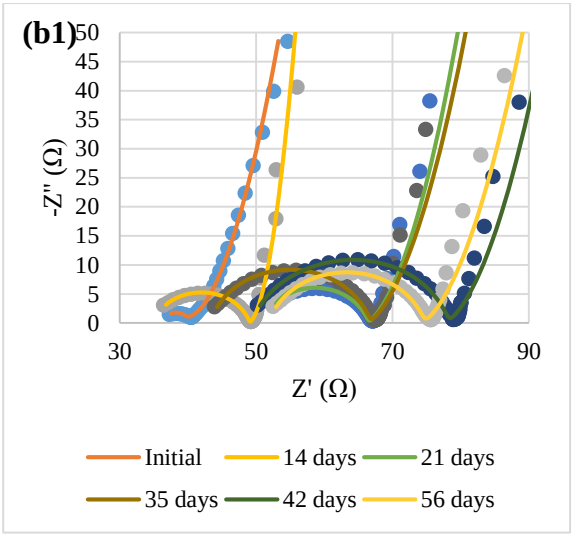
(b1)
-Z'' (Ω)
Z' (Ω)
Initial
14 days
21 days
35 days
42 days
56 days

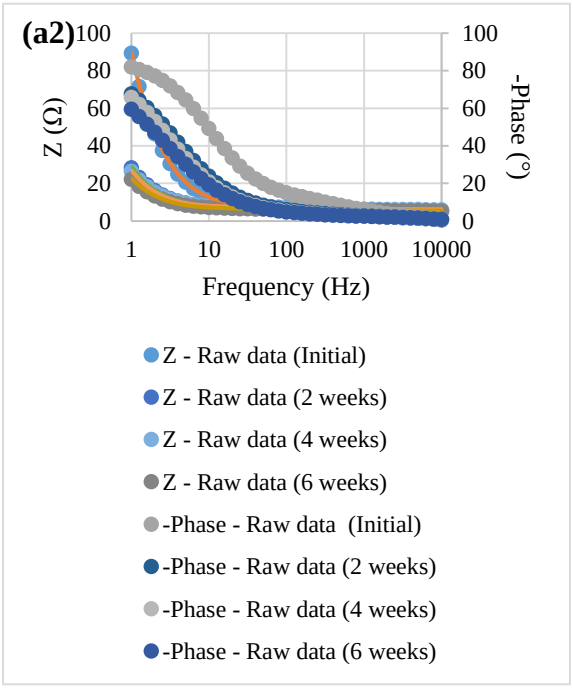
(a2)
Z (Ω)
-Phase (°)
Frequency (Hz)
Z - Raw data (Initial)
Z - Raw data (2 weeks)
Z - Raw data (4 weeks)
Z - Raw data (6 weeks)
-Phase - Raw data (Initial)
-Phase - Raw data (2 weeks)
-Phase - Raw data (4 weeks)
-Phase - Raw data (6 weeks)

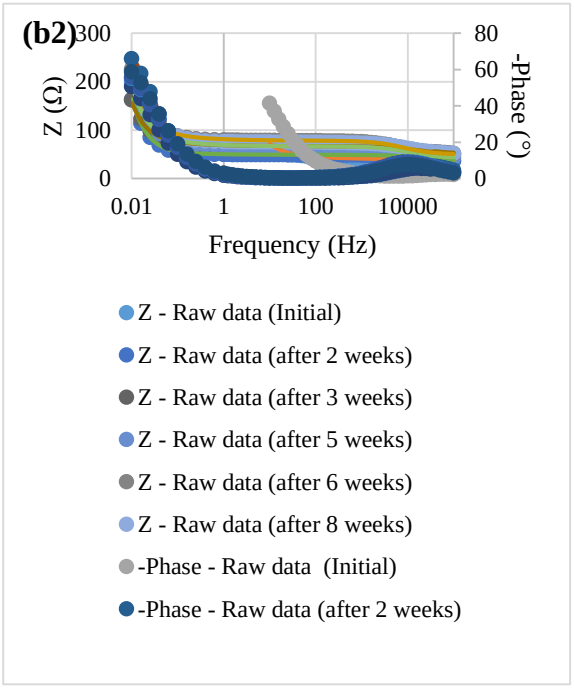
(b2)
Z (Ω)
-Phase (°)
Frequency (Hz)
Z - Raw data (Initial)
Z - Raw data (after 2 weeks)
Z - Raw data (after 3 weeks)
Z - Raw data (after 5 weeks)
Z - Raw data (after 6 weeks)
Z - Raw data (after 8 weeks)
-Phase - Raw data (Initial)
-Phase - Raw data (after 2 weeks)

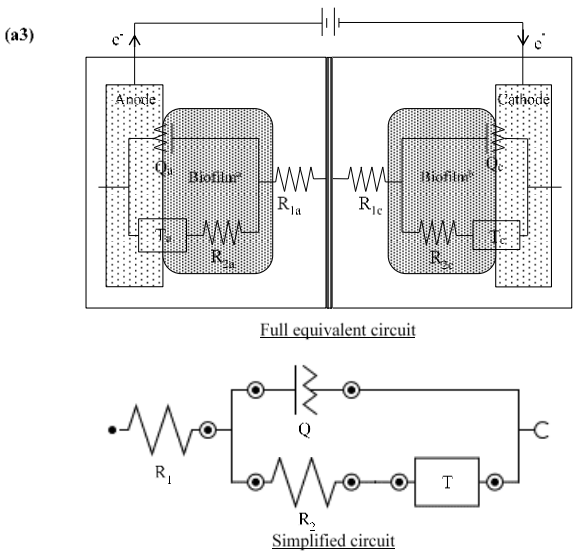
(a3)
Anode
Cathode
Biofilm
Full equivalent circuit
Simplified circuit

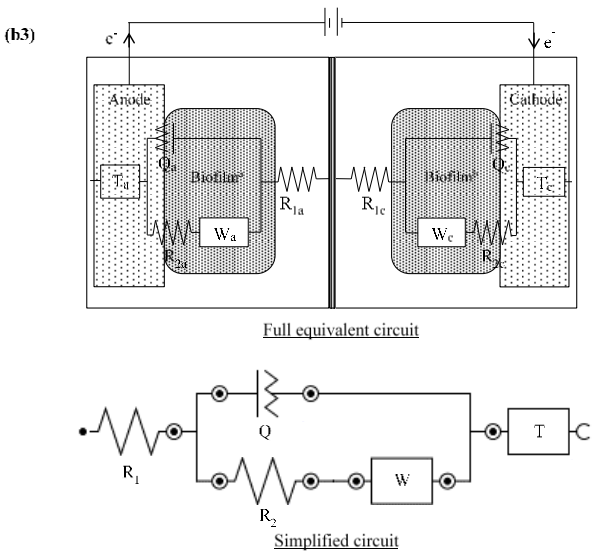
(b3)
Anode
Cathode
Biofilm
Full equivalent circuit
Simplified circuit

Figure B.3 Electrochemical impedance spectrograms for the cells enriched at different stage (a) Nyquist plot, (b) Bode modulus and phase plots and (c) an overview of the full equivalent circuit with its simplified version: $[R_1(Q[R_2W])T]$ where R_1 = solution resistance, R_2 = charge transfer resistance, CPE = constant phase element, W = Warburg diffusion element, and T = finite diffusion element.

Table B.1 Coefficient values determined from the equivalent circuit in Figure B.3 (a3) and (b3)

Day	Solution resistance		Constant phase				Charge transfer resistance		Finite diffusion				Internal Resistance	
			Impedance		Element constant				Impedance		Time constant			
	R1		Q				R2		T				(R1 + R2)	
	Ω	±	Ω^{-1}	±	N	±	Ω	±	Ω^{-1}	±	$s^{1/2}$	±	Ω	±
0	5.435	0.394	0.001	0.000	0.785	0.033	0.151	0.205	0.014	0.001	0.109	0.013	5.586	0.599
14	5.689	0.543	0.005	0.002	0.672	0.033	0.503	0.032	0.046	0.008	0.171	0.043	6.192	0.575
21	5.246	0.503	0.005	0.002	0.673	0.035	0.426	0.036	0.051	0.008	0.166	0.038	5.672	0.540
28	6.233	0.006	0.005	0.002	0.655	0.030	0.499	0.025	0.049	0.009	0.182	0.032	6.732	0.031
35	5.604	0.163	0.010	0.001	0.490	0.089	0.921	0.406	0.069	0.003	0.246	0.011	6.526	0.568
42	5.343	0.122	0.012	0.005	0.529	0.097	0.682	0.158	0.072	0.016	0.241	0.048	6.025	0.280

(a)

Day	Solution resistance		Constant phase				Charge transfer resistance		Semi (Warburg)-diffusion		Finite diffusion				Internal Resistance	
			Impedance		Element constant				Impedance		Impedance		Time constant			
	R1		Q				R2		W		T				(R1 + R2)	
	Ω	±	Ω^{-1}	±	N	±	Ω	±	Ω^{-1}	±	Ω^{-1}	±	$s^{1/2}$	±	Ω	±
0	35.54	1.62	4.09E-06	3.89E-06	0.914	0.187	4.13	0.92	0.007	0.001	0.02	0.01	0.028	0.012	39.67	1.62
14	34.92	1.16	3.62E-06	4.63E-07	0.833	0.002	14.11	1.54	0.238	0.029	2.45	0.04	0.047	0.004	49.04	1.54
21	50.89	0.44	4.00E-06	2.68E-08	0.852	0.025	15.55	4.90	0.128	0.012	5.55	0.01	0.027	0.000	66.44	4.90
35	43.35	1.56	3.43E-06	3.76E-07	0.862	0.007	23.31	9.31	0.103	0.011	4.49	0.48	0.026	0.003	66.65	9.31
42	49.51	0.28	3.34E-06	7.68E-07	0.860	0.002	28.58	18.49	0.095	0.012	3.81	0.72	0.027	0.006	78.08	18.49
56	51.84	0.37	4.44E-06	7.34E-07	0.840	0.004	22.76	6.94	0.088	0.013	3.13	0.26	0.028	0.003	74.60	6.94

(b)

B3. Chronoamperometry test at middle stage (100 days) (3cMEC)

Biocathode in 3cMEC was further investigated to determine the suitable applied voltage for hydrogen production after 100 days of enrichment and operation. Figure B.4 presents the results of the potentials, current and CO_2 diffusion obtained from chronoamperometry test in 3cMEC. Starting from 0.3 V, the applied voltage was increased after the anode cycle was nearly the end by observing the current density dropped to less than 10 % from the peak (Figure B.4 (b)). Meanwhile, the profile of cathode potential was following the anode potentials and based on anode cycle (Figure B.4 (a)). It was found that the peak current density that could be achieved was 0.8 A/m^2 under the applied voltage of 0.9 V. Less than 0.9 V, a large part of electrons was not be utilised in the system because of the sluggish cathode. The cathode reduction process was very slow due to the higher reduction potential. Instead, the electrons were accumulated in the anode, therefore, a plateau current density could be observed from the current profile in Figure B.4 (b) for applied voltages of 0.3 and 0.5 V. A current dropped after the plateau is because of substrate depletion and by-products built up in the anolyte. The cathode began to utilise the electrons from bioanode when more than 0.5 V applied voltage was fixed, peaked at 0.9 V and dropped dramatically when the applied voltage was more than 1.0 V. In Figure B.4 (c), the mass transfer and diffusion coefficients were affected by applied voltage. The trend of the coefficients began to diverge from the control starting 0.5 V and increased until they reached a peak at 0.9 V and decreased back to meet control value. It shows a similar trend as current density. Nevertheless, no hydrogen was detected in this stage even at optimal applied voltage condition. Slow reactions happened in the cathode as indicated in the increase of CO_2 diffusion with no hydrogen production. A different cycle between anode and cathode were first shown in this test. Electricity-generating bioanode was normally dominated by chemoorganotrophic bacteria which required organic matter to grow and produced current while anaerobic electron-consuming biocathode are naturally dominated by autotrophic bacteria to synthesise certain compound from carbon dioxide (Kim *et al.*, 2004; Rabaey and Rozendal, 2010; Choi and Sang, 2016). In addition, the biocathode required a stable and long term energy supply to support its grow and perform a reduction process to synthesise fatty acids and hydrogen. Normally the biocathode could take from weeks to months to accumulate certain products (e.g. acetate, butyrate) up to detected amount (Zaybak *et al.*, 2013; Jourdin *et al.*, 2015). The results were important to serve as a reference to improve overall MEC performance in the latter experiments (See Chapter 7).

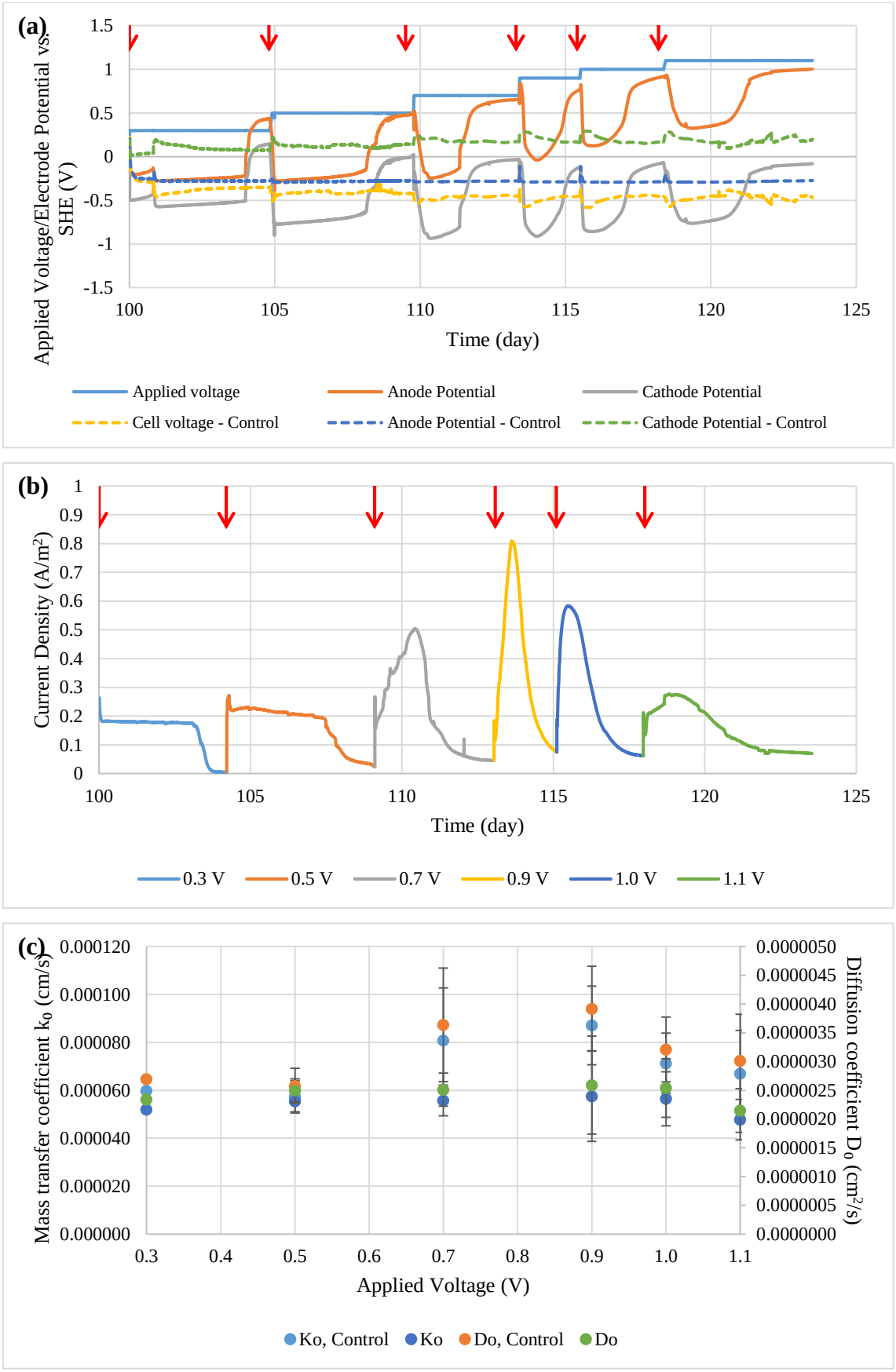

Figure B.4 (a) Potential profile, (b) current density, and (c) the changes of CO_2 mass transfer and diffusion coefficients of the 3cMEC system during the chronoamperometry test

after 100 days of enrichment where bioanode was fully developed. Note: Red arrows represent replacements of the new medium after the current was decreased near a plateau. The timeline on x-axis was set to zero (where the chronoamperometry test started) for comparative purpose.

During the chronoamperometry test, electrolyte pH and conductivity values were measured to study the reason of no hydrogen produced. Figure B.5 exhibits the results of both pH and conductivity value ranged from 0.3 to 1.1 V applied voltage. There are no significant changes in the values except the pH of anolyte. The pH value was first dropped dramatically from 0.3 to 0.7 V and then the second time started from 1.0 V onward. The drop of pH in the anolyte might be the reason of low performance and no hydrogen production. However, there was no direct connection to link the effect of sluggish bioanode to the hydrogen production in the cathode. To further explore the connection, the electrolyte samples were subjected to total carbon and fatty acid analysis. Figure B.6 shows the total carbon contain in both electrolyte and the percentage of fatty acid in the catholyte. Acetate was the only organic carbon added in the anolyte as a carbon source for bioanode. At lower applied voltage (0.3-0.5 V), there was no organic carbon concentration was detected in the effluent at the end of anode cycle (Figure B.6 (a)). Meanwhile, significant organic/inorganic carbon was detected at 0.7 V and above. Even though the current recorded between the region of 0.7 and 1.0 V demonstrating the highest in the study, the consumption of the organic carbon was not correlated to the current density. Higher applied voltage not necessary to drive the oxidation and reduction simultaneously in a fuel cell system. In this case, both anode and cathode were catalysed by microorganisms and it was important to ensure the full functions of the biocatalysts. Besides, it seems that the bioanode was not able to maintain its potential at a higher applied voltage (> 0.7 V) and therefore could not further draw the cathode potential down to certain reduction potential (< 0.9 V) (Figure B.4 (a)). It is well known that standard reduction potential for hydrogen evolution at pH 7.0 is -0.41 V. However, most studies reported that hydrogen-producing biocathode required at least 0.7 V to produce hydrogen (Rozendal *et al.*, 2008; Jeremiasse *et al.*, 2012; Marshall *et al.*, 2012). Lower reduction potentials were also reported and used due to the catholyte conditions (e.g. pH and conductivity) and overpotentials especially when no significant hydrogen was detected (Wagner *et al.*, 2009; Aulenta *et al.*, 2012; Batlle-Vilanova *et al.*, 2014). In the catholyte results (Figure B.6 (b) and (c)), a higher amount of inorganic carbon was detected as a result of CO_2 accumulation in the solution diffused from the nearby gas chamber. It demonstrated that simple attachment of the gas chamber next to cathode could be one of the easiest alternatives to

dissolute CO_2 and increase the accumulation of CO_2 in the catholyte. Apart from the inorganic carbon, a small amount of organic carbon revealed that the cathode was performing specific reduction reactions to produce organic carbon than evolving hydrogen during the test. The biocathode required more time to accumulate the compounds or increase their concentrations (Zaybak *et al.*, 2013; Jourdin *et al.*, 2015).

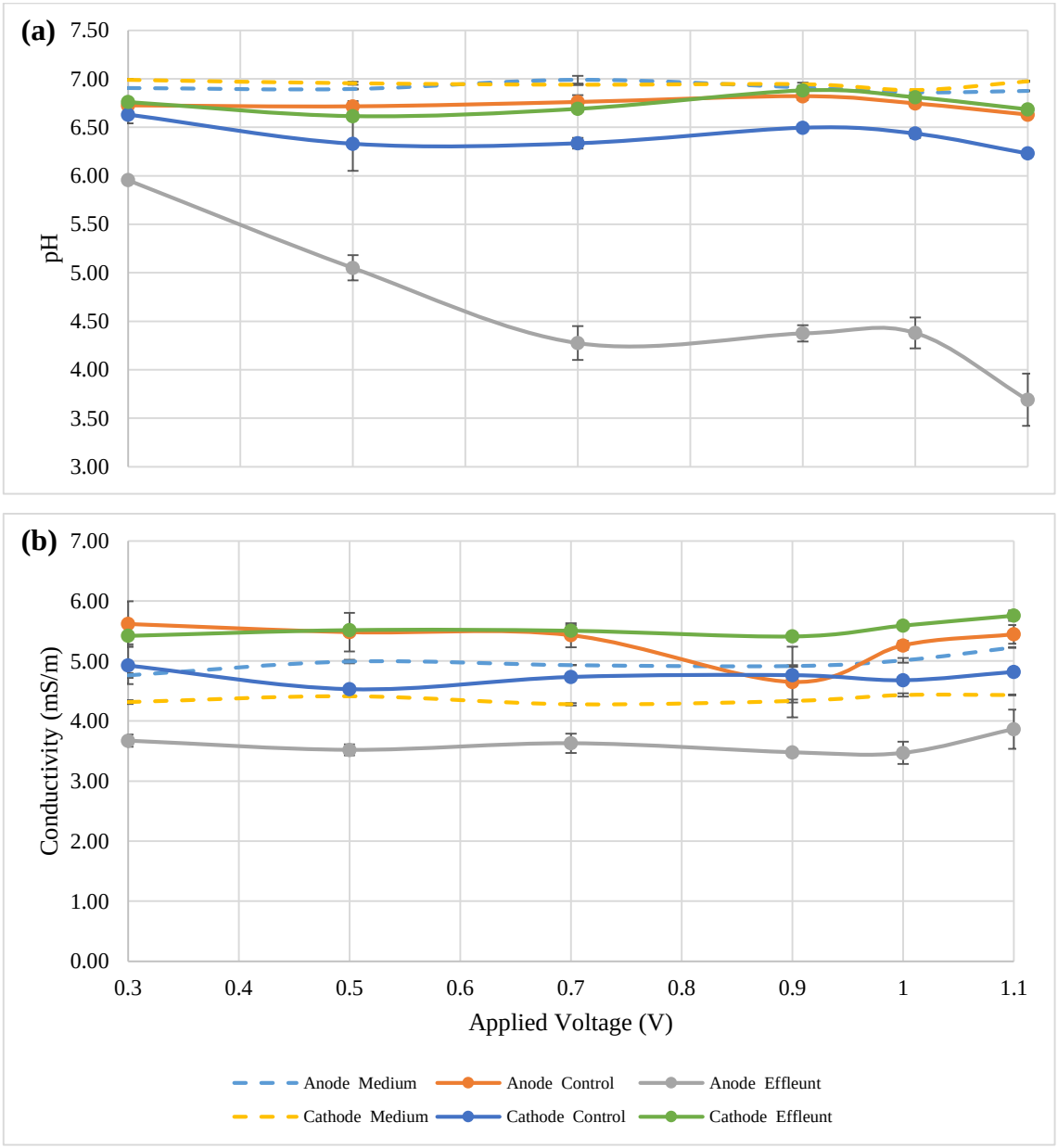

Figure B.5 The profiles of (a) pH and (b) conductivity in anode medium and catholyte relatively to various applied voltages during the chronoamperometry test after 100 days of enrichment. Note: All lines marked with medium and control are not subjected to chronoamperometry test. The samples were collected at the same time with effluents at specific applied voltages during the test. They are shown for comparison.

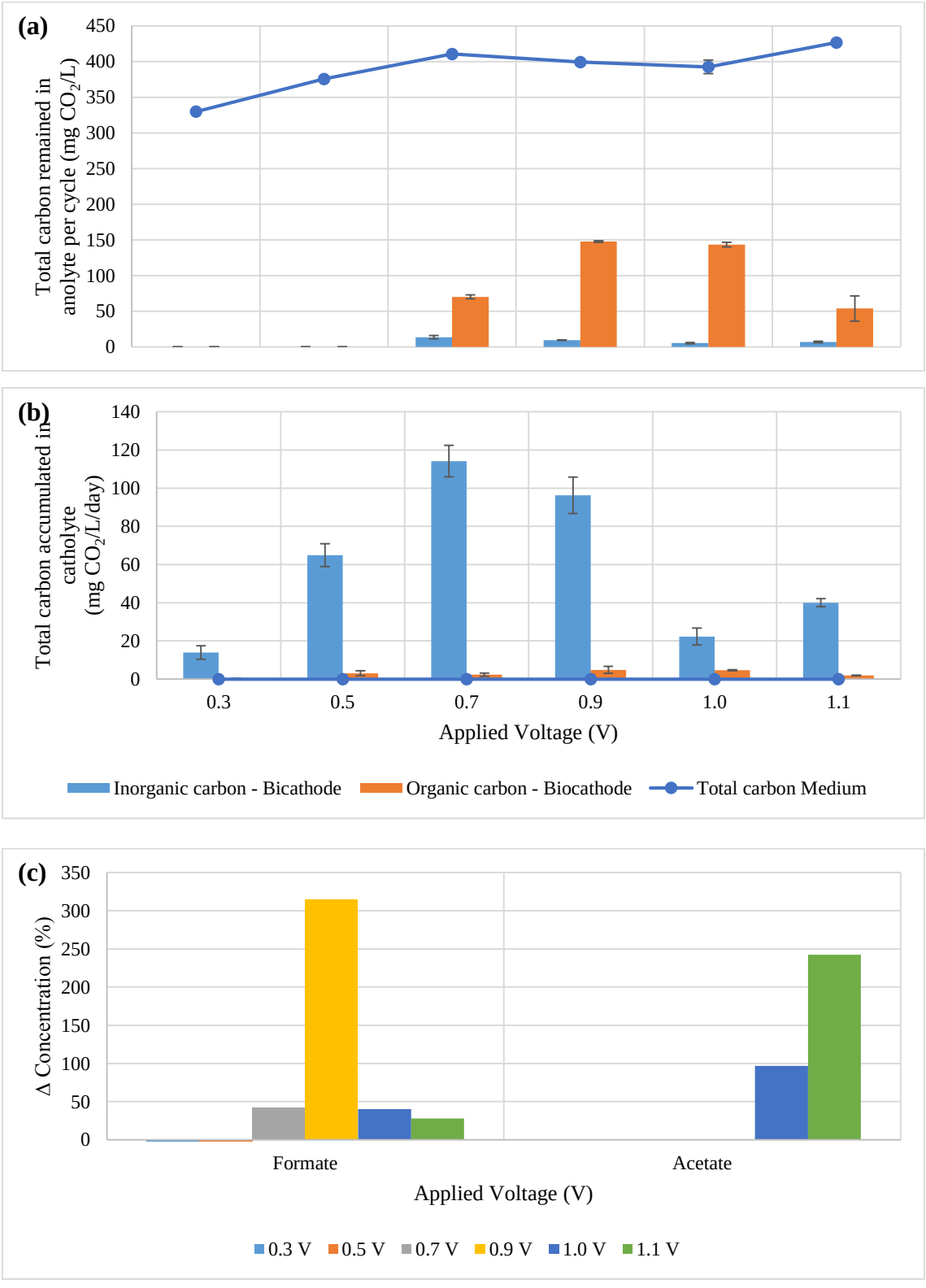

Figure B.6 Total organic/inorganic carbon (a) remained in anolyte, (b) accumulated in catholyte, and (c) percentage of difference in organic carbons in catholyte by compared to control.

At the end of chronoamperometry (after 1.1 V), bioanode and biocathode were instantly subjected to cyclic voltammetry analysis. Figure B.7 shows the records of the CVs after the chronoamperometry test with the bare electrode without microorganisms before the enrichment process. The bioanode was still active at the end and showed oxidation activity. Meanwhile, the cathode reduction activity at -1.0 V was almost similar and hard to notice any differences. However, a small reduction peak was observed at -0.5 V and could be relative to the production of organic carbons (Marshall *et al.*, 2012; Patil *et al.*, 2015; Bajracharya *et al.*, 2017b). In theory, standard hydrogen potential is -0.41 V and higher compared to the standard reduction potential of the short-chain fatty acids such as acetic (-0.28 V). The potential required could go even lower than the standard potentials when the pH of the electrolyte is above neutral. This might be the reason why there was no hydrogen produced because the biocathode potential as observed in Figure B.4 (a) was not lower enough to perform proton reduction activity (minimum potential that it could achieve was -0.9V). After this initial study, some technical issues have been answered. This included the need for longer enrichment process for biocathode while maintaining its potential as low as possible. This can be improved by optimising and maintaining bioanode performance under multiple cycle condition to support the biocathode.

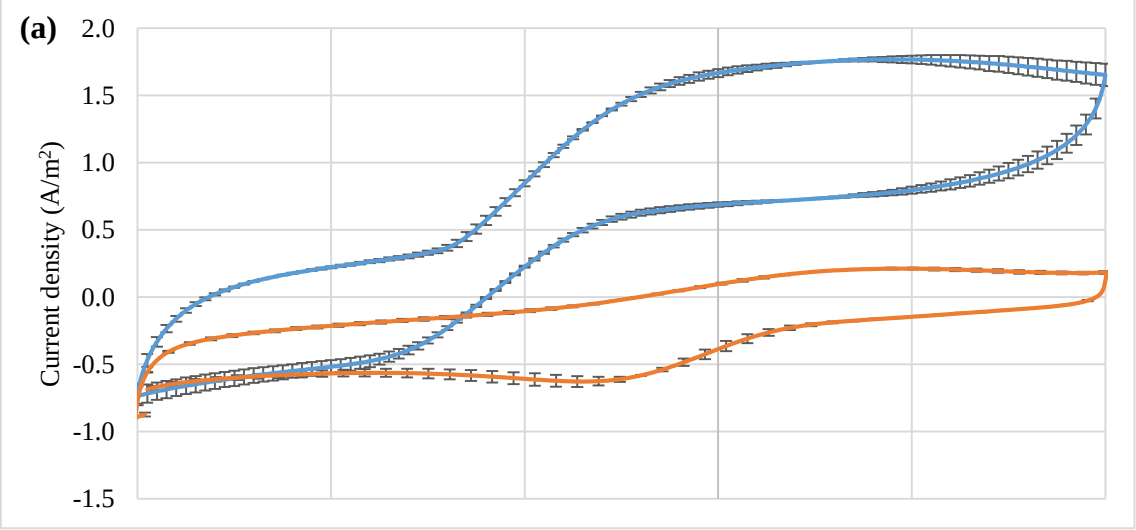

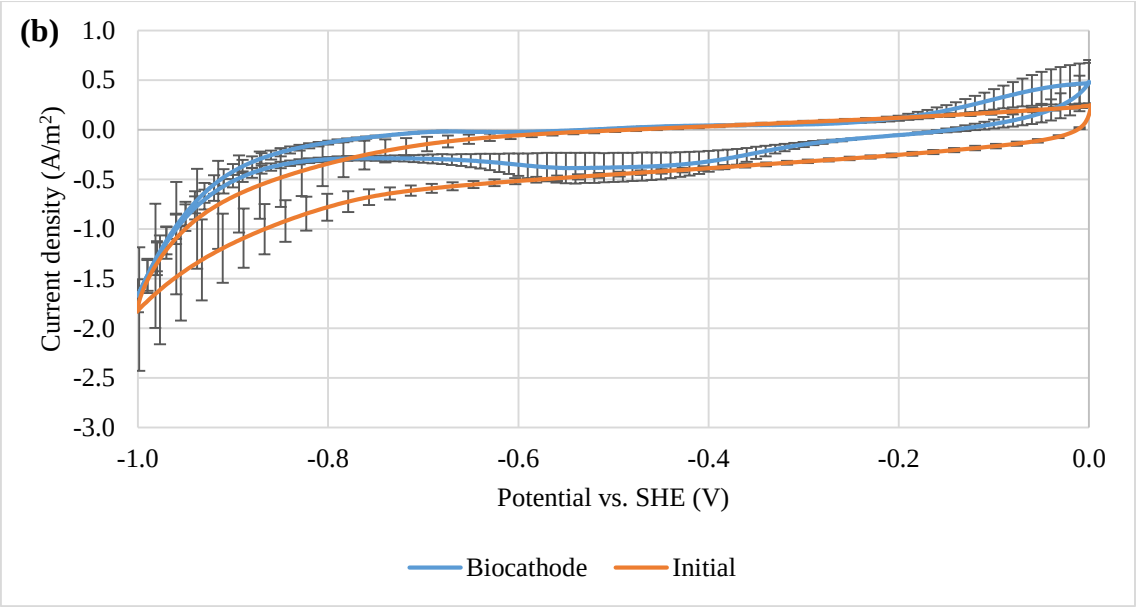

Figure B.7 Cyclic voltammograms of (a) anodic and (b) cathodic catalytic activities after the chronoamperometry test.

References

Abbas, S.Z., Rafatullah, M., Ismail, N. and Syakir, M.I. (2017) 'A review on sediment microbial fuel cells as a new source of sustainable energy and heavy metal remediation: mechanisms and future prospective', *International Journal of Energy Research*, 41(9), pp. 1242-1264.

Aelterman, P., Freguia, S., Keller, J., Verstraete, W. and Rabaey, K. (2008) 'The anode potential regulates bacterial activity in microbial fuel cells', *Appl Microbiol Biotechnol*, 78(3), pp. 409-418.

Ahn, Y. and Logan, B.E. (2013) 'Saline catholytes as alternatives to phosphate buffers in microbial fuel cells', *Bioresource Technology*, 132, pp. 436-439.

An, J. and Lee, H.S. (2014) 'Occurrence and Implications of Voltage Reversal in Stacked Microbial Fuel Cells', *ChemSusChem*, 7(6), pp. 1689-1695.

Anonymous (2007) *Energy and Sewage*.Parliamentary Office of Science and Technology.

Atlas, R.M. (2010) *Handbook of Microbiological Media, Fourth Edition*. CRC Press.

Aulenta, F., Catapano, L., Snip, L., Villano, M. and Majone, M. (2012) 'Linking Bacterial Metabolism to Graphite Cathodes: Electrochemical Insights into the H2-Producing Capability of Desulfovibrio sp', *ChemSusChem*, 5(6), pp. 1080-1085.

Aulenta, F., Reale, P., Canosa, A., Rossetti, S., Panero, S. and Majone, M. (2010) 'Characterization of an electro-active biocathode capable of dechlorinating trichloroethene and cis-dichloroethene to ethene', *Biosens Bioelectron*, 25(7), pp. 1796-1802.

Autolab, M. (2011a) *Application notes: Electrochemical Impedance Spectroscopy (EIS): Part 4 – Equivalent Circuit Models (EIS04)*. Available at: http://www.ecochemie.nl/download/Applicationnotes/Autolab_Application_Note_EIS04.pdf (Accessed: 13 November 2017).

Autolab, M. (2011b) *Electrochemical Impedance Spectroscopy (EIS) Part 2 – Experimental Setup*. Available at: https://www.metrohm.com/en-in/applications/%7B3557CFB6-539A-4CB7-BD78-EF117F1200EA%7D (Accessed: 13 November 2017).

Bagyinka, C. (2014) 'How does the ([NiFe]) hydrogenase enzyme work?', *International Journal of Hydrogen Energy*, 39(32), pp. 18521-18532.

Bajracharya, S., ElMekawy, A., Srikanth, S. and Pant, D. (2016a) 'Cathodes for microbial fuel cells ', in Scott, K.Y., Eileen Hao (ed.) *Microbial Electrochemical and Fuel Cells*. Boston: Woodhead Publishing, pp. 179-213.

Bajracharya, S., Sharma, M., Mohanakrishna, G., Dominguez Benneton, X., Strik, D.P.B.T.B., Sarma, P.M. and Pant, D. (2016b) 'An overview on emerging bioelectrochemical systems (BESs): Technology for sustainable electricity, waste remediation, resource recovery, chemical production and beyond', *Renewable Energy*, 98, pp. 153-170.

Bajracharya, S., Srikanth, S., Mohanakrishna, G., Zacharia, R., Strik, D.P. and Pant, D. (2017a) 'Biotransformation of carbon dioxide in bioelectrochemical systems: State of the art and future prospects', *Journal of Power Sources*, 356, pp. 256-273.

Bajracharya, S., Yuliasni, R., Vanbroekhoven, K., Buisman, C.J.N., Strik, D.P.B.T.B. and Pant, D. (2017b) 'Long-term operation of microbial electrosynthesis cell reducing CO2 to multi-carbon chemicals with a mixed culture avoiding methanogenesis', *Bioelectrochemistry*, 113, pp. 26-34.

Bar-Even, A. (2013) 'Does acetogenesis really require especially low reduction potential?', *Biochimica et Biophysica Acta (BBA) - Bioenergetics*, 1827(3), pp. 395-400.

Batlle-Vilanova, P., Puig, S., Gonzalez-Olmos, R., Vilajeliu-Pons, A., Bañeras, L., Balaguer, M.D. and Colprim, J. (2014) 'Assessment of biotic and abiotic graphite cathodes for hydrogen production in microbial electrolysis cells', *International Journal of Hydrogen Energy*, 39(3), pp. 1297-1305.

Bergel, A., Féron, D. and Mollica, A. (2005) 'Catalysis of oxygen reduction in PEM fuel cell by seawater biofilm', *Electrochemistry Communications*, 7(9), pp. 900-904.

Blanchet, E., Duquenne, F., Rafrafi, Y., Etcheverry, L., Erable, B. and Bergel, A. (2015) 'Importance of the hydrogen route in up-scaling electrosynthesis for microbial CO2 reduction', *Energy & Environmental Science*, 8(12), pp. 3731-3744.

Bond, D.R. and Lovley, D.R. (2003) 'Electricity production by Geobacter sulfurreducens attached to electrodes', *Appl Environ Microbiol*, 69(3), pp. 1548-1555.

Borole, A.P., Aaron, D., Hamilton, C.Y. and Tsouris, C. (2010) 'Understanding Long-Term Changes in Microbial Fuel Cell Performance Using Electrochemical Impedance Spectroscopy', *Environmental Science & Technology*, 44(7), pp. 2740-2745.

Buckel, W. and Thauer, R.K. (2013) 'Energy conservation via electron bifurcating ferredoxin reduction and proton/Na+ translocating ferredoxin oxidation', *Biochimica et Biophysica Acta (BBA) - Bioenergetics*, 1827(2), pp. 94-113.

Burkitt, R., Whiffen, T.R. and Yu, E.H. (2016) 'Iron phthalocyanine and MnOx composite catalysts for microbial fuel cell applications', *Applied Catalysis B: Environmental*, 181, pp. 279-288.

Busalmen, J.P., Esteve-Nuñez, A. and Feliu, J.M. (2008) 'Whole Cell Electrochemistry of Electricity-Producing Microorganisms Evidence an Adaptation for Optimal Exocellular Electron Transport', *Environmental Science & Technology*, 42(7), pp. 2445-2450.

Butler, C.S., Clauwaert, P., Green, S.J., Verstraete, W. and Nerenberg, R. (2010) 'Bioelectrochemical perchlorate reduction in a microbial fuel cell', *Environ Sci Technol*, 44(12), pp. 4685-4691.

Caccavo, F., Lonergan, D.J., Lovley, D.R., Davis, M., Stolz, J.F. and McInerney, M.J. (1994) 'Geobacter sulfurreducens sp. nov., a hydrogen- and acetate-oxidizing dissimilatory metal-reducing microorganism', *Applied and Environmental Microbiology*, 60(10), pp. 3752-3759.

Cai, J., Zheng, P., Qaisar, M. and Xing, Y. (2014) 'Effect of operating modes on simultaneous anaerobic sulfide and nitrate removal in microbial fuel cell', *J Ind Microbiol Biotechnol*, 41(5), pp. 795-802.

Call, D. and Logan, B.E. (2008) 'Hydrogen Production in a Single Chamber Microbial Electrolysis Cell Lacking a Membrane', *Environmental Science & Technology*, 42(9), pp. 3401-3406.

Call, D.F. and Logan, B.E. (2011) 'A method for high throughput bioelectrochemical research based on small scale microbial electrolysis cells', *Biosensors and Bioelectronics*, 26(11), pp. 4526-4531.

Carmalin Sophia, A., Bhalambaal, V.M., Lima, E.C. and Thirunavoukkarasu, M. (2016) 'Microbial desalination cell technology: Contribution to sustainable waste water treatment process, current status and future applications', *Journal of Environmental Chemical Engineering*, 4(3), pp. 3468-3478.

Carmona-Martínez, A.A., Harnisch, F., Kuhlicke, U., Neu, T.R. and Schröder, U. (2013) 'Electron transfer and biofilm formation of Shewanella putrefaciens as function of anode potential', *Bioelectrochemistry*, 93, pp. 23-29.

Cerrillo, M., Viñas, M. and Bonmatí, A. (2017) 'Microbial fuel cells for polishing effluents of anaerobic digesters under inhibition, due to organic and nitrogen overloads', *Journal of Chemical Technology & Biotechnology*, 92(12), pp. 2912-2920.

Chen, G.W., Choi, S.J., Lee, T.H., Lee, G.Y., Cha, J.H. and Kim, C.W. (2008) 'Application of biocathode in microbial fuel cells: cell performance and microbial community', *Appl Microbiol Biotechnol*, 79(3), pp. 379-388.

Chen, J., Tannahill, A.L. and Shuler, M.L. (1985) 'Design of a system for the control of low dissolved oxygen concentrations: critical oxygen concentrations for Azotobacter vinelandii and Escherichia coli', *Biotechnol Bioeng*, 27(2), pp. 151-155.

Chen, Z., Huang, Y.-c., Liang, J.-h., Zhao, F. and Zhu, Y.-g. (2012) 'A novel sediment microbial fuel cell with a biocathode in the rice rhizosphere', *Bioresource Technology*, 108, pp. 55-59.

Chen, Z., Zhu, B.-K., Jia, W.-F., Liang, J.-H. and Sun, G.-X. (2015) 'Can electrokinetic removal of metals from contaminated paddy soils be powered by microbial fuel cells?', *Environmental Technology & Innovation*, 3, pp. 63-67.

Cheng, K.Y., Ginige, M.P. and Kaksonen, A.H. (2012a) 'Ano-cathodophilic biofilm catalyzes both anodic carbon oxidation and cathodic denitrification', *Environ Sci Technol*, 46(18), pp. 10372-10378.

Cheng, K.Y., Ho, G. and Cord-Ruwisch, R. (2008) 'Affinity of Microbial Fuel Cell Biofilm for the Anodic Potential', *Environmental Science & Technology*, 42(10), pp. 3828-3834.

Cheng, K.Y., Ho, G. and Cord-Ruwisch, R. (2012b) 'Energy-efficient treatment of organic wastewater streams using a rotatable bioelectrochemical contactor (RBEC)', *Bioresour Technol*, 126(0), pp. 431-436.

Cheng, S., Liu, H. and Logan, B.E. (2006) 'Increased performance of single-chamber microbial fuel cells using an improved cathode structure', *Electrochemistry Communications*, 8(3), pp. 489-494.

Cheng, S. and Logan, B.E. (2011) 'Increasing power generation for scaling up single-chamber air cathode microbial fuel cells', *Bioresource Technology*, 102(6), pp. 4468-4473.

Choi, O. and Sang, B.-I. (2016) 'Extracellular electron transfer from cathode to microbes: application for biofuel production', *Biotechnology for Biofuels*, 9(1), pp. 11-25.

Coma, M., Puig, S., Pous, N., Balaguer, M.D. and Colprim, J. (2013) 'Biocatalysed sulphate removal in a BES cathode', *Bioresource Technology*, 130, pp. 218-223.

Croese, E., Jeremiasse, A.W., Marshall, I.P.G., Spormann, A.M., Euverink, G.-J.W., Geelhoed, J.S., Stams, A.J.M. and Plugge, C.M. (2014) 'Influence of setup and carbon source on the bacterial community of biocathodes in microbial electrolysis cells', *Enzyme and Microbial Technology*, 61–62, pp. 67-75.

Croese, E., Pereira, M.A., Euverink, G.J., Stams, A.J. and Geelhoed, J.S. (2011) 'Analysis of the microbial community of the biocathode of a hydrogen-producing microbial electrolysis cell', *Appl Microbiol Biotechnol*, 92(5), pp. 1083-1093.

Croft, S. (1987) *Kaye and Laby – Tables of Physical and Chemical Constants (15th edn)*.

Cusick, R.D., Bryan, B., Parker, D.S., Merrill, M.D., Mehanna, M., Kiely, P.D., Liu, G. and Logan, B.E. (2011) 'Performance of a pilot-scale continuous flow microbial electrolysis cell fed winery wastewater', *Applied Microbiology and Biotechnology*, 89(6), pp. 2053-2063.

Daud, S.M., Daud, W.R.W., Kim, B.H., Somalu, M.R., Bakar, M.H.A., Muchtar, A., Jahim, J.M., Lim, S.S. and Chang, I.S. (2018) 'Comparison of performance and ionic concentration gradient of two-chamber microbial fuel cell using ceramic membrane (CM) and cation exchange membrane (CEM) as separators', *Electrochimica Acta*, 259, pp. 365-376.

Desloover, J., Puig, S., Virdis, B., Clauwaert, P., Boeckx, P., Verstraete, W. and Boon, N. (2011) 'Biocathodic nitrous oxide removal in bioelectrochemical systems', *Environ Sci Technol*, 45(24), pp. 10557-10566.

Dominguez-Benetton, X., Sevda, S., Vanbroekhoven, K. and Pant, D. (2012) 'The accurate use of impedance analysis for the study of microbial electrochemical systems', *Chem Soc Rev*, 41(21), pp. 7228-7246.

Escapa, A., Mateos, R., Martínez, E.J. and Blanes, J. (2016) 'Microbial electrolysis cells: An emerging technology for wastewater treatment and energy recovery. From laboratory to pilot plant and beyond', *Renewable and Sustainable Energy Reviews*, 55, pp. 942-956.

Ewing, T., Ha, P.T., Babauta, J.T., Tang, N.T., Heo, D. and Beyenal, H. (2014) 'Scale-up of sediment microbial fuel cells', *Journal of Power Sources*, 272, pp. 311-319.

Fan, L.P. and Li, J.J. (2016) 'Overviews on Internal Resistance and its Detection of Microbial Fuel Cells', *International Journal of Circuits, Systems and Signal Processing*, 10, pp. 316-320.

Fan, Y., Hu, H. and Liu, H. (2007) 'Sustainable Power Generation in Microbial Fuel Cells Using Bicarbonate Buffer and Proton Transfer Mechanisms', *Environmental Science & Technology*, 41(23), pp. 8154-8158.

Fan, Y., Sharbrough, E. and Liu, H. (2008) 'Quantification of the internal resistance distribution of microbial fuel cells', *Environ Sci Technol*, 42(21), pp. 8101-8107.

Ferry, J.G. (2011) 'Fundamentals of methanogenic pathways that are key to the biomethanation of complex biomass', *Current opinion in biotechnology*, 22(3), pp. 351-357.

Foad Marashi, S.K. and Kariminia, H.-R. (2015) 'Performance of a single chamber microbial fuel cell at different organic loads and pH values using purified terephthalic acid wastewater', *Journal of Environmental Health Science and Engineering*, 13, pp. 27-33.

Freguia, S., Teh, E.H., Boon, N., Leung, K.M., Keller, J. and Rabaey, K. (2010) 'Microbial fuel cells operating on mixed fatty acids', *Bioresource Technology*, 101(4), pp. 1233-1238.

Fricke, K., Harnisch, F. and Schroder, U. (2008) 'On the use of cyclic voltammetry for the study of anodic electron transfer in microbial fuel cells', *Energy & Environmental Science*, 1(1), pp. 144-147.

Fu, Q., Kobayashi, H., Kuramochi, Y., Xu, J., Wakayama, T., Maeda, H. and Sato, K. (2013) 'Bioelectrochemical analyses of a thermophilic biocathode catalyzing sustainable hydrogen production', *International Journal of Hydrogen Energy*, 38(35), pp. 15638-15645.

Ge, Z., Wu, L., Zhang, F. and He, Z. (2015) 'Energy extraction from a large-scale microbial fuel cell system treating municipal wastewater', *Journal of Power Sources*, 297, pp. 260-264.

Geelhoed, J.S., Hamelers, H.V.M. and Stams, A.J.M. (2010) 'Electricity-mediated biological hydrogen production', *Current Opinion in Microbiology*, 13(3), pp. 307-315.

Ghasemi Naraghi, Z., Yaghmaei, S., Mardanpour, M.M. and Hasany, M. (2015) 'Produced Water Treatment with Simultaneous Bioenergy Production Using Novel Bioelectrochemical Systems', *Electrochimica Acta*, 180, pp. 535-544.

Gil, G.C., Chang, I.S., Kim, B.H., Kim, M., Jang, J.K., Park, H.S. and Kim, H.J. (2003) 'Operational parameters affecting the performannce of a mediator-less microbial fuel cell', *Biosens Bioelectron*, 18(4), pp. 327-334.

Hari, A.R., Katuri, K.P., Logan, B.E. and Saikaly, P.E. (2016) 'Set anode potentials affect the electron fluxes and microbial community structure in propionate-fed microbial electrolysis cells', *Scientific Reports*, 6, pp. 38690-38701.

Harnisch, F. and Schroder, U. (2010) 'From MFC to MXC: chemical and biological cathodes and their potential for microbial bioelectrochemical systems', *Chemical Society Reviews*, 39(11), pp. 4433-4448.

Hay, J.X.W., Wu, T.Y., Juan, J.C. and Md. Jahim, J. (2013) 'Biohydrogen production through photo fermentation or dark fermentation using waste as a substrate: Overview, economics, and future prospects of hydrogen usage', *Biofuels, Bioproducts and Biorefining*, 7(3), pp. 334-352.

Haynes, W.M. (2010) *CRC Handbook of Chemistry and Physics, 91st Edition*. Taylor & Francis Group.

He, Z. and Mansfeld, F. (2009) 'Exploring the use of electrochemical impedance spectroscopy (EIS) in microbial fuel cell studies', *Energy & Environmental Science*, 2(2), pp. 215-219.

Heidrich, E.S., Curtis, T.P. and Dolfing, J. (2011) 'Determination of the Internal Chemical Energy of Wastewater', *Environmental Science & Technology*, 45(2), pp. 827-832.

Hoogers, G. (2002) *Fuel Cell Technology Handbook*. CRC Press.

Huang, L., Chai, X., Chen, G. and Logan, B.E. (2011) 'Effect of set potential on hexavalent chromium reduction and electricity generation from biocathode microbial fuel cells', *Environ Sci Technol*, 45(11), pp. 5025-5031.

Huang, L., Chai, X., Quan, X., Logan, B.E. and Chen, G. (2012) 'Reductive dechlorination and mineralization of pentachlorophenol in biocathode microbial fuel cells', *Bioresour Technol*, 111(1873-2976 (Electronic)), pp. 167-174.

Huang, Z., Jiang, D., Lu, L. and Ren, Z.J. (2016) 'Ambient CO2 capture and storage in bioelectrochemically mediated wastewater treatment', *Bioresource Technology*, 215, pp. 380-385.

Hussain, S.A., Perrier, M. and Tartakovsky, B. (2018) 'Real-time monitoring of a microbial electrolysis cell using an electrical equivalent circuit model', *Bioprocess and Biosystems Engineering*, 41(4), pp. 543-553.

Jafary, T., Daud, W.R.W., Ghasemi, M., Kim, B.H., Md Jahim, J., Ismail, M. and Lim, S.S. (2015) 'Biocathode in microbial electrolysis cell; present status and future prospects', *Renewable and Sustainable Energy Reviews*, 47, pp. 23-33.

Jain, A., Zhang, X., Pastorella, G., Connolly, J.O., Barry, N., Woolley, R., Krishnamurthy, S. and Marsili, E. (2012) 'Electron transfer mechanism in Shewanella loihica PV-4 biofilms formed at graphite electrode', *Bioelectrochemistry*, 87, pp. 28-32.

Jeremiasse, A.W., Hamelers, H.V.M. and Buisman, C.J.N. (2010) 'Microbial electrolysis cell with a microbial biocathode', *Bioelectrochemistry*, 78(1), pp. 39-43.

Jeremiasse, A.W., Hamelers, H.V.M., Croese, E. and Buisman, C.J.N. (2012) 'Acetate enhances startup of a H2-producing microbial biocathode', *Biotechnology and Bioengineering*, 109(3), pp. 657-664.

Jia, Y.H., Tran, H.T., Kim, D.H., Oh, S.J., Park, D.H., Zhang, R.H. and Ahn, D.H. (2008) 'Simultaneous organics removal and bio-electrochemical denitrification in microbial fuel cells', *Bioprocess Biosyst Eng*, 31(4), pp. 315-321.

Jiang, Y., Liang, P., Zhang, C., Bian, Y., Sun, X., Zhang, H., Yang, X., Zhao, F. and Huang, X. (2016) 'Periodic polarity reversal for stabilizing the pH in two-chamber microbial electrolysis cells', *Applied Energy*, 165, pp. 670-675.

Jourdin, L., Freguia, S., Donose, B.C. and Keller, J. (2015) 'Autotrophic hydrogen-producing biofilm growth sustained by a cathode as the sole electron and energy source', *Bioelectrochemistry*, 102, pp. 56-63.

Jourdin, L., Raes, S.M.T., Buisman, C.J.N. and Strik, D.P.B.T.B. (2018) 'Critical Biofilm Growth throughout Unmodified Carbon Felts Allows Continuous Bioelectrochemical Chain Elongation from CO2 up to Caproate at High Current Density', *Frontiers in Energy Research*, 6(7).

Kadier, A., Simayi, Y., Abdeshahian, P., Azman, N.F., Chandrasekhar, K. and Kalil, M.S. (2016) 'A comprehensive review of microbial electrolysis cells (MEC) reactor designs and configurations for sustainable hydrogen gas production', *Alexandria Engineering Journal*, 55(1), pp. 427-443.

Karthikeyan, R., Selvam, A., Cheng, K.Y. and Wong, J.W.-C. (2016) 'Influence of ionic conductivity in bioelectricity production from saline domestic sewage sludge in microbial fuel cells', *Bioresource Technology*, 200, pp. 845-852.

Keller, K. and Wall, J. (2011) 'Genetics and Molecular Biology of the Electron Flow for Sulfate Respiration in Desulfovibrio', *Frontiers in Microbiology*, 2(135).

Ketep, S.F., Bergel, A., Bertrand, M., Achouak, W. and Fourest, E. (2013) 'Lowering the applied potential during successive scratching/re-inoculation improves the performance of microbial anodes for microbial fuel cells', *Bioresour Technol*, 127, pp. 448-455.

Kiely, P.D., Rader, G., Regan, J.M. and Logan, B.E. (2011) 'Long-term cathode performance and the microbial communities that develop in microbial fuel cells fed different fermentation endproducts', *Bioresour Technol*, 102(1), pp. 361-366.

Kim, B.H. and Gadd, G.M. (2008) *Bacterial Physiology and Metabolism*. New York: Cambridge University Press.

Kim, B.H., Ikeda, T., Park, H.S., Kim, H.J., Hyun, M.S., Kano, K., Takagi, K. and Tatsumi, H. (1999) 'Electrochemical activity of an Fe(III)-reducing bacterium, Shewanella putrefaciens IR-1, in the presence of alternative electron acceptors', *Biotechnology Techniques*, 13(7), pp. 475-478.

Kim, B.H., Lim, S.S., Daud, W.R.W., Gadd, G.M. and Chang, I.S. (2015) 'The biocathode of microbial electrochemical systems and microbially-influenced corrosion', *Bioresource Technology*, 190, pp. 395-401.

Kim, B.H., Park, H.S., Kim, H.J., Kim, G.T., Chang, I.S., Lee, J. and Phung, N.T. (2004) 'Enrichment of microbial community generating electricity using a fuel-cell-type electrochemical cell', *Applied Microbiology and Biotechnology*, 63(6), pp. 672-681.

Kim, H.J., Park, H.S., Hyun, M.S., Chang, I.S., Kim, M. and Kim, B.H. (2002) 'A mediator-less microbial fuel cell using a metal reducing bacterium, Shewanella putrefaciens', *Enzyme and Microbial Technology*, 30(2), pp. 145-152.

Kim, J.R., Min, B. and Logan, B.E. (2005) 'Evaluation of procedures to acclimate a microbial fuel cell for electricity production', *Appl Microbiol Biotechnol*, 68(1), pp. 23-30.

Kim, K.Y., Chae, K.J., Choi, M.J., Ajayi, F.F., Jang, A., Kim, C.W. and Kim, I.S. (2011) 'Enhanced Coulombic efficiency in glucose-fed microbial fuel cells by reducing metabolite electron losses using dual-anode electrodes', *Bioresour Technol*, 102(5), pp. 4144-4149.

Kim, Y. and Logan, B.E. (2011) 'Microbial Reverse Electrodialysis Cells for Synergistically Enhanced Power Production', *Environmental Science & Technology*, 45(13), pp. 5834-5839.

Kodali, M., Santoro, C., Serov, A., Kabir, S., Artyushkova, K., Matanovic, I. and Atanassov, P. (2017) 'Air Breathing Cathodes for Microbial Fuel Cell using Mn-, Fe-, Co- and Ni-containing Platinum Group Metal-free Catalysts', *Electrochimica Acta*, 231, pp. 115-124.

Kracke, F., Vassilev, I. and Krömer, J.O. (2015) 'Microbial electron transport and energy conservation – the foundation for optimizing bioelectrochemical systems', *Frontiers in Microbiology*, 6(575).

Krieg, T., Sydow, A., Schröder, U., Schrader, J. and Holtmann, D. (2014) 'Reactor concepts for bioelectrochemical syntheses and energy conversion', *Trends in Biotechnology*, 32(12), pp. 645-655.

Kumar, G., Bakonyi, P., Zhen, G., Sivagurunathan, P., Koók, L., Kim, S.-H., Tóth, G., Nemestóthy, N. and Bélafi-Bakó, K. (2017) 'Microbial electrochemical systems for sustainable biohydrogen production: Surveying the experiences from a start-up viewpoint', *Renewable and Sustainable Energy Reviews*, 70, pp. 589-597.

Kundu, A., Sahu, J.N., Redzwan, G. and Hashim, M.A. (2013) 'An overview of cathode material and catalysts suitable for generating hydrogen in microbial electrolysis cell', *International Journal of Hydrogen Energy*, 38(4), pp. 1745-1757.

Kyazze, G., Popov, A., Dinsdale, R., Esteves, S., Hawkes, F., Premier, G. and Guwy, A. (2010) 'Influence of catholyte pH and temperature on hydrogen production from acetate using a two chamber concentric tubular microbial electrolysis cell', *International Journal of Hydrogen Energy*, 35(15), pp. 7716-7722.

LaBelle, E., Bond, D. R. (2009) 'Cyclic voltammetry for the study of microbial electron transfer at electrodes', in Rabaey, K., Angenant, L., Schröder, U. and Keller, J. (eds.) *Bio-electrochemical Systems: from extracellular electron transfer to biotechnological application*. Wageningen University, The Netherlands International Water Association (IWA).

LaBelle, E.V., Marshall, C.W., Gilbert, J.A. and May, H.D. (2014) 'Influence of Acidic pH on Hydrogen and Acetate Production by an Electrosynthetic Microbiome', *PLOS ONE*, 9(10), p. e109935.

LaBelle, E.V. and May, H.D. (2017) 'Energy Efficiency and Productivity Enhancement of Microbial Electrosynthesis of Acetate', *Frontiers in Microbiology*, 8(756).

Lee, C.-Y., Ho, K.-L., Lee, D.-J., Su, A. and Chang, J.-S. (2012) 'Electricity harvest from nitrate/sulfide-containing wastewaters using microbial fuel cell with autotrophic denitrifier, Pseudomonas sp. C27', *International Journal of Hydrogen Energy*, 37(20), pp. 15827-15832.

Lee, C.-Y. and Huang, Y.-N. (2013) 'The effects of electrode spacing on the performance of microbial fuel cells under different substrate concentrations', *Water Science and Technology*, 68(9), pp. 2028-2034.

Lee, D.-J., Liu, X. and Weng, H.-L. (2014) 'Sulfate and organic carbon removal by microbial fuel cell with sulfate-reducing bacteria and sulfide-oxidising bacteria anodic biofilm', *Bioresource Technology*, 156, pp. 14-19.

Lee, H.-S. and Rittmann, B.E. (2010) 'Significance of Biological Hydrogen Oxidation in a Continuous Single-Chamber Microbial Electrolysis Cell', *Environmental Science & Technology*, 44(3), pp. 948-954.

Lens, P.N.L., Visser, A., Janssen, A.J.H., Pol, L.W.H. and Lettinga, G. (1998) 'Biotechnological Treatment of Sulfate-Rich Wastewaters', *Critical Reviews in Environmental Science and Technology*, 28(1), pp. 41-88.

Li, L., Kong, X., Sun, Y., Yuan, Z. and Li, Y. (2011) 'Performance of microbial fuel cell in different anode and cathode electrode sizes', *2011 International Conference on Remote Sensing, Environment and Transportation Engineering*, pp. 7707-7710.

Li, Y., Lu, A., Ding, H., Jin, S., Yan, Y., Wang, C., Zen, C. and Wang, X. (2009) 'Cr(VI) reduction at rutile-catalyzed cathode in microbial fuel cells', *Electrochemistry Communications*, 11(7), pp. 1496-1499.

Liang, D., Liu, Y., Peng, S., Lan, F., Lu, S. and Xiang, Y. (2014) 'Effects of bicarbonate and cathode potential on hydrogen production in a biocathode electrolysis cell', *Frontiers of Environmental Science & Engineering*, 8(4), pp. 624-630.

Liang, P., Fan, M., Cao, X. and Huang, X. (2009) 'Evaluation of applied cathode potential to enhance biocathode in microbial fuel cells', *Journal of Chemical Technology & Biotechnology*, 84(5), pp. 794-799.

Liang, P., Huang, X., Fan, M.-Z., Cao, X.-X. and Wang, C. (2007) 'Composition and distribution of internal resistance in three types of microbial fuel cells', *Applied Microbiology and Biotechnology*, 77(3), pp. 551-558.

Lide, D.R. (2006) *CRC Handbook of Chemistry and Physics*. 87th ed. edn. CRC Press.

Lim, S.S., Daud, W.R.W., Md Jahim, J., Ghasemi, M., Chong, P.S. and Ismail, M. (2012) 'Sulfonated poly(ether ether ketone)/poly(ether sulfone) composite membranes as an alternative proton exchange membrane in microbial fuel cells', *International Journal of Hydrogen Energy*, 37(15), pp. 11409-11424.

Lim, S.S., Yu, E.H., Daud, W.R.W., Kim, B.H. and Scott, K. (2017) 'Bioanode as a limiting factor to biocathode performance in microbial electrolysis cells', *Bioresource Technology*, 238, pp. 313-324.

Liu, B., Ji, M. and Zhai, H. (2018) 'Anodic potentials, electricity generation and bacterial community as affected by plant roots in sediment microbial fuel cell: Effects of anode locations', *Chemosphere*, 209, pp. 739-747.

Liu, G., Zhou, Y., Luo, H., Cheng, X., Zhang, R. and Teng, W. (2015) 'A comparative evaluation of different types of microbial electrolysis desalination cells for malic acid production', *Bioresource Technology*, 198, pp. 87-93.

Liu, H., Grot, S. and Logan, B.E. (2005) 'Electrochemically Assisted Microbial Production of Hydrogen from Acetate', *Environmental Science & Technology*, 39(11), pp. 4317-4320.

Liu, L., Chou, T.-Y., Lee, C.-Y., Lee, D.-J., Su, A. and Lai, J.-Y. (2016) 'Performance of freshwater sediment microbial fuel cells: Consistency', *International Journal of Hydrogen Energy*, 41(7), pp. 4504-4508.

Liu, Y., Harnisch, F., Fricke, K., Sietmann, R. and Schröder, U. (2008) 'Improvement of the anodic bioelectrocatalytic activity of mixed culture biofilms by a simple consecutive electrochemical selection procedure', *Biosensors and Bioelectronics*, 24(4), pp. 1006-1011.

Logan, B.E. (2010) 'Scaling up microbial fuel cells and other bioelectrochemical systems', *Applied Microbiology and Biotechnology*, 85(6), pp. 1665-1671.

Logan, B.E., Call, D., Cheng, S., Hamelers, H.V.M., Sleutels, T.H.J.A., Jeremiasse, A.W. and Rozendal, R.A. (2008) 'Microbial Electrolysis Cells for High Yield Hydrogen Gas Production from Organic Matter', *Environmental Science & Technology*, 42(23), pp. 8630-8640.

Logan, B.E., Hamelers, B., Rozendal, R., Schröder, U., Keller, J., Freguia, S., Aelterman, P., Verstraete, W. and Rabaey, K. (2006) 'Microbial Fuel Cells: Methodology and Technology', *Environmental Science & Technology*, 40(17), pp. 5181-5192.

Logan, B.E. and Rabaey, K. (2012) 'Conversion of Wastes into Bioelectricity and Chemicals by Using Microbial Electrochemical Technologies', *Science*, 337(6095), pp. 686-690.

Lovley, D.R. (1991) 'Dissimilatory Fe(III) and Mn(IV) reduction', *Microbiological Reviews*, 55(2), pp. 259-287.

Lu, L., Ren, N., Zhao, X., Wang, H., Wu, D. and Xing, D. (2011) 'Hydrogen production, methanogen inhibition and microbial community structures in psychrophilic single-chamber microbial electrolysis cells', *Energy & Environmental Science*, 4(4), pp. 1329-1336.

Luo, H., Fu, S., Liu, G., Zhang, R., Bai, Y. and Luo, X. (2014) 'Autotrophic biocathode for high efficient sulfate reduction in microbial electrolysis cells', *Bioresource Technology*, 167, pp. 462-468.

Luo, H., Xu, P. and Ren, Z. (2012a) 'Long-term performance and characterization of microbial desalination cells in treating domestic wastewater', *Bioresource Technology*, 120, pp. 187-193.

Luo, H., Xu, P., Roane, T.M., Jenkins, P.E. and Ren, Z. (2012b) 'Microbial desalination cells for improved performance in wastewater treatment, electricity production, and desalination', *Bioresource Technology*, 105, pp. 60-66.

Macdonald, D.D. (2006) 'Reflections on the history of electrochemical impedance spectroscopy', *Electrochimica Acta*, 51(8), pp. 1376-1388.

Madigan, M.T., Martinko, J.M., Bender, K.S., Buckley, D.H., Stahl, D.A. and Brock, T. (2014) *Brock Biology of Microorganisms*. Pearson.

Mand, J., Park, H.S., Jack, T.R. and Voordouw, G. (2014) 'The role of acetogens in microbially influenced corrosion of steel', *Frontiers in Microbiology*, 5(268).

Manohar, A.K. and Mansfeld, F. (2009) 'The internal resistance of a microbial fuel cell and its dependence on cell design and operating conditions', *Electrochimica Acta*, 54(6), pp. 1664-1670.

Marshall, C.W., Ross, D.E., Fichot, E.B., Norman, R.S. and May, H.D. (2012) 'Electrosynthesis of commodity chemicals by an autotrophic microbial community', *Appl Environ Microbiol*, 78(23), pp. 8412-8420.

Marsili, E., Rollefson, J.B., Baron, D.B., Hozalski, R.M. and Bond, D.R. (2008) 'Microbial Biofilm Voltammetry: Direct Electrochemical Characterization of Catalytic Electrode-Attached Biofilms', *Applied and Environmental Microbiology*, 74(23), pp. 7329-7337.

Milner, E.M. (2015) *Development of an Aerobic Biocathode for Microbial Fuel Cells*. thesis. Newcastle University.

Milner, E.M., Popescu, D., Curtis, T., Head, I.M., Scott, K. and Yu, E.H. (2016) 'Microbial fuel cells with highly active aerobic biocathodes', *Journal of Power Sources*, 324, pp. 8-16.

Milner, E.M. and Yu, E.H. (2018) 'The Effect of Oxygen Mass Transfer on Aerobic Biocathode Performance, Biofilm Growth and Distribution in Microbial Fuel Cells', *Fuel Cells*, 18(1), pp. 4-12.

Modestra, J.A. and Mohan, S.V. (2017) 'Microbial electrosynthesis of carboxylic acids through CO2 reduction with selectively enriched biocatalyst: Microbial dynamics', *Journal of CO2 Utilization*, 20, pp. 190-199.

Mohanakrishna, G., Seelam, J.S., Vanbroekhoven, K. and Pant, D. (2015) 'An enriched electroactive homoacetogenic biocathode for the microbial electrosynthesis of acetate through carbon dioxide reduction', *Faraday Discuss*, 183, pp. 445-462.

Mohanakrishna, G., Vanbroekhoven, K. and Pant, D. (2016) 'Imperative role of applied potential and inorganic carbon source on acetate production through microbial electrosynthesis', *Journal of CO2 Utilization*, 15, pp. 57-64.

Moon, J.M., Kondaveeti, S., Lee, T.H., Song, Y.C. and Min, B. (2015) 'Minimum interspatial electrode spacing to optimize air-cathode microbial fuel cell operation with a membrane electrode assembly', *Bioelectrochemistry*, 106, pp. 263-267.

Moussa, M.S., Fuentes, O.G., Lubberding, H.J., Hooijmans, C.M., van Loosdrecht, M.C.M. and Gijzen, H.J. (2006) 'Nitrification Activities in Full-scale Treatment Plants with Varying Salt Loads', *Environmental Technology*, 27(6), pp. 635-643.

Mu, Y., Rozendal, R.A., Rabaey, K. and Keller, J. (2009) 'Nitrobenzene removal in bioelectrochemical systems', *Environ Sci Technol*, 43(22), pp. 8690-8695.

Muyzer, G. and Stams, A.J.M. (2008) 'The ecology and biotechnology of sulphate-reducing bacteria', *Nat Rev Micro*, 6(6), pp. 441-454.

Nielsen, P.H., Smidt, H.D. and Frølund, B. (1998) 'The effect of alkaline pH conditions on a sulphate reducing consortium from a Danish district heating plant AU - Goeres, D M', *Biofouling*, 12(4), pp. 273-286.

Nimje, V.R., Chen, C.-C., Chen, H.-R., Chen, C.-Y., Tseng, M.-J., Cheng, K.-C., Shih, R.-C. and Chang, Y.-F. (2012) 'A Single-Chamber Microbial Fuel Cell without an Air Cathode', *International Journal of Molecular Sciences*, 13(3), pp. 3933-3948.

Nonaka, K., Nguyen, N.T., Yoon, K.-S. and Ogo, S. (2013) 'Novel H2-oxidizing [NiFeSe]hydrogenase from Desulfovibrio vulgaris Miyazaki F', *Journal of Bioscience and Bioengineering*, 115(4), pp. 366-371.

Odom, J.M. and Singleton, R.J. (1993) *The Sulfate-Reducing Bacteria: Contemporary Perspectives*. Springer Science & Business Media.

Oh, S., Min, B. and Logan, B.E. (2004) 'Cathode Performance as a Factor in Electricity Generation in Microbial Fuel Cells', *Environmental Science & Technology*, 38(18), pp. 4900-4904.

Patil, S.A., Arends, J.B.A., Vanwonterghem, I., van Meerbergen, J., Guo, K., Tyson, G.W. and Rabaey, K. (2015) 'Selective Enrichment Establishes a Stable Performing Community for Microbial Electrosynthesis of Acetate from CO2', *Environmental Science & Technology*, 49(14), pp. 8833-8843.

Pernetti, M. and Di Palma, L. (2005) 'Experimental evaluation of inhibition effects of saline wastewater on activated sludge', *Environ Technol*, 26(6), pp. 695-703.

Peters, J.W., Miller, A.-F., Jones, A.K., King, P.W. and Adams, M.W.W. (2016) 'Electron bifurcation', *Current Opinion in Chemical Biology*, 31, pp. 146-152.

Peters, J.W., Schut, G.J., Boyd, E.S., Mulder, D.W., Shepard, E.M., Broderick, J.B., King, P.W. and Adams, M.W.W. (2015) '[FeFe]- and [NiFe]-hydrogenase diversity, mechanism, and maturation', *Biochimica et Biophysica Acta (BBA) - Molecular Cell Research*, 1853(6), pp. 1350-1369.

Pham, T.H., Jang, J.K., Chang, I.S., Kim, B.H (2004) 'Improvement of Cathode Reaction of a Mediatorless Microbial Fuel Cell', *Journal of Microbiology and Biotechnology*, 14(2), pp. 324-329.

Pisciotta, J.M., Zaybak, Z., Call, D.F., Nam, J.Y. and Logan, B.E. (2012) 'Enrichment of microbial electrolysis cell biocathodes from sediment microbial fuel cell bioanodes', *Appl Environ Microbiol*, 78(15), pp. 5212-9.

Premier, G.C., Michie, I.S., Boghani, H.C., Fradler, K.R. and Kim, J.R. (2016) *Reactor design and scale-up*. 1st edn. Elsevier Science.

Puig, S., Serra, M., Coma, M., Cabré, M., Dolors Balaguer, M. and Colprim, J. (2011a) 'Microbial fuel cell application in landfill leachate treatment', *Journal of Hazardous Materials*, 185(2), pp. 763-767.

Puig, S., Serra, M., Vilar-Sanz, A., Cabre, M., Baneras, L., Colprim, J. and Balaguer, M.D. (2011b) 'Autotrophic nitrite removal in the cathode of microbial fuel cells', *Bioresour Technol*, 102(6), pp. 4462-4467.

Rabaey, K., Read, S.T., Clauwaert, P., Freguia, S., Bond, P.L., Blackall, L.L. and Keller, J. (2008) 'Cathodic oxygen reduction catalyzed by bacteria in microbial fuel cells', *ISME J*, 2(5), pp. 519-527.

Rabaey, K. and Rozendal, R.A. (2010) 'Microbial electrosynthesis — revisiting the electrical route for microbial production', *Nat Rev Micro*, 8(10), pp. 706-716.

Raes, S.M.T., Jourdin, L., Buisman, C.J.N. and Strik, D.P.B.T.B. (2017) 'Continuous Long-Term Bioelectrochemical Chain Elongation to Butyrate', *ChemElectroChem*, 4(2), pp. 386-395.

Rago, L., Monpart, N., Cortes, P., Baeza, J.A. and Guisasola, A. (2016) 'Performance of microbial electrolysis cells with bioanodes grown at different external resistances', *Water Sci Technol*, 73(5), pp. 1129-1135.

Rahimnejad, M., Ghoreyshi, A.A., Najafpour, G.D., Younesi, H. and Shakeri, M. (2012) 'A novel microbial fuel cell stack for continuous production of clean energy', *International Journal of Hydrogen Energy*, 37(7), pp. 5992-6000.

Ramos, A.R., Grein, F., Oliveira, G.P., Venceslau, S.S., Keller, K.L., Wall, J.D. and Pereira, I.A. (2015) 'The FlxABCD-HdrABC proteins correspond to a novel NADH dehydrogenase/heterodisulfide reductase widespread in anaerobic bacteria and involved in ethanol metabolism in Desulfovibrio vulgaris Hildenborough', *Environmental microbiology*, 17(7), pp. 2288-2305.

Rismani-Yazdi, H., Carver, S.M., Christy, A.D. and Tuovinen, O.H. (2008) 'Cathodic limitations in microbial fuel cells: An overview', *Journal of Power Sources*, 180(2), pp. 683-694.

Rivera, I., Bakonyi, P. and Buitrón, G. (2017) 'H2 production in membraneless bioelectrochemical cells with optimized architecture: The effect of cathode surface area and electrode distance', *Chemosphere*, 171, pp. 379-385.

Rosenbaum, M., Aulenta, F., Villano, M. and Angenent, L.T. (2011) 'Cathodes as electron donors for microbial metabolism: Which extracellular electron transfer mechanisms are involved?', *Bioresource Technology*, 102(1), pp. 324-333.

Rozendal, R.A., Hamelers, H.V.M., Euverink, G.J.W., Metz, S.J. and Buisman, C.J.N. (2006) 'Principle and perspectives of hydrogen production through biocatalyzed electrolysis', *International Journal of Hydrogen Energy*, 31(12), pp. 1632-1640.

Rozendal, R.A., Hamelers, H.V.M., Molenkamp, R.J. and Buisman, C.J.N. (2007) 'Performance of single chamber biocatalyzed electrolysis with different types of ion exchange membranes', *Water Research*, 41(9), pp. 1984-1994.

Rozendal, R.A., Jeremiasse, A.W., Hamelers, H.V.M. and Buisman, C.J.N. (2008) 'Hydrogen Production with a Microbial Biocathode', *Environmental Science & Technology*, 42(2), pp. 629-634.

Ruiz, Y., Baeza, J.A. and Guisasola, A. (2013) 'Revealing the proliferation of hydrogen scavengers in a single-chamber microbial electrolysis cell using electron balances', *International Journal of Hydrogen Energy*, 38(36), pp. 15917-15927.

Saeed, H.M., Husseini, G.A., Yousef, S., Saif, J., Al-Asheh, S., Abu Fara, A., Azzam, S., Khawaga, R. and Aidan, A. (2015) 'Microbial desalination cell technology: A review and a case study', *Desalination*, 359, pp. 1-13.

Santoro, C., Arbizzani, C., Erable, B. and Ieropoulos, I. (2017) 'Microbial fuel cells: From fundamentals to applications. A review', *Journal of Power Sources*, 356, pp. 225-244.

Sawasdee, V. and Pisutpaisal, N. (2015) 'Effect of Nitrogen Concentration on the Performance of Single-Chamber Microbial Fuel Cells', *Energy Procedia*, 79, pp. 620-623.

Schneider, G., Kovács, T., Rákhely, G. and Czeller, M. (2016) 'Biosensoric potential of microbial fuel cells', *Applied Microbiology and Biotechnology*, 100(16), pp. 7001-7009.

Schuchmann, K. and Muller, V. (2014) 'Autotrophy at the thermodynamic limit of life: a model for energy conservation in acetogenic bacteria', *Nat Rev Micro*, 12(12), pp. 809-821.

Sekar, N. and Ramasamy, R.P. (2013) 'Electrochemical Impedance Spectroscopy for Microbial Fuel Cell Characterization', *Journal of Microbial & Biochemical Technology*, p. S6:004.

Selembo, P.A., Merrill, M.D. and Logan, B.E. (2009) 'The use of stainless steel and nickel alloys as low-cost cathodes in microbial electrolysis cells', *Journal of Power Sources*, 190(2), pp. 271-278.

Shcherbakov, V.V., Artemkina, Y.M., Ponomareva, T.N. and Kirillov, A.D. (2009) 'Electrical conductivity of the ammonia-water system', *Russian Journal of Inorganic Chemistry*, 54(2), pp. 277-279.

Shea, C., Clauwaert, P., Verstraete, W. and Nerenberg, R. (2008) 'Adapting a denitrifying biocathode for perchlorate reduction', *Water Sci Technol*, 58(10), pp. 1941-1946.

Sleutels, T.H.J.A., Darus, L., Hamelers, H.V.M. and Buisman, C.J.N. (2011) 'Effect of operational parameters on Coulombic efficiency in bioelectrochemical systems', *Bioresource Technology*, 102(24), pp. 11172-11176.

Sleutels, T.H.J.A., Heijne, A.T., Buisman, C.J.N. and Hamelers, H.V.M. (2013) 'Steady-state performance and chemical efficiency of Microbial Electrolysis Cells', *International Journal of Hydrogen Energy*, 38(18), pp. 7201-7208.

Snoeyink, V.L. (1980) *Water chemistry* New York: Wiley.

Spurr, M.W.A. (2016) *Microbial Fuel Cell-based Biosensors for Estimation of Biochemical Oxygen Demand and Detection of Toxicity*. Newcastle University, UK.

Srikanth, S., Singh, D., Vanbroekhoven, K., Pant, D., Kumar, M., Puri, S.K. and Ramakumar, S.S.V. (2018) 'Electro-biocatalytic conversion of carbon dioxide to alcohols using gas diffusion electrode', *Bioresource Technology*, 265, pp. 45-51.

Su, M., Jiang, Y. and Li, D. (2013) 'Production of Acetate from Carbon Dioxide in Bioelectrochemical Systems Based on Autotrophic Mixed Culture', *Journal of Microbiology and Biotechnology*, 23(8), pp. 1400-1146.

Sydow, U., Wohland, P., Wolke, I. and Cypionka, H. (2002) 'Bioenergetics of the alkaliphilic sulfate-reducing bacterium Desulfonatronovibrio hydrogenovorans', *Microbiology*, 148(Pt 3), pp. 853-60.

Tandukar, M., Huber, S.J., Onodera, T. and Pavlostathis, S.G. (2009) 'Biological chromium(VI) reduction in the cathode of a microbial fuel cell', *Environ Sci Technol*, 43(21), pp. 8159-8165.

Tartakovsky, B., Manuel, M.F., Wang, H. and Guiot, S.R. (2009) 'High rate membrane-less microbial electrolysis cell for continuous hydrogen production', *International Journal of Hydrogen Energy*, 34(2), pp. 672-677.

Tender, L.M., Gray, S.A., Groveman, E., Lowy, D.A., Kauffman, P., Melhado, J., Tyce, R.C., Flynn, D., Petrecca, R. and Dobarro, J. (2008) 'The first demonstration of a microbial fuel cell as a viable power supply: Powering a meteorological buoy', *Journal of Power Sources*, 179(2), pp. 571-575.

Thompson, L.J., Gray, V., Lindsay, D. and von Holy, A. (2006) 'Carbon : nitrogen : phosphorus ratios influence biofilm formation by Enterobacter cloacae and Citrobacter freundii', *J Appl Microbiol*, 101(5), pp. 1105-1113.

Timmers, R.A., Strik, D.P.B.T.B., Hamelers, H.V.M. and Buisman, C.J.N. (2012) 'Characterization of the internal resistance of a plant microbial fuel cell', *Electrochimica Acta*, 72, pp. 165-171.

Torres, C.I., Krajmalnik-Brown, R., Parameswaran, P., Marcus, A.K., Wanger, G., Gorby, Y.A. and Rittmann, B.E. (2009) 'Selecting Anode-Respiring Bacteria Based on Anode Potential: Phylogenetic, Electrochemical, and Microscopic Characterization', *Environmental Science & Technology*, 43(24), pp. 9519-9524.

van den Brand, T.P.H., Roest, K., Chen, G.H., Brdjanovic, D. and van Loosdrecht, M.C.M. (2015) 'Potential for beneficial application of sulfate reducing bacteria in sulfate containing domestic wastewater treatment', *World Journal of Microbiology and Biotechnology*, 31(11), pp. 1675-1681.

van Eerten-Jansen, M.C.A.A., Jansen, N.C., Plugge, C.M., de Wilde, V., Buisman, C.J.N. and ter Heijne, A. (2015) 'Analysis of the mechanisms of bioelectrochemical methane production by mixed cultures', *Journal of Chemical Technology & Biotechnology*, 90(5), pp. 963-970.

Vassilev, I., Ledezma, P., Freguia, S., Kromer, J.O., Keller, J. and Virdis, B. (2017) *General Meeting of the International Society for Microbial Electrochemistry and Technology (ISMET 2017)*. Lisbon, Portugal.

Venzlaff, H., Enning, D., Srinivasan, J., Mayrhofer, K.J.J., Hassel, A.W., Widdel, F. and Stratmann, M. (2013) 'Accelerated cathodic reaction in microbial corrosion of iron due to direct electron uptake by sulfate-reducing bacteria', *Corrosion Science*, 66, pp. 88-96.

Villano, M., Aulenta, F., Ciucci, C., Ferri, T., Giuliano, A. and Majone, M. (2010) 'Bioelectrochemical reduction of CO(2) to CH(4) via direct and indirect extracellular electron transfer by a hydrogenophilic methanogenic culture', *Bioresour Technol*, 101(9), pp. 3085-3090.

Villano, M., De Bonis, L., Rossetti, S., Aulenta, F. and Majone, M. (2011) 'Bioelectrochemical hydrogen production with hydrogenophilic dechlorinating bacteria as electrocatalytic agents', *Bioresource Technology*, 102(3), pp. 3193-3199.

Wagner, R.C., Regan, J.M., Oh, S.-E., Zuo, Y. and Logan, B.E. (2009) 'Hydrogen and methane production from swine wastewater using microbial electrolysis cells', *Water Research*, 43(5), pp. 1480-1488.

Wang, A., Liu, W., Ren, N., Zhou, J. and Cheng, S. (2010) 'Key factors affecting microbial anode potential in a microbial electrolysis cell for H2 production', *International Journal of Hydrogen Energy*, 35(24), pp. 13481-13487.

Wang, A., Sun, D., Cao, G., Wang, H., Ren, N., Wu, W.-M. and Logan, B.E. (2011a) 'Integrated hydrogen production process from cellulose by combining dark fermentation, microbial fuel cells, and a microbial electrolysis cell', *Bioresource Technology*, 102(5), pp. 4137-4143.

Wang, A.J., Cheng, H.Y., Liang, B., Ren, N.Q., Cui, D., Lin, N., Kim, B.H. and Rabaey, K. (2011b) 'Efficient reduction of nitrobenzene to aniline with a biocatalyzed cathode', *Environ Sci Technol*, 45(23), pp. 10186-10193.

Wang, C.-T., Sangeetha, T., Yan, W.-M., Chong, W.-T., Saw, L.-H., Zhao, F., Chang, C.-T. and Wang, C.-H. (2018) 'Application of interface material and effects of oxygen gradient on the performance of single-chamber sediment microbial fuel cells (SSMFCs)', *Journal of Environmental Sciences*, 75, pp. 163-168.

Wang, X., Feng, Y., Ren, N., Wang, H., Lee, H., Li, N. and Zhao, Q. (2009) 'Accelerated start-up of two-chambered microbial fuel cells: Effect of anodic positive poised potential', *Electrochimica Acta*, 54(3), pp. 1109-1114.

Wang, Y.-P., Liu, X.-W., Li, W.-W., Li, F., Wang, Y.-K., Sheng, G.-P., Zeng, R.J. and Yu, H.-Q. (2012) 'A microbial fuel cell–membrane bioreactor integrated system for cost-effective wastewater treatment', *Applied Energy*, 98, pp. 230-235.

Wei, J., Liang, P., Cao, X. and Huang, X. (2010) 'A New Insight into Potential Regulation on Growth and Power Generation of Geobacter sulfurreducens in Microbial Fuel Cells Based on Energy Viewpoint', *Environmental Science & Technology*, 44(8), pp. 3187-3191.

Wenzel, J., Fiset, E., Batlle-Vilanova, P., Cabezas, A., Etchebehere, C., Balaguer, M.D., Colprim, J. and Puig, S. (2018) 'Microbial Community Pathways for the Production of Volatile Fatty Acids From CO2 and Electricity', *Frontiers in Energy Research*, 6(15).

Winfield, J., Gajda, I., Greenman, J. and Ieropoulos, I. (2016) 'A review into the use of ceramics in microbial fuel cells', *Bioresource Technology*, 215, pp. 296-303.

Xie, D., Yu, H., Li, C., Ren, Y., Wei, C. and Feng, C. (2014) 'Competitive microbial reduction of perchlorate and nitrate with a cathode directly serving as the electron donor', *Electrochimica Acta*, 133(0), pp. 217-223.

Xing, D., Cheng, S., Regan, J.M. and Logan, B.E. (2009) 'Change in microbial communities in acetate- and glucose-fed microbial fuel cells in the presence of light', *Biosensors and Bioelectronics*, 25(1), pp. 105-111.

Yates, M.D., Kiely, P.D., Call, D.F., Rismani-Yazdi, H., Bibby, K., Peccia, J., Regan, J.M. and Logan, B.E. (2012) 'Convergent development of anodic bacterial communities in microbial fuel cells', *Isme j*, 6(11), pp. 2002-2013.

Yuan, H., Hou, Y., Abu-Reesh, I.M., Chen, J. and He, Z. (2016) 'Oxygen reduction reaction catalysts used in microbial fuel cells for energy-efficient wastewater treatment: a review', *Materials Horizons*, 3(5), pp. 382-401.

Zaybak, Z., Pisciotta, J.M., Tokash, J.C. and Logan, B.E. (2013) 'Enhanced start-up of anaerobic facultatively autotrophic biocathodes in bioelectrochemical systems', *Journal of Biotechnology*, 168(4), pp. 478-485.

Zhang, B., Feng, C., Ni, J., Zhang, J. and Huang, W. (2012a) 'Simultaneous reduction of vanadium (V) and chromium (VI) with enhanced energy recovery based on microbial fuel cell technology', *Journal of Power Sources*, 204, pp. 34-39.

Zhang, G., Zhang, H., Zhang, C., Zhang, G., Yang, F., Yuan, G. and Gao, F. (2013) 'Simultaneous nitrogen and carbon removal in a single chamber microbial fuel cell with a rotating biocathode', *Process Biochemistry*, 48(5-6), pp. 893-900.

Zhang, G., Zhao, Q., Jiao, Y., Wang, K., Lee, D.J. and Ren, N. (2012b) 'Efficient electricity generation from sewage sludge using biocathode microbial fuel cell', *Water Res*, 46(1), pp. 43-52.

Zhang, P.-Y. and Liu, Z.-L. (2010) 'Experimental study of the microbial fuel cell internal resistance', *Journal of Power Sources*, 195(24), pp. 8013-8018.

Zhang, Y., Min, B., Huang, L. and Angelidaki, I. (2011) 'Electricity generation and microbial community response to substrate changes in microbial fuel cell', *Bioresource Technology*, 102(2), pp. 1166-1173.

Zhen, G., Kobayashi, T., Lu, X., Kumar, G., Hu, Y., Bakonyi, P., Rózsenberszki, T., Koók, L., Nemestóthy, N., Bélafi-Bakó, K. and Xu, K. (2016) 'Recovery of biohydrogen in a single-chamber microbial electrohydrogenesis cell using liquid fraction of pressed municipal solid waste (LPW) as substrate', *International Journal of Hydrogen Energy*, 41(40), pp. 17896-17906.

Zhen, G., Lu, X., Kumar, G., Bakonyi, P., Xu, K. and Zhao, Y. (2017) 'Microbial electrolysis cell platform for simultaneous waste biorefinery and clean electrofuels generation: Current situation, challenges and future perspectives', *Progress in Energy and Combustion Science*, 63, pp. 119-145.

Zheng, Y., Xiao, Y., Yang, Z.-H., Wu, S., Xu, H.-J., Liang, F.-Y. and Zhao, F. (2014) 'The bacterial communities of bioelectrochemical systems associated with the sulfate removal under different pHs', *Process Biochemistry*, 49(8), pp. 1345-1351.

Zhu, X., Tokash, J.C., Hong, Y. and Logan, B.E. (2013) 'Controlling the occurrence of power overshoot by adapting microbial fuel cells to high anode potentials', *Bioelectrochemistry*, 90, pp. 30-35.